

DOE/NASA/0260-1

NASA CR-174713

GBI ER-11

(NASA-CR-174713) DESIGN OF AN ADVANCED WOOD
COMPOSITE ROTOR AND DEVELOPMENT OF WOOD
COMPOSITE BLADE TECHNOLOGY Final Report
(Gougeon Bros., Inc.) 195 p CSCI 11D

N87-17861

Unclass

G3/24 43382

Design of an Advanced Wood Composite Rotor and Development of Wood Composite Blade Technology

IN-24
58133
DATE OVERDUE
P-195

Thomas Stroebel,
Curtis Dechow and
Michael Zuteck

Gougeon Brothers, Inc.
Bay City, Michigan

December 1984

Date for general release ————— DECEMBER 1986

Prepared for
NATIONAL AERONAUTICS AND SPACE ADMINISTRATION
Lewis Research Center
Under Contract DEN 3-260

for

U.S. DEPARTMENT OF ENERGY
Conservation and Renewable Energy
Wind Energy Technology Division



DISCLAIMER

This report was prepared as an account of work sponsored by an agency of the United States Government. Neither the United States Government nor any agency thereof, nor any of their employees, makes any warranty, express or implied, or assumes any legal liability or responsibility for the accuracy, completeness, or usefulness of any information, apparatus, product, or process disclosed, or represents that its use would not infringe privately owned rights. Reference herein to any specific commercial product, process, or service by trade name, trademark, manufacturer, or otherwise, does not necessarily constitute or imply its endorsement, recommendation, or favoring by the United States Government or any agency thereof. The views and opinions of authors expressed herein do not necessarily state or reflect those of the United States Government or any agency thereof.

Printed in the United States of America

Available from

National Technical Information Service
U.S. Department of Commerce
5285 Port Royal Road
Springfield, VA 22161

NTIS price codes¹

Printed copy:

Microfiche copy: A01

¹Codes are used for pricing all publications. The code is determined by the number of pages in the publication. Information pertaining to the pricing codes can be found in the current issues of the following publications, which are generally available in most libraries: *Energy Research Abstracts (ERA)*; *Government Reports Announcements and Index (GRA and I)*; *Scientific and Technical Abstract Reports (STAR)*; and publication, NTIS-PR-360 available from NTIS at the above address.

Design of an Advanced Wood Composite Rotor and Development of Wood Composite Blade Technology

Thomas Stroebe,
Curtis Dechow and
Michael Zuteck

Gougeon Brothers, Inc.
Bay City, Michigan

December 1984

Prepared for
NATIONAL AERONAUTICS AND SPACE ADMINISTRATION
Lewis Research Center
Cleveland, Ohio 44135
Under Contract DEN 3-260

for
U.S. DEPARTMENT OF ENERGY
Conservation and Renewable Energy
Wind Energy Technology Division
Washington, D.C. 20585

CONTENTS

	Page
1.0 SUMMARY	1
2.0 INTRODUCTION	2
3.0 ROTOR DESIGN SPECIFICATION	2
3.1 Geometry and Aerodynamics	
3.2 Loads and Design Cases	
3.3 Rotor to Drivetrain Interface	
4.0 ROTOR DESIGN CONCEPT	4
4.1 Structural Concepts	
4.2 Rotor Geometry	
4.3 Inner Rotor Hardware and Load Take-Off	
4.4 Instrumentation	
4.5 Miscellaneous Provisions	
5.0 FABRICATION CONCEPT and DESIGN DETAILS	9
5.1 Molds and Tooling	
5.2 Outer Rotor (Blades)	
5.3 Inner Rotor (Composite Hub)	
5.4 Rotor Assembly	
5.5 Manufacturing Plan	
6.0 DESIGN SUPPORT TESTS	13
6.1 Qualification of Splice Joint	
6.2 Composite Hub	
7.0 STRUCTURAL ANALYSIS	14
7.1 Outer Rotor	
7.1.1 Normal operating loads	
7.1.2 Maximum operating loads	
7.1.3 Hurricane loads	
7.1.4 Buckling and Edgewise loads	
7.2 Splice Joint	
7.3 Inner Rotor	
7.4 General Rotor Properties	

PRECEDING PAGE BLANK NOT FILMED

8.0 COST ANALYSIS	17
8.1 Capital Costs	
8.2 Materials and Labor Breakdown	
8.3 Cost Summary	
8.4 Cost Reduction and Cost Control	
9.0 MISCELLANEOUS HARDWARE	20
9.1 Prototype Tooling and Fixtures	
9.2 Handling and Shipping Provisions	
10.0 SECONDARY TASKS	21
10.1 Load Take-Off Stud Test Program	
10.2 Wood/Epoxy Laminate Test Program	
10.3 Advanced Wood Composite Technology Tests	
11.0 DISCUSSION	22
11.1 Primary Task	
11.2 Secondary Tasks	
12.0 CONCLUDING REMARKS	24
13.0 APPENDIX A - Teetered Hub Principal Stud Load Analysis	77
14.0 APPENDIX B - Summary of Aerodynamic Tip Brake Design Concepts	78
15.0 APPENDIX C - Rotor Design Allowables Analysis	83
16.0 APPENDIX D - Exploratory Testing of a Wood/Epoxy/Graphite Composite Concept	110
17.0 APPENDIX E - An Evaluation of Wood/Epoxy Laminate with Scarf Jointed Plies in Compression	137
18.0 APPENDIX F - Prototype Rotor Manufacturing Plan	155
19.0 REFERENCES	189

1.0 SUMMARY

Following a successful demonstration of the field performance of laminated wood composite blades, on intermediate size MOD-0A wind turbines, a contract (DEN3-260) was awarded for the Development of Advanced Wood Composite Blade Technology. Tasks contained within this contract were:

Primary Task - Design and Fabrication of a Two-Bladed, MOD-0 Research Rotor, with Complete Tip to Tip Wood Composite Construction (flow through hub design).

Secondary Tasks -

1. Design of a Load Take-Off Stud Test Program and Fabrication of Stud Test Samples for Evaluation Under a Separate NASA Sponsored Program.
2. Design of a Wood/Epoxy Laminate Test Program and Fabrication of Laminate Test Material for Evaluation Under a Separate NASA Sponsored Program.
3. Design and Conduct Test Programs to Qualify Advanced Composite Concepts.
4. Design and Fabrication of a Splice Joint Test Article.
5. Design and Fabrication of an Inner Rotor (Hub) Test Article.

Items 4 and 5 above were to be tested at U.S. Government facilities under NASA-Lewis Research Center (NASA-LeRC) direction and are to support the design developed within the principal task.

The wood composite rotor structure was designed featuring epoxy laminated Douglas Fir veneers for the principal structure with some use of synthetic fibers (E-glass and graphite) for reinforcement of the prototype hub. Synthetic fiber augmentation was recommended due to the size and quantity of holes present in the hub region. Variations and simplifications on the outer rotor structural design, utilized in earlier wood/epoxy blades, were justified and documented during the conceptual design phase. Adhesive splicing of the two blades to the hub by use of structural finger joints is another key feature of this design. Final blade shape was developed in accordance with a stall-limited, 400 kW (maximum power), 90 foot diameter specification.

Calculations of margins of safety for various load conditions have been examined and are documented. The lowest positive margin of safety (3 percent) was calculated in the hub at rotor centerline for the 125 mph wind (with gusts) extreme wind load case.

Fabrication costs have been estimated for a production version of the rotor design presented within this report. The costed rotor is assumed to be simplified, relative to the prototype, by elimination of research specific features. In 1983 dollars, the cost per rotor was estimated at \$25,452 for the 100th rotor at a production rate of 120 rotors per year (Note that this estimate excludes the cost of teetering hardware).

A DOE/NASA reassessment of Wind Energy Program needs resulted in a termination of the prototype rotor fabrication task. Partially completed tooling has been placed in storage.

2.0 INTRODUCTION

Wind energy capture technology continues to be developed to compete, in particular geographical areas, with petroleum fuels and other energy alternatives for electrical power generation. Much of the continuing interest in wind energy is due to the encouraging results of earlier DOE/NASA projects. These efforts succeeded in overcoming many of the numerous technical obstacles to developing wind energy conversion as a workable technology. Although wind turbine blade costs have been significantly reduced due to the application of wood/epoxy composite technology (refs. 1, 2 and 3), it is expected that rotor costs can be lowered further by continuing the wood/epoxy composite structure across the rotor centerline. Such a composite hub concept offers two specific cost advantages over current rotors:

1. Most metallic hub elements are eliminated, thereby avoiding the cost of expensive forgings.
2. The use of relatively high cost load take-off studs, which transfer blade loads into the hub, is eliminated.

Conceptual and Preliminary Design efforts were conducted to review and explore various structural, configuration, and manufacturing options for the Final Rotor Design effort. Due to the NASA-LeRC reassessment of both aerodynamic performance as well as the limited MOD-0 generator capability at NASA's Plumbrook Station, where the prototype was scheduled for test, the rotor diameter specification was changed from 125 feet to 90 feet at the conclusion of the Conceptual Design phase.

3.0 ROTOR DESIGN SPECIFICATION

The contract required the design of the wood composite rotor to be within parameters described in this section. The final design specifications are listed in Table I. Compliance of rotor aerodynamics with specified power producing characteristics was verified by NASA-LeRC throughout the design effort.

3.1 Geometry and Aerodynamics

As specified by NASA-LeRC, the final design rotor was to feature a planform with the following key parameters:

Diameter	90 ft
Tip Airfoil	NACA 64(3)-6XX*
Maximum Power	400 kW

*Thickness to Chord Ratio to be contractor recommended

The tip airfoil was specified by NASA-LeRC due to good lift versus drag and drag versus thickness characteristics. These features combine to provide aerodynamically and structurally efficient sections. Furthermore, the same family of airfoils had been selected for the MOD-5A rotor and commonalty was considered desirable. The MOD-5A rotor refers to the 400 foot diameter rotor program conducted by the General Electric Company under DOE/NASA sponsorship.

3.2 Loads and Design Cases

Preliminary and Final Design operating loads were furnished by NASA-LeRC as developed from their MOSTAB computer model. These loads are given in Table II. In Table II, loads are given as a function of radial distance from rotor centerline, referred to as rotor 'station', in inches, from centerline.

3.3 Rotor to Drivetrain Interface

The contract required that NASA and the contractor jointly develop a load take-off concept for the teetering hub bearing assembly which is to be NASA designed and supplied. Here, load take-off refers to a mechanical transfer of loads from the rotor to the driveshaft assembly. A teetering hub is a hub design which allows for shedding of peak wind gust loads by allowing the rotor to pivot about its centerline on a shaft which is perpendicular to the wind direction. A hard teeter stop load of 170,000 foot-pounds was specified by NASA during the Final Design phase. A hard teeter stop load is the highest load to be experienced by the teetering hub mechanism. This load would occur when the rotor teeters against its mechanical limits. The rotor is expected to experience this load for less than 5 percent of rotor operation, which would be approximately 20,000,000 cycles.

4.0 ROTOR DESIGN CONCEPT

The contractual effort entailed an evolutionary approach to arrive at a final design which would meet the NASA-LeRC requirements. This section describes the rotor design following completion of the final design phase.

4.1 Structural Concepts

The rotor structure can be subdivided into three principal elements. These are the two blades and the hub, all to be fabricated of wood/epoxy-based composite plies. Each of the three elements is initially fabricated in halves which are then bonded into single pieces. Finally all three elements are joined to form an integral rotor. Clarification of this scheme is given in Sections 5.3 and 5.4 as well as in Figure 44.

The three elements are joined using two splice joints. These joints are centered at radial station 43 (inches) to each side of the rotor centerline. This location was chosen for the following reasons:

1. Allows construction of the hub using single (96 inch long) veneer sheets, thereby maintaining ease of manufacture and higher design allowables (by elimination of butt joints within the laminate plies) in the critically stressed area.
2. Allows rotor contour to change from a constant section non-tapering hub to a tapering blade shape without manufacturing restrictions imposed by veneers.
3. Allows all hub hardware to be precisely installed without added complication of an assembly at rotor centerline.
4. Moment loads at the joint are reduced from that existing at rotor centerline.

Three basic outer rotor structural design cases were presented for NASA review during the Conceptual Design phase. Each case could be engineered to have acceptable capability against identified loads. The cases were:

- A. All veneer structure, with constant thickness from leading edge to single shear web and decreasing thickness from shear web to trailing edge as shown in Figure 1. Note that dimensions given in all figures are in inches.
- B. Principal structural laminate forward with single shearweb and paper honeycomb/plywood skin tailpanel construction as shown in Figure 2.
- C. All veneer structure, with constant thickness from leading to trailing edge and with single shear web as shown in Figure 3.

At the time of the Conceptual Design Review, upon Gougeon Brothers, Inc. (GBI) recommendation, NASA rejected Concept B for further study. The cost/benefit relationship of Concept B did not compare favorably with Concepts A and C. This was primarily due to the more efficient placement of structural material in the latter two concepts and significantly lower manufacturing complexity and cost.

At the time of the Preliminary Design Review, NASA accepted Concept C for the Final Design effort. This decision was based upon a GBI demonstration that the aerodynamic flutter susceptibility difference between the Concepts A and C was insignificant when the torsional stiffness of the respective sections was taken into account. It was also shown that, due to panel buckling concerns, any weight savings expected from Concept A relative to Concept C would be minimal. Furthermore, it was identified that any such weight savings would be negated in rotor cost due to the additional manufacturing complexity involved in stepping down the shell thickness in the proposed chordwise fashion.

4.2 Rotor Geometry

A final rotor geometry was approved by NASA-LeRC featuring the following principal dimensions and is shown in Figure 4:

Tip Airfoil	NACA 64(3)-618 (modified)
Tip Chord	24.0 in.
Inner Airfoil (at Station 156*)	NACA 0028**
Chord at Inner Airfoil	64.75 in.
Twist	Zero degrees
Splice Joint Centerline	Station 43
Hub Chord	57.5 in.
Hub Thickness	21.9 in.
Est. Prototype Weight	4522 lbs.

*Station number is dimension in inches from rotor centerline.

**Defined inner airfoil is used for developing all intermediate airfoils through linear interpolation. The actual airfoils from Stations 156 to 180 are modified due to the need to smoothly transition from the aerodynamic portion of the rotor into a hub shape.

Airfoil selection was guided by structural as well as aerodynamic considerations. The NACA 64(3)-series foils (also specified for MOD-5A) provide good lift versus drag characteristics. A symmetrical NACA 00-series foil was proposed for the defining inboard station. This foil simplifies the transition of airfoil shapes into a nearly symmetrical hub section, over limited span, which minimizes wood veneer compounding complications. Asymmetric and particularly reflexive inboard foils would have made the inboard shape transition task extremely challenging for simplified wood composite construction techniques. All foils between this symmetric foil and the tip would be straight line interpolations of the two defined foils.

The inner airfoil thickness-to-chord ratio was minimized while maintaining structural adequacy. Also, the outer rotor design was adjusted slightly to provide NASA with the option of fabricating individual blades, with a root geometry suitable for a bonded stud load take off, from the same tooling. These individual blades would incorporate the standard MOD-OA stud pattern and could be used for a related wind energy development project.

The outer rotor was designed with zero degrees actual twist between the defining airfoils at Stations 156 and 540. However, due to a shift in the angle of zero lift, the aerodynamic twist between these same two airfoils would be 3 to 3.5 degrees.

The proposed final design contour was evaluated by Wichita State University, under a separate NASA contract, for annual energy capture. Although GBI recommended zero degrees of geometric blade twist, for desirable progressive stalling properties, it was shown that a trade-off existed between maximizing energy capture and optimizing power limiting characteristics. The final design rotor was accepted by NASA, with no geometric twist from centerline to tip, while acknowledging the recognized energy capture shortcomings.

The rotor diameter was the only physical dimension initially specified by NASA, while those dimensions pertaining to the aerodynamic portion of the rotor were initially recommended by GBI during the preliminary design phase and evaluated for acceptable performance by NASA. The outer rotor geometry was developed by coordinating airfoil selection with structural assessment. The geometry of the inner, non-power producing portion of the rotor was driven strictly by structural and load take-off considerations. A summary of geometric properties is presented in Table III. The final general hub configuration can be seen in Figures 5 and 6 (Note that both the upwind and downwind rotor configurations are shown).

4.3 Inner Rotor Hardware and Load Take-Off

The hardware proposed for the rotor hub generally falls into two categories. First, there is hardware which is removable and was to undergo detailed design and be provided by NASA. Secondly, hardware which is to be bonded

into the laminate structure as the specific load take-off element, was designed by the contractor, and was to be furnished with the rotor.

Two principal load take-off schemes were under consideration during the conceptual stage of design. One concept featured a load take-off through the edge laminate via bonded in place teeter bearings as is shown in Figure 7. This design featured flexibility for upwind as well as downwind configuring of a prototype rotor. This could take place by bringing the low speed shaft of the machine into the hub through holes in both the upwind and downwind faces of the hub. Hardware access and removal also appeared to be straightforward with this concept.

The other concept shared similarities to the first with the exception of a load take-off through metallic sleeves bonded into a thickened laminate in the hub and attaching to the teeter bearing bases with through-bolts as is shown in Figure 8. Because of the thickened laminate, the load transfer plane would be very near the flatwise neutral axis of the hub section, minimizing the effect of bending strain. Fastening, rather than bonding, of the teeter bearings would allow indexing the delta-three angle of the prototype rotor by providing multiple attachment options. The delta-three angle is the angle between the rotor's teeter axis and a line perpendicular to the rotor's spanwise centerline as shown in Figure 8. It couples blade pitching to blade teetering (or flapping). Non-zero delta-three settings of a teetered rotor are known to offer the following effects:

1. Positive delta-three angles couple the blade pitching to blade teetering in such a way that an aerodynamic force component is generated that opposes the teeter motion. Positive delta-three angles have been shown to allow for more rapid yaw rates of a wind turbine while restraining teeter motion, and suppressing teeter motion at high yaw angles (refs. 4 and 5).
2. Non-zero delta-three angles have been shown to improve the accuracy with which a wind turbine machine, in free yaw, will align itself with the wind, thereby maximizing wind energy capture.

NASA-LeRC desired to investigate the effects of various delta-three settings on this rotor because earlier work (ref. 4) indicated that the interrelationship of delta-three angle and other rotor parameters such as coning and airfoil shape upon wind turbine machine operating characteristics are not precisely known. Delta-three angles of zero as well as ± 22.5 , ± 45 , and ± 67.5 degrees are offered.

The ease of access to the teeter hardware was not as apparent with this design. However, a three dimensional mockup was fabricated by NASA which demonstrated that the access would be adequate. Following this demonstration, NASA elected the concept offering variable delta-three angles for the Final Design effort.

As discussed previously, the hub hardware serving to interface the composite hub to the low speed shaft is principally an array of fastener sleeves

bonded into a thickened region of the composite hub structure. The actual attachment of the metal teeter hardware to the composite hub takes place via through-bolts. These bolts capture both the teeter bearing bases near the interior laminate surface and also a welded teeter stop structure to the exterior laminate surface. The fastener arrangement, as shown in Figure 9, serves principally to transfer rotor torque and thrust into the teeter shaft through two teeter bearing bases. See Appendix A for the analysis of torque loads on these fasteners. The evaluated loads will yield very high positive margins in this area of the design. Sufficient numbers of the bonded fastener sleeves are placed in the hub laminate to allow the prototype rotor to be configured for all specified delta-three angles. The teeter shaft completes the transfer of rotor torque and thrust to the low speed shaft while relieving the rotor of gust loads.

For the prototype rotor, two teeter stop and damping schemes were considered. The first incorporated elastomeric 'bumpers' to stabilize intermediate teeter excursions. Direct contact between the low speed shaft and a steel weldment attached to the laminated hub would occur only when the elastomeric bumpers failed to singularly react higher rotor teeter moments.

The second scheme was to use a pair of hydraulic dampers or shock absorber mechanisms. These would attach externally to the hub and extend to a low speed shaft attachment. The dampers would serve to reduce the normal teeter stop loads on the rotor and could also be designed with internal 'hard stops'. An added feature of this system was the capability of developing variable damping as a function of teetering angle. Dampers could also be utilized, on the prototype machine, with adjustable valving to allow for optimizing the teetering behavior. Stock, high-capacity dampers were identified which might serve in this function. A load take-off provision for the first teeter stop scheme was designed by NASA, while provisions for the second scheme were designed by GBI and are shown in Figure 10.

4.4 Instrumentation

Principal instrumentation on the prototype rotor was to include pressure taps, angle of attack indicators, ice detection, and strain gages. The pressure taps and angle of attack indicators were specified for installation on only one blade of the rotor.

Stainless steel pressure taps were specified by NASA to be installed at three spanwise locations (near 50, 75, and 90 percent of span). Twenty four pressure taps were to be arrayed chordwise (twelve on each surface) at each spanwise location as shown in Figure 11. Provisions for the installation of three angle-of-attack probes, to be installed near each of the pressure tap sets were also developed as required. This is shown in Figure 12. It was also specified that the contractor provide three watertight enclosures and conduit for electrical cables, for the necessary electronic signal conditioning devices, in proximity to the pressure tap locations. Access to

these enclosures was to be provided via cover plates. These provisions were designed and are illustrated in Figures 13, 14, 15, and 16.

4.5 Miscellaneous Provisions

At the conceptual design level, the design specification included incorporation of aerodynamic tip brakes. The tip brake design concepts are summarized in Appendix B. Further aerodynamic tip brake design and development was not pursued.

It was specified by NASA that GBI furnish provisions for ice detectors, addition of tip weights, and tip venting. Ice detection may be desired at specific sites where icing conditions would necessitate rotor shutdown. Tip weights could be added if any post-production balancing of the rotor would be required. The venting serves to prevent pressurization of the structure with changes in temperature or atmospheric pressure experienced when shipped over routes with extreme altitude changes and also to prevent internal moisture buildup. Figure 17 illustrates the details proposed to meet these requirements.

Provisions for rotor lightning strike protection were proposed by both NASA and the contractor. A laminated aluminum screen system, essentially the same as utilized for MOD-OA blades, was NASA's final choice. Externally attached aluminum strike diverter straps and a laminated aluminized fiberglass cloth had also been proposed and evaluated for material and installation cost. Although it was felt by both GBI and NASA that all three systems would be technically feasible, the chosen system had been previously qualified (ref. 6) and represented therefore, minimal overall risk. Coverage of the rotor was proposed strictly for the blade elements. Ground straps would be installed just outboard of the splice joint, as shown in Figure 18. An evaluation of conductive epoxies would be necessary to assure best electrical connection from the screen to the ground straps and from other conductive installations (such as pressure taps) to the screen as shown in Figure 13.

5.0 FABRICATION CONCEPT and DESIGN DETAILS

The fabrication concept serves as one of the practical advancements of the proposed design relative to previous efforts (ref. 7). Because of the acceptance by NASA of chordwise centers of gravity which are further aft from the airfoil leading edge, relative to previous programs, manufacturing simplifications occur. These simplifications also permit more efficient placement of structural material to counter critical flatwise design loads.

Many of the descriptions and design details furnished in this area of the report pertain to and assume a rotor produced from prototype tooling. However, some of the illustrated general manufacturing processes assume production operations with the availability of production level tooling.

Some of the assumptions made for the production version of this rotor include:

- a) Use of 50 inch wide, 96 inch long, 0.1 inch thick rotary peeled Douglas Fir Veneers (Prototype is baselined on 25 inch wide veneers of same type)
- b) Use of WEST SYSTEM (R) Epoxy
- c) Use of ultrasonically graded veneer (GBI specified Blade Grade 2 in the outer rotor and Blade Grade 1 in the hub; see Appendix C)
- d) Use of spanwise butt joints in outer rotor laminate with controlled 3 inch stagger as shown in Figure 19.

The instrumentation enclosures will be installed in the prototype prior to the bonding of blade halves.

5.1 Molds and Tooling

The general molding concept has not changed dramatically from earlier efforts. As before, female half shell molds using vacuum bag lay up were proposed. The machining of the laminated blade halves after lay up is accomplished with a circular saw which is guided by the mold so that cut angle and elevation are properly controlled.

For the prototype rotor, four molds were to be built. For fabrication of the outer rotor, female high pressure and low pressure molds would be formed from a full scale male pattern. In turn, all four outer rotor halves would be manufactured from these tools. For fabrication of the constant section inner rotor (hub), two female molds would be fabricated, without the need for a male pattern. This is because of the relative simplicity of the outer surfaces and the lower exterior contour tolerance requirements of the hub.

Other tooling necessary for fabrication of the prototype includes fixtures for drilling and bonding stud hole bushings in the hub laminate, and miscellaneous machining jigs for manufacturing holes in both hub surfaces as well as access to instrumentation enclosures. Finally, some simple clamping devices are necessary for bonding the assembled outer rotor parts (blades) to the hub.

For early units, machining of the finger joints, which will allow for a structural assembly of the three rotor parts, is assumed to take place at a facility which supported a similar machining requirement under the MOD-5A program.

5.2 Outer Rotor (Blades)

Fabrication of the outer rotor or blades consists of the following principal operations.

Materials Preparation- Graded veneers are conditioned to a stable moisture content and trimmed to dimensions required for molding. Fiberglass cloth is checked for quality of weave and trimmed to dimensions required for molding. Vacuum bagging materials are prepared for molding.

Half shell molding- The mold surface is coated with epoxy gelcoat. Required layers of fiberglass cloth and veneer are epoxy coated and placed in mold. Entire layup is vacuum bag cured at room temperature. This is shown in Figures 20, 21 and 22.

Half shell trimming- Circular saws are used to accurately trim the leading and trailing edges of each blade half. This is shown in Figure 23.

Half shell bonding- The shear web is bonded into position prior to bonding the trimmed blade halves together. This is shown in Figures 24 and 25.

Preliminary finishing- Cleanup of excess adhesive at bonded joints takes place.

Finger Joint Machining- Each blade is accurately positioned with respect to the cutting machinery. The ends are machined flush and then fingers are carefully machined in vertical passes into the blade end. This is shown in Figures 26 and 27.

Detail of the outer rotor structure is given in Figure 28.

5.3 Inner Rotor (Composite Hub)

Fabrication of the inner rotor, or hub, consists of the following principal operations.

Materials Preparation- Graded veneers are conditioned to a stable moisture content and trimmed to dimensions required for molding. Fiberglass cloth is checked for quality of weave and trimmed to dimensions required for molding. Vacuum bagging materials are prepared for molding.

Half Shell Molding- The mold surface is coated with epoxy gelcoat. Required layers of fiberglass cloth and veneer are epoxy coated and placed in mold. Entire layup is vacuum bag cured at room

temperature. This sequence (minus gelcoat application) is repeated once in the low pressure shell to manufacture the thicker structural buildup. This is shown in Figures 29, 30, 31 and 32.

Load Take-Off Hardware Installation- Following accurate trimming of the half shell edges, holes for load take-off studs are machined into the compression side half shell. Then, a special jig is used to accurately position and hold the load take-off studs during adhesive bonding. This is shown in Figures 33 and 34.

Half Shell Bonding- Teeter hardware is installed and protected from adhesive as the hub halves are bonded. This is shown in Figure 35.

Preliminary Shell Machining- A hole is machined to provide for low speed shaft clearance. This is shown in Figure 36.

Preliminary Finishing- Cleanup of excess adhesive at bonded joints takes place.

Finger Joint Machining- The hub is accurately positioned with respect to the cutting machinery. Each end is machined flush and then fingers are carefully machined in vertical passes into the hub ends.

Details of the hub structure and finger joint are given in Figures 37 through 43. The figures illustrate the location of structural laminate and hole reinforcements, as well as finger joint machining and joining details and tolerances. Note that Figure 42 does not illustrate an inner rotor element but is included in this section for completeness.

5.4 Rotor Assembly

Because the rotor is composed of three basic structural elements: two blades and a hub, a plan to assemble the three pieces was developed. This consists of bonding each blade to the hub in separate operations.

During each operation, care must be taken to maintain critical alignments while the rotor components are positioned with the low pressure surfaces facing up. The first of these alignments is the maintenance of linearity of a reference line scribed on the common flatwise surface of all three pieces with respect to a vertical plane. This maintains proper aerodynamic relationships as well as keeps the center of gravity as close as possible to the chordwise centerline of the hub, minimizing tower excitations. The other alignment is the maintenance of linearity of a common leading/trailing edge line with respect to a horizontal plane. Due to the lack of twist, this becomes easier to accomplish and serves to maintain close tip alignment of the two blades of the rotor with respect to the rotor disk. Figure 44 illustrates this configuration.

While maintaining these alignments, each blade is brought into contact with the hub during separate splice joint bonding operations. Clamping force is then applied and maintained via balance-loaded external polyester cables which compress the joint and keep the load relatively constant during cure.

5.5 Manufacturing Plan

A detailed Manufacturing Plan was developed by GBI and serves to identify all manufacturing operations necessary for the fabrication of a prototype rotor as designed. It is included in Appendix F for reference. Included in the Manufacturing Plan are key quality control and quality assurance provisions.

6.0 DESIGN SUPPORT TESTS

Several design support tests were specified within the original scope of the project. General test plans were to be designed by GBI and the necessary test articles were to be fabricated by GBI. These are described within this section.

6.1 Qualification of Splice Joint

The structural joint which is utilized to bond the outer rotor pieces to the inner rotor is perhaps the most innovative structural feature of this rotor design. The specific joint type is a set of form fitting fingers as selected for the baseline MOD-5A splice joints (reference Figures 41, 42, and 43). Because of the NASA specified commonality which is to exist between the finger joint geometry of these two projects, a finger length of 11.5 inches (with a slope of 10:1) and a pitch of approximately 2.75 inches was used.

A cantilevered test article, as shown in Figures 45 and 46, was designed by GBI to subject a set of these machined and bonded finger joints to alternating bending stresses. Actuator loading at the extreme tip end of the 20 foot long test article would generate the desired outer fiber stresses. The actuator loads are reacted at the root end of the article by advanced load take-off studs (Design 4) which are similar to previous MOD-0A blade concepts. The studs are epoxy bonded to laminate blocking at the root end and attached to a rigid strongback. The test section of the test article is a constant section wood/epoxy laminate box-beam containing the bonded set of finger joints. The fundamental parameters guiding the design of the test article were maximum actuator load and deflection, estimated extreme fiber stress in the test area to yield a high cycle fatigue failure, and load take-off stud capability.

The structural pieces were fabricated at GBI and supported 'prove out' of the MOD-5A finger cutting machinery. The machined structural pieces were

returned to GBI for final assembly. Shipment was made to NASA-LeRC after final bonding of the joint and load take-off studs.

Installation of strain gages was performed by NASA-LeRC. The test article was fatigue tested at Ft. Eustis, Virginia under a separate NASA-LeRC contract.

6.2 Composite Hub

The final hub design featured wood/epoxy laminate structure augmented with E-glass fibers placed between each veneer layer at an orientation of ± 45 degrees relative to wood fiber. The principal purpose in augmenting the wood/epoxy laminate with glass fiber was to reduce the significant stress concentrating effects of the large holes existing on both the upwind and downwind faces of the hub. Both faces of the prototype rotor hub were required to have an access hole so that the prototype rotor could be operated both upwind and downwind of the tower. Furthermore, strength augmentation is desirable due to the significant number of smaller disruptions of the laminate in the thickened, low pressure side laminate. These disruptions are created by the large number of load take-off sleeves bonded in this region. For flexibility in the prototype rotor test program, many additional bolt locations were provided so that the rotor could be operated over a range of delta-three angles. To create additional positive margin in the prototype rotor, the glass fiber augmentation was proposed by GBI and accepted by NASA. Furthermore, the high pressure or tension side hole was designed with both an oblong shape and with a carbon fiber/epoxy liner to reduce the classic stress concentrating effects of such a structural disruption. It is likely however, that a production version of such a rotor would not require a large hole in each surface. It is also unlikely that the numerous bonded sleeves for load take-off would be present in a production rotor version.

NASA elected to waive any qualification testing requirements relative to the hub design because of adequate positive margins in the area of the hub and low assessed risk of prototype failure.

7.0 STRUCTURAL ANALYSIS

The structural analysis of the rotor consists principally of an assessment of flatwise and edgewise section physical properties of the designed structure. These properties were then evaluated against different NASA furnished final design load cases to determine design margin levels. A flatwise margins summary is provided in Table IV. It can be seen from Table IV that the rotor's smallest positive (flatwise) margin is calculated as 3 percent for the extreme wind case at rotor centerline (Station 0 inches). Edgewise margins, as expected, were large, and will be discussed later. Where necessary, the design was modified to obtain positive flatwise

margins. A preliminary evaluation of margins against combined loads was also conducted at a limited number of rotor locations to determine magnitudes of margin change.

Design allowables were also developed, based on materials test data, for specific loading conditions. The allowables analysis is presented in Appendix C. Data from references 8, 9, and 10 were utilized in the development of allowables. Summaries of the structural analysis of the different rotor components for different loading conditions are presented in this section.

7.1 Outer Rotor

7.1.1 Normal Operating Loads

A normal operating load allowable was used to determine section capabilities against defined flatwise and edgewise loads separately. Positive flatwise margins were calculated for the entire rotor and are summarized in Table V and in Figure 47. A minimum positive flatwise margin of 12 percent is calculated at Station 276.

An analysis of margins against combined flatwise and edgewise loads was also conducted for the normal operating load case. This analysis was conducted at the rotor centerline (Station 0), at the splice joint centerline (Station 43), and at the rotor 'breakpoint' (Station 156). The 'breakpoint' is the location of maximum chord as shown in Figure 4. Extreme fiber minimum and maximum tensile stresses were evaluated around the high pressure perimeter at the rotor centerline. Extreme fiber minimum and maximum compressive stresses were evaluated around the low pressure forward perimeter of the two outboard stations (Stations 43 and 156) by adding peak flatwise and peak edgewise stresses. These stresses change linearly with distance from the flatwise and edgewise neutral axes. Flatwise extreme fiber stresses were adjusted, at rotor centerline, for the effects of the high pressure surface (tension surface), low speed shaft cutout hole. Allowables for the highest stressed surface fiber were utilized in accordance with the established Goodman diagram (Appendix C, Figure 66) for each perimeter location evaluated.

As shown in Tables VI, VII, and VIII, the combined loads analysis does show reductions from the positive margins calculated for the flatwise design operating case. The calculated combined minimum positive margins range from 14 to 149 percent.

7.1.2 Maximum Operating Loads

A maximum operating load allowable was used to determine inner and outer rotor section capabilities against defined flatwise and edgewise loads. Positive flatwise margins are seen throughout the rotor and are summarized

in Table IX and in Figure 48. A minimum positive flatwise margin of 24 percent is calculated at Station 324.

7.1.3 Hurricane Loads

A static load allowable was used to determine inner and outer rotor section capabilities against a fixed aerodynamic load of 70.1 lb/sq.ft. This value is equivalent to a wind speed of 125 mph with an aerodynamic drag coefficient of 1.25 and with a 1.4 multiplier for gusts. Positive margins are seen throughout the rotor and are summarized in Table X and in Figure 49. A minimum positive flatwise margin of 3 percent is calculated at Station 0.

7.1.4 Buckling and Edgewise Loads

The designed structure was also checked for positive margins against flatwise buckling loads and was spot checked at three locations for expected high margins against edgewise bending loads. The results are presented in Tables XI and XII. A minimum positive flatwise buckling margin of 102 percent is calculated at Station 324; a minimum positive edgewise moment capability of 569 percent is calculated at Station 156.

7.2 Splice Joint

The rotor section at which the splice joint is centered (Station 43) was given a flatwise bending capability knockdown of 2 percent following an assessment of available finger joint design data generated within the MOD-5A program. The 2 percent knockdown does not imply a 98 percent joint efficiency. Rather, it reflects the fact that a much larger total scale effect knockdown must be taken for the overall rotor than just for the limited volume finger joint area. Also, it accounts for the fact that butt joints, which occur in the bulk outer blade laminate, have been systematically excluded from the finger joint area. This 2 percent knockdown was applied against the Station 43 section capabilities for normal and maximum operating conditions, as well as hurricane gust conditions. Positive margins are still present.

7.3 Inner Rotor

Hub sections were evaluated with allowances for low speed shaft cutouts and with an additional stress concentration factor of 2.3, assumed for the critical tension side (elongated) hole, due to classical analysis. Figure 50 shows the critical hub section element evaluated at rotor centerline (Station 0) which is one half of the high pressure shell. Due to symmetry, the other half of the high pressure shell benefits from the same analysis relative to flatwise loads. The assumed distribution of outer fiber stress,

due to flatwise loads, over this same section is plotted in Figure 51. It is felt that the analytical treatment of the holes was conservative because the ± 45 degree (relative to wood grain) glass fiber augmentation of the hub laminate would reduce shear lag and stress concentrations below classical levels. Benefits of E-glass fiber augmenting of the wood/epoxy laminate are not accounted for in the parallel to grain allowable values, thereby providing additional conservatism. The evaluation of stress levels and material allowables in the hub near the low speed shaft cutouts is presented in further detail in Appendix C.

Teeter stop loads, as presented by NASA, were evaluated against the design capability of the load take-off provisions for both hydraulic and rigid structure teeter stops, and positive margins are indicated against conservatively estimated load take-off stud capability.

Paired 24 inch long studs are proposed with a moment arm approximately 29 inches from the teeter axis. Assuming simple single-acting hydraulic teeter dampers, each stud would be required to perform for 20 million cycles at a peak tensile load of 40,000 pounds. Recent stud fatigue data (generated through the program described in Section 10.1) suggests such performance can be easily attained.

7.4 General Rotor Properties

General rotor properties have been calculated by determining section properties (weight per spanwise foot and flatwise and edgewise stiffness) at twentyone spanwise locations. The computed weight and stiffness properties have been combined with specified loads to calculate rotor deflections and resonant frequencies through use of cantilevered beam relationships. The ability of GBI to accurately compute and apply section properties to predict overall rotor (or blade) deflection and frequency properties has been demonstrated in previous design and fabrication efforts. General rotor properties are presented in Tables XIII, XIV, and XV and in Figures 52, 53, and 54.

8.0 COST ANALYSIS

A Final Design Cost Analysis was conducted. The analysis focused on a production version of the Final Design Prototype at different production rates. Different capital equipment assumptions were applied to the different production rate cases. Also, it was assumed that a production variation of the prototype design would be lighter by 530 pounds. This weight savings would be realized mostly through hub design simplifications including fewer load takeoff provisions and less fiberglass augmentation. The cost analysis is detailed in this section.

8.1 Capital Costs

Capital cost assumptions were made for the three distinct production rates of 2, 10, and 120 rotors per year. The costing basis for 2 rotors per year production assumed use of existing prototype equipment. At this production rate, continued dependence on subcontracting of finger joint machining has been assumed.

At a production rate of 10 rotors per year, continued utilization of the prototype tooling, with slight refinements, is assumed. Depreciation costs over a ten year life is, however included in this case. In addition, the capitalization of a finger joint cutting machine is assumed at this production volume.

While the lower production rates assume usage of existing GBI plant facilities, the final case, at a rate of 120 Rotors per year, includes capital costs for a dedicated production facility with a 20 year life. Also present in this case are capital costs for higher production tooling with a 10 year life and production molds with a 5 year life.

A summary of plant capital costs for all three cases is provided in Table XVI.

8.2 Materials and Labor Breakdown

The breakdown of production rotor materials into basic quantities was accomplished and is summarized in Table XVII. Note that the production weight of 3991 pounds is less than the prototype weight of 4522 pounds. This is principally due to reductions in hub reinforcing fiberglass and epoxy, hub hardware, and the instrumentation package. These reductions are possible due to an elimination of the need for variable delta-three angle capability, instrumentation, and flexibility for upwind or downwind configuring.

A similar breakdown of production rotor direct labor hours at a 120 rotors/year production rate was developed and is summarized in Table XVIII. Certain labor efficiency improvement factors have been utilized in translating the direct labor component of production rotor costs from the lowest to the highest production volume case.

Labor costs for the prototype rotor will be significantly higher than for the 2 rotor/year case. This is not only because of learning curve factors, but also because the prototype would have multiple configuration capability and would be fully instrumented.

Total cost figures exclude the cost of teeter hardware which was not evaluated under this contract. The cost of a wood composite rotor of the type designed in this effort should be lower, not only than that of rotors employing other methods of manufacture and material, but also than that of rotors composed of a metallic hub and wood/composite blades such as in the case of MOD-0A.

8.3 Cost Summary

A summary of rotor costs for all three evaluated rotor production per year cases is presented in Table XIX. These costs range from \$25,452 to \$38,783 for 120 rotors per year to 2 rotors per year respectively. For the 120 rotors per year production case, the material component of final unit cost is 26.9 percent while the labor and overhead component is 47.3 percent. A similar relationship was shown in a previous effort (ref. 11). Cost reduction efforts would therefore be best served by focusing on reducing direct labor hours per blade by investing in plant and capital equipment sufficient to realize substantial labor reductions.

Cost data was based on several years of commercial blade fabrication during which time GBI built more than 775 blades (or 200,000 pounds of such structures). Therefore, the figures can be viewed as considerably more realistic than those generated in previous efforts.

8.4 Cost Reduction and Cost Control

In the process of estimating the 2nd, 10th, and 100th unit rotor costs (Table XIX), an effort was made to assume the greatest possible labor force learning and efficiency improvement factors. The result of such an improvement is a reduction in both the total and proportionate costs of labor per rotor when going from low volume production rates to producing a rotor every other work day.

Implementation of such a program would involve two basic elements. First, all appropriate tooling and equipment was identified to allow production to move from inefficient, prototype dedicated hardware to more streamlined production oriented systems. Additional capital costs were assumed for further production hardware development in support of improvements which, although not identified, should be anticipated and supported.

Secondly, it is felt that a dynamic philosophy of constant task reassessment is necessary to further reduce total labor hours per rotor. This can happen both by better utilization and refinement of existing hardware and by development of new hardware.

Material cost improvements result from an aggressive competitive purchase program, judicious inventory control, and an ongoing process improvement program.

Manufacturing costs are collected and reported in a computer equipped accounting system so that management, shop supervision, and process improvement engineers have an up-to-date cost history available in the ongoing effort to reduce costs.

9.0 MISCELLANEOUS HARDWARE

Additional hardware which was designed under this contract included special clamping fixtures and sleeve installation hardware for manufacture of the prototype rotor. Furthermore, necessary hardware for handling and shipment of both the partially completed and fully assembled rotor were designed. Descriptions of this hardware is provided in this section.

9.1 Prototype Tooling and Fixtures

At an early stage in the manufacture of the composite hub, holes are machined and the large number of sleeves needed for the load take-off are bonded into place. Principally the hardware consists of a plate which has been machined in accordance with the selected fastener pattern. Slip bushings are inserted into the plate holes to support the hand performed drilling operation. Finally, slip pins are later inserted into the plate holes to hold and align the sleeves prior to and during the bonding operation as shown in Figure 55. A second flat plate is provided to retain the planar relationship of these slip pins by sandwiching the slip pin shoulders between the two plates. Four steel hangers attach to the main plate and serve to position the plate properly with respect to the machined hub laminate edges. The hardware designed for accomplishing this operation on the prototype is shown in Figure 56.

The hardware illustrated in Figure 57 serves to provide the necessary tip end attachment and adjustment of external cables needed during the splice joint bonding operation described in Section 5.4.

9.2 Handling and Shipping Provisions

General shipping configurations were developed for preliminary rotor shipment to the finger joint machining subcontractor. Form fitting shipping cradles were designed for containing the rotor elements during preliminary shipment and for containing the fully assembled rotor during final shipment. Provisions are shown in Figure 58 for final rotor shipment.

A modified MOD-OA spreader bar would be used for handling the fully assembled rotor. For the prototype rotor, it is assumed that this hardware would be furnished by NASA-LeRC. Use of the bar is shown in Figure 59.

10.0 SECONDARY TASKS

The contractual effort included tasks unrelated to the rotor design but supporting the development of advanced wood composite rotor technology. The work on these tasks is summarized in this section.

10.1 Load Take-Off Stud Test Program

The program included the design of advanced load take-off stud concepts. A set of designs were proposed which would serve to identify the contribution of specific design variables to static and fatigue performance. Also the designs were developed to elevate the overall level of stud performance relative to previous evaluations (ref. 12). GBI was also tasked under this contract with the fabrication of up to 92 test samples containing the NASA selected studs from the proposed designs. The test program is being conducted by another NASA-LeRC contractor.

From the ten designs proposed, NASA-LeRC made a final selection of eight stud designs to be manufactured. This selection included five of the proposed designs, with NASA adding a full-scale MOD-OA, a 3/4 scale MOD-OA design and a non-tip drilled derivative of one of the first five designs. Figures 60 and 61 illustrate the eight designs selected for evaluation.

To introduce simulated blade loads into the test studs, a laminated wood/epoxy composite block was required for bonding of studs. Two test block designs were specified by NASA-LeRC. These designs are shown in Figure 62. The test studs were bonded into the test blocks by GBI.

The thrust of the test program has been on an initial evaluation of all eight designs with larger sample populations finally designated for Designs 4 and 5. Because of the thin wall thicknesses needed in the tip region for Designs 4 and 5, a number of machining procedure iterations as well as slight respecification of the designs were necessary to improve delivery time and reduce the cost of the test studs. Initial performance data provided by NASA-LeRC indicates that both Design 4 and 5 studs are very promising for significant gains in static and fatigue performance, as compared to the MOD-OA blade studs (ref. 12).

10.2 Wood/Epoxy Laminate Test Program

GBI was tasked under the contract to propose to NASA-LeRC a test program for the evaluation of wood/epoxy laminate and to fabricate the basic laminate from which fatigue samples would be built by NASA or another contractor. Following review of the proposal, NASA-LeRC indicated what laminate types would be required. The fabrication and shipment of these laminate billets has been completed. The testing of these fatigue samples has been conducted by another NASA-LeRC contractor.

10.3 Advanced Wood Composite Technology Tests

GBI was tasked to evaluate several concepts for advancements in wood/epoxy laminate technology. The first of these concepts was developed in support of the load take-off stud test program. This involved an evaluation of a scheme where the basic laminate is augmented with unidirectional graphite fabric to increase the elastic modulus. Increasing the laminate elastic modulus reduces the modulus mismatch between the laminate and steel load take-off studs, thereby reducing the shear stress levels in the epoxy utilized to transfer load from one material to the other. These reduced stress levels are expected to be associated with improved levels of fatigue performance for load take-off studs. Ultimately the concept was shown to be sound. Some performance degradation was noted at tests conducted near 120 degrees Fahrenheit. The summary of this evaluation is presented in Appendix D.

The second program was an evaluation of wood/epoxy laminates, with scarf jointed plies, under compressive static and fatigue loads. The effects of scarf joint slopes on laminate performance, particularly in fatigue, had not previously been investigated. Also evaluated was the effect on laminate performance of non-optimum scarf joints, namely overlaps or gaps, formed during a manufacturing operation. This test program is summarized in Appendix E.

11.0 DISCUSSION

A comprehensive review of the Final Rotor Design and secondary tasks progress was conducted by NASA-LeRC personnel. This section provides a summary of the work performed under this contract.

11.1 Primary Task

The design of an Advanced Wood Composite Rotor has been completed and undergone review, by NASA's Lewis Research Center. The design was approved by NASA on the basis of structural integrity and estimated aerodynamic performance. The manufacturing plan was considered to be practical and cost-effective.

The lowest positive design margin was calculated at rotor centerline for the extreme wind condition (125 mph wind plus gusts). This calculation was based on conservative laminate strength and hole stress concentration assumptions. For a production version of the rotor, simplifications of the hub design should increase the calculated margins.

The design is a 90 foot diameter, 400 kW (max. rated power) rotor, which weighs 3991 pounds in production configuration (the prototype weight was calculated to be 4522 pounds). The rotor could be field assembled, however one piece shipment has been assumed.

Cost of production units, at a rate of 120 rotors per year, has been estimated to be \$25,452 (1983 dollars). This figure excludes teeter hardware. A cost per unit weight analysis shows that such a rotor, at \$6.38 per pound, is seventeen percent lower in per pound cost than adjusted MOD-0A blade data (refs. 7 and 11). The economics should become even more attractive when comparisons on a complete rotor basis would be made.

Miscellaneous design features such as lightning protection, instrumentation and ice detection provisions were all accepted by NASA at the time of the Final Design Review. The lightning protection and ice detection provisions are proven concepts used in previous programs. Shipping and handling provisions were reviewed and determined by NASA to be practical and in accordance with previously accepted practice.

Fabrication of the prototype pattern, from which the prototype tooling would be made, commenced following NASA approval of rotor contour drawings. Work on the tooling was terminated, following NASA direction to delete fabrication of the rotor from the program.

11.2 Secondary Tasks

The results of the secondary tasks are summarized in this section.

1. Advanced stud designs were finalized and samples were produced for testing at a NASA contracted test facility.
2. A wood composite test program was reviewed by NASA and elements of the program were selected for testing at a NASA contracted test facility. Wood/Epoxy laminate was produced by GBI in support of this activity.
3. Test Programs were designed and conducted in support of two advanced composite concepts. One program was a scheme for augmenting wood composite with unidirectional graphite. The other involved compression evaluation of scarf jointed laminate plies. Both concepts were shown to offer performance benefits, although the modest amounts of data generated may not sufficiently support the development of specific design allowables.
4. A test article for fatigue evaluation of full-scale finger joints was designed and fabricated. The article was tested at a U.S. Government facility.

12.0 CONCLUDING REMARKS

The relative simplicity of the rotor structural design and stall-limiting scheme offers potential savings in capital costs as well as machine operating and maintenance costs. These savings are expected to be offset to some degree by lower annual energy capture. Actual data on the resulting cost of energy would significantly influence future commercial rotor designs.

The opportunity to enhance the properties of basic wood/epoxy laminate via high strength fiber augmentation or scarf jointed construction was demonstrated in the secondary tasks of this contract. Further testing would serve to refine such advancements and allow for the development of statistically credible design data.

TABLE I.- FINAL PROTOTYPE ROTOR DESIGN SPECIFICATIONS

Rated Power(max.),kW		400
Rotor Diameter, feet		90
Number of Blades		2
Blade Twist, Deg	Physical	0
	Aerodynamic	3.5
Rotor Speed, RPM	Nominal	55
	Maximum	60
Rotor Location*		Upwind or Downwind
Rotor Tilt, Deg		Less than 5
Rotor Coning, Deg		0
Rotor Teetering, Deg		+/-6
Hub Delta-3 Angle, Deg**		+/-67.5 in 22.5 increments
Tip Airfoil Type		NACA 64(3) 6XX
Type of Power Control		Stall Limited
Normal Shutdown Mode		Yaw Control
Emergency Shutdown Mode		Mechanical Brake
Starting Mode		Motoring
Design Windspeed, mph		25
Cutout Windspeed, mph		50

* with respect to tower

** rotation of teeter axis with respect to rotor spanwise centerline

TABLE II. - 90-FOOT DIAMETER WOOD ROTOR DESIGN MOMENTS*

STATION (inches)	FLATWISE MOMENT, lb-ft		CHORDWISE MOMENT, lb-ft	
	STEADY	CYCLIC	STEADY	CYCLIC
0	-142,400	24,400	-28,600	35,200
45	-123,200	21,800	-26,700	26,300
100	-100,400	18,400	-19,800	19,100
155	-79,000	15,400	-16,300	13,100
210	-59,000	12,400	-13,000	8,700
265	-41,000	9,400	-9,500	5,500
320	-25,200	6,400	-6,300	3,200
375	-13,200	3,800	-3,800	1,600
430	-5,000	1,900	-1,900	700
485	-600	500	-700	150
540	0	0	0	0

*NASA specified at 4×10^8 cycles.

TABLE III. - BLADE GEOMETRIC PROPERTIES

Blade Twist: 0°

STATION (inches)	CHORD (inches)	THICKNESS (inches)	THICKNESS/CHORD	SHELL THICKNESS (inches)	SHEAR WEB LOCATIONS L.E. to Fwd Face (inches)
0 - 43	57.5	21.88	.381	2.7	-----
43	57.5	21.88	.381	2.7	-----
60	58.41	21.27	.364	2.38 - 2.48*	-----
84	59.85	20.42	.341	1.18 - 1.28	-----
132	63.12	18.72	.297	1.08 - 1.18	24.69
156	63.7	17.87	.281	1.08	24.00
180	62.2	17.02	.274	.98 - 1.08	23.13
228	57.11	15.33	.268	.88 - .98	21.38
276	52.02	13.65	.262	.88	19.62
324	46.92	11.96	.255	.68 - .78	17.88
372	41.83	10.28	.246	.58 - .68	16.13
420	36.73	8.59	.234	.58	14.38
468	31.64	6.91	.218	.58	12.63
516	26.55	5.22	.197	.58	10.88
540	24.0	4.38	.182	.58	10.00

*Double numbers indicate a veneer terminates at station.

TABLE IV. - FLATWISE MARGINS SUMMARY

STATION (inches)	MARGINS, Percent			MINIMUM MARGIN	
	EXTREME WIND CASE	DESIGN OPERATING CASE	MAXIMUM OPERATING CASE	PERCENT	CASE
0	3	64	104	3	Extreme Wind
3	7	70	110	7	Extreme Wind
6	15	82	126	15	Extreme Wind
9	31	107	156	31	Extreme Wind
17	156	298	392	156	Extreme Wind
20	159	302	396	159	Extreme Wind
35	179	216	290	179	Extreme Wind
43*	184	218	292	184	Extreme Wind
43*	177	197	266	177	Extreme Wind
60	138	171	232	138	Extreme Wind
84	49	49	83	49	Extreme Wind
132	41	32	58	32	Design Oper.
156	38	22	47	22	Design Oper.
180	39	19	42	19	Design Oper.
228	43	14	33	14	Design Oper.
276	52	12	28	12	Design Oper.
324	61	15	24	15	Design Oper.
372	83	32	27	27	Max Oper.
420	167	84	62	62	Max Oper.
468	410	211	155	155	Max Oper.
516	2661	1130	960	960	Max Oper.
540	∞	∞	∞	∞	All

*Two different calculations were made at the splice joint centerline (Station 43). The higher margins as indicated for the inner rotor are due to the use of higher grade unjointed laminate; the lower outer rotor margins are due to the use of jointed lower grade veneer laminates.

TABLE V. - DESIGN OPERATING CASE, FLATWISE SUMMARY
175 kW OUTPUT, 25 MPH WIND SPEED

STATION (inches)	r RATIO MIN STRESS MAX STRESS (NASA SPECIFIED)	ALLOWABLE (psi)	DESIGN OPERATING LOAD NASA SPECIFIED (inch-lbs x 10 ⁶)	FLATWISE CAPABILITY AGAINST ALLOWABLE (inch-lbs x 10 ⁶)	FLATWISE LOAD MARGIN (percent)
0	.700	2831	2.000	3.286	64
3	.700	2831	1.980	3.359	70
6	.700	2831	1.965	3.582	82
9	.700	2831	1.940	4.021	107
17	.700	2831	1.900	7.559	298
20	.700	2831	1.880	7.559	302
35	.700	2831	1.795	5.679	216
43**	.700	2774	1.750	5.564	218
43**	.700	2372	1.750	5.194	197
60	.700	2420	1.650	4.467	171
84	.696	2415	1.520	2.270	49
132	.684	2405	1.245	1.640	32
156	.676	2395	1.130	1.382	22
180	.669	2385	1.005	1.193	19
228	.649	2355	.770	.876	14
276	.622	2320	.558	.626	12
324	.592	2280	.366	.422	15
372	.554	2225	.206	.272	32
420	.474	2135	.100	.184	84
468	.25	1845	0.034	.106	211
516	-.24*	1490	0.004	.049	1130
540	-.50*	1310	0	.029	∞

*extrapolated values
**see explanation in Table IV.

TABLE VI. - COMBINED LOADS STRESS ANALYSES
(175 kW Output, 25 MPH Wind Speed, 4x10⁸ Cycles)

SUMMARY FOR ROTOR CENTERLINE (STATION 0)
(High Pressure Surface)

EXTREME FIBER LOCATION		EXTREME FIBER FLATWISE STRESS COMPONENT*		COMBINED EXTREME FIBER STRESS		STRESS RATIO (Min.Stress) (Max.Stress)	DESIGN ALLOWABLE** (psi)	DESIGN MARGIN (percent)
DISTANCE FROM LEADING EDGE (inches)	DISTANCE FROM CHORDLINE (inches)	Max (psi)	Min (psi)	Max (psi)	Min (psi)			
0	0	114	80	341	103	0.30	2258	562
1	2.46	325	228	544	250	0.46	2469	354
2	4.63	511	358	722	379	0.52	2562	255
3	6.23	649	454	852	474	0.56	2609	206
4	7.44	752	527	947	547	0.58	2644	179
5	8.35	830	581	1017	600	0.59	2668	162
7	9.63	940	658	1112	675	0.61	2703	143
9	10.37	1004	703	1160	719	0.62	2714	134
11	10.70	1032	722	1172	736	0.63	2738	134
13	10.78	1309	916	1433	928	0.65	2761	93
15	10.78	1719	1203	1827	1214	0.66	2784	52
17	10.78	1984	1389	2077	1398	0.67	2796	35
19	10.78	2389	1672	2466	1680	0.68	2808	14

* Based on Stepwise Linear Approximation of Smoothly Varying Stress Field in Region of Low Speed Shaft Hole
** These Values Have Received An Additional 17% Upgrade From Goodman Curve Values By Assuming Use of Unjointed,
Blade Grade 1 Veneer. An Additional Upgrade From Adjusting Allowables in Accordance With Highly Stressed,
Small Structural Volumes Was Not Implemented.

CALCULATION PARAMETERS

FLATWISE NEUTRAL AXIS: 1.33 inches from chordline toward low pressure surface
EDGEWISE NEUTRAL AXIS: 28.75 inches from leading edge

Extreme Edgewise Stress
Maximum: 227 psi
Minimum: 23 psi

TABLE VII. - COMBINED LOADS STRESS ANALYSIS
(175 kW OUTPUT, 25 MPH WIND SPEED, 4×10^8 CYCLES)

SUMMARY FOR STATION: 43

EXTREME FIBER LOCATION		COMBINED STRESS		STRESS RATIO (Min.Stress) (Max.Stress)	DESIGN ALLOWABLE (psi)	DESIGN MARGIN* (percent)
DISTANCE FROM L.E. (inches)	DISTANCE FROM CHORDLINE (inches)	Max. (psi)	Min. (psi)			
0	0	-173	-17	.10	-1905	1001
1	2.46	-358	-151	.41	-2181	509
2	4.63	-521	-268	.51	-2256	333
3	6.23	-639	-354	.55	-2287	258
4	7.44	-727	-419	.57	-2304	217
5	8.35	-791	-468	.59	-2317	193
7	9.63	-878	-536	.61	-2328	165
9	10.37	-924	-575	.62	-2333	153
11	10.70	-937	-592	.63	-2337	149
13	10.78	-931	-595	.63	-2340	151
15	10.78	-919	-594	.64	-2343	155
21	10.79	-884	-591	.66	-2353	166
27	10.79	-848	-588	.69	-2364	179
28.75	10.79	-837	-586	.70	-2368	183

* These Values Are Downgraded By 2% From Goodman Curve Values Because of Splice Joint Adjustments

CALCULATION PARAMETERS

EXTREME FLATWISE STRESS

EXTREME EDGEWISE STRESS

Flatwise Neutral Axis: Chordline
Edgewise Neutral Axis: 28.75 in. from Leading Edge

Max: -837 psi
Min: -586 psi

Max: -173 psi
Min: -17 psi

TABLE VIII. - COMBINED LOADS STRESS ANALYSES
(175 kW OUTPUT, 25 MPH WIND SPEED, 4×10^8 CYCLES)

SUMMARY FOR STATION: 156

EXTREME FIBER LOCATION		COMBINED STRESS		STRESS RATIO (Min.Stress) (Max.Stress)	DESIGN ALLOWABLE (psi)	DESIGN MARGIN* (percent)
DISTANCE FROM L.E. (inches)	DISTANCE FROM CHORDLINE (inches)	Max. (psi)	Min. (psi)			
0	0	-253	-25	.10	-1944	668
1	3.17	-938	-493	.52	-2311	146
2	4.36	-1189	-668	.56	-2340	96
4	5.84	-1495	-885	.59	-2364	58
7	7.26	-1780	-1092	.61	-2377	33
13	8.59	-2018	-1284	.63	-2387	18
19	8.96	-2048	-1333	.65	-2393	16
25	8.73	-1946	-1294	.66	-2400	23
31	8.14	-1765	-1202	.68	-2407	36
37	7.27	-1523	-1068	.70	-2416	58
43	6.03	-1200	-880	.73	-2430	102
49	4.53	-821	-653	.79	-2459	199
55	2.80	-392	-391	1.00	-2578	560
58	1.90	-257	-168	.65	-2395	1327

EXTREME FLATWISE STRESS

EXTREME EDGEWISE STRESS

Flatwise Neutral Axis: Chordline
Edgewise Neutral Axis: 29.32 in. from Leading Edge

Max: -1958 psi
Min: -1324 psi

Max: -253 psi
Min: -25 psi

ORIGINAL PAGE IS
OF POOR QUALITY

TABLE IX. - MAXIMUM OPERATING CASE
400 kW OUTPUT, 33 MPH WIND SPEED

STATION (inches)	r RATIO MIN STRESS MAX STRESS NASA SPECIFIED	ALLOWABLE (psi)	MAX OPERATING LOAD (Inch-lbs x 10 ⁶)	FLATWISE CAPABILITY AGAINST ALLOWABLE (Inch-lbs x 10 ⁶)	FLATWISE LOAD MARGIN (percent)
0	.700	4210	2.398	4.887	104
3	.700	4210	2.378	4.996	110
6	.700	4210	2.358	5.327	126
9	.700	4210	2.318	5.979	156
17	.700	4210	2.285	11.241	392
20	.700	4210	2.265	11.241	396
35	.700	4210	2.165	8.445	290
43 **	.700	4126	2.112	8.276	292
43 **	.700	3526	2.112	7.721	266
60	.700	3598	2.000	6.641	232
84	.696	3583	1.843	3.368	83
132	.684	3561	1.536	2.428	58
156	.676	3542	1.388	2.044	47
180	.669	3518	1.243	1.760	42
228	.649	3468	0.970	1.289	33
276	.622	3406	0.720	0.919	28
324	.592	3330	0.499	0.617	24
372	.554	3240	0.312	0.396	27
420	.474	3077	0.164	0.266	62
468	.250	2700	0.0606	0.155	155
516	-.240 *	2032	0.00633	0.067	960
540	-.50 *	1775	0	0.040	∞

*extrapolated values

**see explanation in Table IV.

TABLE X. - EXTREME WIND LOAD CASE

70.1#/ft² Airlord
(50.1#/ft² x 1.4 Instantaneous Peak Dynamics Multiplier)

STATION (inches)	ALLOWABLE (psi)	EXTREME WIND LOAD (Inch-lbs x 10 ⁶)	CAPABILITY AGAINST ALLOWABLE (Inch-lbs x 10 ⁶)	FLATWISE LOAD MARGIN (percent)
0	3612	3.060	3.145	3
3	3612	3.018	3.215	7
6	3612	2.978	3.428	15
9	3612	2.937	3.848	31
17	3612	2.831	7.233	156
20	3612	2.790	7.233	159
35	3612	2.600	7.242	179
43*	3540	2.500	7.098	184
43*	3160	2.500	6.916	177
60	3225	2.271	5.951	138
84	3225	2.031	3.018	49
132	3225	1.558	2.192	41
156	3225	1.349	1.859	38
180	3225	1.159	1.605	39
228	3225	0.8303	1.188	43
276	3225	0.5657	0.857	52
324	3225	0.3594	0.580	61
372	3225	0.2058	0.377	83
420	3225	0.0990	0.264	167
468	3225	0.0335	0.171	410
516	3225	0.00349	0.096	2661
540	3225	0	0.064	∞

*see explanation in Table IV.

TABLE XI. - FLATWISE BUCKLING MARGINS

STATION (inches)	EXTREME WIND (PEAK psi IN SHELL)	DESIGN OPERATING (PEAK psi IN SHELL)	MAX OPERATING (PEAK psi IN SHELL)	BUCKLING STRENGTH (psi)	FLATWISE MINIMUM MARGIN (percent)
43	1142	800	965	12569	1000
60	1231	894	1084	10999	794
84	2170	1617	1961	5441	151
132	2292	1826	2252	5447	138
156	2341	1958	2405	5595	133
180	2329	2009	2484	5595	125
228	2255	2071	2609	5582	114
276	2128	2068	2668	5516	107
324	1999	1975	2693	5433	102
372	1761	1686	2554	5394	111
420	1208	1158	1899	6374	236
468	633	594	1058	7759	633
516	117	121	192	10519	5379
540	0	0	0	12049	∞

TABLE XII. - EDGEWISE MOMENT LOAD MARGINS

STATION (inches)	STRESS RATIO	ALLOWABLE (psi)	PEAK EDGEWISE LOAD (psi x 10 ⁶)	EDGEWISE CAPABILITY AGAINST ALLOWABLE (inch-lbs x 10 ⁶)	EDGEWISE LOAD MARGIN (percent)
0	0.1	1989	.7656	6.717	777
43	0.1	1666	.636	6.136	865
156	0.1	1700	.3528	2.361	569

TABLE XIII. - INNER ROTOR PHYSICAL PROPERTIES

STATION (inches)	WEIGHT/FT (lbs)	CG LOCATION (% of chord)	EDGEWISE EI (lbs-in ²)	FLATWISE EI (lbs-in ²)	EDGEWISE* CAPABILITY (inch-lbs x 10 ⁶)	FLATWISE* CAPABILITY (inch-lbs x 10 ⁶)
0	128.7	50	274.064	45.510	15.269	3.145
3	131.6	50	274.202	45.948	15.338	3.215
6	141.6	50	274.455	47.203	15.574	3.428
9	175.0	50	274.924	48.873	15.704	3.848
17	186.6	50	275.358	57.409	15.728	7.233
20	186.6	50	275.358	57.409	15.728	7.233
35	122.5	50	213.555	48.182	12.198	7.242
43	122.5	50	213.555	48.182	12.198	7.242

*Capabilities calculated against 5-minute duration loading (extreme wind) 3612 psi allowable
glass augmentation credit not taken, carbon fiber hole liner credit not taken

ORIGINAL PAGE IS
OF POOR QUALITY

TABLE XIV. - OUTER ROTOR PHYSICAL PROPERTIES

STATION (inches)	WEIGHT/FT (lbs)	CG LOCATION (% of chord)	GJ* lbs-in ² x 10 ⁹	EDGEWISE EI lbs-in ² x 10 ⁹	FLATWISE EI lbs-in ² x 10 ⁹	EDGEWISE* CAPABILITY (in-lbs x 10 ⁶)	FLATWISE** CAPABILITY (in-lbs x 10 ⁶)
43	100.8	50.0	10.54	211.90	47.89	11.639	6.916
60	92.1	49.5	9.000	197.19	39.86	10.586	5.951
84	52.3	48.5	4.804	108.40	19.86	5.459	3.018
132	49.4	47.2	3.129	103.56	13.28	4.816	2.192
156	47.2	46.9	2.470	97.908	10.74	4.480	1.859
180	45.0	47.0	2.055	89.720	8.933	4.194	1.605
228	37.3	47.3	1.414	61.267	5.960	3.122	1.188
276	30.9	47.2	.91888	41.295	3.808	2.288	.857
324	25.1	47.0	.56863	26.741	2.317	1.619	.580
372	19.6	47.4	.33308	15.775	1.309	1.069	.377
420	16.0	47.5	.18615	9.6436	.7239	.806	.264
468	13.6	47.7	.09719	5.9425	.3790	.578	.171
516	11.2	47.7	.04128	3.3487	.1641	.388	.096
540	9.9	47.2	.02318	2.3586	.09069	.299	.064

* Torsional stiffness

** Capabilities calculated against 5-minute duration loading (extreme wind) 3225 psi allowable

TABLE XV. - MISCELLANEOUS ROTOR PROPERTIES

<u>NATURAL FREQUENCIES (HERTZ)</u>		
	<u>With Centrifugal Stiffening</u>	<u>Without Centrifugal Stiffening</u>
Flatwise	3.80 (4.15P)	3.64 (3.97P)
Edgewise	10.42 (11.37P)	10.36 (11.30P)
<u>TIP DEFLECTION:</u> 16.1 inches (70.1 lb/ft ² wind loading)		
<u>ROTATIONAL MOMENT OF INERTIA:</u> 4.80×10^5 lb-in-sec ²		
<u>WEIGHTS:</u>		
Hub Weight	1679.5 lbs	
Hub CG	STA 0	
Outer Blade Weight	1421 lbs	
Outer Blade CG	STA 174	
TOTAL ROTOR WEIGHT 4521.5 lbs		

TABLE XVI. - PLANT CAPITAL COSTS (mid 1983 K\$)

North of Bay City Agrarian Plant Site

I.	<u>2 ROTOR/YEAR PRODUCTION</u>	(Assume Use of Prototype Equipment)
	No Additional Equipment	
II.	<u>10 ROTOR/YEAR PRODUCTION RATE</u>	(Assume Use of Prototype Equipment)
	Additional Equipment*	200
	(10 year life)	
	TOTAL	200
	Depreciation as straight line at 10 units per year	
III.	<u>120 ROTOR/YEAR PRODUCTION RATE</u>	
	Plant (20 year life)	1440
	Tooling (10 year life)	790
	Molds (5 year life)	180
	TOTAL	2410
	Depreciation as straight line at 120 units per year	

*Includes finger joint cutter

TABLE XVII. - NET ROTOR WEIGHT (Pounds)

Veneer	2501
Epoxy	1057
Fiberglass	205
Hub Hardware	86
Lightning Protection	34
Miscellaneous	108
TOTAL	3991

Veneer Preparation and Layout	53
Shear Web Preparation	14
Stringer Preparation	5
Fiberglass Layout	14
Mold Preparation and Gelcoat	39
Glass Wet Out	69
Veneer and Fiberglass Molding	70
Shell Trim	8
Shear Web Cut and Bond	16
Half Shell Bonding	26
Clean Up and Balancing	37
Routing and Drilling for Studs	8
Bonding Studs, Anchors and Damper Stud Blocks	9
Cutting Holes for Hub	14
Manufacture and Install Hub Cutout Sleeves	5
Splice Joint Alignment and Cut	23
Splice Joint Alignment and Bond	35
Joint Clean Up and Finishing	7
Final Finishing	60
Preparation for Shipping	23
Lightning Protection	15
ROTOR TOTAL	550

NOTE: Total Labor & Overhead = direct labor above x 1.15 (hrs paid/hrs worked) x \$6.50/hr (North of Bay City 1983 Agrarian Labor Rate) x 1.5 (total manpower/direct labor x 1.95 (shop overhead))

ORIGINAL PAGE IS
OF POOR QUALITY

TABLE XIX. - ROTOR COST SUMMARY (1983\$)

ITEM	PRODUCTION RATE (rotors per year)					
	2		10		120	
	\$	%	\$	%	\$	%
Veneer	2041	5.3	1916	5.3	1790	7.0
Epoxy	2855	7.4	2855	7.9	2624	10.3
Fiberglass	1081	2.8	1081	3.0	981	3.9
Hub Hardware	942	2.4	876	2.4	674	2.6
Lightning Protection	248	0.6	235	0.6	213	0.8
Miscellaneous	703	1.8	674	1.9	573	2.3
TOTAL MATERIALS	7870	20.3	7637	21.1	6855	26.9
Labor & Overhead	22774	58.7	19403	53.6	12025	47.3
13% G&A	3984	10.3	3515	9.7	2454	9.6
12% Fee & Guarantee	4155	10.7	3667	10.1	2560	10.1
Depreciation	----	----	2000*	5.5	1558*	6.1
TOTAL	38783	100	36222	100	25452	100

Assumptions:

- (1) Mature plant at full production and 100% efficiency (no start-up costs)
- (2) Plant location north of Bay City in agrarian area where direct labor rate is \$6.50/hour
- (3) Existing Gougeon plant can handle up to 10 units per year production
- (4) Subcontracted cost for cutting finger joints is unknown and not included

*No cost of money, only straight line depreciation rate for capital costs

ORIGINAL FILE
OF POOR QUALITY

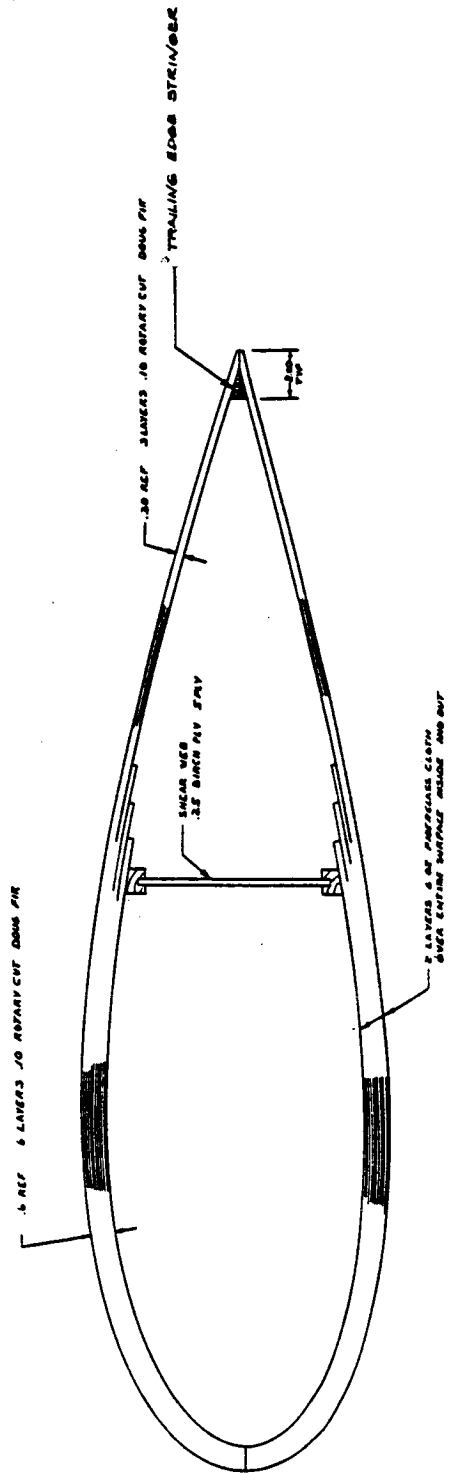


Figure 1.- Variable Thickness Section Concept

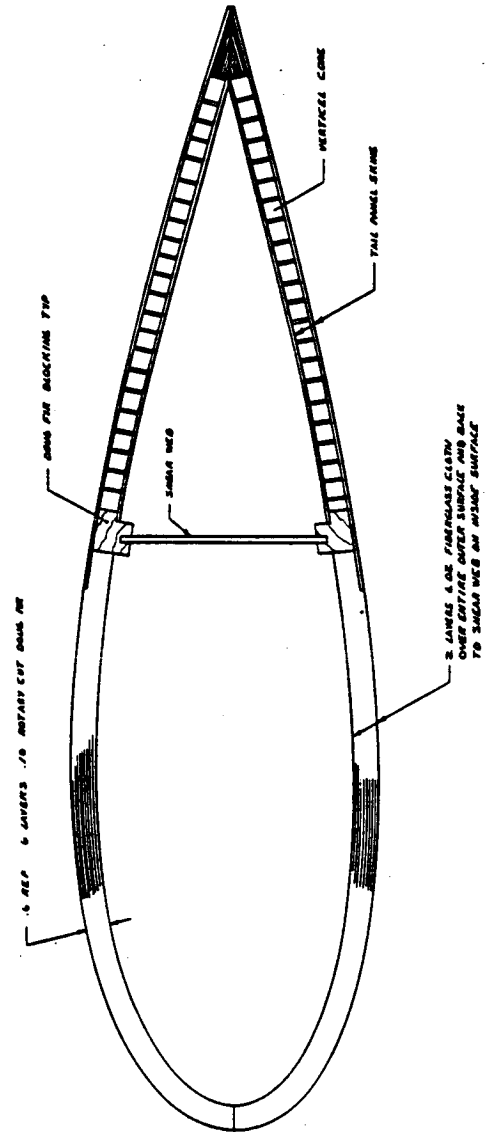


Figure 2.- Cored Tail Panel Section Concept

ORIGINAL PAGE 10
OF POOR QUALITY

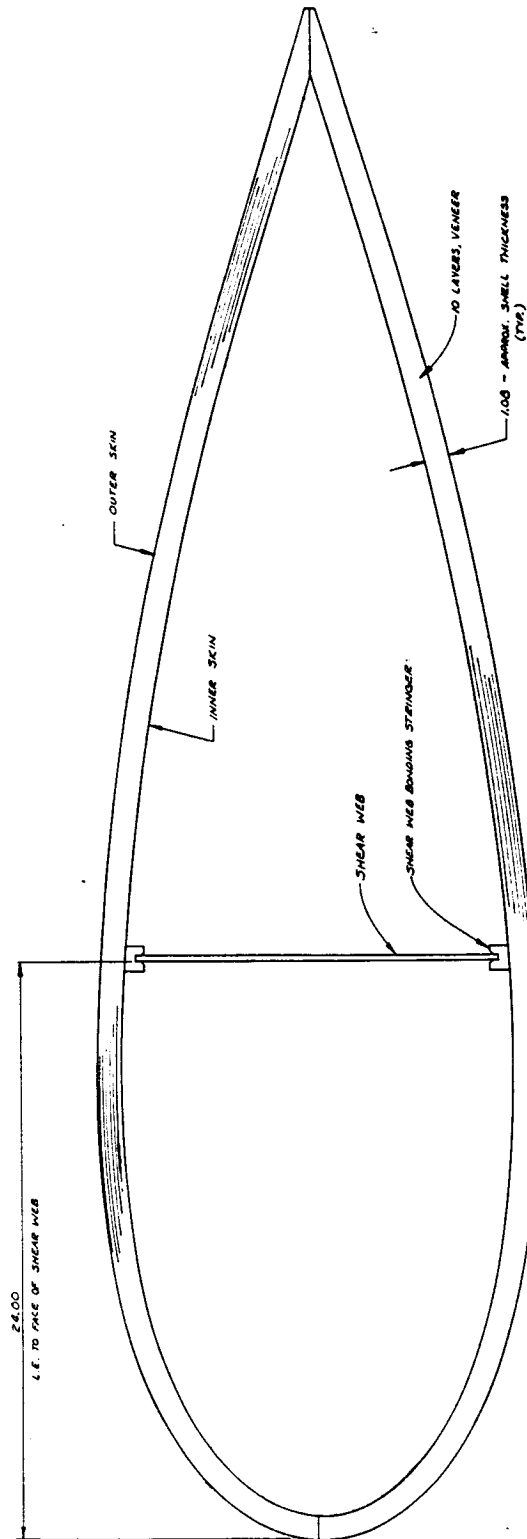


Figure 3. - Final Design Constant Thickness Section

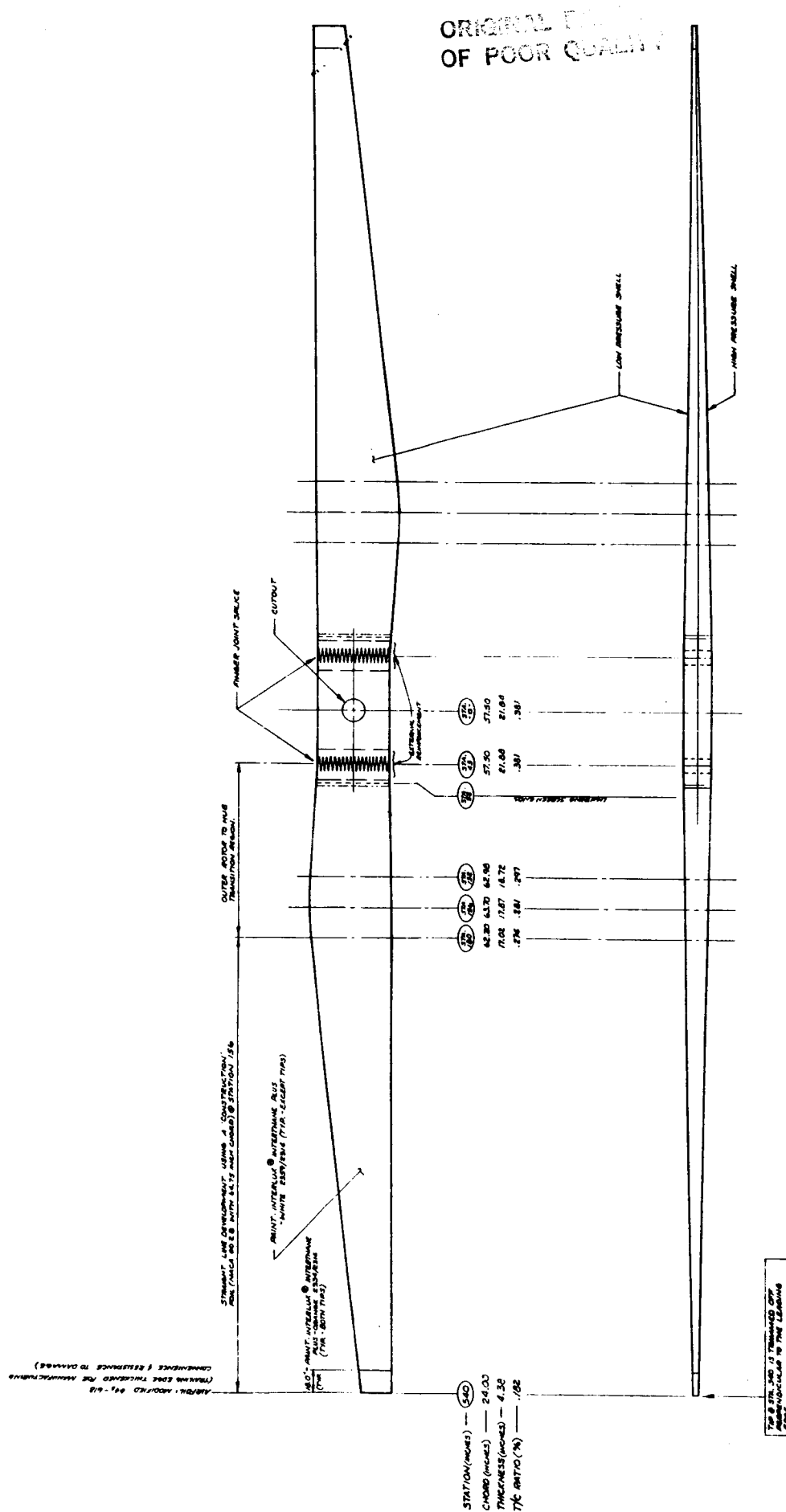


Figure 4. - Rotor Platform

ORIGINAL PAGE IS
OF POOR QUALITY

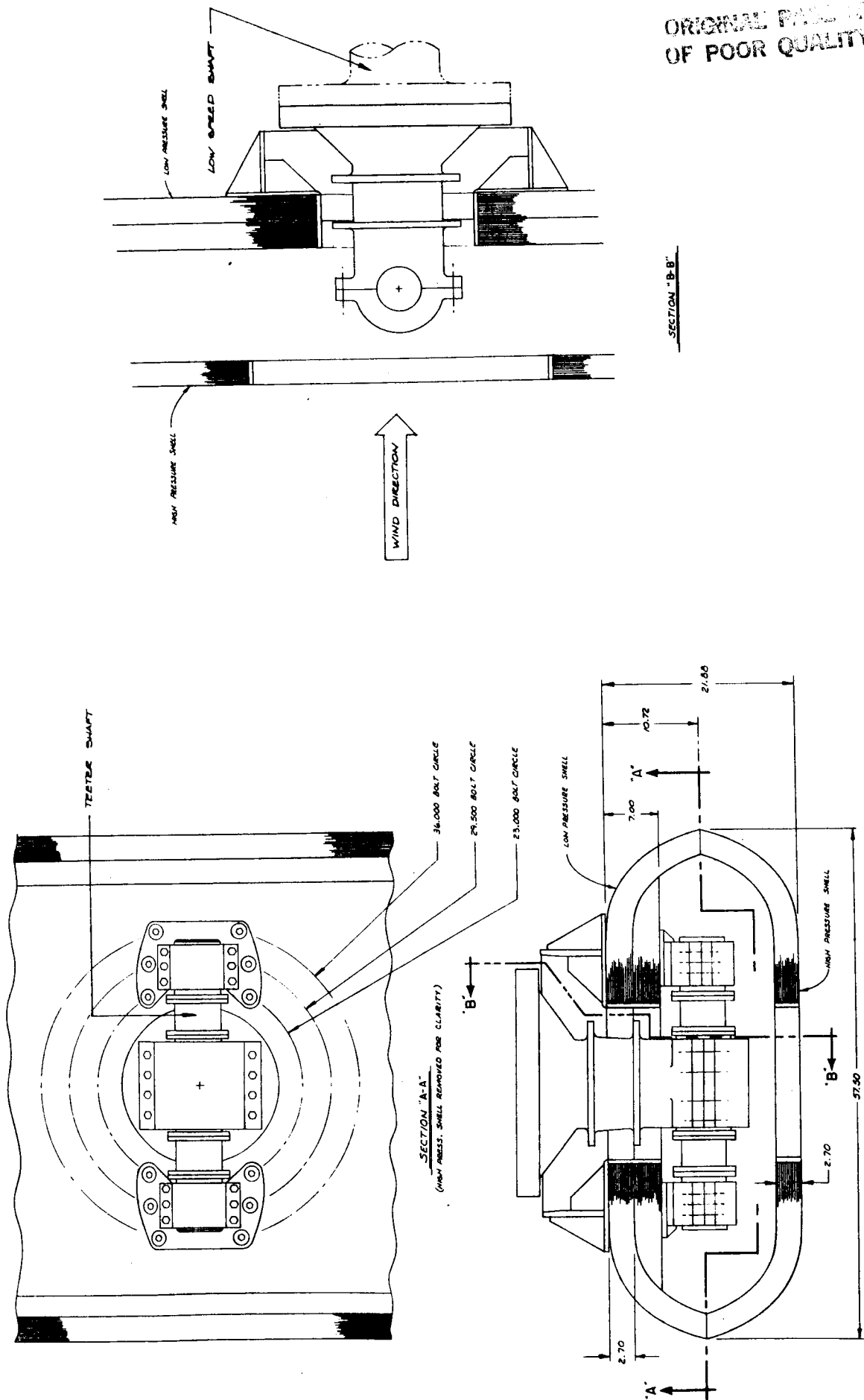


Figure 5. - Teetering Hub Scheme - Upwind Configuration

SECTION "A-A"
OF FOUR COLUMNS

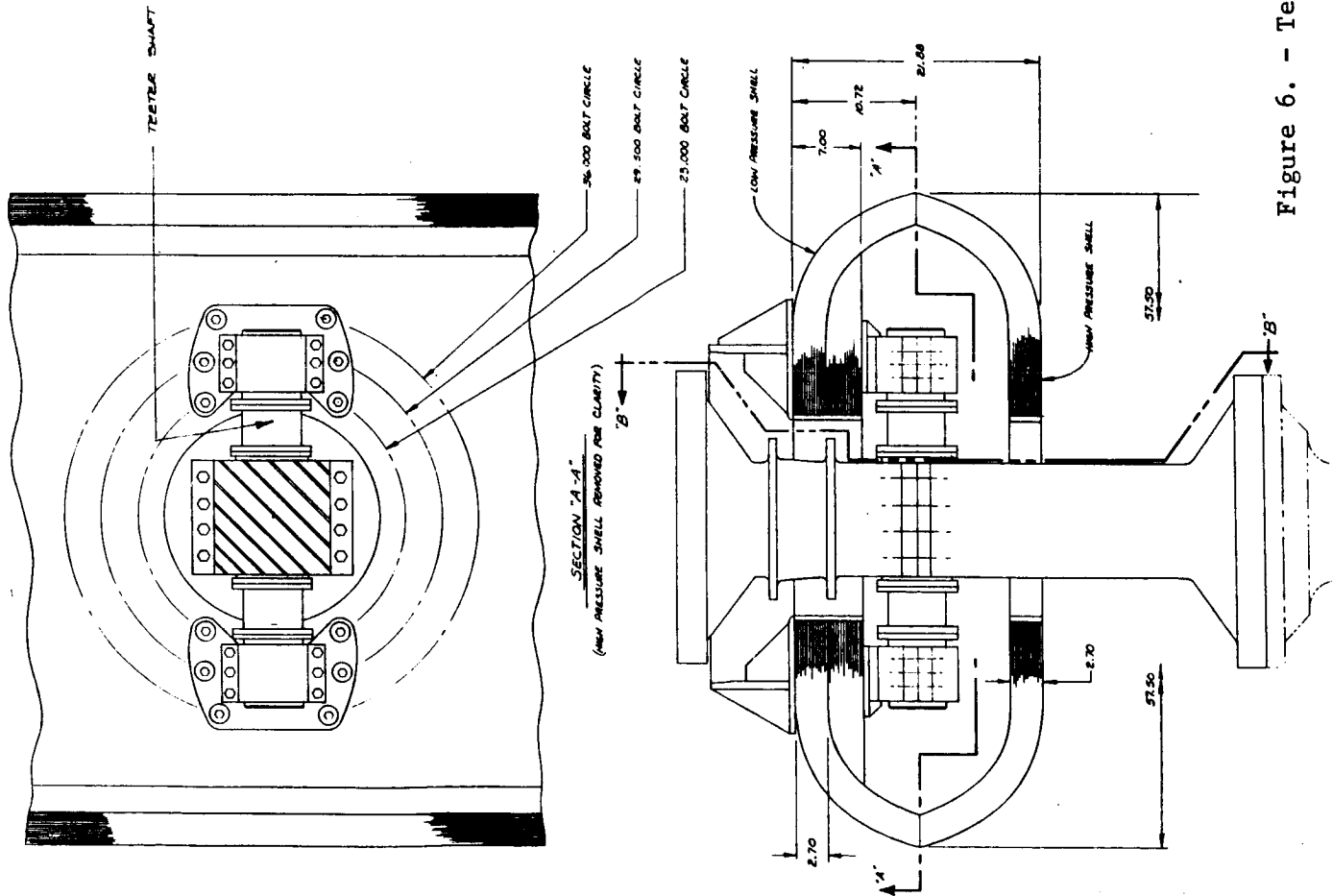


Figure 6. - Teetering Hub Scheme - Downwind Configuration

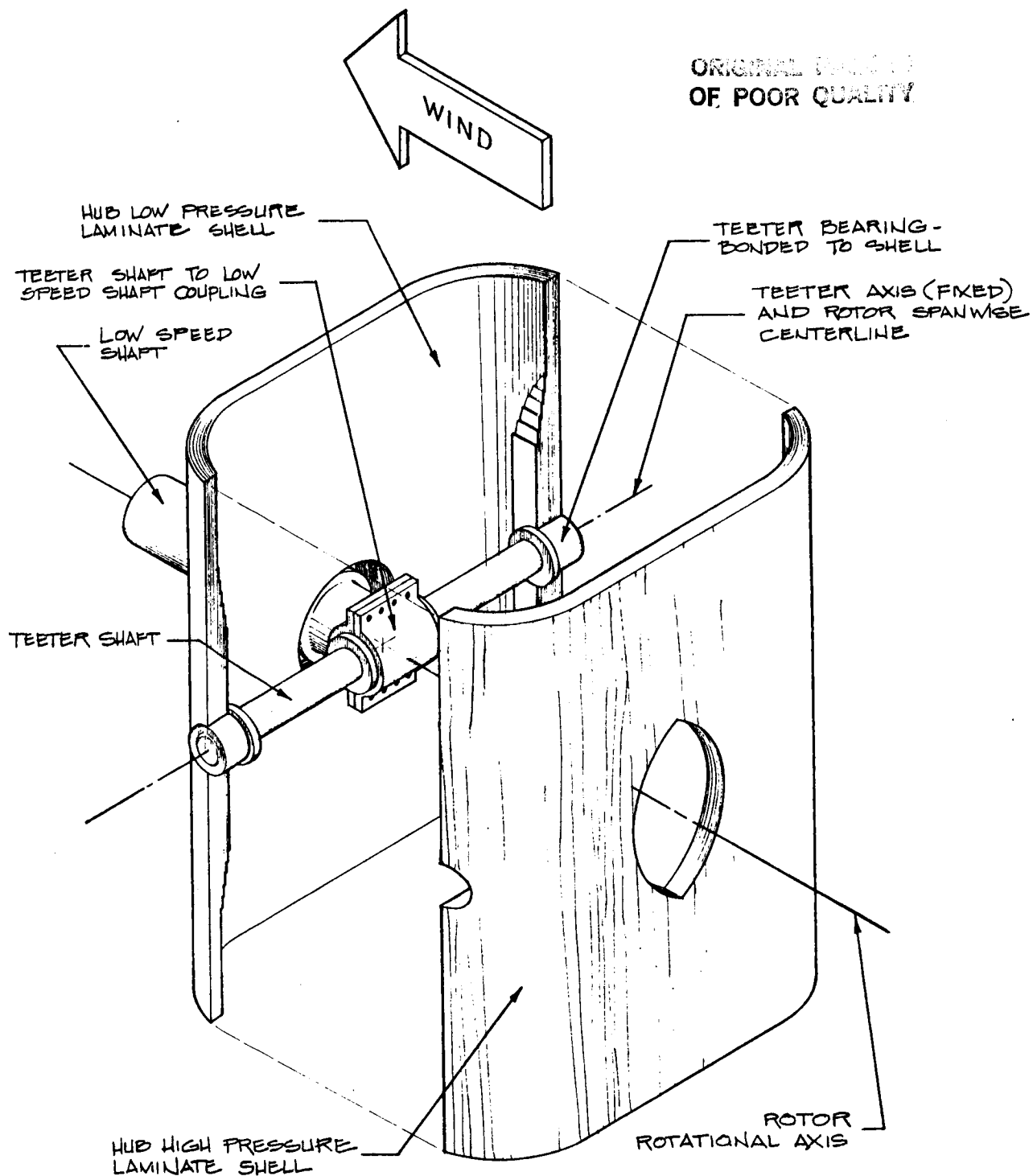


Figure 7. - Fixed Teeter Axis Hub Concept - Upwind Configuration, Exploded Schematic

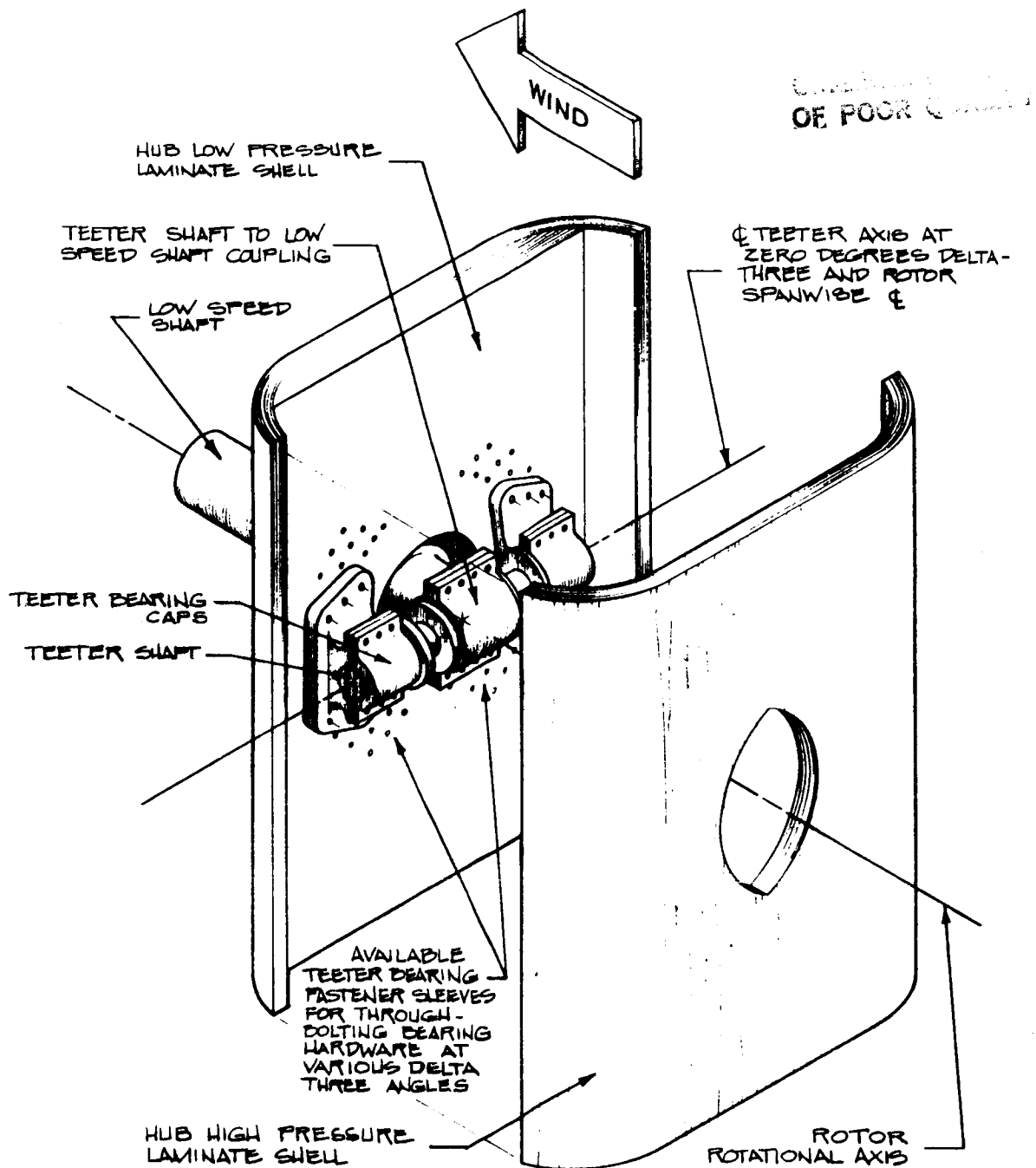


Figure 8. - Variable Delta-Three Angle Hub Concept - Upwind Configuration, Exploded Schematic

GRAPHICAL SYMBOLS OF POOR QUALITY

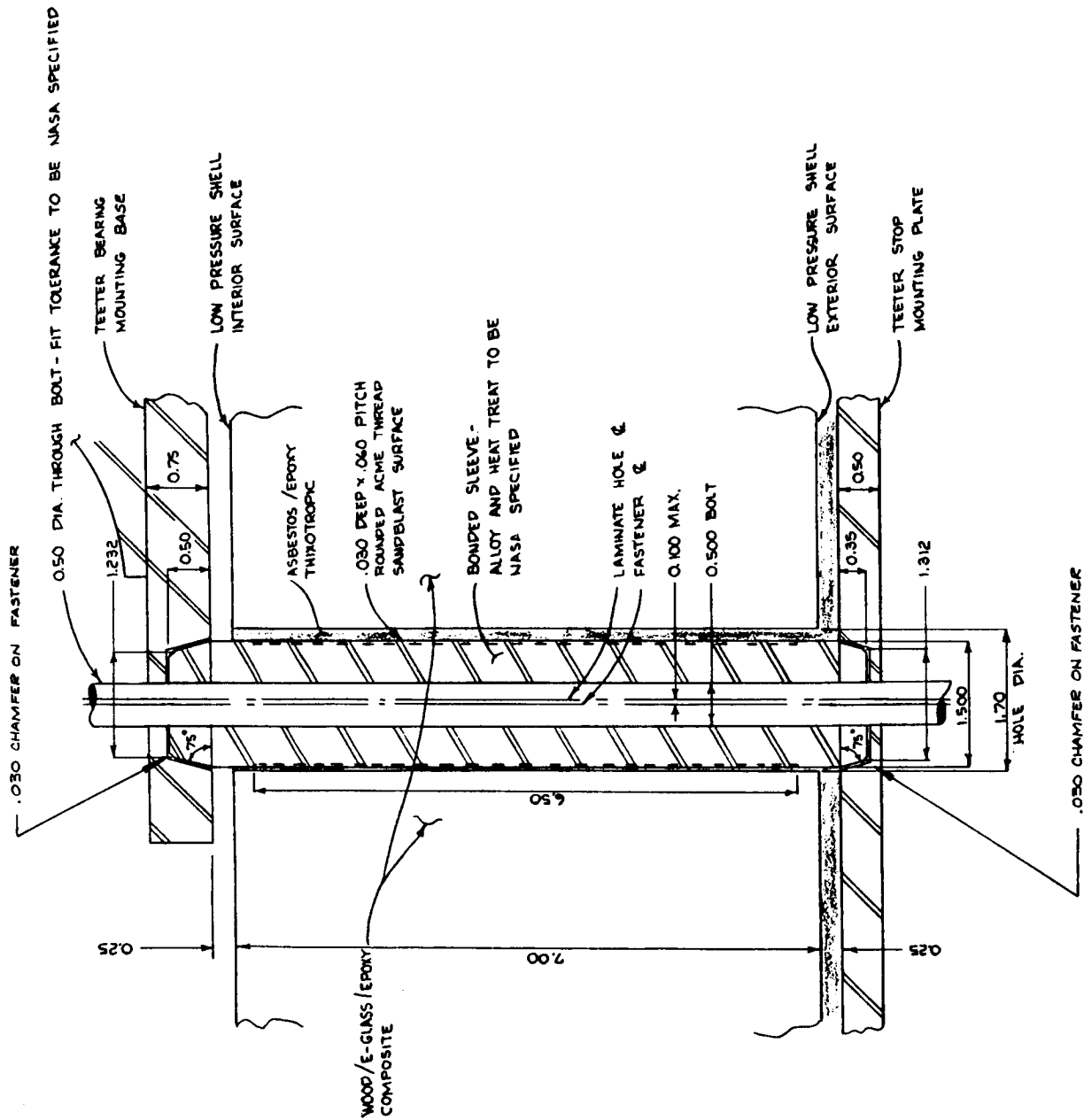


Figure 9. - Rotor to Teeter Hardware Load Take-Off Fastener

ORIGINAL PAGE IS
OF POOR QUALITY

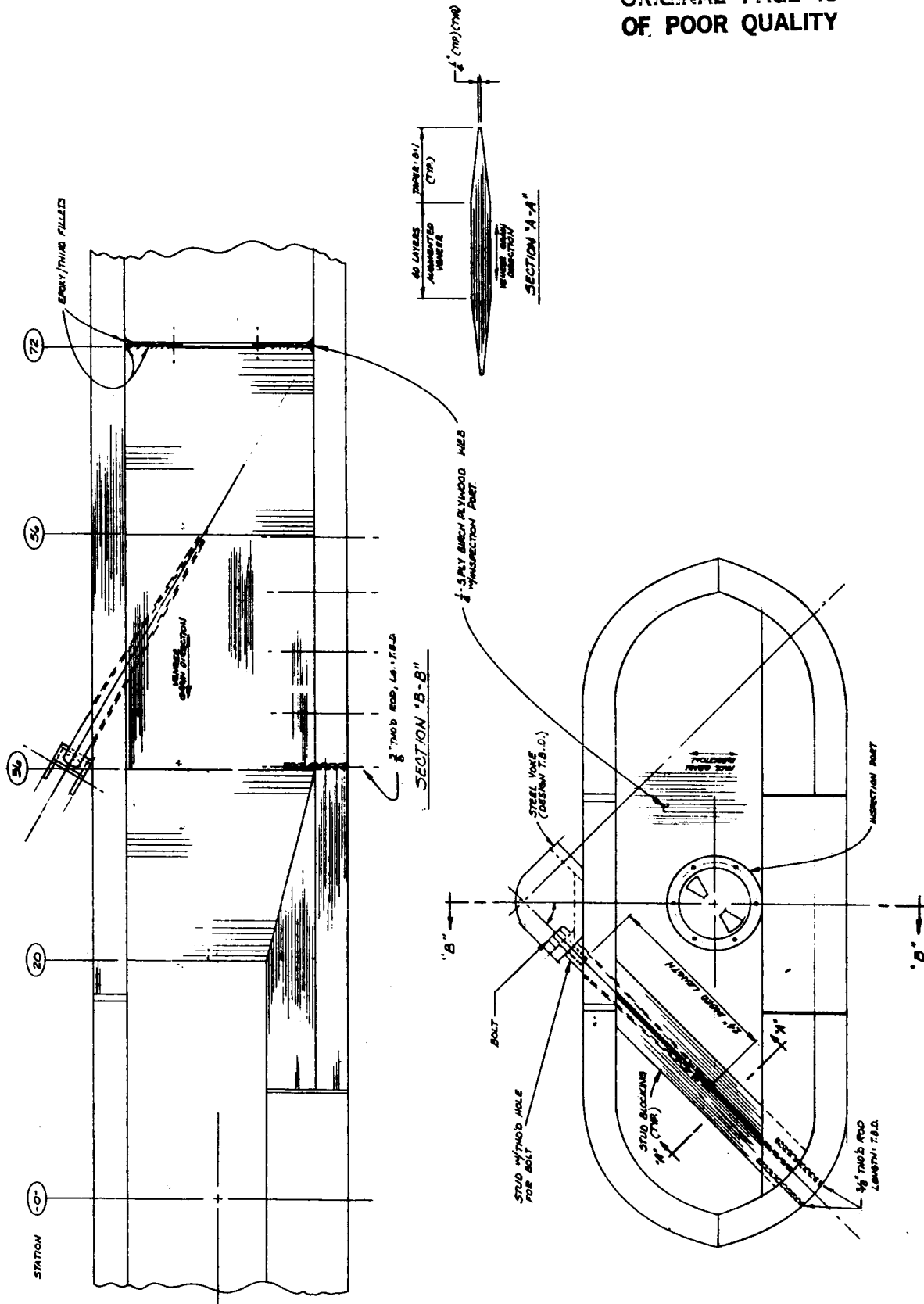


Figure 10.- Load Take-Off for Hydraulic Teeter Dampers

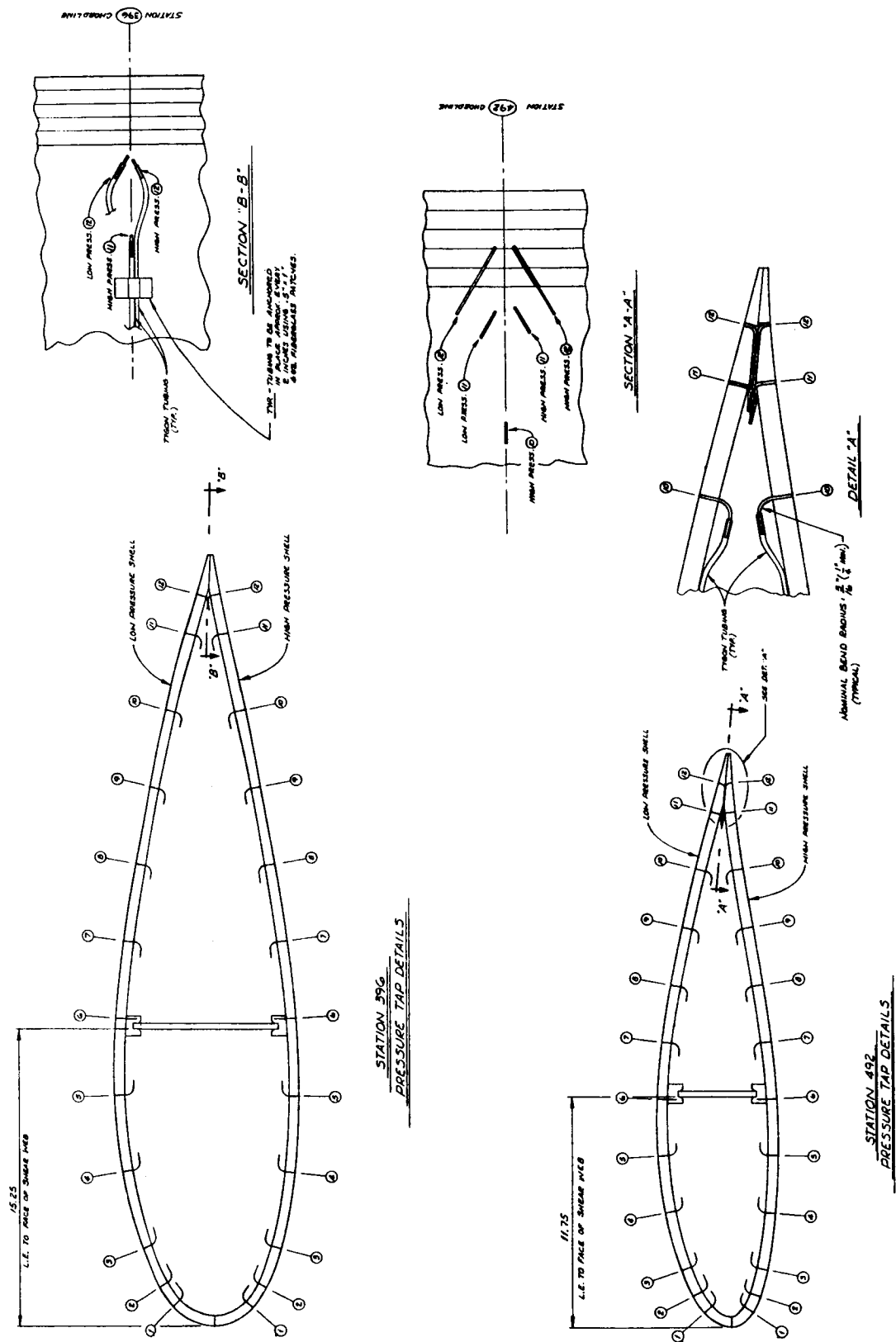


Figure 11.- Pressure Tap Arrangement, Two Typical Sections

ORIGINAL PAGE IS
POOR QUALITY

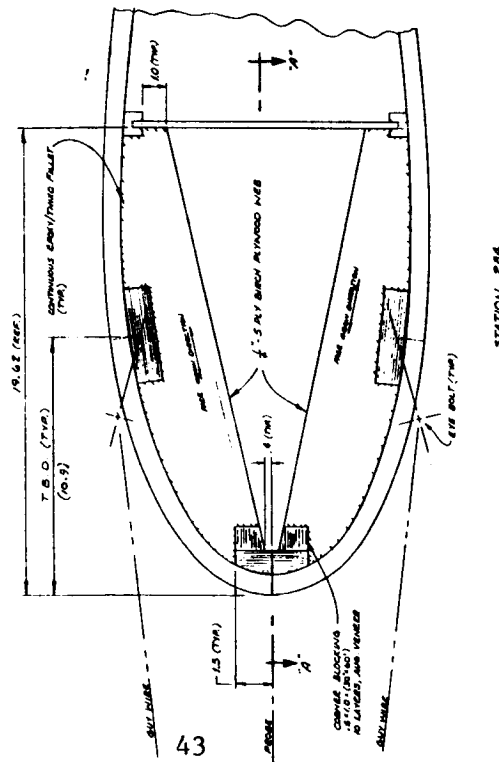
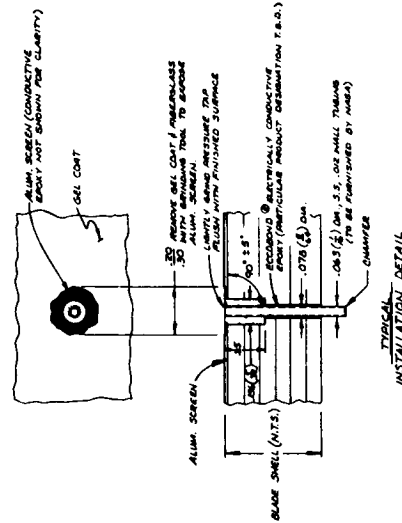
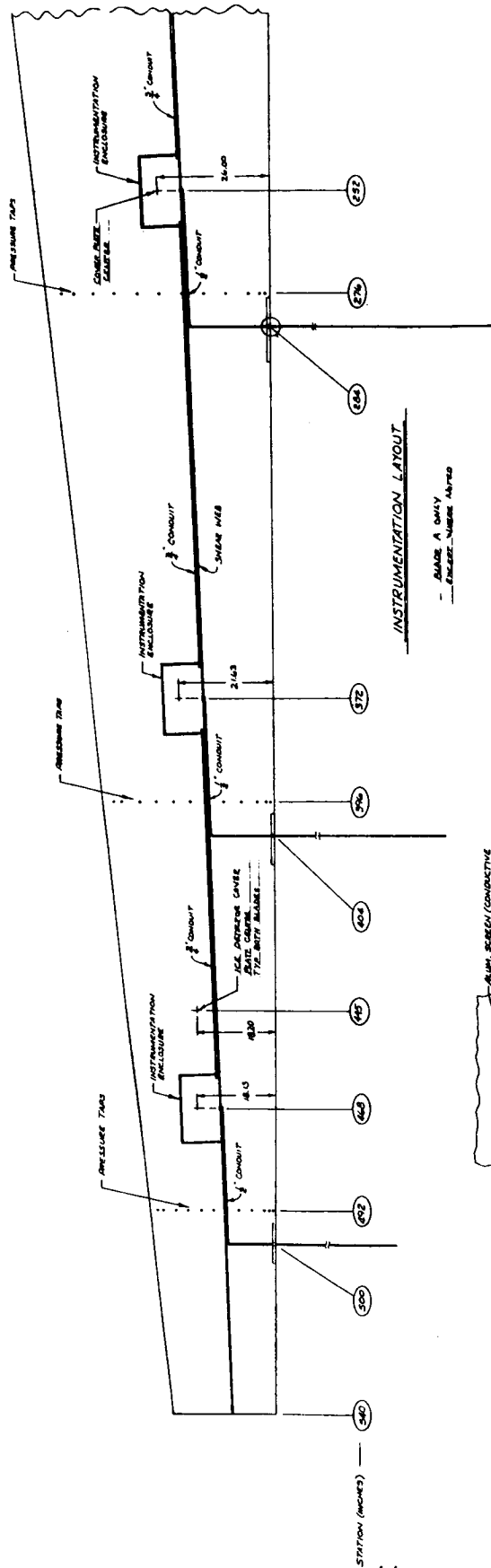


Figure 12.- Angle of Attack Probe Load Take-Off Scheme



PRESSURE TAP LOCATIONS				
WATER AT OR I.E. ALONG CHASE LINE				
STA. 276	STA. 376	STA. 476	STA. 576	STA. 676
276.00	376.00	476.00	576.00	676.00
1) 276.00	376.00	476.00	576.00	676.00
2) 276.00	376.00	476.00	576.00	676.00
3) 276.00	376.00	476.00	576.00	676.00
4) 276.00	376.00	476.00	576.00	676.00
5) 276.00	376.00	476.00	576.00	676.00
6) 276.00	376.00	476.00	576.00	676.00
7) 276.00	376.00	476.00	576.00	676.00
8) 276.00	376.00	476.00	576.00	676.00
9) 276.00	376.00	476.00	576.00	676.00
10) 276.00	376.00	476.00	576.00	676.00
11) 276.00	376.00	476.00	576.00	676.00
12) 276.00	376.00	476.00	576.00	676.00
13) 276.00	376.00	476.00	576.00	676.00
14) 276.00	376.00	476.00	576.00	676.00
15) 276.00	376.00	476.00	576.00	676.00
16) 276.00	376.00	476.00	576.00	676.00
17) 276.00	376.00	476.00	576.00	676.00
18) 276.00	376.00	476.00	576.00	676.00
19) 276.00	376.00	476.00	576.00	676.00
20) 276.00	376.00	476.00	576.00	676.00

DETAIL "A" - PRESSURE TAPS

Figure 13.- General Instrumentation Arrangement Planform View

ORIGINAL PAGE IS
OF POOR QUALITY

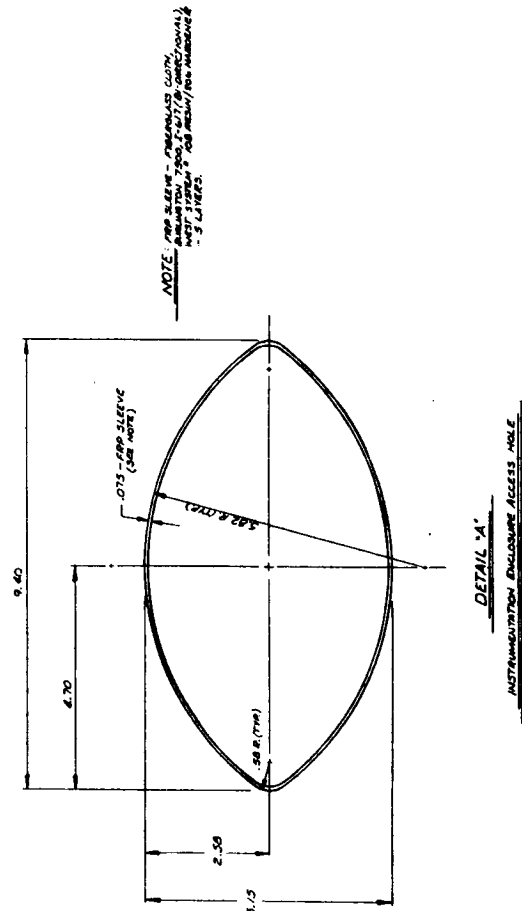
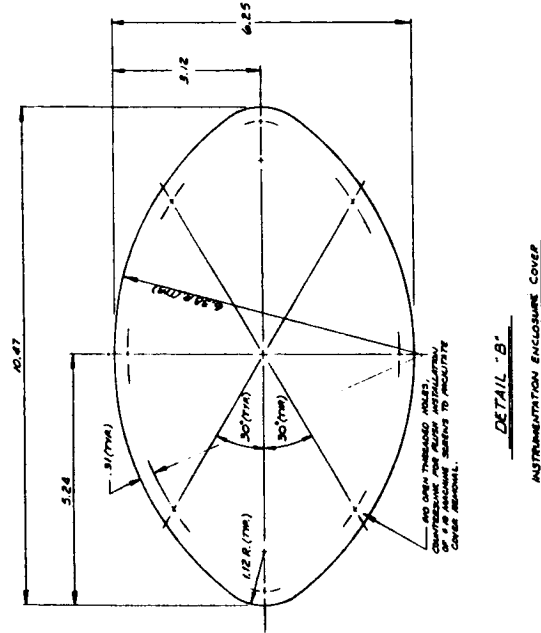
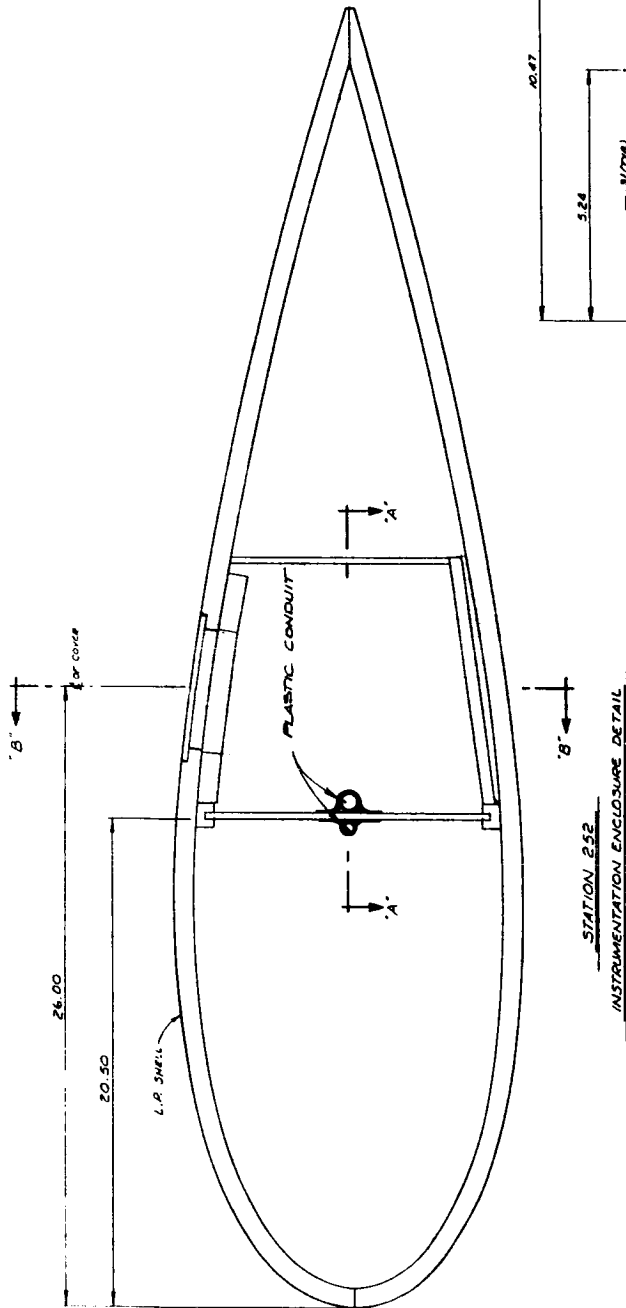


Figure 14. - Instrumentation Enclosure and Typical Cover Detail

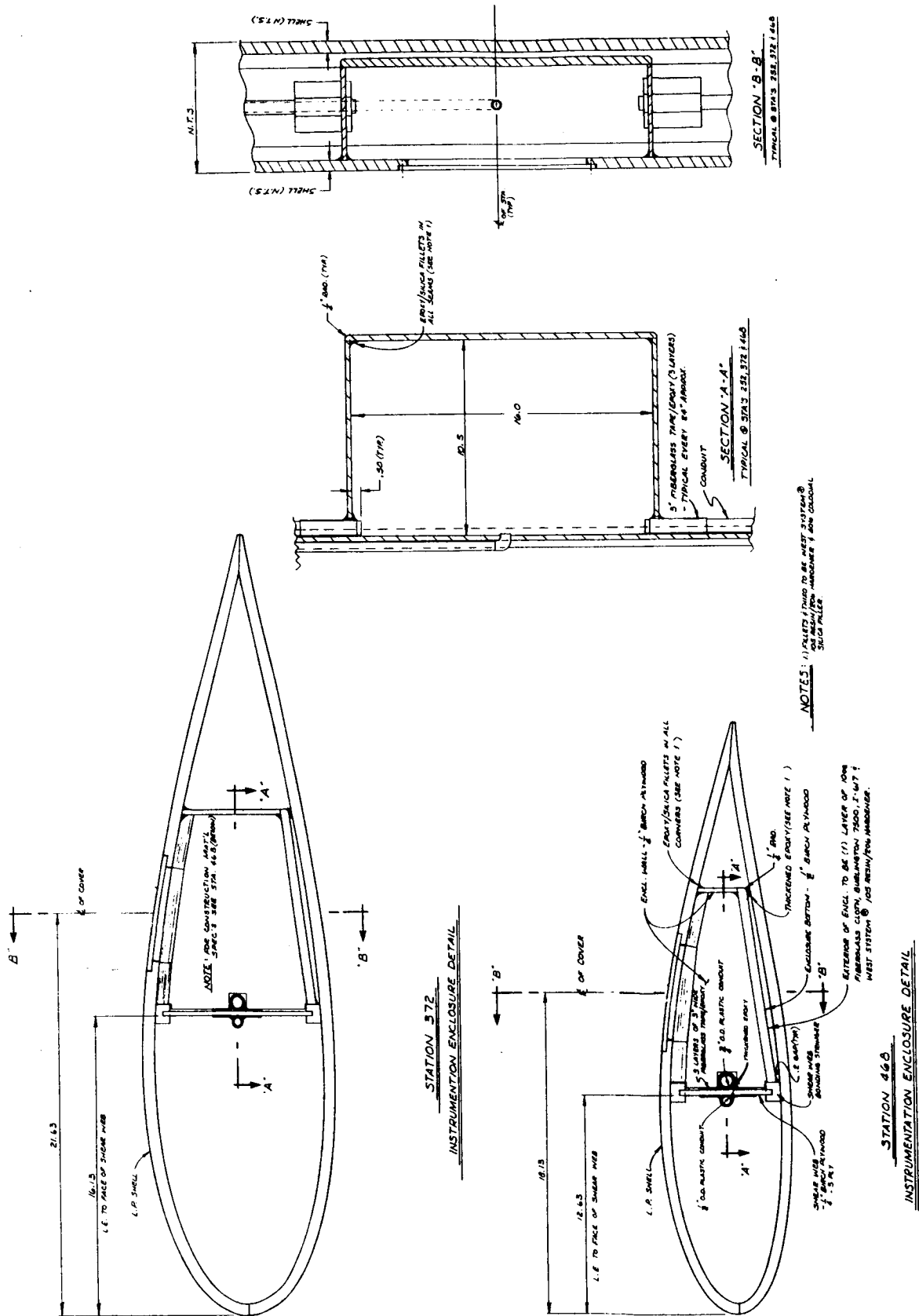


Figure 15.- Instrumentation Enclosures and Construction Detail

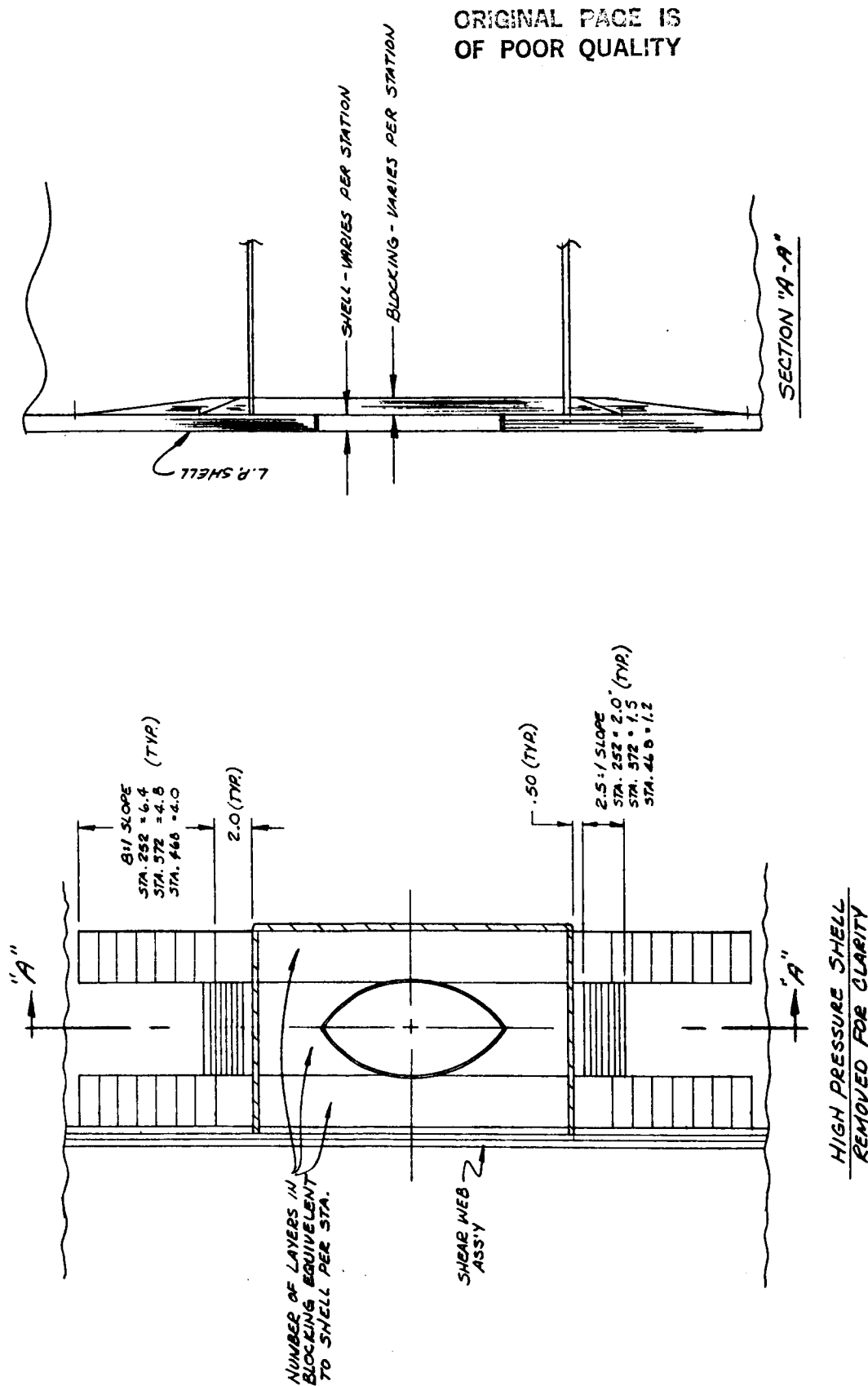


Figure 16.- Instrumentation Enclosure - Structural Details

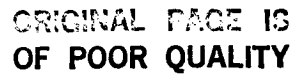
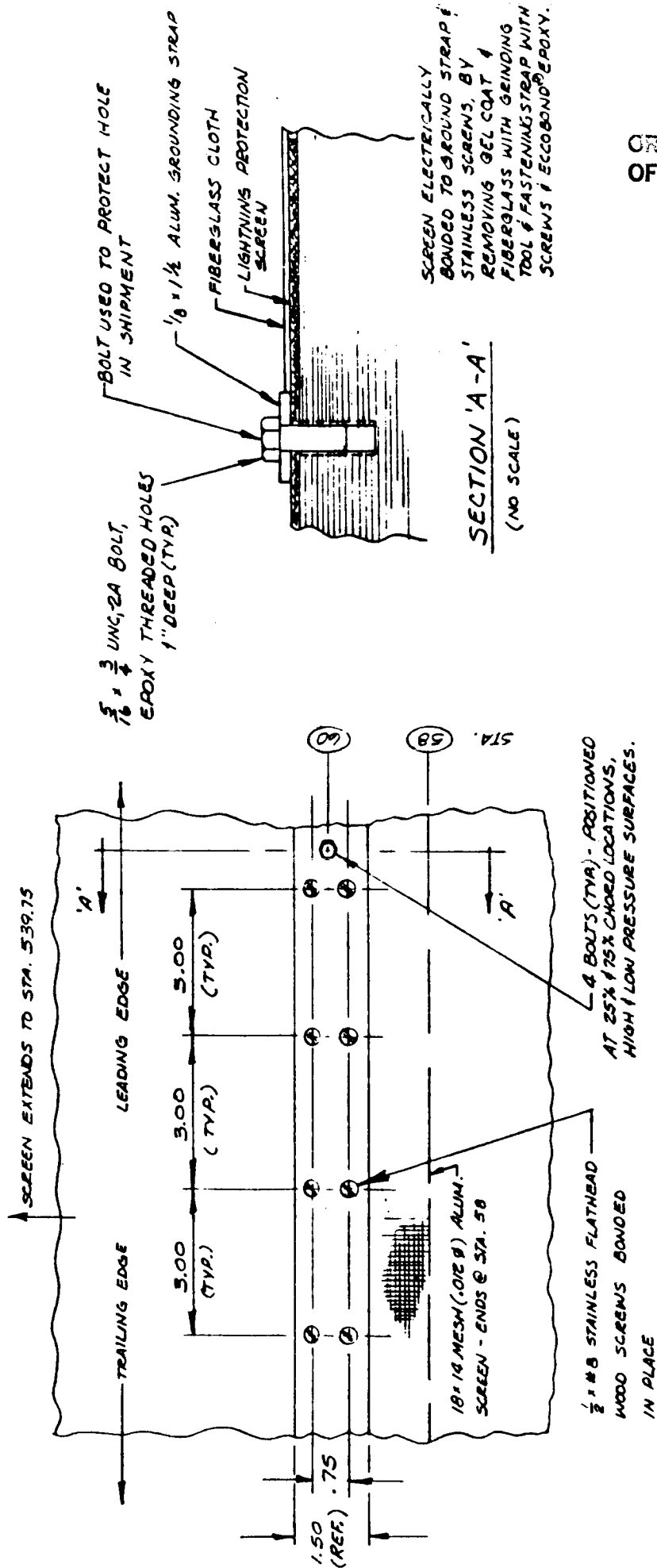


Figure 17.- Tip Weight, Tip Venting and Ice Detection Provisions

TIP VENT / TIP WEIGHT BLOCKING DETAILS



ORIGINAL FACE IS
OF POOR QUALITY

Figure 18.- Ground Strap Lightning Protection Details

ORIGINAL PAGE IS
OF POOR QUALITY

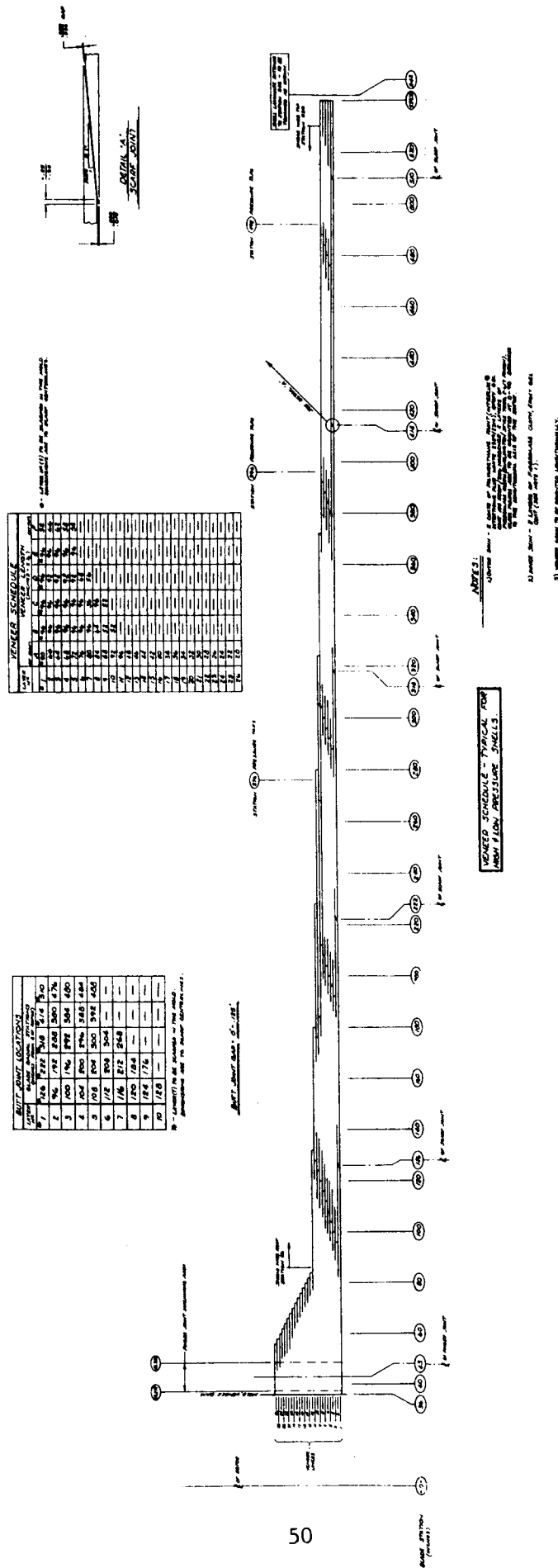


Figure 19. - Outer Rotor Veneer Schedule

ORIGINAL FACE IS
OF POOR QUALITY

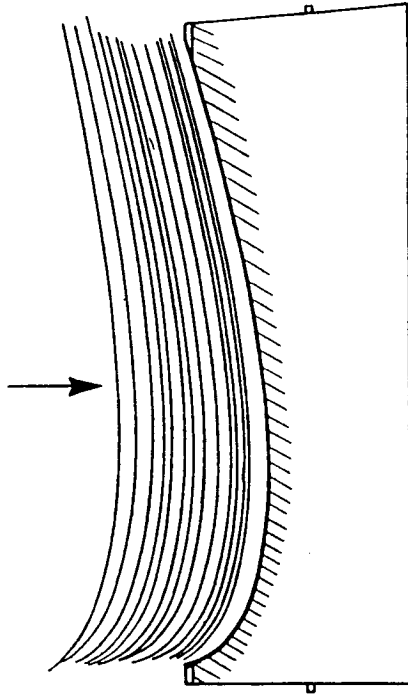


Figure 21. - Epoxy Coated Veneers Placed In Mold

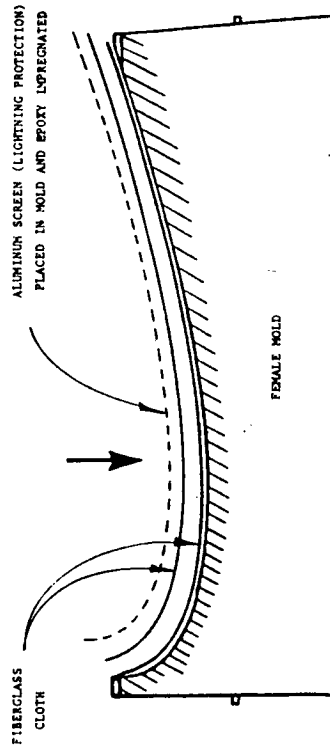


Figure 20. - Epoxy Gelcoat And 2 Layers 10 Oz. Fiberglass Cloth Placed In Mold And Wet Out

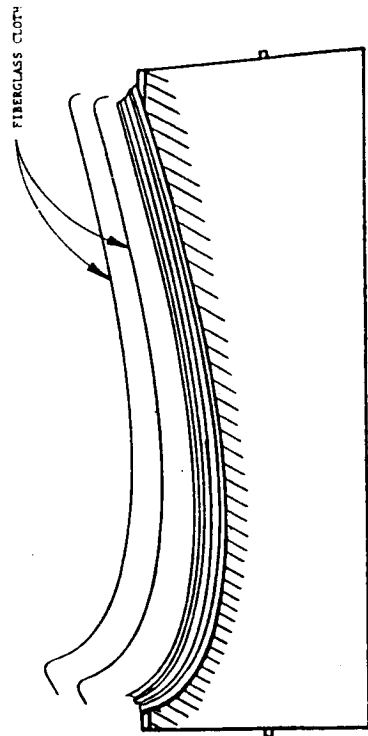


Figure 22. - 2 Layers 10 oz Fiberglass Cloth Placed On Veneer Then Vacuum Bag Is Sealed And Vacuum Applied During Cure

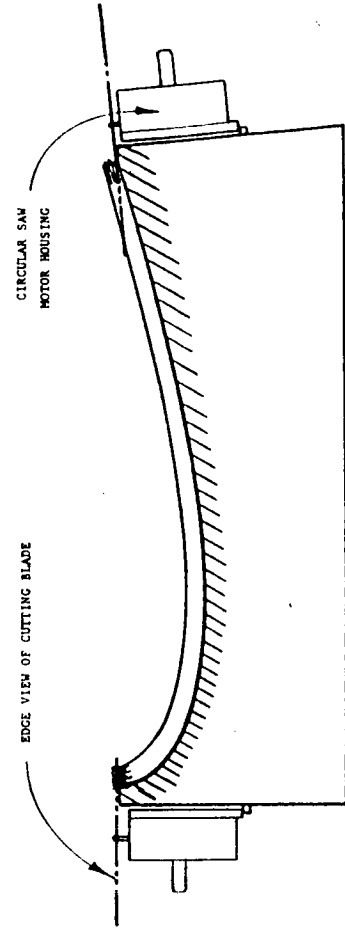


Figure 23. - Circular Saw Trim Half Shell

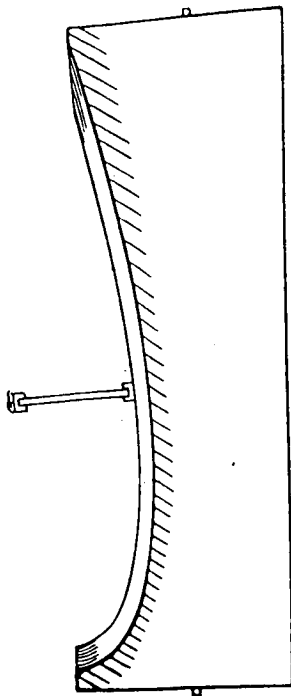


Figure 24. - Bonding of Shear Web To Lower Half Shell Placement Is Checked

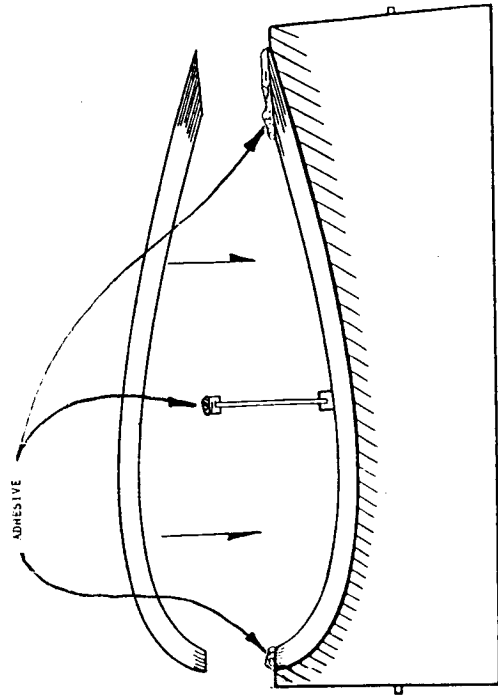


Figure 25. - Bonding of Two Half Shells

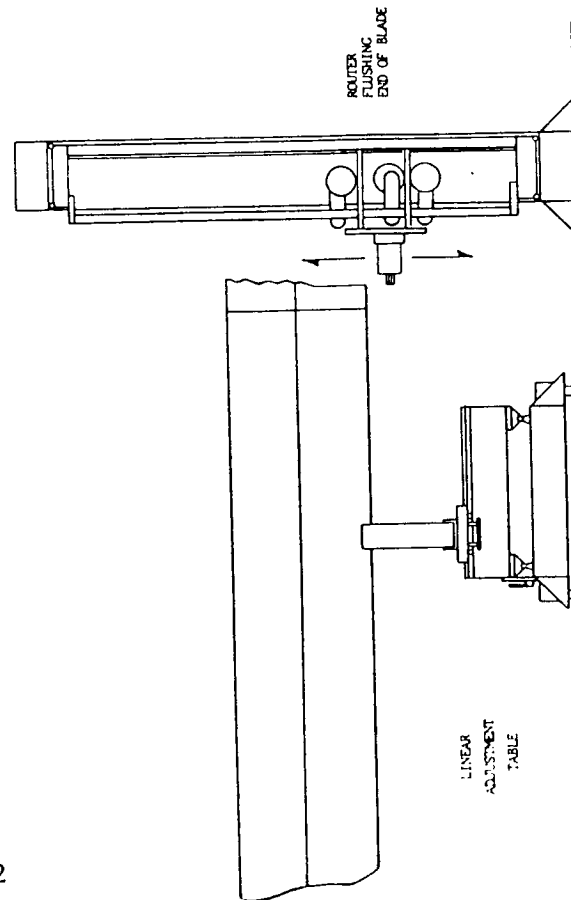


Figure 26 .- Blade Positioned and Trued To Finger Joint Machine (Production Configuration)

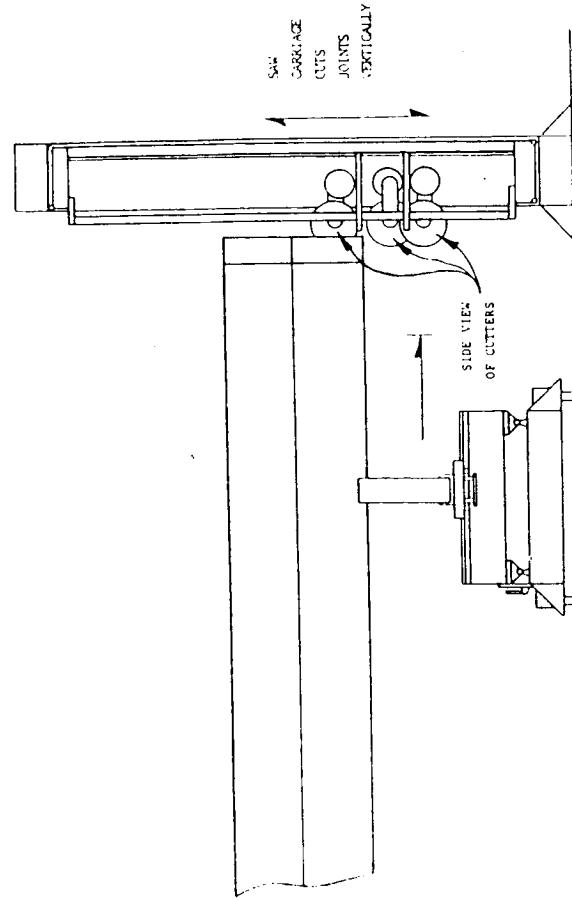


Figure 27. - Blade Indexed Into Finger Joint Machine (Production Configuration)



2 LAYERS 10 OZ. FIBERGLASS CLOTH

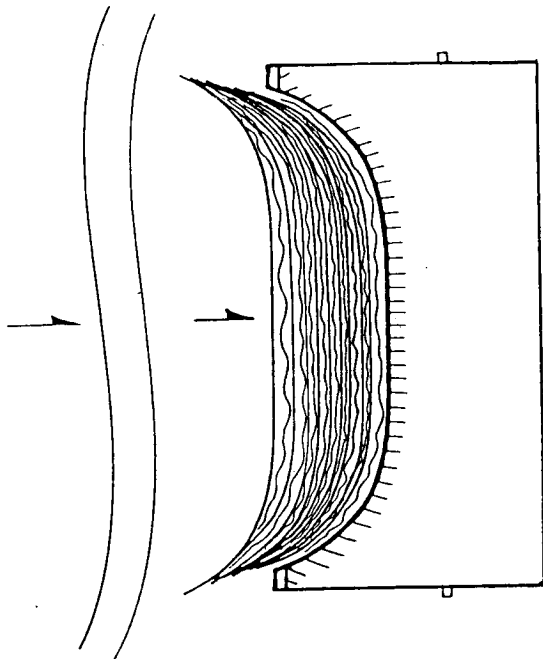


Figure 29. — Epoxy Gelcoat And Wet Out Fiberglass Cloth Placed in Mold

2 LAYERS 10 OZ. FIBERGLASS CLOTH

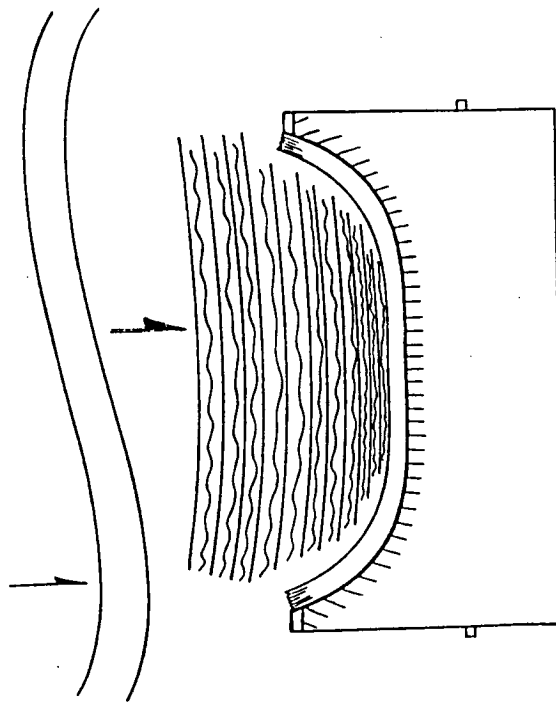


Figure 30 . - Veneers And Augmenting Glass Placed in Mold For First Vacuum Bagging Sequence With Two Layers 10 oz. Fiberglass Cloth

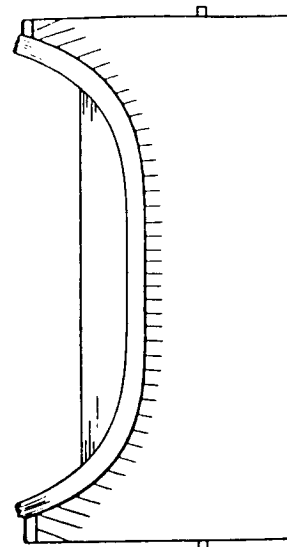


Figure 31 . - Veneer And Augmenting Glass Buildup For Teeeter Bearing

Figure 32 . - Vacuum Molding Completed (Low Pressure Shell Shown)

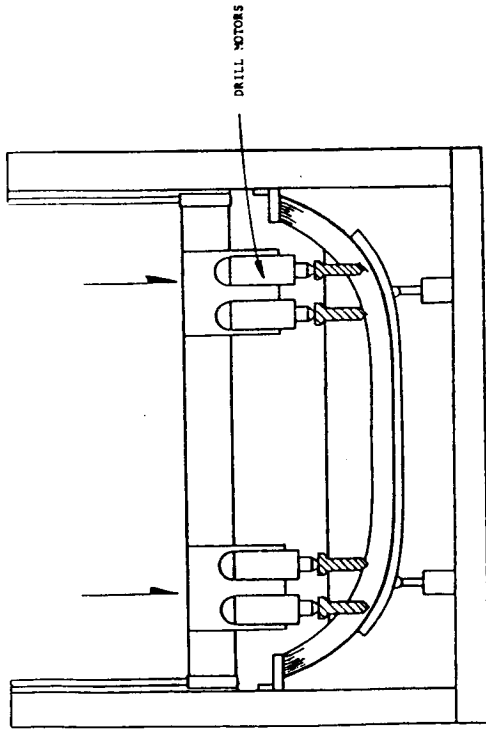


Figure 33. - Holes For Studs Drilled By Multiple Drill Jig (Production Configuration)

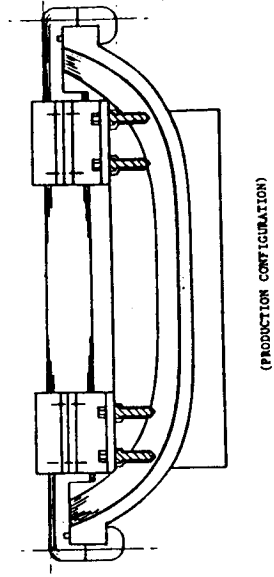


Figure 34. - Pillow Blocks And Studs Bonded To Hub Half-Shell

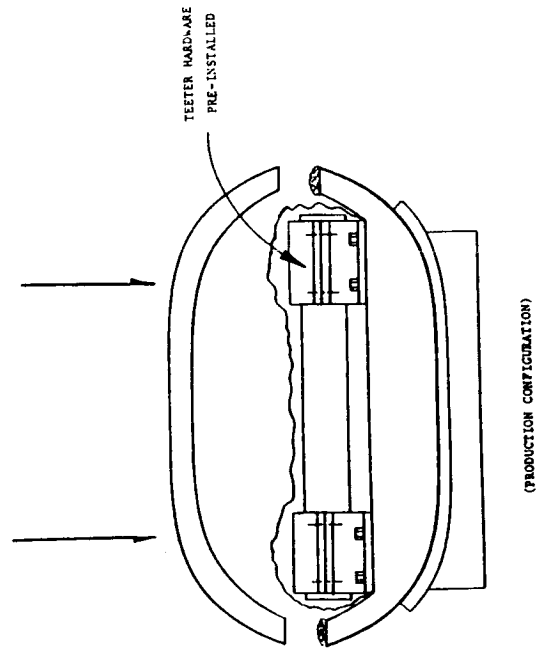


Figure 35 . - Hub Half-Shell Pieces Bonded Together

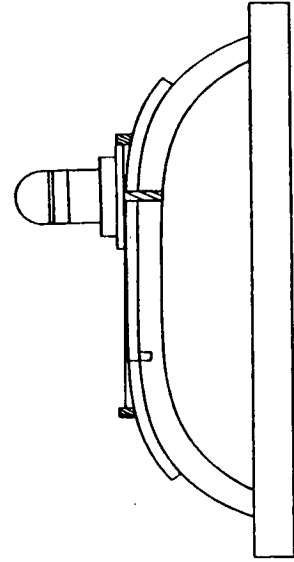


Figure 36. - Router Runs Against Fence And Cuts Hole For Rotor Shaft

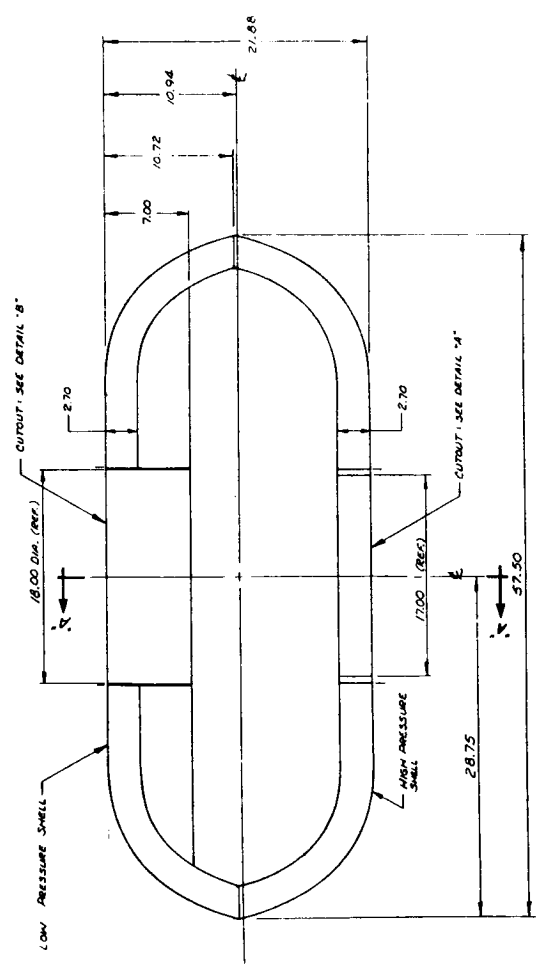
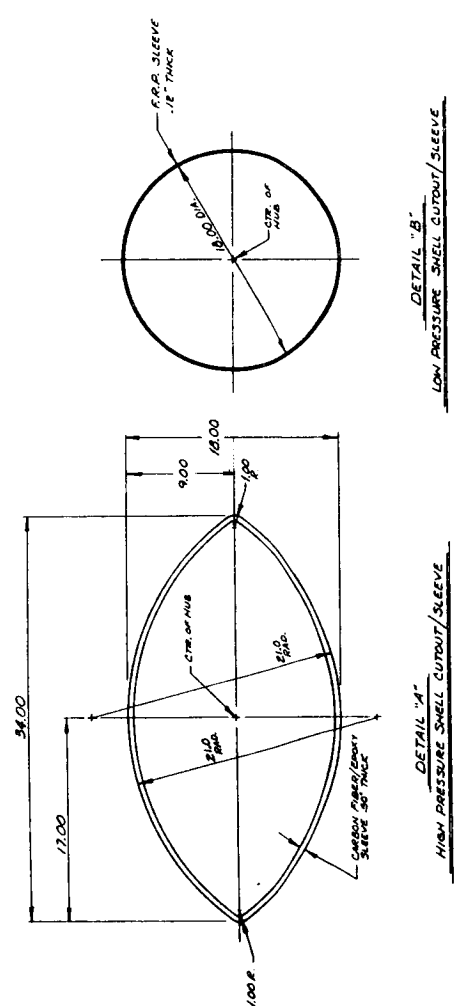
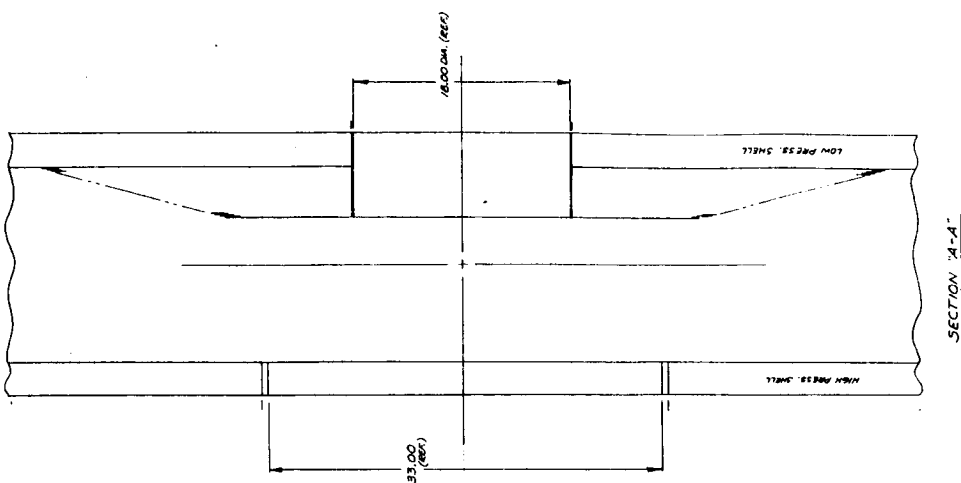


Figure 37. - Inner Rotor (Hub) Structural Detail

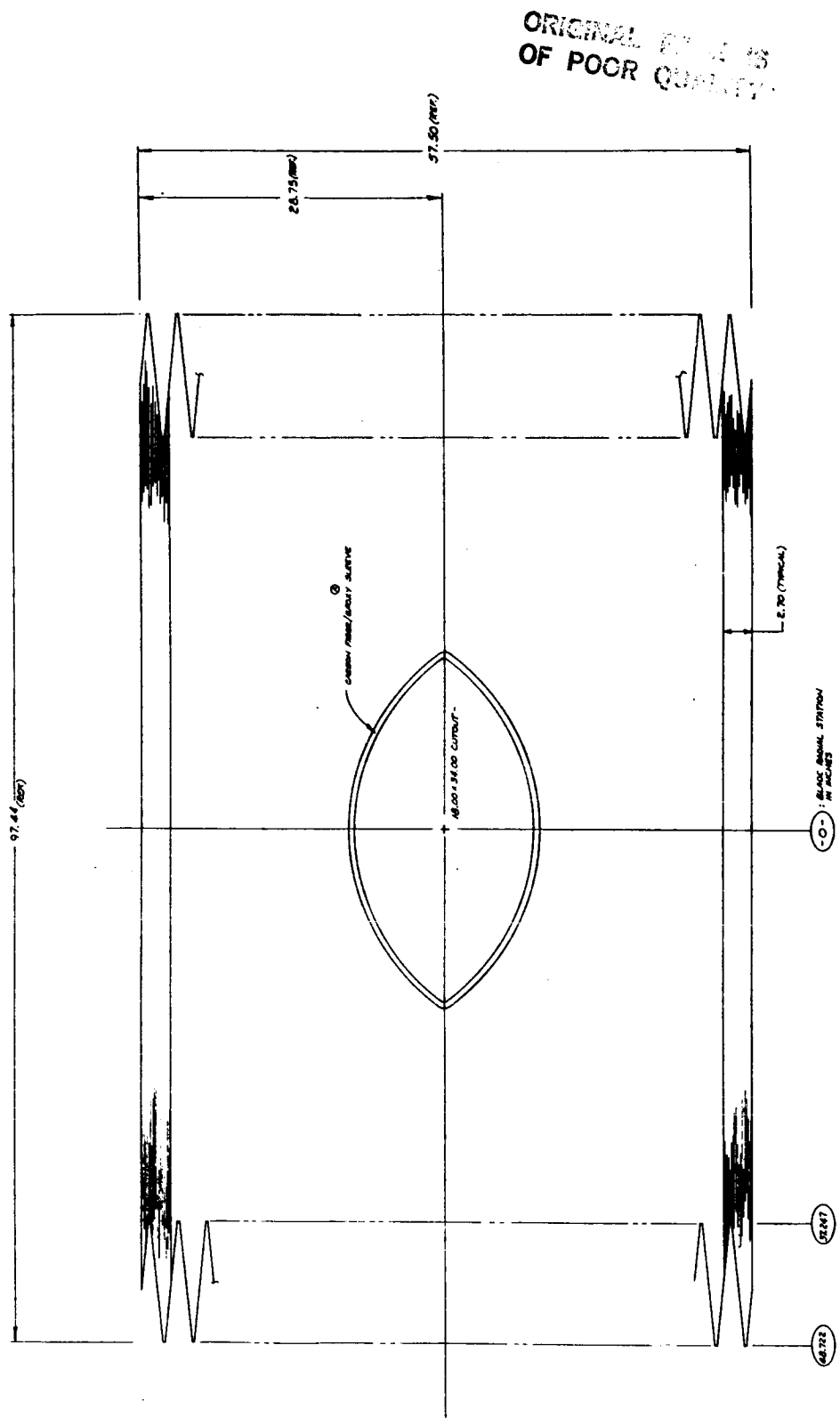
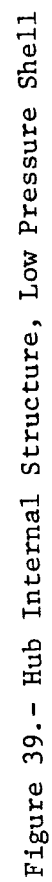
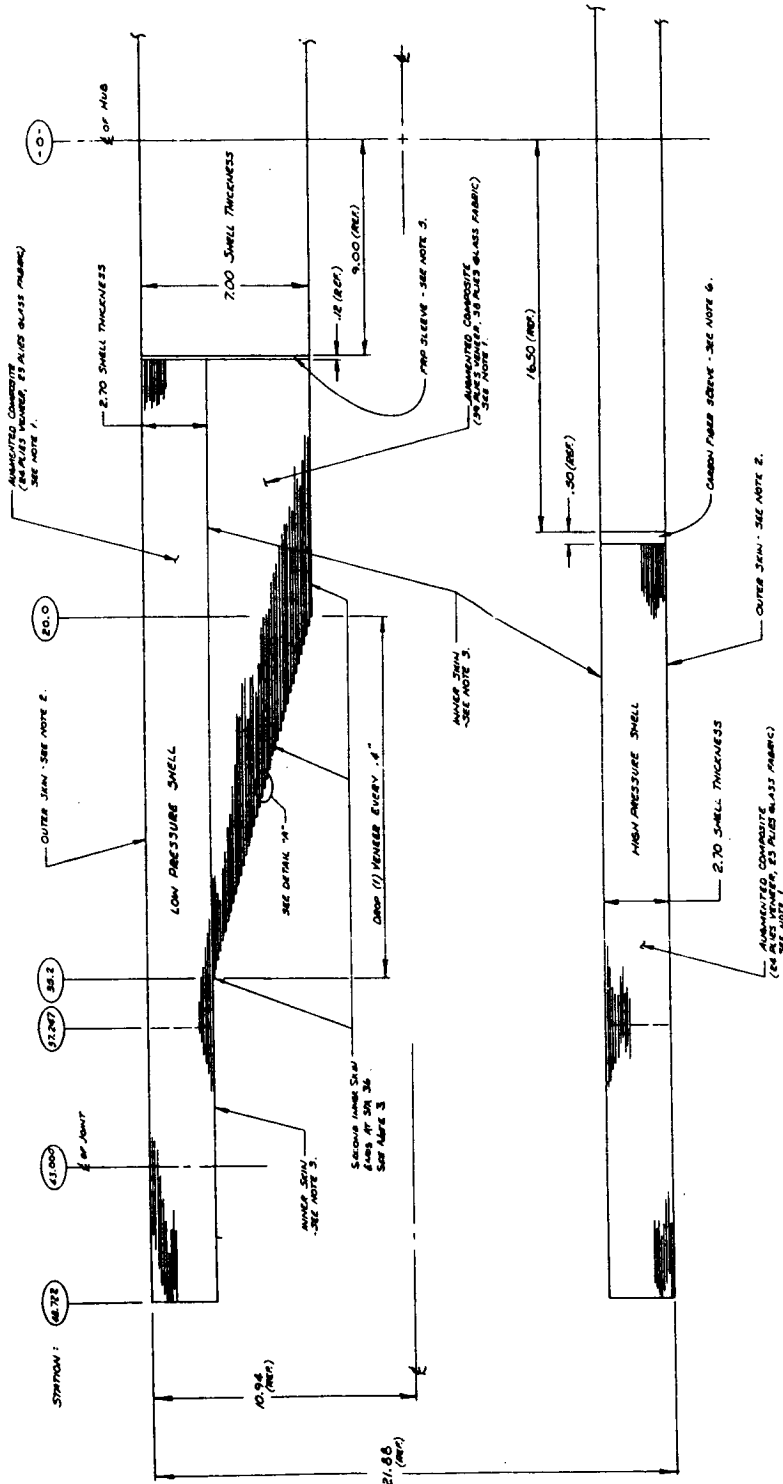


Figure 38.- Hub Internal Structure, High Pressure Shell





- NOTES:**
- 1) UNBLENDED COMPOSITE - ALTERNATING RAILS OF 10" GLASS CLOTH (BLENDED WITH 20% CARBON FIBER) AND 10" CARBON FIBER (BLENDED WITH 20% GLASS CLOTH) SHALL BE USED TO CONSTITUTE THE COMPOSITIONAL RAILS OF THE RAILS.
 - 2) OUTER JEWEL - 2 COATS OF POLYURETHANE ADHESIVE (NOT VENEER) SHALL BE APPLIED TO THE OUTER JEWEL. THE OUTER JEWEL SHALL BE 10" WIDE AND 10" HIGH. THE OUTER JEWEL SHALL BE 10" WIDE AND 10" HIGH. THE OUTER JEWEL SHALL BE 10" WIDE AND 10" HIGH.
 - 3) INNER JEWEL - 2 COATS OF POLYURETHANE ADHESIVE (NOT VENEER) SHALL BE APPLIED TO THE INNER JEWEL. THE INNER JEWEL SHALL BE 10" WIDE AND 10" HIGH. THE INNER JEWEL SHALL BE 10" WIDE AND 10" HIGH.
 - 4) VENEER BEHIND THE COMPOSITE - CONDITIONALLY.
 - 5) CARBON FIBER SLEEVE - 10" WIDE AND 10" HIGH. THE CARBON FIBER SLEEVE SHALL BE 10" WIDE AND 10" HIGH. THE CARBON FIBER SLEEVE SHALL BE 10" WIDE AND 10" HIGH.
 - 6) CARBON FIBER SLEEVE - 10" WIDE AND 10" HIGH. THE CARBON FIBER SLEEVE SHALL BE 10" WIDE AND 10" HIGH. THE CARBON FIBER SLEEVE SHALL BE 10" WIDE AND 10" HIGH.

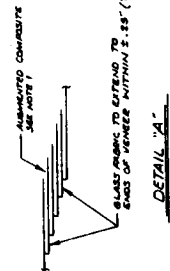


Figure 40. - Hub Veneer Schedule

ORIGINAL DESIGN
OF POOR QUALITY.

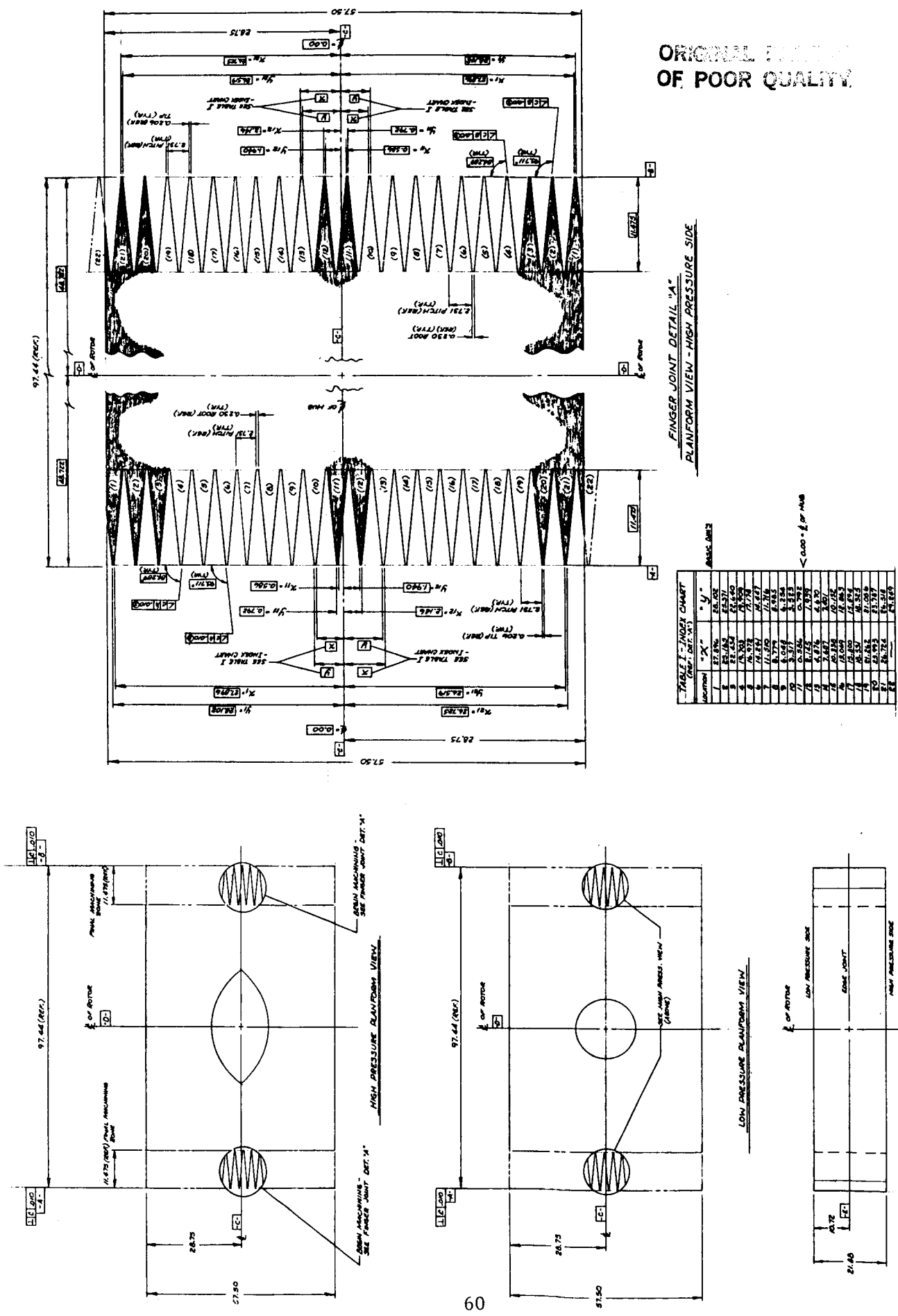


Figure 41.- Hub Splice Machining Details

ORIGINAL SET
OF POOR QUALITY

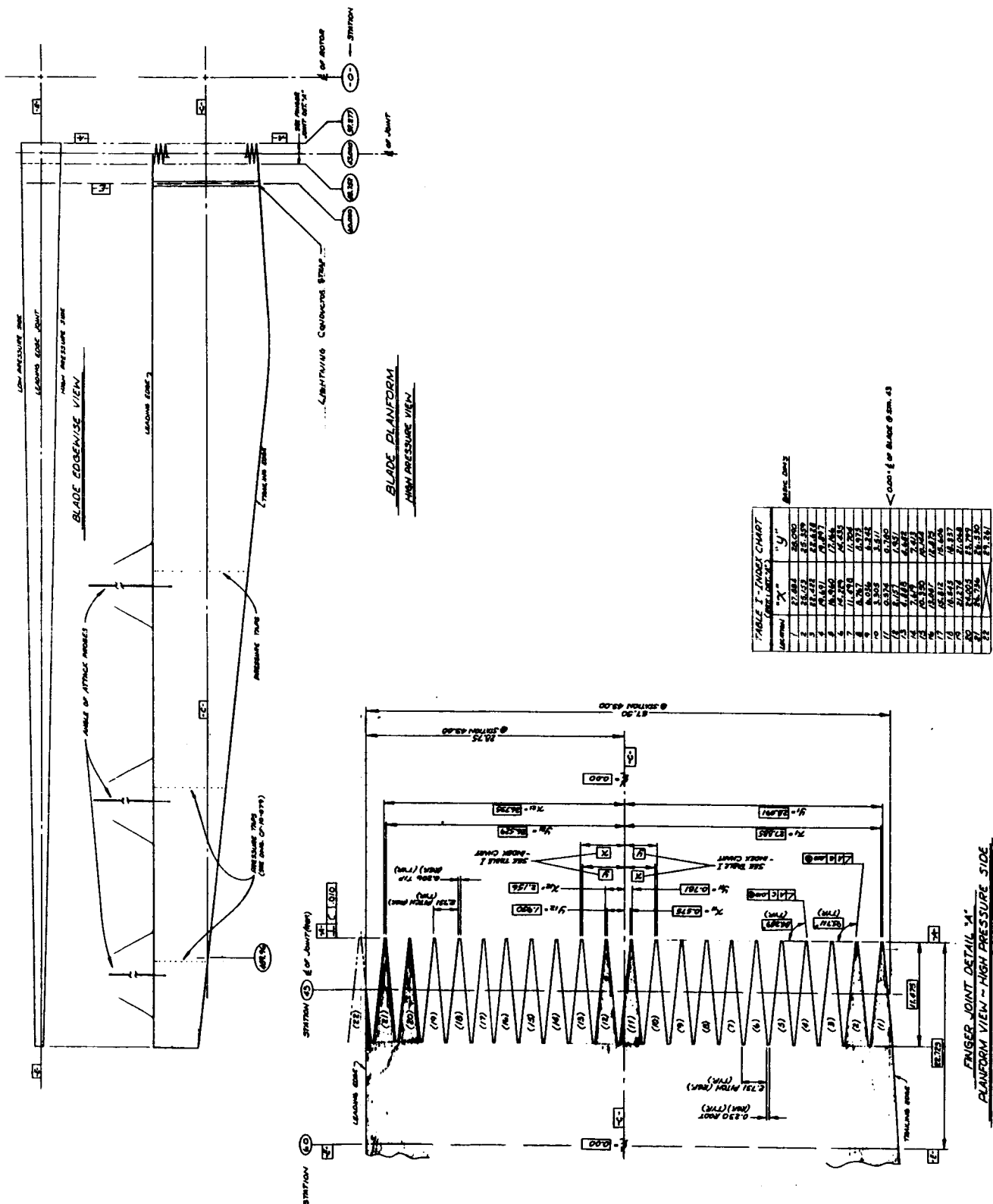
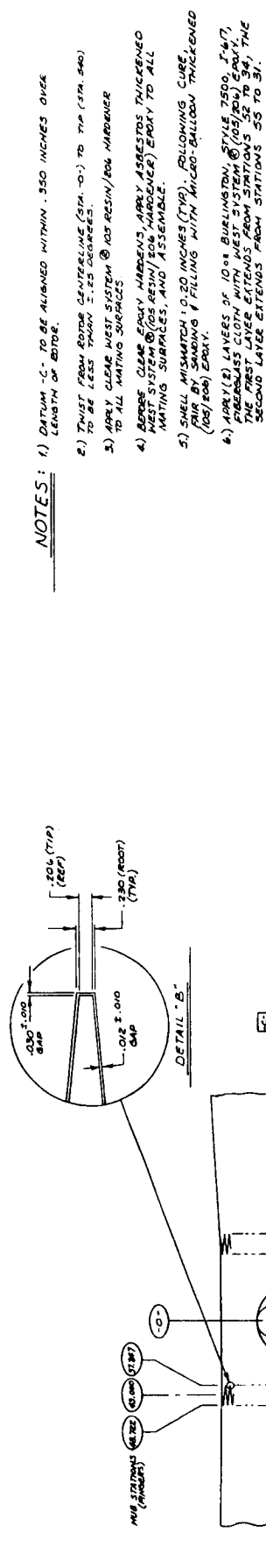


Figure 42. - Outer Rotor Planform View and Splice Joint Machining Details



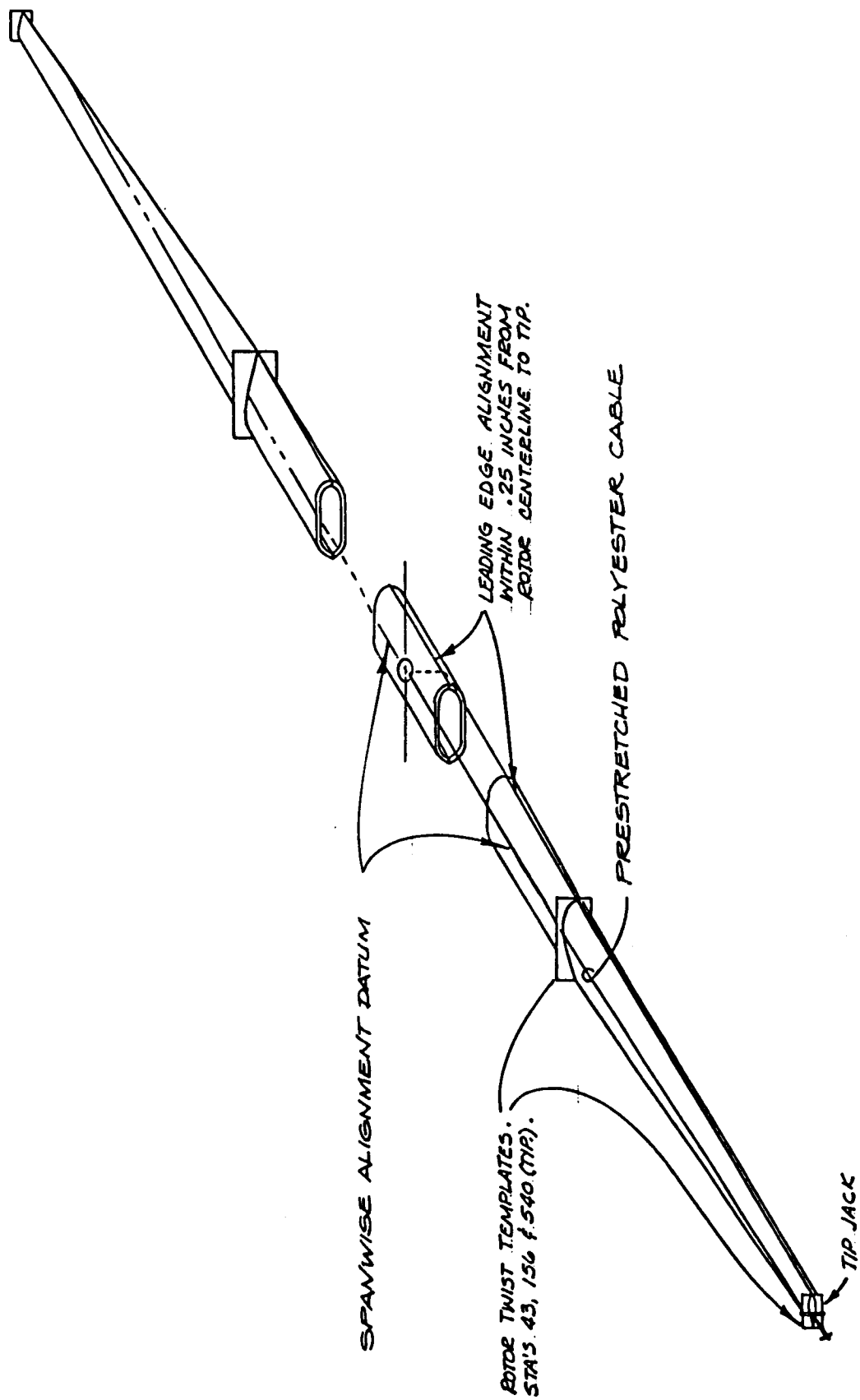


Figure 44.- Rotor Assembly Alignment and Clamping Schematic

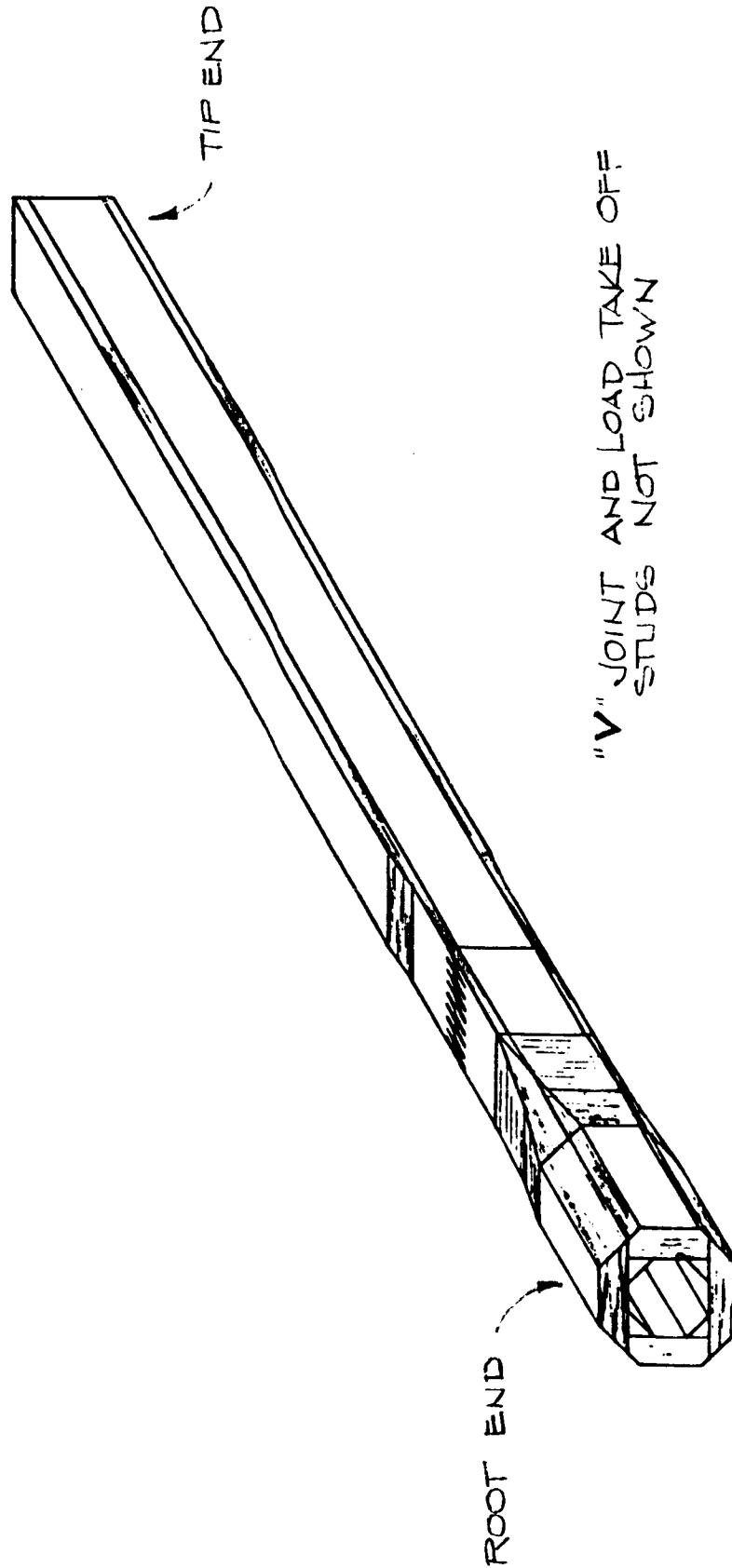


Figure 46.- Cantilevered Splice Joint Test Article, Auxiliary View

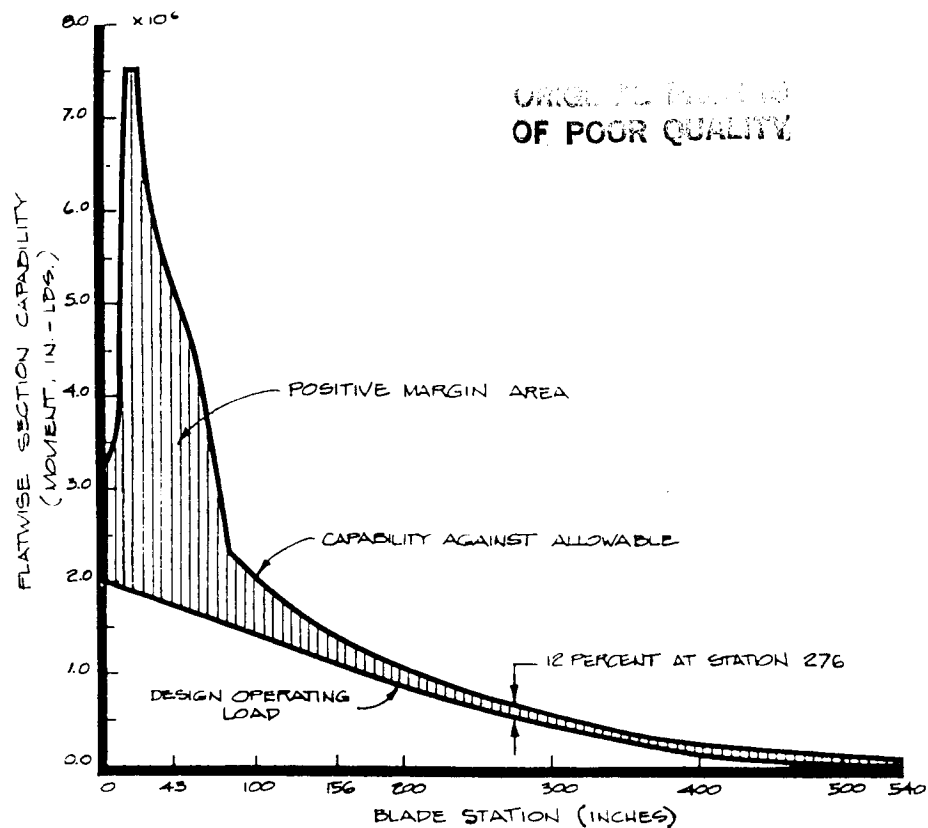


Figure 47.—Design Operating Load Capability vs. Blade Station 175 kW Output - 25 MPH Windspeed

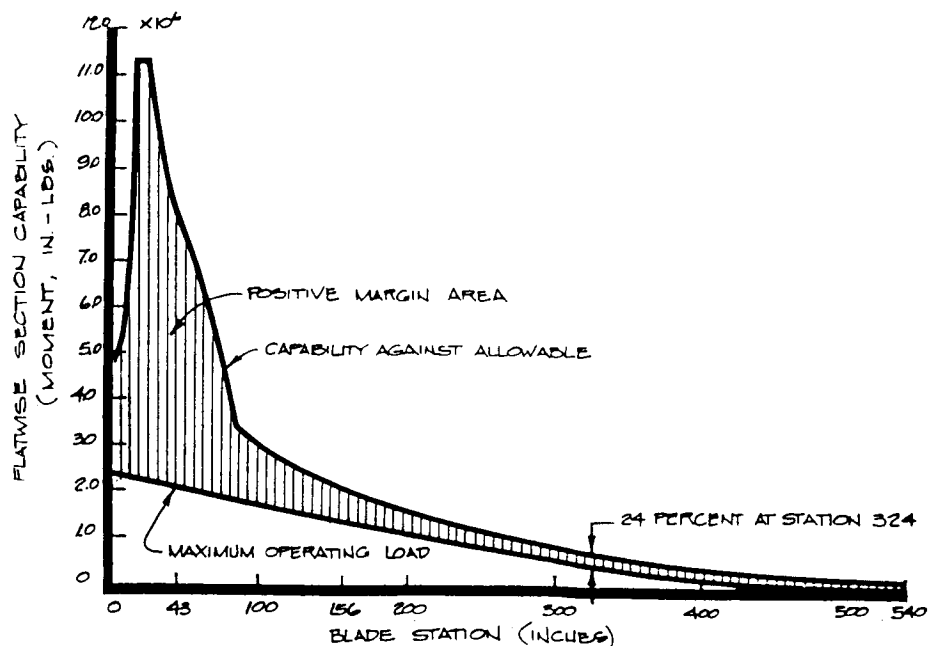


Figure 48.—Maximum Operating Load Capability vs Blade Station 400 kW Output - 33 MPH Windspeed - Variable PSI Allowable

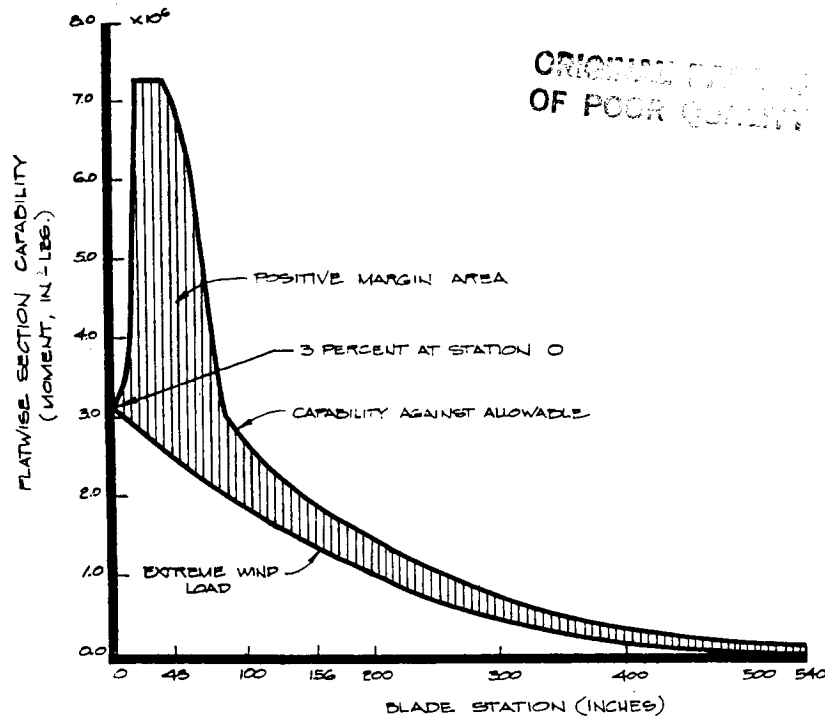


Figure 49.—Extreme Wind Load Capability vs. Blade Station
70.1#/Ft² Airload (50.1#/Ft² x 1.4 Instantaneous Peak
Dynamics Multiplier)

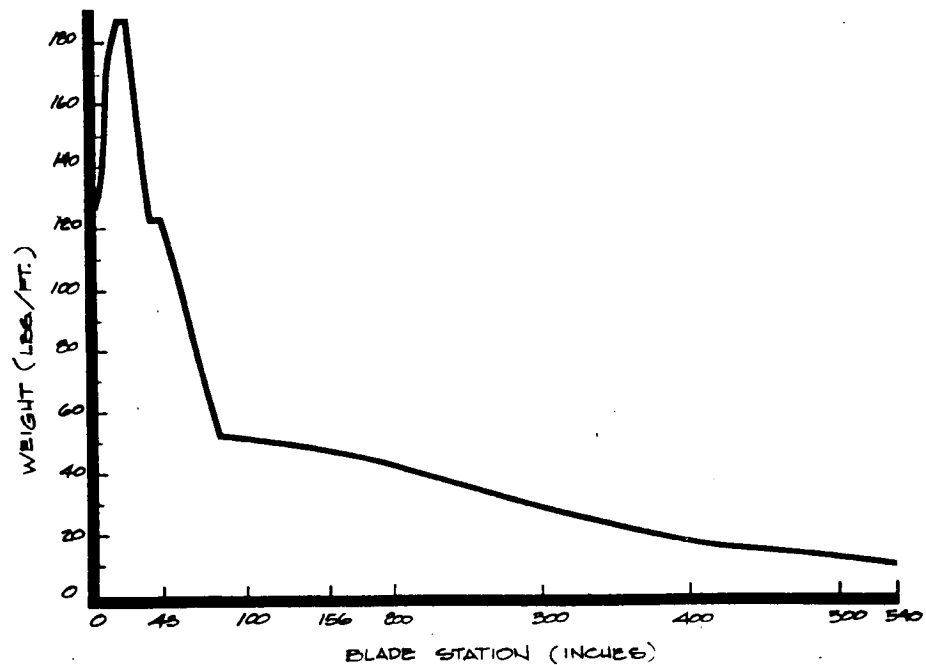


Figure 52.—Weight vs. Blade Station
(Without Instrumentation)

OF POOR QUALITY

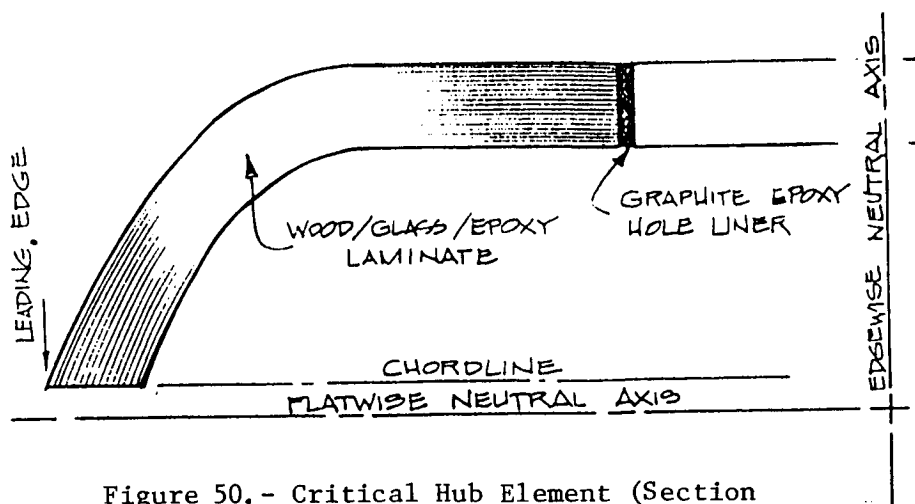


Figure 50.- Critical Hub Element (Section View) at Rotor Centerline. (Note that only one-half of High Pressure Shell Is Shown)

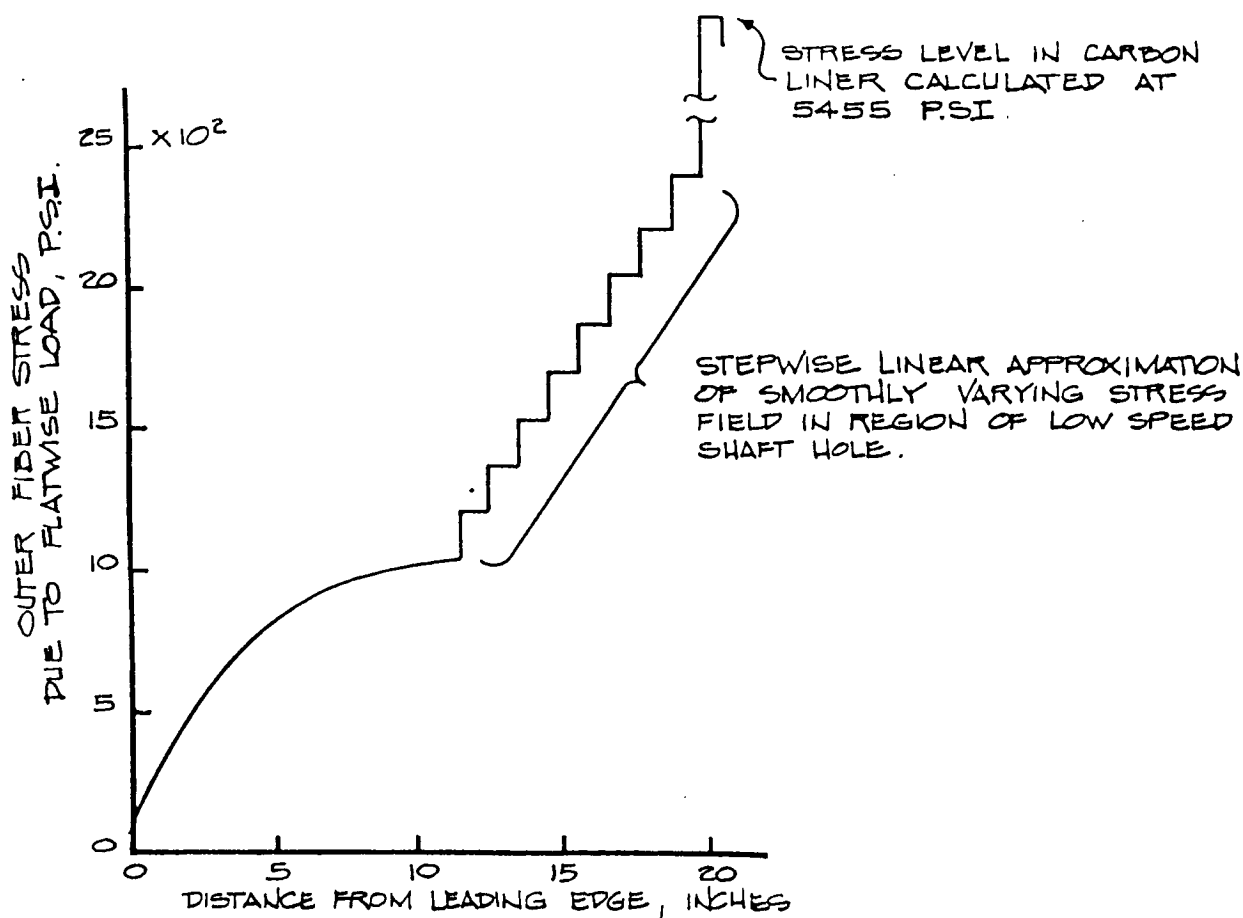


Figure 51.- Calculated Distribution of Outer Fiber Stress for Element Shown in Figure 50.

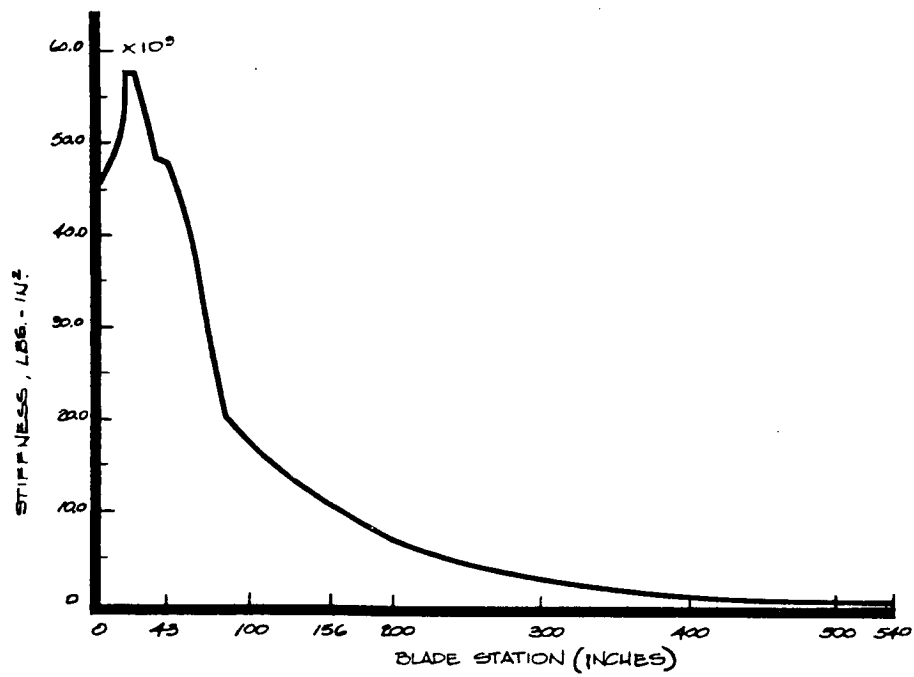


Figure 53.—Flatwise EI vs. Blade Station

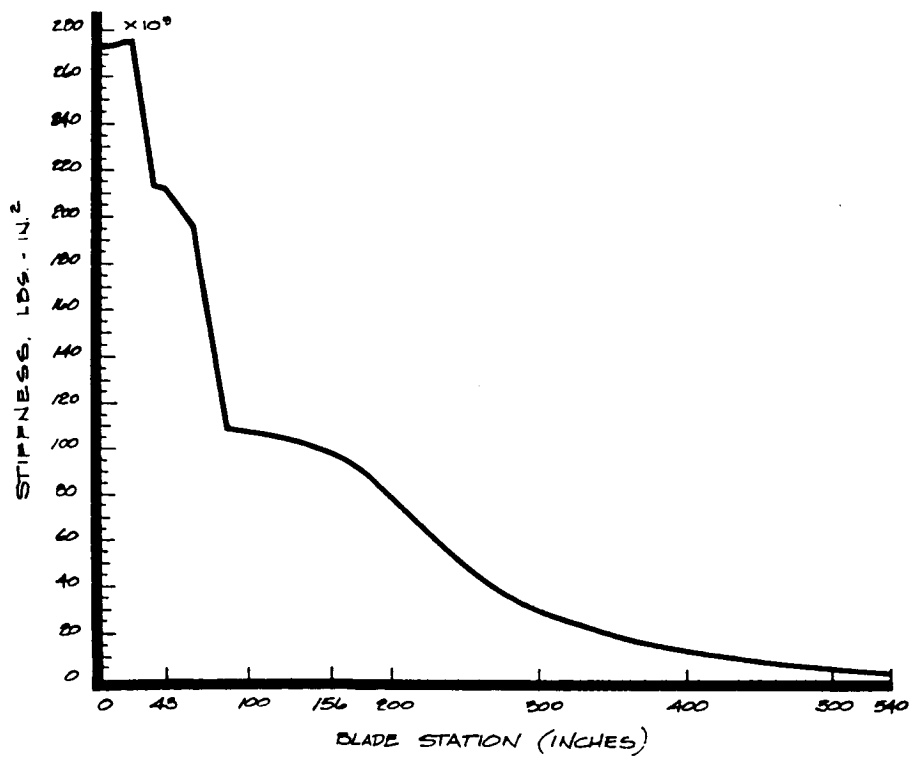


Figure 54.—Edgewise EI vs. Blade Station

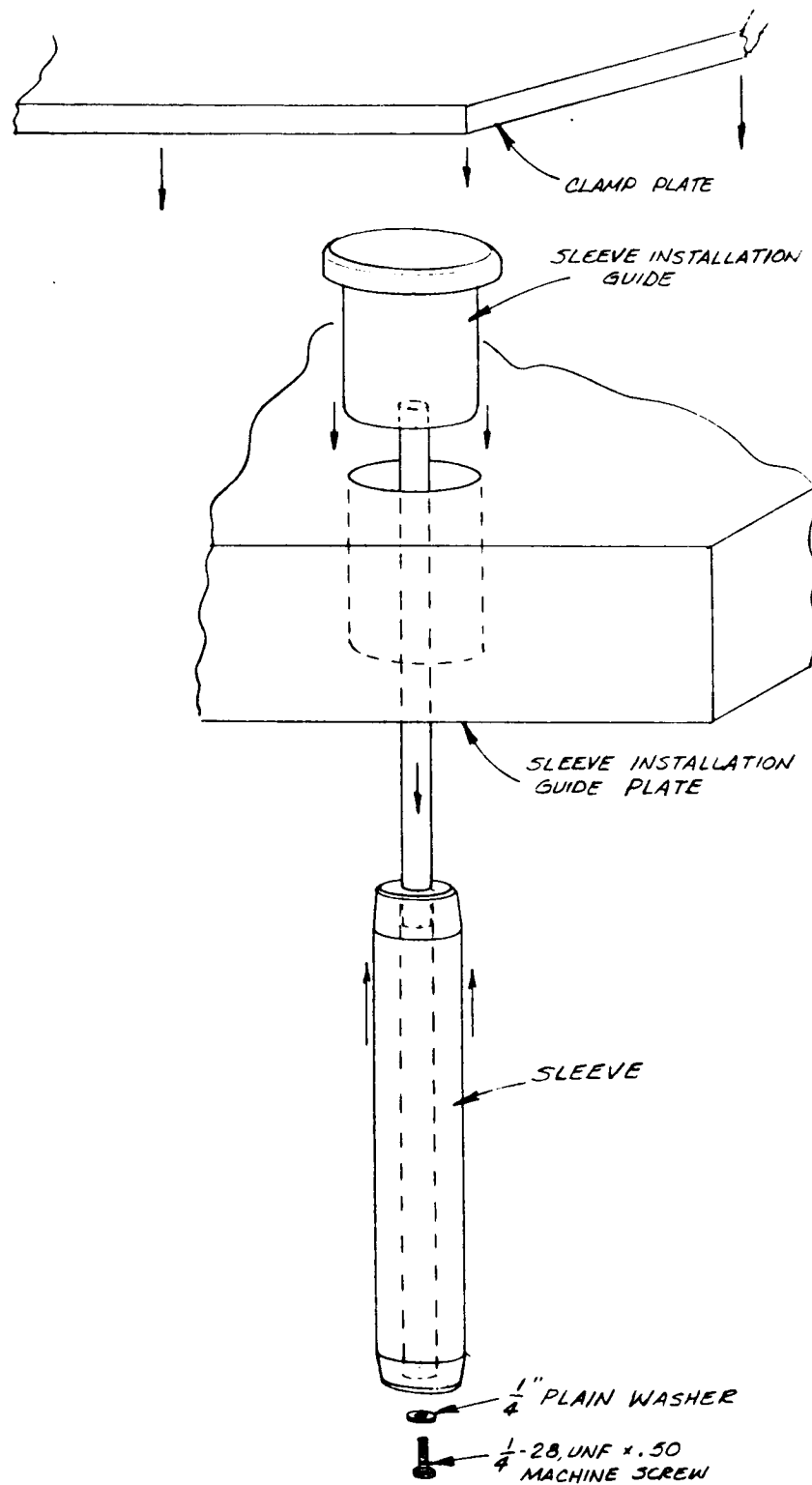


Figure 55.- Hub Fastener Sleeve Installation Schematic

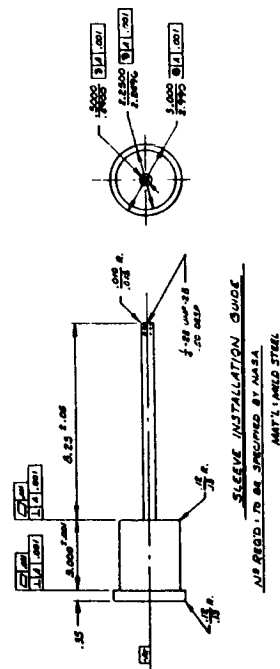
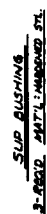
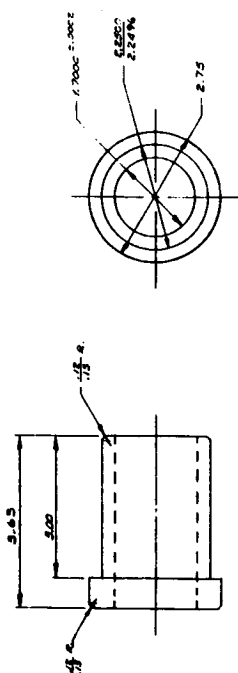
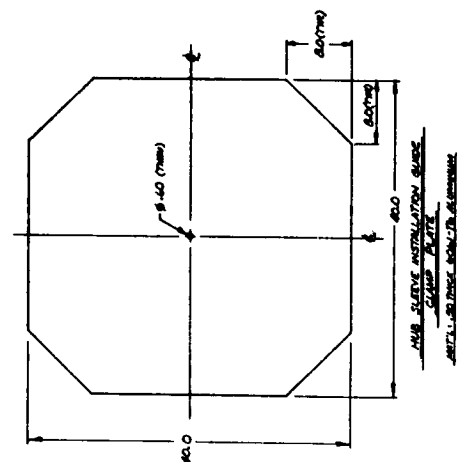
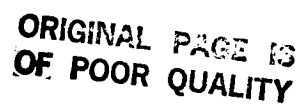
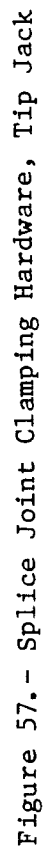


Figure 56.-- Hub Fastener Installation Hardware Details



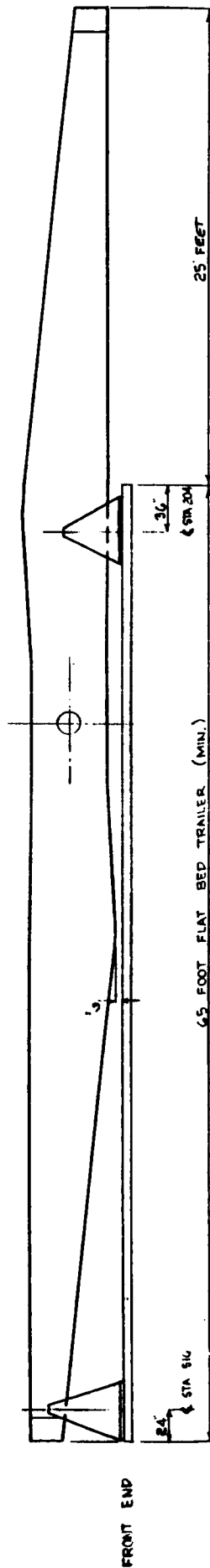


Figure 58 - Assembled Rotor Shipment Configuration

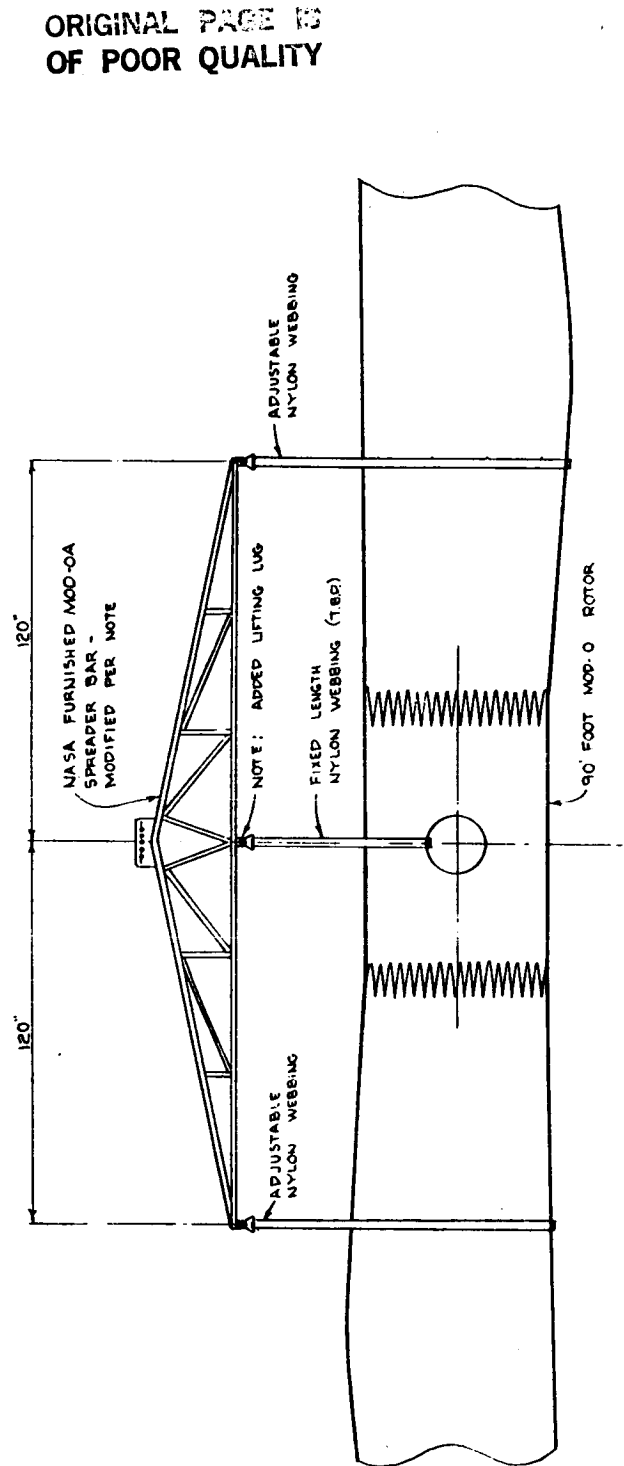


Figure 59.- Rotor Lifting Scheme

ORIGINAL PAGE IS
OF POOR QUALITY

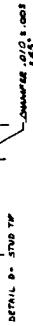


Figure 60. - Primary Set of Advanced Stud Designs

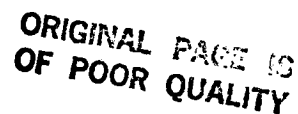
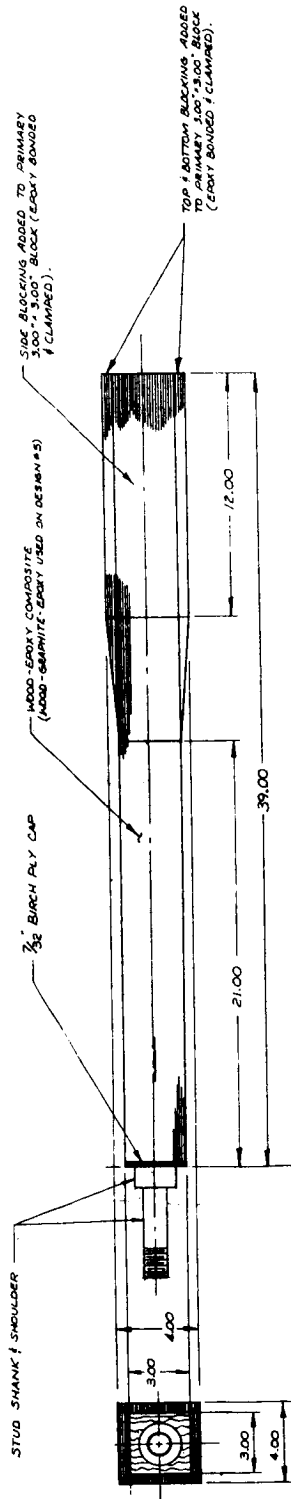
[illegible]

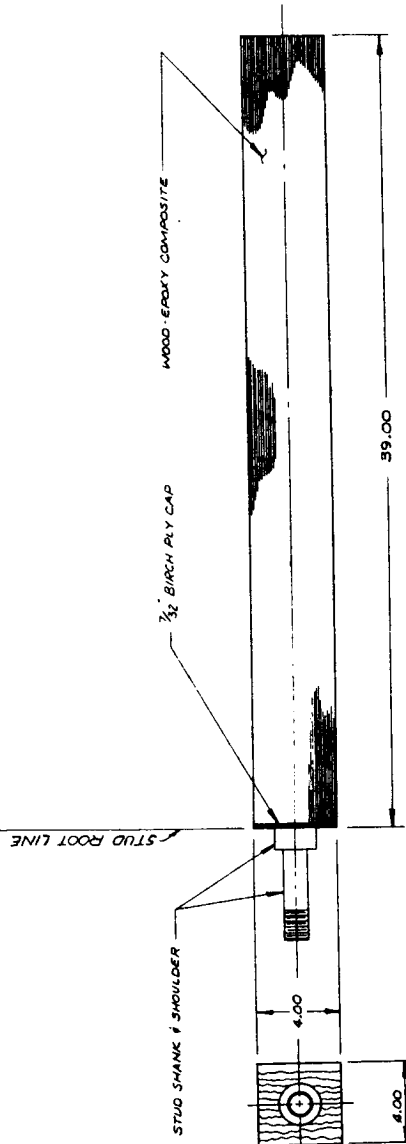
Figure 61.- Secondary Set of Advanced Stud Designs

NOTES

- 1) STUD HOLES TO BE CENTERED WITHIN 0.015 INCHES AT ROOT END OF BLOCK.
- 2) HOLE CONCENTRICITY WITH BLOCK CENTERLINE WITHIN 0.030 INCHES IS REQUIRED FOR ENTIRE LENGTH OF HOLE.
- 3) STUDS TO BE BONDED CONCENTRIC WITH HOLE CENTERLINE WITHIN 0.015 INCHES FOR ENTIRE LENGTH OF HOLE.
- 4) STUD INSERT DEPTH IS TO BE WITHIN .030 INCHES OF NOMINAL DESIGN DEPTH (PER DRAWINGS OF 10505A & 0710-035).



TEST STUD ASSEMBLY ~ DESIGNS 1 THRU 7



TEST STUD ASSEMBLY ~ DESIGN 8

Figure 62.- Test Stud Block Designs

ORIGINAL DESIGNS
OF POOR QUALITY

13.0 APPENDIX A - Teetered Hub Principal Stud Load Analysis

Assumptions:

- 1) 90 foot diameter rotor/400kW output
- 2) Gear box/generator efficiency of 0.85
- 3) Four inner row studs 11.5 inches from centerline, four middle row studs 14.75 inches from centerline, and four outer row studs 18.0 inches from centerline (two inner, two middle, and two outer studs on each bearing base - two such bases)
- 4) 55 rpm machine speed
- 5) Each inner row stud is $(11.5/18)^2$ as effective at transmitting torque as each outer row stud. Each middle row stud is $(14.75/18)^2$ as effective at transmitting torque as each outer row stud. This conservatively assumes that the load on any stud will increase linearly as its distance from the centerline increases.

Calculation:

Power at shaft (Hp) = $400 \text{ Kw} \times 1.34 \text{ (Hp/Kw)}/0.85 \text{ (system efficiency)}$
= 631 Hp

Operating torque (in-lbs) = $63030 \times \text{Hp}/\text{rpm} = 63030 \times 631/55 =$
723,126 in-lbs

The four inner studs are equal to $4 \times (11.5/18)^2$ or 1.633 of the outer studs

The four middle studs are equal to $4 \times (14.75/18)^2$ or 2.686 of the outer studs

Total equivalent number of outer studs = $1.633 + 2.686 + 4 = 8.319$

Shear load carried by each outer stud (lbs) = $723,193 \text{ in-lbs}/(8.319 \text{ studs} \times 18 \text{ inches}) = 4830 \text{ lbs.}$

14.0 APPENDIX B - Summary of Aerodynamic Tip Brake Design Concepts

Background

Contract DEN3-260 has supported work to develop a reliable aerodynamic brake as a secondary system for the 90-foot diameter rotor. The secondary system could control rotor over speed in the event the generator drops off line and the primary brake system fails.

Two tip brake designs were presented by Gougeon Brothers, Inc. (GBI) to NASA at the Conceptual Design Review (CDR). The primary design at that time was Concept A which is described below. The second design was a balanced winglet brake which could provide problems in manufacturing and with respect to tower clearance. At the CDR, NASA directed the contractor to do no further work on the balanced winglet brake concept.

The following narrative describes Concept A and two additional conceptual designs (Concepts B and C) proposed at the conclusion of the Rotor Preliminary Design phase. Figure 63 illustrates the three concepts.

Concept A

Concept A is a power modulating tip brake which deploys by pitching as it translates along the rotor spanwise axis. The pivot axis of this design is 35 percent of chord aft of the leading edge and the tip pitches nose down during deployment.

The pivot shaft is secured to the actuating tip. Located on this shaft is an adjustable stop collar and a compression spring that seats against the outboard bearing case.

The inboard bearing is a non-metallic, low-friction, bushing which is bonded into the blade. The outer bearing is a helical roller bearing that reacts against raised followers on the pivot shaft. This bearing is slip fit into the rotor and secured in place with machine screws around the perimeter of the flange.

Pre-compression of the spring holds the tip and shaft in proper operating orientation during normal machine operation. In the event of some specific rotational rotor over speed, the centrifugal load of the tip and shaft begin to overpower the spring which in turn allows spanwise translation of the tip. As the tip translates, the helical bearing and follower produce a nose down rotation of the tip, thereby decreasing lift and eventually increasing drag. The tip will further deploy should the rotor continue to increase its rotational speed, effectively controlling the rotor from a runaway over speed.

This tip design will modulate itself to match fluctuating power in the rotor during an emergency situation. Concept A was not developed to completely stop the rotor. It will only limit maximum rotor rotational speed during a potential emergency over speed condition.

Disassembly of this tip brake would be accomplished by removing the machine screws from the outer bearing flange and sliding the outer bearing, tip, shaft, spring and stop collar out of the blade as a unit. Any adjustment to the pre-compression of the spring can be done with this complete assembly removed from the blade.

There is concern that the compression spring for this design may not be practical. In order to react the weight of the tip and pivot shaft in a 40-50 G field, a high spring preload is required while maintaining a sufficiently low spring constant to allow the proper amount of linear translation of the tip (approximately 4 inches minimum) during a 10 percent over speed. Centrifugal load varies as the square of rotation speed, so a 10 percent over speed would equate to an incremental force of 21 percent on the spring to provide adequate translation. There might not be enough internal volume at the tip brake's junction to properly incorporate such a spring. Also, the outer bearing would likely not be an off the shelf item, since it has to combine rotary and linear motion via a helical spline.

Concept B

In order to simplify the bearing and spring design for the pitching tip brake, an alternative concept (Concept B) was developed. This design does not translate along the rotor spanwise axis, therefore allowing a simple roller design to be incorporated for the outer bearing. This outer bearing would slip fit into the rotor and be held in position by means of a bearing flange and machine screws.

The inboard bearing can, as with Concept A, be a low friction, nonmetallic bushing that is bonded into the rotor. The pivot shaft for this design is located at 35 percent chord aft of the leading edge and is bonded into the tip. A spanwise translating slide weight, which is restricted from rotary movement, features a helical guide that reacts against a raised follower on the pivot shaft. A precompressed spring that bears against the outer bearing shell holds the slide weight in proper position during normal operation of the rotor. If a rotor rotational over speed condition develops, centrifugal force on the slider weight increases, overcoming the spring force, and allowing outboard translation of the slider weight. This translation causes the tip to pitch nose down due to the helical spline and follower.

The tip is initially balanced aerodynamically, but as the tip rotates far enough for stall to begin, the resultant drag vector reacts further and further back on the foil such that a higher torque will be required to hold the tip at 90 degrees to the apparent wind. Fast initial rotation with a final high braking torque can be accomplished with a progressively steeper helix angle inside the slide weight. If the machine speed increases, the

slide will translate further spanwise and cause increased rotation of the tip, thereby preventing a runaway rotor. Similar to Concept A, Concept B will only regulate the rotor at a given RPM during an over speed condition. It will not bring the rotor to a stop.

Disassembly of the unit can be accomplished by removing the machine screws from the outboard bearing flange and sliding the entire unit from the rotor. An adjustable stop for the spring can be used to facilitate fine tuning the specific rotor rotational speed at which the tip will begin deployment. This adjustment can be done while the unit is removed from the rotor.

The bearings for this design should be off the shelf items. However, the slide weight will be a specialized part to design and manufacture. The spring sizing becomes much more reasonable than that for Concept A since only the weight of the slide must be reacted as opposed to the weight of the tip and shaft as in Concept A. The spring pre-load will still be larger than the normal centrifugal force below some specified deployment initiating rotational speed.

Concept C

A third concept (Concept C) was developed to alleviate the more complex bearing and spring requirements of Concepts A and B. This concept is termed a "one shot" unbalanced pitching tip brake. It differs from the previous two in that once deployment is initiated, full tip rotation takes place and is held until the rotor rotational speed approaches zero.

This style of brake is particularly attractive because once the tip brake commences deployment the generator has dropped off line and the primary rotor brake system has failed to function properly. This concept serves to significantly reduce the rotor's rotational speed rather than avoiding runaway as in Concepts A and B. In addition, before the rotor would again be operational, Concept C would require service personnel to manually reset the brake. This may be sound practice because, to experience emergency tip brake deployment, difficulties with the wind turbine generator system have developed and merit be checking before the machine is again started.

Both inboard and outboard bearings can be a low friction, non-metallic bushing type. The outboard bearing is slip fit into the blade and fastened with machine screws through a bearing flange. The inboard bearing is bonded into the rotor.

The pivot shaft is bonded to the tip and is located at 50 percent chord aft of the leading edge at the tip-rotor junction. The shaft is oriented parallel to the leading edge of the rotor causing the center of area to be located ahead of the pivot axis. Located on the shaft just inboard of the outer bearing would be a torsion spring that will hold the tip in the 90 degree, fully deployed, position and help stabilize the tip while the rotor

speed is decreasing or when it is at a stop. Incorporated in the same area of the shaft would be a rotary damper to reduce the full deployment loads of the tip.

As the rotor rotational speed reaches a pre-set limit, the centrifugal latch mechanism releases, allowing aerodynamic forces and the torsion spring to rotate and hold the tip in a 90 degree orientation. The rotor rotational speed would then decrease.

Disassembly is accomplished in a manner similar to Concepts A and B in that machine screws are removed from the flange of the outboard bearing and the entire unit can slide out of the rotor. The centrifugal latch should also be easily removable and could be adjusted for proper deployment load while removed.

With the pivot shaft located at 50 percent chord, there is less internal volume available for the necessary mechanisms. However, with the simplicity of this design available volume should not present significant problems. Should design efforts continue on tip brakes, there are several variations of the damper and latch mechanisms for Concept C that could be even more simple and reliable in long-term adverse conditions.

Summary

The length of these brakes has been consistently determined assuming only one tip would deploy. This conservative approach drives both the length of the tip and the size of the actuating mechanisms up considerably.

However, it has been recognized that if only one tip were to deploy, a large rotor thrust load imbalance would result, causing excessive teeter forces, therefore it might be more practical to develop a fail safe system whereby both tips deploy together. A method of interconnecting the release mechanisms in Design C by means of a cable could result in near simultaneous deployment. This would allow the length of the tip to decrease to 48 inches as opposed to the 102 inch length originally sized. A design such as Concept C, incorporating the interconnecting latch mechanisms, might approach a level of reliability such that the 48 inch tip length could be used. This would serve to minimize the complexity and weight penalty of an aerodynamic tip brake assembly.

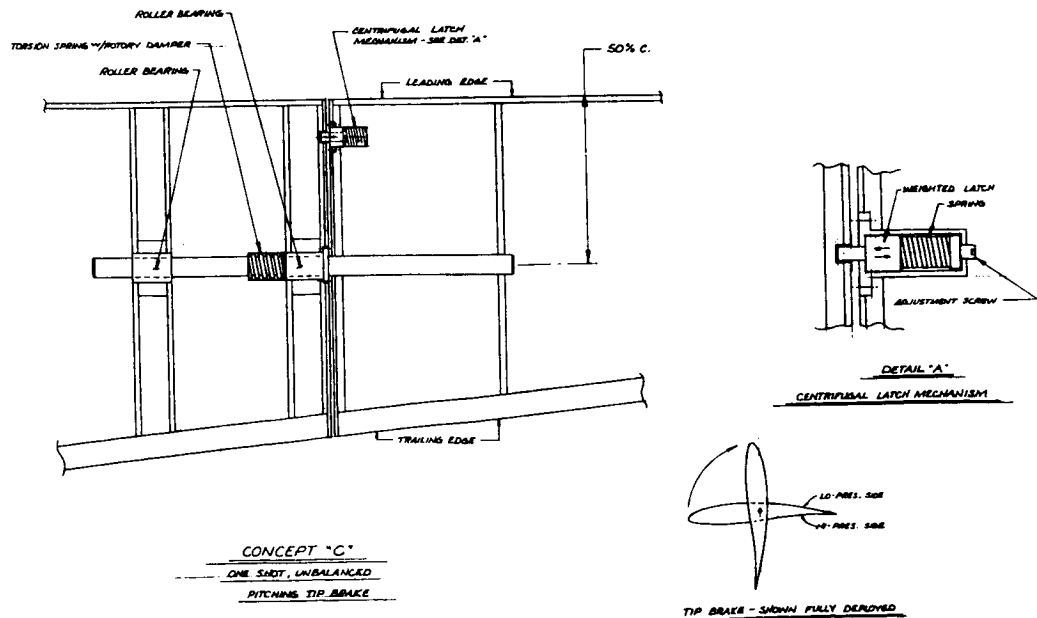
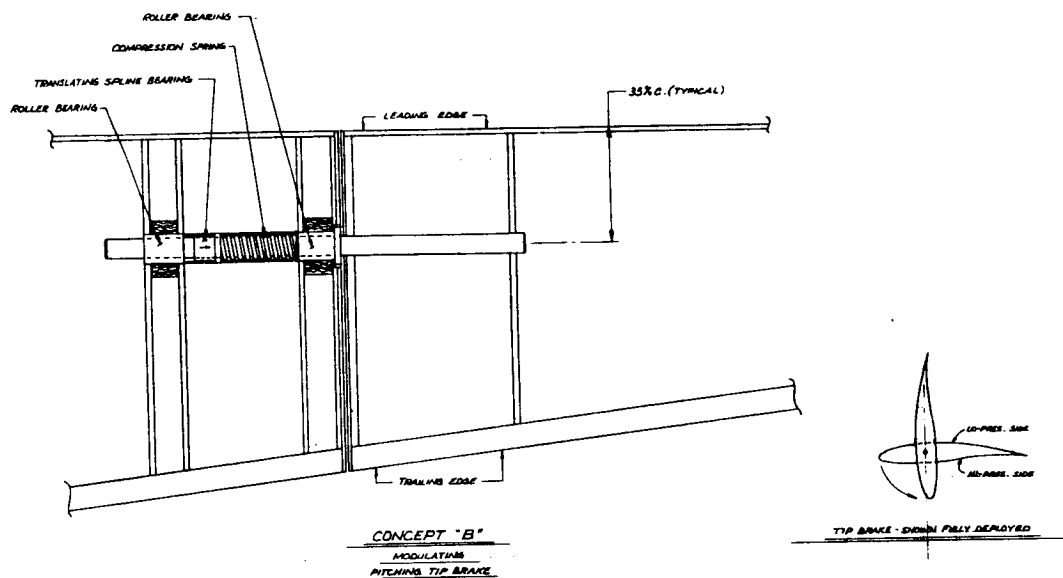
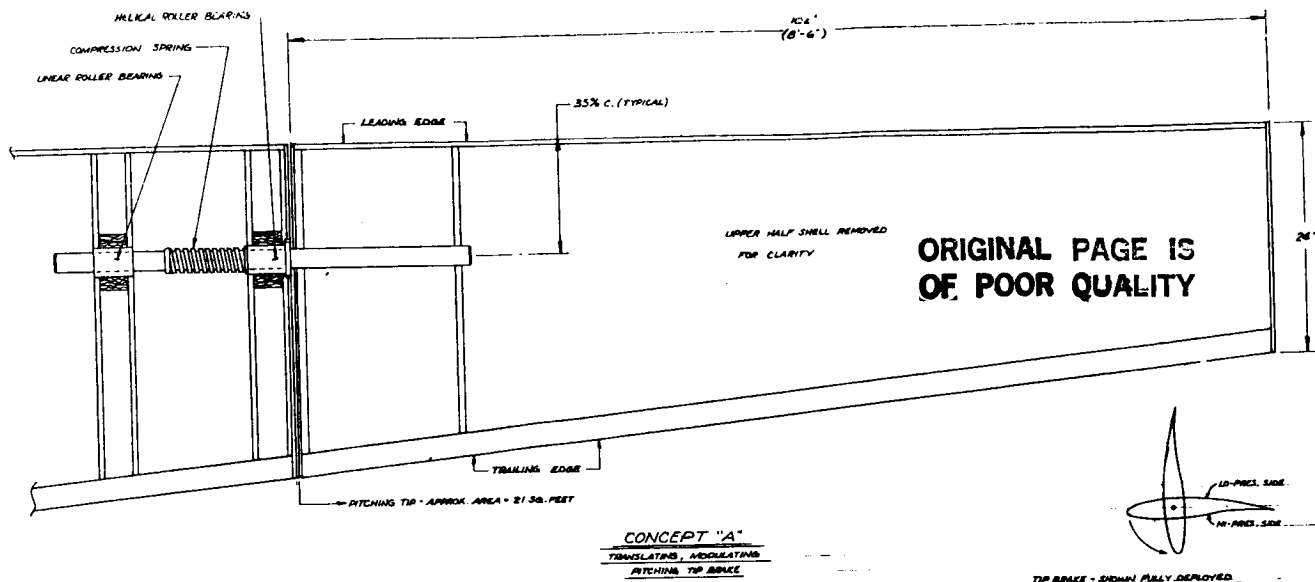


Figure 63.- Pitching Aerodynamic Tip Brake Concepts

15.0 APPENDIX C - Rotor Design Allowables Analysis

Introduction

The development of a complete set of fatigue and static wood/epoxy laminate capabilities, or design allowables, was completed within this contractual effort. Materials test data utilized as a basis for deriving allowables, were generally taken from the MOD-5A rotor materials test program.

Several general concepts have been applied in the adjustment of mean test data values to a final set of design allowables for the specific rotor design developed in this effort. Clarification of these concepts will aid in understanding the allowables computations in the following sections.

Fatigue data generated under the MOD-5A rotor materials test program did not extend beyond ten million cycles and revealed no 'endurance limit.' Log-log plots of maximum cyclic stress against accumulated cycle data were mathematically curve fitted using the least squares linear regression technique as shown in Figure 64. The resulting empirical description of the material's fatigue behavior was used to extrapolate maximum cyclic stress levels to cycle counts beyond those which were tested. This approach yields values which may be conservative from the point of view that at some unknown non-zero stress level, an essentially infinite fatigue life may exist. The linear regression curve used however, maintains a constant negative slope, generating stress values which may be increasingly conservative as the extrapolation extends beyond the actual test data. Figure 64 illustrates this relationship.

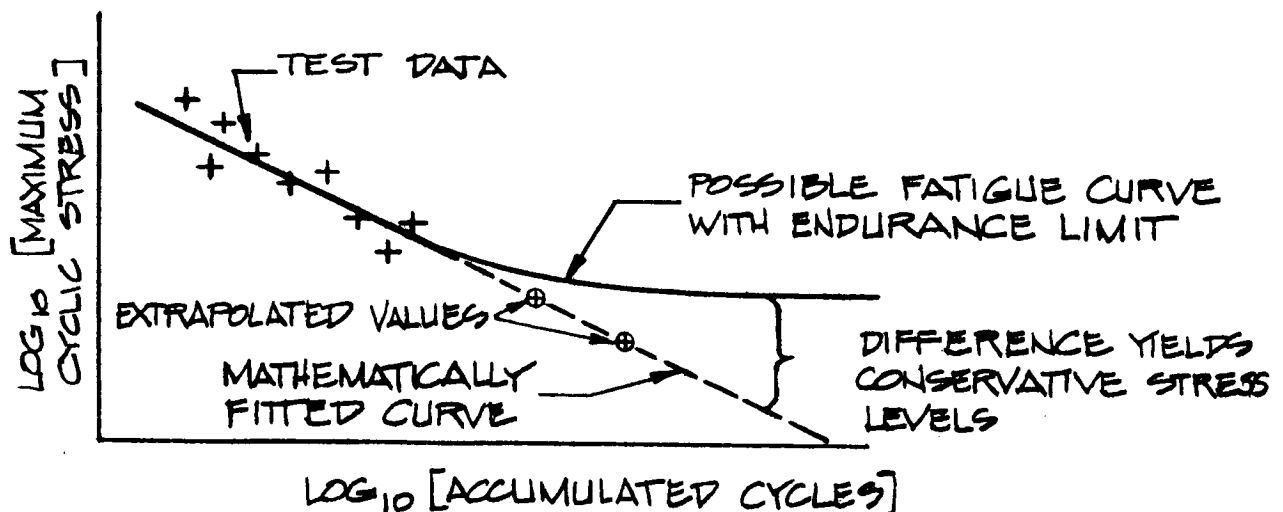


Figure 64. - Possible vs. Mathematical/Empirical Fatigue Curve

Although the same species (Douglas fir) and visual grade of veneer was used throughout the MOD-5A rotor materials test program, two different stress

grades of veneer were used. The difference between these two grades, namely Blade Grade 1 (BG1) and Blade Grade 2 (BG2), stems from a determination of the stress wave propagation time in each veneer sheet, during processing, using automated stress wave timing technology. Stress wave propagation times generally correlate inversely with properties such as elastic modulus and strength. Specifications for BG1 and BG2 veneer are contained within GBI Materials Specification GMS-001. Basically, BG1 graded veneers are those yielding stress wave times below a prescribed threshold while BG2 graded veneers are those yielding stress wave times within a range directly above the threshold of BG1 veneers. Veneers yielding stress wave times above the upper limit of the BG2 range are rejected for wind turbine application as their strength and modulus values are generally too low to be desirable for a stress critical application of this nature.

Some testing was conducted under the MOD-5A materials test program which permits correlation of BG1 and BG2 veneer based laminate performance. The calculated correlation factors have been used, when necessary, to adjust one veneer grade data base to design allowables which assume use of the other veneer grade.

A statistical evaluation of MOD-5A materials test data scatter was conducted to determine bounds of lowest expected performance. The product of the standard deviation (σ), multiplied by two, was used to establish a 95 percent confidence lower bound.

Generally, the static and fatigue performance of wood and wood fiber materials are known to decrease as the fiber moisture content increases. MOD-5A materials test data was normalized to 12 percent wood moisture content (wmc) using an equation developed by the Forest Products Laboratory (Madison, Wisconsin; ref. 8). That equation was developed for the adjustment of static values but it was found, within the MOD-5A materials test program, that it performed a very commendable job of reducing the scatter of plotted, non-moisture content normalized fatigue data. The 12 percent normalizing value was selected because it is a standard choice in the wood industry and it is also expected to be the highest moisture content level experienced by a wood/epoxy rotor in any normal operating environment.

The static and fatigue performance of wood-based laminates are somewhat sensitive to temperature over the range a rotor is expected to encounter. Higher ambient temperatures will degrade static and fatigue capabilities of the laminate, particularly in compression. Therefore, a temperature spectrum adjustment factor has been used in the computation of design allowables.

Duration of load, or creep, is another effect which existing literature shows to be significant in wood fiber-based structures. Wood fiber exhibits better static and fatigue capability against loads imposed over shorter (single or accumulated cycle) spans of time. Adjustments for this effect have been made on the design allowables, which thereby account for the influence of extended duration loads.

The effect whereby material performance decreases as a stressed volume increases was also studied and shown to be significant for wood/epoxy laminates under the MOD-5A materials test program. Analysis of the data allowed the derivation of empirical static and fatigue scale effect equations. These equations were applied to determine adjustments to design allowables relative to the specific volume of structural material within this rotor design.

With this introduction of rotor design allowables concepts complete, presentations shall be made in the following sections detailing the computation of all relevant final design allowables. Stress ratio (R) refers to the ratio of minimum stress to maximum stress, during cyclic fatigue. Consistency with the development of MOD-5A design allowables exists throughout the following calculations although some design specific adjustment factors have been appropriately applied. Finally, note that all allowables are strictly developed for the parallel to wood fiber direction. In the outer rotor, the design is similar to previous designs where secondary force flows (crossgrain) are known not to be limiting factors in the design. For this rotor, secondary force flows are recognized as an influence on the design, strictly in the hub, due to the large cutouts for the low speed shaft and are treated by the use of bidirectional fiberglass augmentation of the hub laminate.

R = +1 (Steady Load) Tension Fatigue Allowable

Analysis

The MOD-5A static tension size effect testing included many butt jointed laminate samples. Analysis of the BG1 butt-jointed laminate data suggested a static tension scale effect line of the form:

$$\text{Mean Tensile Strength} = 13500 \times \text{Volume}^{-.05815}$$

where strength is in psi and volume is in cubic inches.

For a characteristic (equivalent stress) volume of 6250 cubic inches (cu.in.), the computed tensile strength is:

$$13500 \times 6250^{-.05815} = 8121 \text{ psi}$$

The 90 foot rotor characteristic volume is taken to be 1 percent of the total enclosed volume within the rotor shell, as was done for MOD-5A.

A BG1 to BG2 veneer adjustment is needed because the outer rotor will use BG2 veneer. This adjustment factor is the ratio of the MOD-5A material test

results for BG2 veneer with 3 inch staggerred butt joints (8534 psi) to the results for BG1 veneer with 3 inch staggerred butts (10183 psi).

The 2σ adjustment (.84), temperature spectrum adjustment (.975), and duration of load adjustment (.53) are the same as used in the derivation of the MOD-5A allowables. 14 years is 4×10^8 cycles at 55 rpm.

Calculation

Mean Tensile Strength at 12% wmc
(BG1 laminate, 3 inch staggerred butt
joints, 6250 cu.in. volume) =8121 psi

BG1 to BG2 adjustment	.838
2σ adjustment	.84
Temperature spectrum adjustment	.975
Duration of load adjustment	.53

R = +1 Tension Fatigue Allowable =2954 psi

Summary

R = +1 Tension Fatigue Allowable

2954 psi

mean - 2σ , 6250 cu.in., 12% wmc
BG2 veneer, temperature spectrum, 14 year duration

R = 0.1 Tension Fatigue Allowable

Analysis

The mean peak tensile stress at 10^6 cycles (6369 psi), the exponent (B) for the strength vs. cycles curve (-.0897), the mean peak tensile stress at 4×10^8 cycles are all taken from available MOD-5A materials test data. The data is for a mixed group of BG2 and BG1 test results with 16 samples total. The samples feature a cylindrical cross section with a 32 cu.in. test volume with three butt joints staggered 3 inches in the inner three laminations. No attempt was made to remove the BG1 data or to compensate for its presence because the two data groups overlay each other rather well. Additionally,

the results are known to include a conservative factor in that there is about twice too much butt joint in the sample volume compared to normal rotor laminate.

The size effect volume exponent (-.09583) is based on a comparison of the MOD-5A large scale tension fatigue test results with the smaller scale tension fatigue results.

The 10% wmc to 12% wmc correction is necessary because the initial MOD-5A data is based on a 10% wmc level. The adjustment factor used (.969) is the standard moisture correction for static tension as derived by the FPL.

The 2σ correction (.84), and temperature spectrum adjustment (.975) are the same values used in the derivation of the MOD-5A allowables.

Calculation

Mean Peak Tensile Stress at 10^6 cycles, 10% wmc =6369 psi

10^6 to 4×10^8 cycle adjustment (400^B) .5842

Mean Peak Tensile Stress at 4×10^8 cycles,
10% wmc =3721 psi

2σ adjustment	.84
10% wmc to 12% wmc adjustment	.969
Size effect adjustment ($6250/32$) ^{-0.09583}	.595
Temperature spectrum adjustment	.975

R = 0.1 Tension Fatigue Allowable =1757 psi

Summary

R = 0.1 Tension Fatigue Allowable

1757 psi

mean - 2σ , 6250 cu.in., 12% wmc
BG2 veneer, temperature spectrum, 4×10^8 cycles

R = -1 (Fully Reversed), Fatigue Allowable

Analysis

The mean peak stress at 10^6 and 4×10^8 cycles, the exponent B, and the 95% confidence lower bound are taken from available MOD-5A materials test data. The 10% wmc to 12% wmc adjustment (.897) is the standard FPL derived moisture correction for static compression. The size effect exponent (-.05815) is the same as used for static tension. The 65 cu.in. volume attributed to the test samples is to adjust for the ratio of butt joints per unit volume in the test volume versus the rotor laminate volume (ie. it is the volume of rotor laminate which has the same amount of butt joint as did the test pieces). The BG1 to BG2 veneer adjustment is the ratio of MOD-5A butt jointed compression results corrected to 12% wmc for BG2 veneer (6452 psi) to the similar results for BG1 veneer (6968 psi). The 2σ adjustment (.84) and the temperature spectrum adjustment (.94) are identical to those used in the derivation of the MOD-5A allowables.

Calculation

Mean Peak Fully Reversed Strength at 10^6 cycles, 10% wmc	=3415 psi
10^6 to 4×10^8 cycle adjustment	.599
Mean Peak Fully Reversed Strength at 4×10^8 cycles, 10% wmc	=2045 psi
2σ adjustment	.84
10% wmc to 12% wmc adjustment	.897
Size effect adjustment $(6250/65)^{-.05815}$.767
Temperature spectrum adjustment	.94
BG1 to BG2 veneer adjustment (6452/6968)	.926

R = -1 (Fully Reversed), Fatigue Allowable =1029 psi

Summary

R = -1 (Fully Reversed), Fatigue Allowable

1029 psi

mean - 2σ , 6250 cu.in., 12% wmc
BG2 veneer, temperature spectrum, 4×10^8 cycles

R = 0.1 Compression Fatigue Allowable

Analysis

The mean peak compressive stress at 10^6 cycles (5586 psi), the exponent B (-0.0590), and the 95% confidence lower bound are taken from the MOD-5A materials test data. The 10% wmc to 12% wmc correction (.897) is the standard FPL derived method for static compression. The size effect exponent (-0.0075) is the same as used in derivation of the MOD-5A allowables. The conservative 32 cu.in. volume for the test samples is again used to balance the fact that a BG1/BG2 mix is present in the data base. As was the case for the tension-tension fatigue data, the two data sets are reasonably well interspersed and no attempt was made to explicitly remove the BG1 data. The duration adjustment is taken to reflect the fact that an 8 Hertz (Hz) compression test to 4×10^8 cycles would take 13,900 hours (8 Hz was the test rate), but a 4×10^8 cycle design life is 13.8 years at 55 rpm. The duration correction for 13.8 years is virtually identical to that for 20 years, so the MOD-5A factor of .755 is applied.

The 2σ adjustment (.84) and temperature spectrum adjustment (.9) are identical to those used in the derivation of the MOD-5A allowables.

Calculations

Mean Peak Compressive Stress at 10^6 cycles, 10% wmc	=5586 psi
10^6 to 4×10^8 cycle adjustment (400^B)	.7022
Mean Peak Compressive Stress at 4×10^8 cycles, 10% wmc	=3923 psi
2σ adjustment	.84
10% wmc to 12% wmc adjustment	.897
Size effect adjustment $(6250/32)^{-0.0075}$.961
Temperature spectrum adjustment	.900
Duration of load adjustment (13900 hours to 20 years)	.755

R = 0.1, Compression Fatigue Allowable = 1930 psi

Summary

R = 0.1 Compression Fatigue Allowable
1930 psi
mean - 2σ , 6250 cu.in., 12% wmc
BG2 veneer, temperature spectrum, 4×10^8 cycles

R = +1 (Steady Load), Compression Fatigue Allowable

Analysis

The mean compressive strength value is taken from the MOD-5A material test data corrected to 12% wmc. The standard .84 adjustment factor for 2σ is applied and is nearly identical to the calculated 2σ factor for the data set (.834).

The duration of load adjustment (.53) from 5 minutes to 14 years and the temperature spectrum adjustment (.90) are identical to those used in the derivation of the MOD-5A allowables.

Calculation

Mean Static Compressive Strength at 12% wmc	=6452 psi
2σ adjustment	.84
Size effect adjustment	
(none for compression, R=+1)	1.00
Temperature spectrum adjustment	.90
Duration of load adjustment	.53

R = +1 (Steady Load), Compression Fatigue Allowable =2585 psi

Summary

R = +1 (Steady Load), Compression Fatigue Allowable
2585 psi
mean - 2σ , 6250 cu.in., 12% wmc
BG2 veneer, temperature spectrum, 14 years

Goodman Diagram, 4×10^8 Cycles

The graph in Figure 65 is the Goodman diagram which results when the preceding allowables are plotted. The curve is skewed a little toward the compression side by the explicit treatment of scale effect, which is currently assumed to have its maximum depressive effect upon tension-tension allowables in the vicinity of $R = 0.1$. This causes the tension side of the diagram to be relatively linear, and the performance advantage of tension relative to compression observed in laboratory sized samples no longer exists. On the whole, the diagram is relatively symmetrical and the tension and compression sides of the rotor can be stressed about equally. It appears that using equal thickness for high and low pressure shells is a reasonable procedure for wood/epoxy rotors of intermediate (MOD-0) size.

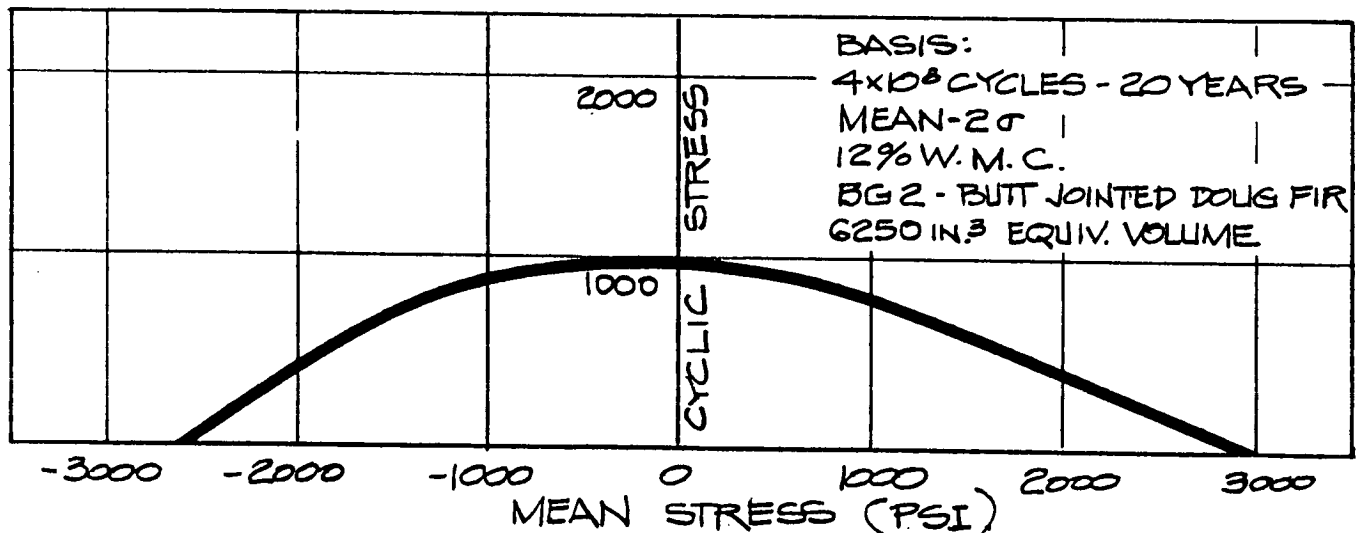


Figure 65. - Goodman Diagram - 4×10^8 Cycles

Fatigue Allowables for 10^7 Cycle Loading

As an additional design check, the fatigue capability of the design was evaluated against a set of elevated loads which reflect a maximum operating load condition. It is clear that such loads will only be present occasionally because they represent an elevated wind condition of roughly 33 mph. Therefore it would be inappropriate to use the 4×10^8 cycle allowable in evaluating performance for this infrequent high load condition. A second Goodman diagram for 10^7 cycles was therefore developed for this elevated

load case. The 10^7 cycle choice is equivalent to about 3000 hours at 55 rpm, or roughly 1/3 of a year. That is far more than the prototype rotor will experience on the NASA MOD-0 machine at Plumbrook, Ohio (as is 4×10^8 cycles at normal operating loads). The elevated load, 10^7 cycle level was chosen as representative of what a commercial rotor might see in a lifetime of operation, consistent with choosing 4×10^8 cycles to represent a lifetime of normal operating loads.

Adjustment to the 10^7 cycle level is straightforward, only the load duration adjustment or cycle adjustment shown in the previous sections need be changed. A summary of the changes and results is shown in the following table.

<u>Loading Condition</u>	<u>3000 hr Duration Factor</u>	<u>10^6 to 10^7 Cycle Factor</u>	<u>Adjusted Allowable Stress, psi</u>
R = +1 Tension	.805	1.0	4487
R = .1 Tension	1.0	.813	2446
R = -1 Reversed	1.0	.821	1410
R = .1 Compression	.936*	.873	2975
R = +1 Compression	.805	1.0	3926

$$* .936 = \frac{.777}{.830} = \frac{347 \text{ hour duration factor}}{3000 \text{ hour duration factor}}$$

where 347 hours is 10^7 cycles at 8 Hz as actually tested, and 3000 hours is 10^7 cycles at 55 rpm as machine would operate

Goodman Diagram, 10^7 and 4×10^8 Cycles

Figure 66 is a Goodman Diagram which shows the allowable stress curves for both the normal operating load case of 4×10^8 cycles (20 years) and the maximum operating load case of 10^7 cycles (3000 hours). A substantial increase in allowable stress for the reduced cycle case is evident, as would be expected.

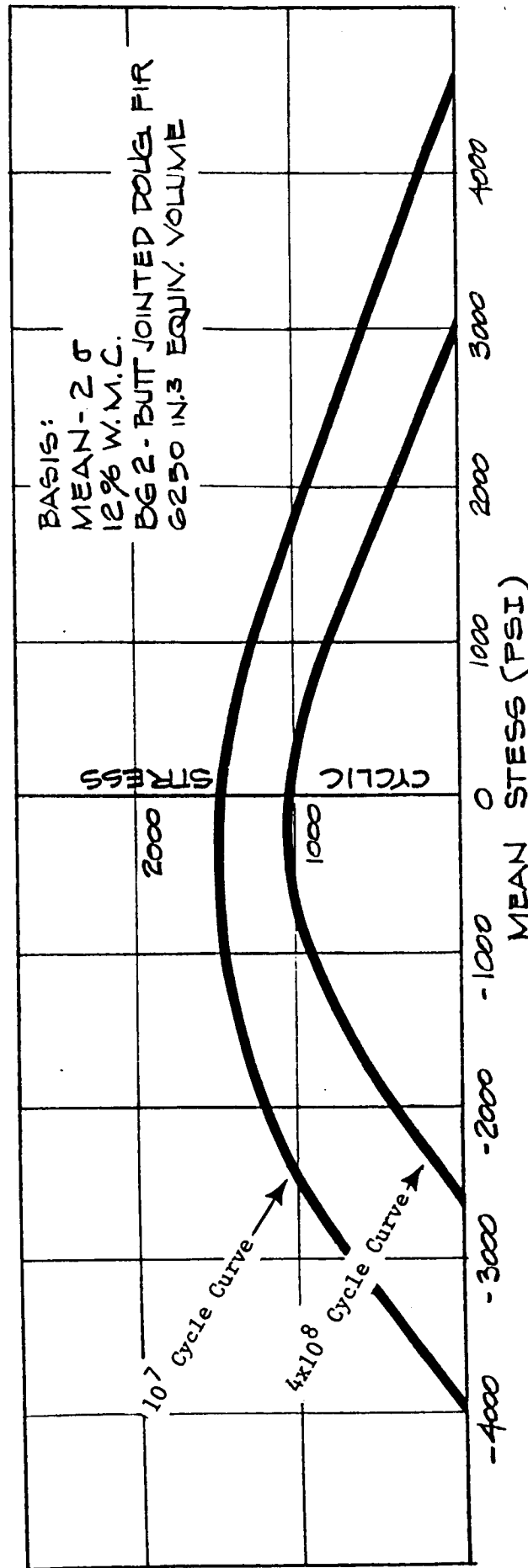


Figure 66. - Goodman Diagram - 10^7 Cycle and 4×10^8 Cycles

The basic character of the curve is the same in both cases, with compression showing slightly higher allowable stresses, except near $R = +1$, where tension is favored.

Allowables Upgrade for BG1 Unjointed Hub Material

As part of the MOD-5A fatigue allowables development, a comparison was made between butt jointed fatigue results and those for scarf jointed laminates. Comparing performance at 10^6 cycles, so that uncertainties associated with extrapolating outside the test data range are eliminated, we find:

<u>Data Type</u>	<u>Number of Data Points</u>	<u>Mean Peak Stress at 10^6 Cycles, psi</u>	<u>Improvement</u>
Tension-Tension			
Butt Joints/BG1 & BG2	16	6373	+21%
Scarf Joints/BG1	5	7716	
Fully Reversed			
Butt Joints/BG1	10	3415	+14%
Scarf Joints/BG1	9	3897	
Compression-Compression			
Butt Joints/BG1	17	5997*	+13%
Scarf Joints/BG1	7	6767*	

*Comparison conducted at 3×10^5 cycles because of high cycle data anomalies in the scarf data set

It should be noted that the data sets for tension-tension and compression-compression scarfs are small (5 points and 7 points respectively) and thus the associated improvement percentages have a rather large uncertainty and should be used with care. Much of the following discussion is devoted to trying to draw reasonable conclusions from sometimes rather sparse or anomalous data sets. The reader who does not really need or desire that level of detail can save considerable effort by skipping ahead to the overall conclusion relative to the Goodman Diagram Upgrade. This conclusion is presented on page 98.

As mentioned in developing the butt jointed material allowables, the butt jointed test samples had twice the amount of butt joints of bulk rotor laminate, per unit volume. A volume correction factor is easily applied to



the above improvement percentages to approximately account for volume differences, and the results of such a correction are shown in the next table.

Test Type	Volume Adjustment	Scarf vs. Butt Improvement	
		Unadjusted	Adjusted
Tension-Tension	2 ⁻ .09853 = .93 (-7%)	21%	14%
Fully Reversed	2 ⁻ .05815 = .96 (-4%)	14%	10%
Compression-Compression	2 ⁻ .0075 = .99 (-1%)	13%	12%

The difference between BG2 and BG1 veneer in fatigue has not been specifically established via test. The best which can be done at this time is to assume that the difference in fatigue would be the same as the difference in the associated static properties.

From the MOD-5A materials testing we find (adjusted to 12% wmc):

	Maximum Tensile Strength (psi)		Maximum Compressive Strength (psi)	
	BG1	BG2	BG1	BG2
No joints	9706*	10016	7345	7149
Butt joints	10183	8534	6968	6452

*This value appears to be anomalously low - see later discussion in this section.

Combining both the no joint and butt joint samples into an overall comparison of BG1 vs. BG2 to reduce the effect of possible data anomalies, we find:

$$\text{Tension: } \frac{9706 + 10183}{10016 + 8534} = 1.072, +7\%$$

$$\text{Compression: } \frac{7345 + 6968}{7149 + 6452} = 1.052, +5\%$$

In order to arrive at an overall improvement for going from BG2 to BG1 and also eliminating butt joints, we proceed as follows:

Tension-Tension - Since the butt joint test population was a BG2 and BG1 mix, presumably about half of the BG1 vs. BG2 correction is already present in the butt vs. scarf fatigue comparison, so add 1/2 of the BG2 to BG1 tension improvement ($7\%/2 = 3.5\%$). Use 3 percent conservatively.

Fully Reversed - Apply the compressive correction as is done for moisture.

Compression-Compression - Apply the compression correction.

<u>Property</u>	<u>Overall Improvement</u>
Tension-Tension (R=0.1)	17% (14% + 3%)
Fully Reversed Fatigue (R=0.1)	15% (10% + 5%)
Compression-Compression (R=0.1)	17% (12% + 5%)

Design Driver Tension-Tension (R=0.1) Improvement = 17%
adjusted from BG2 to BG1 veneer and adjusted from butt joints to unjointed laminate

The BG2 vs. BG1 allowables upgrade for both tension and compression is already given on this page. The static butt jointed vs. unjointed upgrade is also required to determine the overall hub static upgrade for the R = +1 allowable.

Some care must be exerted in determining the butt jointed vs. unjointed tension upgrade because there is evidence to suggest that the unjointed BG1 results were artificially low and with high scatter, probably due at least in part to the effect of rough surfaced veneer. (An unusually high coefficient of variation for this data supports that hypothesis. The same is true for the anomalous compression results cited in the following discussion of the compression upgrade.) Perhaps the best that can be done is to average together the results for BG1, BG2, and C veneer grades in order to minimize the anomalous BG1 results, since additional testing was not conducted to resolve the initial anomaly. (An ultrasonically screened, C-grade veneer had been evaluated in the MOD-5A materials test program in 1981.) The MOD-5A tension results for the three veneer grades are shown in the following table.

Tensile Strength for Veneer Grades at 12% wmc, psi			
	BG1	BG2	C
Unjointed	9706	10016	8972
Butt-jointed	10183	8534	7392

$$\text{Average Upgrade: } \frac{9706 + 10016 + 8972}{10183 + 8534 + 7392} = 1.10, +10\%$$

With a BG2 to BG1 tension upgrade of 7 percent, the combined upgrade for the unjointed BG1 hub material is 17 percent (10% from jointed to unjointed + 7% from BG2 to BG1).

Tension Upgrade for Unjointed BG1 Hub Material

$$R = +1, \text{ Tension} = +17\%$$

An anomalous condition of a lesser degree also appears to exist in the MOD-5A compression data in that the results for BG2 butted material are inexplicably lower than those for butted C grade material. A similar averaging procedure is again called into use to reduce the effect of this anomalous result.

Compressive Strength for Veneer Grades at 12% wmc, psi			
	BG1	BG2	C
Unjointed	7345	7149	6912
Butt-jointed	6968	6452	6674

$$\text{Average Upgrade: } \frac{7345 + 7149 + 6912}{6968 + 6452 + 6674} = 1.065, +7\%$$

With a BG2 to BG1 compression upgrade of 5 percent, the combined upgrade for the unjointed BG1 hub material is 12 percent.

Compression Upgrade for Unjointed BG1 Hub Material

$$R = +1, \text{ Compression} = +12\%$$

The $R = +1$ tension upgrade of 17 percent is the same as the $R = 0.1$ tension-tension upgrade of 17 percent, and is nearly the same as the $R = -1$ (fully reversed) upgrade of 15 percent. Since it is the tension side of the Goodman diagram which drives the design, that alone is sufficient justification to choose a 17% hub allowables upgrade. In addition, note that the compression-compression upgrade of 17% is slightly higher than is likely, and this is probably due to a statistical variability associated with having only seven scarf fatigue data points. The 12 percent, $R = +1$ compression upgrade is more believable, but the issue is academic since neither drive the design.

Overall Upgrade for BG1 Hub Material

$$\text{Goodman Diagram Upgrade} = 17\%$$

Static Tension Allowable

Analysis

The basis for the static tension allowable is the curve fit to the static tension size effect data from the MOD-5A materials test data. With a characteristic volume of 6250 cu.in. for this 90 foot diameter rotor, the mean tensile strength allowable is 8121 psi for butt-jointed BG1 material. A 2σ adjustment factor of .84 is used as was done for MOD-5A. The BG1 to BG2 adjustment of .838 is again used, as was done in the derivation of the $R = +1$ tension fatigue allowable. The MOD-5A extreme temperature adjustment factor of .95 is replaced by an extreme temperature adjustment factor of .93 to reflect the fact that this rotor is being designed to an upper temperature extreme of 120 degrees Fahrenheit (F), rather than the MOD-5A value of 104 degrees F (against assumed average test temperature in both cases of 68 degrees F).

Calculation of extreme temperature adjustment factor:

$$100\% - [5\% \times (120 - 68) / (104 - 68)] = 93\%$$

Calculation

Mean tensile strength =8121 psi
(12% wmc, butt-jointed, BG1, 6250 cu. in.)

2 σ adjustment .84
BG1 to BG2 adjustment .838
Extreme temperature adjustment factor .93

Outer Rotor Static Tension Allowable =5316 psi

Butt-jointed BG2 to Unjointed BG1 upgrade
(Same as calculated for R = +1 tension) 1.17

Inner Rotor (Hub) Static Tension Allowable =6220 psi

Summary

Static Tension Allowable

Outer Rotor = 5316 psi (butt-jointed BG2)

Inner Rotor (Hub) = 6220 psi (unjointed BG1)

mean - 2 σ , 5 minute load duration, 120 degrees F, 6250 cu.in.

Static Compression Allowable

Analysis

The Coefficient of Variation (COV = standard deviation/mean strength) of the MOD-5A BG2, butt-jointed compressive test data is suspiciously high, and the mean compressive strength of 6452 psi is lower than the mean of 6674 psi for the C grade butt-jointed material. This lends a conservative factor to the following calculation. The extreme temperature factor of .70 for 120 degrees F is the same as was used in the MOD-OA wood/epoxy blade design. The 2 σ correction of .84 and the proportional limit factor of .85 are the same as were used in the MOD-5A allowables derivation. The butted BG2 to unjointed BG1 upgrade is the 12% factor as calculated for R = +1 compression.

Calculation

Mean Compressive Strength
(12% wmc, butt jointed BG2) =6452 psi

2 σ adjustment	.84
Extreme temperature adjustment	.70
Proportional limit adjustment	.85

Outer Rotor Static Compression Allowable =3225 psi

Butt-jointed BG2 to unjointed BG1 upgrade 1.12

Inner Rotor (Hub) Static Compression Allowable =3612 psi

Summary

Static Compression Allowable

Outer Rotor = 3225 psi (butt-jointed/BG2)

Inner Rotor (Hub) = 3612 psi (unjointed BG1)

mean - 2 σ , 5 minute load duration, 120 deg.F, proportional limit

Finger Joint Allowables

Overview

It has been generally accepted that the presence of finger joints would cause the greatest loss of performance in tension-tension fatigue, and therefore a series of finger joint fatigue tests have been performed at R = 0.1 tension fatigue. Samples like those used to test butt-jointed and scarf-jointed laminates were used, so direct comparisons can be made. From the MOD-5A test data, the mean peak tensile stress for a BG2/BG1 mix of butt-jointed samples at 10⁶ cycles was 6369 psi at 10% wmc. This value is corrected downward by 3 percent to go from the mix to pure BG2 veneer, and by an additional 3.2 percent to go from 10% wmc to 12% wmc.

Peak tensile stress at 10^6 cycles
(butt-jointed) =6369 psi

BG2/BG1 mix to BG2 adjustment (1/1.03) .971
10% wmc to 12% wmc adjustment (1/1.032) .969

Peak tensile stress at 10^6 cycles
(butt-jointed, BG2, 12% wmc) =5992 psi

Peak finger joint stress at 10^6 cycles
(BG2, 12% wmc) =4550 psi

The peak finger joint stress comes from the current plot of the finger joint test results corrected to 12% wmc. The value of 4550 psi is 76 percent of the comparable 5992 psi value for butt-jointed BG2 veneer at 12% wmc. At first look this would appear to imply a need to substantially thicken the joint region to compensate the lowered allowable, and this could be so, but the rotor has a much larger volume of laminate than do the finger joints, and thus a separate size correction must be made in order to properly determine the finger joint allowable.

Analysis

The volume of the test region of the finger joint samples is the standard 32 cu.in. test volume. The configuration tested was a 6 inch long finger with an additional inch of cylinder beyond each finger tip. The characteristic volume can be taken to be the 4 square inch (sq.in.) circular cross-section times the 6 inch finger length equals 24 cu.in., directly within the joint region.

The rotor cross-sectional area at the finger joints is:

$$[21.8 \times 34.2 + \pi(10.9)] = 1119 \text{ sq.in.}$$

There are two finger joint regions, each 11.5 inches long, so the overall finger joint spanwise length is a total of 23 inches. Multiplying the above two numbers gives the total finger joint region total enclosed volume of 25,737 cu.in. Because the stress is not uniform across the rotor volume, a form factor should be applied to calculate an equivalent (uniformly stressed) volume. The 1 percent form factor used in calculating the rotor allowables for the MOD-5A and elsewhere on this rotor will again be used here.

Calculation

Finger joint test sample
characteristic volume: 24 cu.in.

Rotor finger joint characteristic
volume (25,737 x 0.01): 257 cu.in.

Size adjustment $(257/24)^{-.09853}$: .792

Peak finger joint stress, corrected for volume
(BG2, 12% wmc, 10^6 cycles) =3604 psi

2 σ adjustment	.84
10^6 to 4×10^8 adjustment $[400^{-.0897}]$.584
Temperature spectrum adjustment	.975

Peak finger joint tensile stress =1724 psi

Summary

Finger Joint Allowable
R = 0.1, Tension Fatigue

1724 psi

mean - 2 σ , 257 cu.in. volume, 12% wmc
BG2, temperature spectrum, 4×10^8 cycles

Discussion

The R = 0.1 tension finger joint allowable of 1724 psi calculated above is within 2 percent of the allowable of 1757 psi for the butt-jointed BG2 veneer which makes up the bulk of the outer rotor. In effect, the size effect correction has compensated the loss of strength associated with the finger joints. The butt jointed material is already suffering a strength knockdown due to the detrimental effect of the butt joints, and one should note that butt joints are eliminated from the finger joint region so that it is beginning with an elevated basic strength. In addition, the finger joint region is only a small fraction of the overall rotor volume, so it does not experience as large a reduction due to scale effect. The perhaps surprising result is that very little reduction in the allowable is required in the finger joint region. Since a data base of finger joint fatigue data exists only for R = 0.1 tension, it is not possible at this time to directly calculate finger joint allowables at other stress ratios. However, the detrimental effect of defects appears to be greatest for tension-tension

fatigue, and evidence to support this exists in that the fatigue curve slope for butt-jointed material is much larger in tension-tension fatigue than it is in fully reversed or compression fatigue. So we should already be seeing the worst effect of the finger joint induced stress raisers (defects) in the existing tension-tension fatigue results. It would thus appear to be a conservative position to take 98% of the outer blade Goodman diagram as a characterization of the finger joint fatigue performance, provided that the 11.5 inch fingers have proportions geometrically similar to those used in the MOD-5A materials test program.

Finger Joint Fatigue Performance Assumed
To Be 98 Percent of Outer Rotor Goodman Diagram

Low Speed Shaft Hole - Tension Side

The shape finally chosen for the tension side low speed shaft hole was a football shaped hole formed with 21 inch radius circular arcs, as illustrated in Figure 67.

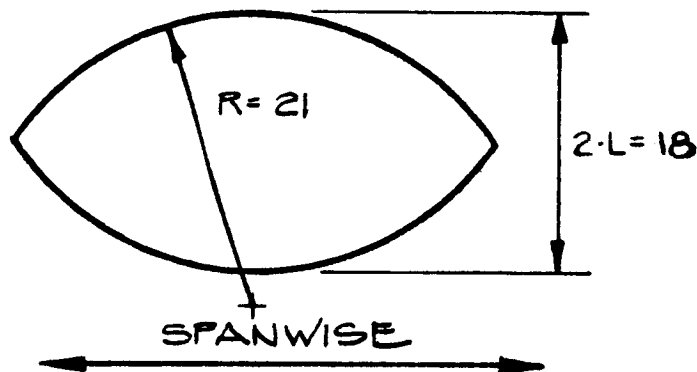


Figure 67. - Tension Side Low-Speed Shaft Hole Geometry

The primary motivation for this choice was the desire to obtain a lower value of stress concentration along the edge of the hole than would exist for a circular hole. The classical result for the stress concentration at the tip of an elliptical hole in a homogeneous isotropic material is:

$$S = S_o \times [1 + 2 \times (L/R)^{.5}]$$

where S_o is the average stress away from the hole, L is 1/2 of the hole width, and R is the radius of curvature

For the football shape chosen:

$$S/S_o = [1 + 2 \times (9/21)^5] = 2.31$$

By comparison, a circular hole has a stress concentration factor (S/S_o) of 3.0, so a circular hole would exhibit a peak stress 30 percent higher than does the selected football shaped hole. This is a useful and easily obtained reduction of peak stress.

Neither wood nor laminated wood/epoxy composite is a homogeneous isotropic material. The lamination process does improve overall homogeneity significantly, but the highly anisotropic nature of the underlying wood is still very evident. This is where +/- 45 degree fiberglass augmentation plies become useful. The purpose of this augmentation is to increase the shear stiffness of the augmented laminate to a level where the ratio of longitudinal stiffness along the major stress direction to shear stiffness is about the same as the 2.66 ratio which exists for classical homogeneous isotropic materials such as metals.

$$E/G = 2 \times (1 + \nu)$$

where E is the Modulus of Elasticity, G is the Shear Modulus, and ν is Poisson's ratio

Note that if the shear stiffness could be raised to arbitrarily high levels without changing the longitudinal stiffness, this would mean that the shear lag would approach zero and only a vanishingly small stress concentration would exist along the side of the hole.

The football shaped tension side hole is to be provided with a 0.5 inch thick hole liner. Ignoring for the moment that this hole liner is of relatively high modulus unidirectional carbon fiber/epoxy laminate and will therefore accept higher loading than the fiberglass augmented wood/epoxy laminate, the purely geometric effect the change in hole dimensions has upon the idealized stress concentration factor can be calculated:

$$S/S_o = [1 + 2 \times (8.5/20.5)^5] = 2.29$$

This calculation makes it clear that the stress concentration factor is not sensitive to small changes in hole dimensions, and one can use a 2.3 to 1 stress concentration factor for the tension side low speed shaft hole without worry that small manufacturing variations could upset the calculations.

The 2.3 to 1 stress concentration factor is applied directly to the edge of the hole at rotor spanwise centerline (the widest part of the hole). In order to estimate the hole edge stress at other locations along the rotor spanwise centerline, it was assumed that the chordwise stress distribution

could be approximately modeled by a triangular distribution of excess stress superimposed on a rectangular base of normalized stress, as shown in Figure 68.

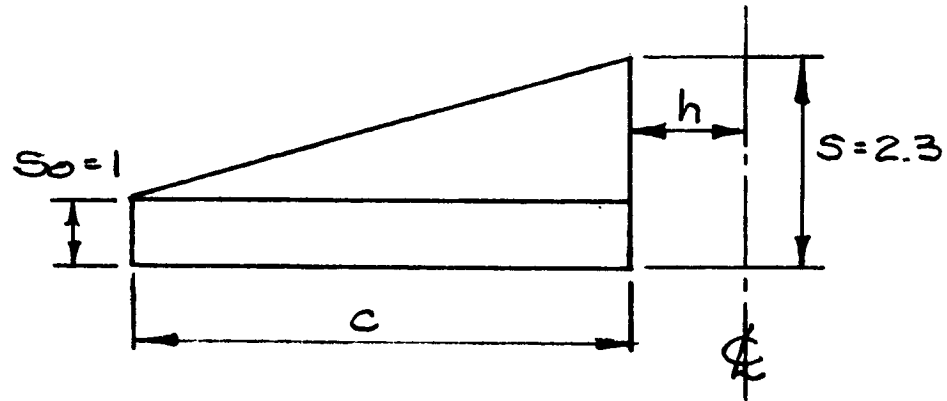


Figure 68. - Geometry of Stress Redistribution Due to Cutout

We require that the triangular distribution of excess stress produce a stress concentration of 2.3 at the hole edge when $h = 9$ at rotor centerline. We also require that the excess stress vanish beyond the hole, so that a normalized stress equals 1 when $h = 0$. A final constraint is that the total area under the stress curve must remain constant everywhere along the hole, so that overall stress is not being created or destroyed, but is simply being moved from the cutout into the remaining nearby material. These conditions taken together dictate a characteristic chordal width dimension for the assumed stress field, which can be shown to be 22.85 inches for $S = 2.3$ and $h = 9$. We can then write:

$$h + c = 22.85$$

and

$$k = 1 + 2 (h / c)$$

where 22.85 is the characteristic chordwise dimension and k is the hole edge stress concentration factor, S/S_0 for other values of hole half width h .

If one attributes to the carbon fiber liner the properties of the augmented fir laminate, the equations become:

$$h + c = 21.58$$

and again,

$$k = 1 + 2 (h / c)$$

Assuming that the flatwise stress distribution extends about 22 inches either side of hole centerline is seen to be quite consistent with the rotor hub shape and 57.5 inch chordal dimension.

Tension Hole Allowable Perspective

As will be seen in the discussion of the compression side hole at the end of the section, a wood or wood composite test sample with a hole in it may perform in a way which seems to largely ignore the classical effects of stress concentration. A perfect example of this is the effect of butt joints upon laminate performance. Butt joints are certainly holes in the spanwise fiber composing the laminate, and their corner radii are worse (smaller) than those for a perfectly circular hole. So we might expect the presence of butt joints to degrade laminate performance by a factor of three or even more, since three is the stress concentration factor for a circular hole. This does not occur. The worst effects are seen in fatigue, and even there the percentage reductions due to butt joints are rather modest, as shown below.

Scarf Joint Improvement on 10⁶ Cycle Butt Joint Performance

Tension-Tension	+14%
Fully Reversed	+10%
Compression-Compression	+12%

Note: See upgrade analysis for BG1 unjointed hub material

These facts argue that using classical stress concentration factors for holes in wood composite structures is a very conservative procedure in at least some known cases.

The explanation for this behavior seems to lie at least in part in the realm of scale effect i.e. the allowable for the very small high stress volume near the butt can be taken to be much higher than for the majority of the wood away from the butt. There is still a difficulty in that we consider that there is little or no scale effect in compression, and yet the hole toleration effect is still strong in compression. One can take recourse to the argument that failed fiber must still carry considerable load in compression (unlike tension) and this is surely so. Nonetheless, the matter of wood laminate's ability to tolerate holes must be regarded as rather remarkable when considered from the viewpoint of classical stress concentration factors.

As an illustrative example we can calculate the strength of the tension side hole by imagining it as a very large butt joint and using scale effect to relate its performance to the measured performance of butt jointed laminate.

Test sample butt joint volume
(0.1 x 0.1 x 6.75): 0.0675 cu.in.

Circular rotor hole volume
(12 x 18 x 22): 7128 cu.in.

Form factor (account for non-uniform
stress with depth): 0.01

Effective rotor hole volume
(7128 x 0.01): 71.3 cu.in.

Volume ratio (71.3/0.0675): 1056

Tensile fatigue scale factor
 $1056^{-0.09853}$: 0.504

Peak Tension-Tension stress
(butt-jointed laminate, 4×10^8 cycles) =3721 psi

2σ adjustment .84
10% wmc to 12% wmc adjustment .969
Temperature spectrum adjustment .975
Size effect adjustment .504

Tension Hole Fatigue Allowable	=1488 psi
--------------------------------	-----------

The basic $R = 0.1$ tension fatigue allowable derived for the BG1 hub material is:

$$1757 \times 1.17 = 2056 \text{ psi}$$

where 1757 is the allowable (in psi) for butt jointed BG2 veneer laminate and 1.17 is the upgrade factor for unjointed BG1 veneer laminate

If scaling a butt joint to 18 inch size were a valid procedure, an allowable of 1488 psi could be used against net cross-section with stress concentration effect already accounted for (since stress concentration near butt joints was present during the tests). In our analysis, we have

explicitly accounted for a stress concentration of 2.3 to 1, with an allowable of 2056 psi:

$$2056/2.3 = 894 \text{ psi (So in Figure 68)}$$

therefore,

$$894 \times 1.65 = 1475 \text{ psi}$$

where 1.65 is the average stress where a triangular distribution of concentrated stress (2.3 times the normal stress) is superimposed over the normal stress as is shown in Figure 69.

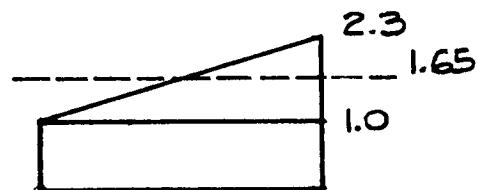


Figure 69. - Geometric Determination of Average Stress

That the 1475 psi (against net cross-section) allowable actually used in the design is so close to the 1488 psi (also against net cross-section) calculated above must be regarded as largely fortuitous since the calculations involve many approximations and simplifications. Nonetheless, it is interesting that scale effect does seem to provide some unification between two very different hole sizes, and there is some added confidence in seeing two very different methods produce similar allowable values.

Low Speed Shaft Hole - Compression Side

The rotor compression side hole has been given relatively less attention than the tension side hole for four basic reasons:

1. Compression side material in this hub operates at lower strain because the neutral axis is shifted toward the hub compression side by the thick interior buildup.
2. The compression side hole receives considerable help from the steel hole liner/teeter stop weldment which carries load across the hole.

3. Compression side failure would be gradual if it did occur.

4. Some fatigue data exists (from MOD-5A testing) which indicates that a rather modest knockdown is sufficient to account for a hole in compression.

A brief summary of the existing data on holes in compression will be given here. The work referred to was performed in support of the MOD-5A materials test program at a time when it appeared that an internal teeter with a hole through the compression side might be used. Rectangular samples 12 inches long, 6 inches wide, and 15 laminations thick (0.1 inch thick veneer) with a 2 inch diameter hole in the center were tested both statically and in fatigue. Samples were both normal fir laminate and fir laminate augmented with +/- 45 degrees fiberglass. Both unreinforced holes, and holes with a 1/8 inch fiberglass reinforcing ring were tested.

After adjustment to 12% wmc, the compressive fatigue results ($R = 0.1$) taken at 10^6 cycles were approximately as follows:

Unaugmented Laminate, Unreinforced Hole	} 4000 psi at 10^6 cycles
Augmented Laminate, Unreinforced Hole	
Unaugmented Laminate, Reinforced Hole	
Augmented Laminate, Reinforced Hole:	5000 psi at 10^6 cycles

Note: stress computed against net cross-section at 12% wmc

The 5000 psi result at 10^6 cycles is virtually the same performance level as was obtained for butt jointed laminate at 10^6 cycles during the MOD-5A test program (5011 psi at 10^6 cycles and 12% wmc). The conclusion is that the compression side hole does not show much stress concentration knockdown, particularly when augmented and in the presence of a hole liner, as this hub will be. The design margin is consequently large.

16.0 APPENDIX D - Exploratory Testing of a Wood/Epoxy/Graphite Composite Concept

Summary

In support of improving load take-off stud performance, relative to wood/epoxy composite wind turbine blade applications, a concept was proposed for increasing the elastic modulus of the laminate, by fifty percent, in the region of the studs. The proposed scheme for achieving the stiffness increase was to alternate plies of unidirectional graphite fabric with the standard plies of 0.1 inch thick Douglas fir veneer. A minimum scope test program was designed and implemented to explore the concept.

Results of testing the graphite augmented wood/epoxy laminate in compression ramp-to-failure and compression fatigue over a range of temperatures indicate that the concept is appropriate for stud applications with the only indicated limitation being at elevated temperatures. In tension stud ramp-to-failure and fatigue tests, the augmented laminate was examined relative to its interaction with a bonded stud. The results, although clouded by steel fatigue, were also encouraging. Finally, several ramp-to-failure and fatigue tests were conducted on compression samples simulating the region where the basic wood/epoxy laminate would transition (or merge) into the graphite augmented laminate. The results of these tests provide additional confidence for applications of the concept.

Background

Currently, bonded load take-off studs are utilized for the transfer of all loads from wood/epoxy composite wind turbine blades to a mating metal hub. A series of five stud designs were recommended by GBI for testing because they isolate principal variables capable of extending performance of load take-off studs while maintaining reasonable materials and manufacturing costs.

In this group of proposed stud designs, one of the designs (Design 5) assumes the use of augmented laminate, in the region of the tapered stud. The augmented laminate would have nearly a fifty percent higher elastic modulus over the baseline wood/epoxy laminate. Such a scheme would serve to reduce the elastic modulus difference between the steel studs ($E=3.0$ million psi) and the wood/epoxy laminate ($E=2.0$ to 2.2 million psi) into which the studs are bonded. Reducing this difference in modulus should serve to reduce peak shear stress levels in the epoxy. Epoxy shear failure has been the prevailing fatigue failure mechanism in all stud testing programs to date.

It is also anticipated that the one-time load carrying capability of bonded-in-studs would be enhanced because this failure mode is typically linked to the bulk laminate shear strength. The bulk laminate shear strength is also expected to improve along with the increase in bulk laminate elastic

modulus due to the introduction of parallel fibers which are higher in stiffness and strength than the wood fibers.

The use of unidirectional graphite, placed between each veneer ply and oriented parallel to the wood fiber in the laminate, was proposed by GBI for achieving the desired modulus enhancement. Because a preliminary investigation indicated that unidirectional fabric thicknesses of more than 0.015 inches (dry), when alternated between plies of Douglas Fir veneer, result in no further increase (and in some cases a decrease) in compressive strength, a fabric of nominally 0.010 inches thick was selected as the principal augmenting candidate. This determination of an optimum fabric thickness may be attributed to the compressive dependence of the thin layers of carbon fiber on the thicker wood layers for column stability. These wood layers, of a relatively constant thickness, may be limited in their ability to support slightly thicker layers of carbon fiber. To further explore this issue, very limited evaluation of a unidirectional fabric with dry thickness of 0.015 inches was conducted in this test program.

GBI was tasked with developing and executing a minimal scope test program to ensure that this graphite augmentation concept was sound.

Test Program Design

The test program matrix is shown in Table XX (Note that Tables and Figures for this appendix are included within this section). Number of samples are indicated for each defined sample configuration and test type. Control samples (containing no graphite augmentation) were also taken from each laminate billet to both characterize the laminate and to allow relative performance comparisons between graphite augmented and unaugmented laminate to be made.

Most tests were to be conducted at room temperatures (65 to 75 degrees Fahrenheit). Some ramp-to-failure and very low cycle fatigue tests were to be conducted at temperature extremes of approximately -40 and 120 degrees Fahrenheit. Tests included compression ramp-to-failure, compression fatigue, tension stud ramp-to-failure, and tension stud fatigue. All fatigue tests were to be conducted at a constant stress ratio (R) of 0.1 ($R = \text{minimum magnitude stress} / \text{maximum magnitude stress}$). Fatigue tests were to be targeted to 10,000, 100,000 and 1,000,000 cycles.

The basic compression sample design was a 2 inch thick by 2 inch wide by 8 inch high laminate block. All fiber was aligned parallel to the major dimension. The blocks would be composed of approximately 19 Douglas fir veneer plies (and 18 unidirectional graphite fiber plies if fully augmented). If augmented, the two materials would be alternated and bonded with WEST SYSTEM (R) Epoxy. Some specimens were also specified as 'augmented transition' samples and were to be only partially augmented to simulate the structural region where graphite fiber is introduced into the laminate. Details are illustrated in Figure 70 which also describes the tension stud sample and the general compression sample.

Strain measurements would be taken, on a limited basis, during compression ramp tests. The strain values would be used to confirm the elastic modulus of fully augmented and unaugmented samples. Modulus values of 2 million psi and 3 million psi were expected for the unaugmented and fully augmented laminates respectively.

Tension stud samples were designed with 48 inch laminate block lengths and with a 0.75 inch diameter, high strength steel rod, with rolled threads, bonded into each end of the block as illustrated in Figure 70. The threaded steel rod studs would serve to introduce the load to the laminate block. This would simulate the interaction between the laminate and more sophisticated load take-off stud designs (such as Design 5). To match the unaugmented and augmented laminate stiffnesses surrounding the threaded rod, different width and thickness dimensions were specified for the unaugmented (control) and the augmented laminate tension samples. These dimensions were to be 2.40 by 2.40, and 2.13 by 2.13 inches respectively.

Sample Fabrication

A total of five laminate billets (designated 1 through 5), of different dimensions were fabricated from GBI specified Blade Grade 2 (BG2), 0.1 inch thick, rotary peeled Douglas fir veneers. BG2 is the second highest structural classification for ultrasonically screened veneer used by GBI in wind turbine blade construction. Earlier tests had shown the BG2/Graphite fiber combination yielded the elastic modulus desired, namely 3 to 3.2 million psi. The principal unidirectional graphite fabric used was ORCOWEB Graphite (4.75 oz./sq. yd. and 0.010 inches dry thickness) for the augmentation in billets 1, 2, 4, and 5 which are detailed in Figure 71. Also used, but for fewer samples was FIBERITE Style W-1705 (5.86 oz./sq. yd. and 0.015 inches dry thickness) for the augmentation in billet 3 which is also detailed in Figure 71. Earlier tests had suggested that the FIBERITE Style W-1705 may have degraded fatigue performance, perhaps due to abrasion from the fiberglass fill yarns which are used to hold the fabric together. The ORCOWEB fabric has a less 'compromising' construction with no interweaving of fill fiber. The two fabrics are illustrated in Figures 72 and 73. The adhesive used in all samples was WEST SYSTEM (R) 105 Epoxy Resin and 206 Hardener. Billets were laminated under 20 to 24 inches Hg of vacuum.

Veneers for each billet were conditioned to average wood moisture contents of 5 to 8 percent. The veneers were taken at random from available BG2 inventory.

To minimize variation among test sample groups, each laminate billet was designed so that a large dispersion of variable groups would be fabricated from the same material. Furthermore, veneers were split lengthwise from billets 1, 2, and 3. One part of the split veneer was utilized for the augmented portion of the billet while the remainder went into the unaugmented portion of the billet. Again, this was done to minimize the influence of wood fiber variation. This scheme is illustrated in Figure 71.

Testing Methods

Tests were conducted both at GBI's Materials Test Laboratory and at the University of Dayton's Structural Test Laboratory (under GBI Purchase Order No. 11674). At GBI's facility, an MTS (model 810.14-2) two column, 110,000 pound load capacity, servo-hydraulic, closed loop test system was utilized to perform all tests. At the University of Dayton, a similar MTS system (STL Machine No. 2), with 50,000 pound rated load cell and hydraulic actuator, was utilized to perform all tests. Calibration of both system's electronics for accuracy of load, stroke, and strain measurements was conducted within 6 months of all tests. Typical setups are shown in Figures 74 and 75.

Five minute ramp-to-failure tests were conducted per ASTM Standard D198. The selected ramps were 8000 pounds per minute for unaugmented compression samples, 12,000 pounds per minute for augmented compression samples, 6000 pounds per minute for unaugmented tension stud samples, and 8000 pounds per minute for augmented tension stud samples. Tests were conducted at room temperatures ranging from 65 to 75 degrees Fahrenheit. A uniform failure criteria of 0.2 inch actuator deflection (from start of ramp) was established for compression tests while a similar criteria of 0.5 inches was applied to tension stud tests.

A knife edge extensometer was used over a typical gage length of 2.0 inches, on randomly selected compression samples, for measurement of strain. A total of 13 augmented and 9 unaugmented samples were evaluated for strain.

All fatigue tests were conducted at a constant stress ratio of 0.1. An 8 Hz sinusoidal load was typically applied to compression fatigue samples, while tension stud fatigue samples were typically subjected to a 4 Hz sinusoidal load. All fatigue tests were conducted under closed-loop load control. Progressive damage could, in most cases, be monitored via measurement of peak-to-peak actuator movement as a constant peak-to-peak load was applied to the sample. This feature was useful in monitoring failure trends and aided in identifying runout tests (tests which were excessively outperforming a failure prediction) which eventually required termination. Failure criteria identical to those for ramp-to-failure tests were used for fatigue samples. All fatigue tests were conducted at room temperatures ranging from 65 to 75 degrees Fahrenheit.

To minimize the cyclic fatigue stress imposed on the threaded rod used in tension stud tests, nuts were used to lightly pretension the rod against the test grips.

High and low temperature compression tests were carried out by allowing the samples to stabilize in controlled temperature environments. The samples would then be individually removed from the conditioning environment and placed in an insulating jacket before being put between the test platens. When possible, post failure temperature measurements were taken. Although

this procedure did not precisely maintain constant specimen temperature, the results still reveal the general performance trends at temperature extremes.

Test Results and Conclusions

Augmented and unaugmented samples were manufactured from the same veneers, therefore relative comparisons of results, without normalizing wood moisture content (WMC) to a standard level, are valid. For a limited number of failed ramp-to-failure compression samples, laminate moisture content (LMC) was determined. This was accomplished using the oven drying method (ASTM Method D143, Sections 124 and 125) which involves principally, the following calculation:

$$\text{LMC (\%)} = \frac{100 \times (\text{Post Test Weight} - \text{Oven Dry Weight})}{\text{Oven Dry Weight}}$$

Test results for ramp-to-failure compression tests are given in Table XXI. Test results for compression fatigue tests are presented in Table XXII and are plotted in Maximum Stress versus Total Cycle (S-N) format in Figure 76. Test results for compression samples, evaluated for elastic modulus only, are given in Table XXIIa. These results are summarized and discussed later in this section.

Test results for tension stud ramp-to-failure tests are given in Table XXIII. Test results for tension stud fatigue tests are tabulated in Table XXIV and are plotted in S-N format in Figure 77. These results are summarized and discussed later in this section.

Test results for extreme temperature compression results are included in Tables XXI and XXII. Temperature extreme fatigue results are plotted in S-N format in Figure 78. These results are summarized and discussed later in this section.

The average control laminate elastic modulus value was 2.2 million psi for billet 1 samples and 2.0 million psi for billet 2 samples. For laminate augmented with ORCOWEB Graphite, the average elastic modulus was 3.0 million psi for billet 1 samples and 2.6 million psi for billet 2 samples. For laminate augmented with FIBERITE Style W-1705 Graphite, the average elastic modulus was 3.1 million psi.

Ramp-to-failure compression results are summarized in Table XXV. The control material for billets 1, 2, and 3 performed similarly. This allowed direct comparisons to be made between the ORCOWEB Graphite (contained in billets 1 and 2) and the FIBERITE Style W-1705 (contained in billet 3). Control samples from billets 4 and 5, which were partially augmented to simulate augmented transition material, performed respectively 5 percent below and 11 percent above billet 1, 2, and 3 values.

Compressive ramp-to-failure results are characterized by relatively low scatter. Highest coefficients of variation (COV) were seen in the mixed billet 1 and 2 results. Four trends can be summarized from the results of these tests.

1. ORCOWEB Graphite augmentation provides a 38 percent static performance enhancement at room temperature, while the FIBERITE W-1705 augmentation (although based on far fewer samples) showed a 58 percent performance gain.
2. At reduced temperatures (approx. -40 deg. F), the static performance of control material was enhanced by 26 percent while the graphite augmented material static performance increased by an average of 24 percent. Reference 8 predicts a nominal 31 percent improvement in performance when going from 68 degrees to -40 degrees (Fahrenheit).
3. At elevated temperatures (approx. 120 deg. F), the performance of control material was degraded by 13 percent while the graphite augmented material performance dropped by an average of 22 percent. Reference 8 predicts a nominal 13 percent drop in performance when going from 68 degrees to 120 degrees Fahrenheit. The large performance drop for the augmented material may point to the dependence of the graphite on the wood fiber for column support.
4. The ramp-to-failure tests conducted on partially augmented samples from billet 4 performed slightly better (2%) than the control material from the same billet. Sample populations in this comparison were small, nevertheless the results indicate that the augmentation transition scheme generates no adverse stress concentrating effects for static type loads.

The compression fatigue summary (Table XXVI), suggests some significant trends. Comparing linear regression values from the developed S-N curves at 10,000 and 1,000,000 cycles shows that augmented transition material experienced an average 4 percent drop in fatigue performance from that of control laminate. This was likely due to the stress concentrating effects of terminated fibers of relatively high elastic modulus within the laminate. On the other hand, the fully augmented material performed an average of 44 percent above the control laminate in fatigue. It is also worth noting that the FIBERITE W-1705 augmented laminate typically performed near the upper end of the scatter band, dispelling much of the concern that interwoven, transverse glass fiber may contribute to an accelerated degradation of the carbon fiber. However, the observed increase in performance was not in proportion to the increase in graphite material, again indicating that a limit, in the ability of the wood laminate to support the increased graphite content, may be coming into play.

Comparisons of high and low temperature low-cycle compressive fatigue tests do show that, at reduced temperatures (approx. -40 deg. F), both unaugmented and augmented samples performed approximately 24 to 27 percent above the

room temperature trend line. At elevated temperatures (approx. 120 degrees Fahrenheit) the augmented material seemed to take a proportionately greater performance loss (approx. 22 percent) over the loss of unaugmented material (approx. 12 percent) when comparing results with room temperature trend lines. Although the test technique was unrefined, and samples were observed to be as much as 20 degrees off of their extreme temperature by the end of test, these results compare closely to the ramp-to-failure extreme temperature results.

The partially augmented (transition) sample fatigue tests yielded results which were initially a cause for concern. After manufacturing a second billet (billet 5) of partially augmented material, it was evident that the relatively poor results of the billet 4 test samples was due more to weaker wood fiber than any other factor. This is evident from the compression ramp-to-failure results of billet 4 and 5 control samples. Linear regression fatigue data trends for the partially augmented samples show that from 10,000 to 1,000,000 cycles, partially augmented laminate performed on average at 96% of the control laminate level. Therefore, it can be concluded that the stress concentrating effect of the terminated graphite fibers is very small in this configuration in fatigue.

Tension stud ramp-to-failure results are summarized in Table XXVII. The control samples showed the performance level of billet 2 samples to be lower by 14 percent relative to billet 1 samples and billet 3 samples to be lower than billet 1 samples by 9 percent. This performance level gap was slightly reduced between billet 1 and billet 2 samples (from 14 to 10 percent) following the introduction of ORCOWEB graphite as augmentation fiber into each sample group. The performance level gap between billet 1 and billet 3 samples was essentially eliminated following the introduction of FIBERITE W-1705 graphite as augmentation fiber into billet 3. If the observed reduction of variability is a consistent trend for augmented material, that would be a significant additional advantage in the use of augmented material in stress critical stud applications.

The tension stud fatigue summary, as shown in Table XXVI, was somewhat obscured by fatigue problems with the high strength steel studs. It can be seen that failures were steel dominated between 100,000 and 1,000,000 cycles which resulted in the convergence of augmented and unaugmented data. Nevertheless, the performance benefits for studs bonded into augmented laminate are clearly shown at lower cycles. Based on the linear regression curves of the augmented and unaugmented data sets, from 10,000 to 1,000,000 cycles, studs bonded into augmented laminate perform at an average load 10 percent higher than studs bonded into unaugmented laminate. On a basis of stress level, this performance gain is increased to 39 percent due to the smaller cross section of the augmented tension samples.

Upon completion of this concept qualification test program, it was recommended to NASA that the benefits of graphite augmenting of wood/epoxy laminate were substantial. Therefore, the advanced load take-off stud design based on such augmented laminate could be tested with confidence that the laminate performance and stud interfacing behavior were sound.

TABLE XX. - GRAPHITE AUGMENTED WOOD/EPOXY LAMINATE TEST MATRIX

(Number of Samples)

Test Type	SAMPLE CONFIGURATION (Reference Figure 70)		
	Control (No Augmentation)	Transition Laminate* (Partially Augmented)	Fully Augmented Laminate*
Compression Ramp-to-Failure At Room Temperature	17	2	12(2)**
Compression Ramp-to-Failure at -40°F	7	0	5
Compression Ramp-to-Failure At 120°F	11	0	9
Compression Fatigue Target 10 ⁴ Cycles At Room Temperature	3	2	3(1)**
Compression Fatigue Target 10 ⁴ Cycles At -40°F	4	0	2
Compression Fatigue Target 10 ⁴ Cycles At 120°F	4	0	2
Compression Fatigue Target 10 ⁵ Cycles At Room Temperature	2	5	2(1)**
Compression Fatigue Target 10 ⁶ Cycles At Room Temperature	2	6	4(1)**

*Unless otherwise noted, augmenting fabric is ORCOWEB Graphite

**Value in brackets is the number of samples using Fiberite W-1705 Graphite

TABLE XX. (continued) - GRAPHITE AUGMENTED WOOD EPOXY LAMINATE TEST MATRIX

(Number of Samples)

Test Type	SAMPLE CONFIGURATION (Reference Figure 70)	
	Control (No Augmentation)	Fully Augmented Laminate*
Tension Stud Ramp-to-Failure At Room Temperature	6	6(2)**
Tension Stud Fatigue Target 10^4 Cycles At Room Temperature	2	3
Tension Stud Fatigue Target 10^5 Cycles At Room Temperature	2	2(1)**
Tension Stud Fatigue Target 10^6 Cycles At Room Temperature	2	2

*Unless otherwise noted, augmenting fabric is ORCOWEB Graphite

**Value in brackets is the number of samples using Fiberite W-1705 Graphite

Table XXI. - COMPRESSION RAMP-TO-FAILURE RESULTS
UNGAUGMENTED SAMPLES

Specimen Number	Weight (pounds)	Crosssection (inches ²)	Length (inches)	Laminate Moisture Content (percent)	Ultimate Stress (psi)	Test Temperature (°F)	Ramp Length (secs)
1-10F	.588	3.48	7.44	NM*	10,310	75	300
1-9G	.584	3.53		NM	10,500		
1-10H	.586	3.52		5.3	9,540		
1-9I	.588	3.52		NM	10,160		
1-9J	.586	3.52		NM	10,210		
2-9D	.538	3.50		5.0	9,100		
2-9E	.535	3.49		NM	9,040		
2-10F	.535	3.49			8,740		
2-9G	.532	3.47			8,960		
2-9J	.528	3.48			9,180		
3-4A	.556	3.51	7.47		9,850		
3-4C	.552	3.50	7.44	5.6	9,340		
4-4A	.680	4.03	8.00	NM	9,150		
4-2D	.672	4.01			9,000		
5-2D	.726	3.99			10,730		370
5-3D	.733	4.00			10,720		370
5-5D	.718	4.02			10,510		360
1-9A	.588	3.53	7.44		8,650	123	300
1-9D	.589	3.53			8,600	120	
1-9B	.586	3.53			8,750	124	
1-10L	.592	3.51			9,140	119	
1-10A	.586	3.50			8,690	120	
1-10D	.591	3.47			8,620	121	
2-10D	.539	3.48			7,540	120	
2-9I	.528	3.49			7,810	120	
2-9K	.529	3.49			7,800	121	
2-10A	.549	3.50			7,900	121	
2-9L	.540	3.52			7,640	121	
1-9E	.585	3.53			12,990	-40 to -23	200
1-9L	.587	3.53			12,580	-16	380
1-10E	.590	3.47			13,210	-22	390
2-9A	.543	3.51			11,770	-30	180
2-9H	.528	3.50			11,050	-27	330
2-10B	.546	3.48			11,420	-23	340
2-10L	.544	3.51			11,120	-17	330

*Not measured

TABLE XXI. (continued) - COMPRESSION RAMP-TO-FAILURE RESULTS
FULLY AND PARTIALLY AUGMENTED (TRANSITION) SAMPLES

Specimen Number	Weight (pounds)	Crosssection (inches ²)	Length (inches)	Laminate Moisture Content (percent)	Ultimate Stress (psi)	Test Temperature (°F)	Ramp Length (secs)	Fabric Type
1-2F	.665	3.50	7.44	NM	14,870	75	300	ORCOWEB
1-1G	.650	3.51			14,260			
1-2H	.660	3.51			14,470			
1-1J	.641	3.50		4.9	13,950			
2-2C	.599	3.47		4.5	13,040			
2-1E	.579	3.52		NM	11,830			
2-2F	.605	3.50			12,420			
2-1G	.577	3.48			11,910			
2-2K	.611	3.49			12,670			
2-1B	.591	3.51			12,390			
3-1C	.641	3.51	7.47		16,320			FIBERITE
3-1E	.640	3.52	7.44	4.7	13,990			ORCOWEB
4-4B*	.708	4.03	8.00	NM	9,260			
4-3C*	.704	4.02	8.00		9,270			
1-1B	.648	3.50	7.44		10,520	121		ORCOWEB
1-1E	.658	3.53			10,990	122		
1-2K	.645	3.50			10,760	114		
1-2B	.667	3.51			11,800	120		
1-2D	.664	3.51			12,510	121		
2-2H	.610	3.51			9,270	120		
2-1J	.587	3.51			8,280	120		
2-1I	.584	3.50			9,270	121		
2-1K	.598	3.54			9,330	121		
1-1D	.656	3.52			16,940**	-40 to -20	510	ORCOWEB
1-1I	.653	3.51			16,950**			
1-2C	.659	3.50			17,030**		230	
2-2D	.606	3.49			15,600		490	
2-2I	.613	3.49			15,030			

* Partially Augmented
** Specimen Strength Exceeded
Test Machine Capability

TABLE XXII. - COMPRESSION FATIGUE RESULTS
UNGAUGMENTED SAMPLES (R = 0.1)

Specimen Number	Weight (pounds)	Crosssection (inches ²)	Length (inches)	Elastic Modulus @ 75°F (million psi)	Maximum Compressive Stress (psi)	Test Temp (°F)	Accumulated Cycles	Test Frequency (Hertz)
1-9H	.590	3.53	7.44	NM	8,600	75	31,970	10
2-10E	.542	3.49			7,910		11,960	
3-4B	.558	3.52			8,140		15,328	
1-10I	.590	3.52			7,850	120	4,307	8
1-10B	.585	3.49			7,640		10,233	
2-10I	.539	3.53			7,580		5,578	
2-10K	.538	3.49			6,720		15,499	
1-9K	.591	3.52			10,190	-40 to -20	16,400*	
1-10K	.602	3.51			10,690		24,100	
2-9B	.540	3.49			10,270		300	
2-10H	.538	3.52			10,650		900	
1-9F	.587	3.54	7.47	2.30	8,38	75	281,400	
2-10G	.543	3.51		2.00	7,660		307,900	
1-10G	.588	3.51		2.30	8,020		3,632,400 ⁺	
2-9F	.532	3.50		2.00	6,940		5,185,700 ⁺	

*No Failure, Test Terminated Due to Specimen Warming

+No Failure, Test Terminated

TABLE XXII. (continued) - COMPRESSION FATIGUE RESULTS
FULLY AND PARTIALLY AUGMENTED SAMPLES (R = 0.1)

Specimen Number	Weight (pounds)	Crosssection (inches ²)	Length (inches)	Elastic Modulus @ 75°F (million psi)	Maximum Compressive Stress (psi)	Test Temp (°F)	Accumulated Cycles	Test Frequency (Hertz)
1-1H	.649	3.52	7.44	NM	12,240	75	13,658	10
2-2E	.601	3.48	→	→	10,720	→	9,961	→
3-1B	.642	3.48	→	→	12,160	→	15,946	→
1-2E	.663	3.51	→	→	9,980	120	7,856	8
2-1H	.575	3.50	→	→	7,630	120	3,444	→
1-2I	.672	3.51	7.47	→	14,640	-40 to -20	10,000**	→
2-1D	.581	3.51	→	→	14,640	-40 to -20	5,900	→
1-1F	.663	3.52	→	3.10	11,860	75	1,316,600	→
1-2G	.656	3.49	→	2.90	12,130	→	4,209,500	→
2-1F	.574	3.49	→	2.50	10,320	→	37,800	→
2-2G	.614	3.50	→	2.50	10,330	→	1,534,300	→
3-1D	.639	3.51	→	3.00	12,300	→	64,200	→
3-1F	.644	3.52	→	3.20	11,500	→	4,269,000+	→
4-5B*	.711	4.02	8.00	NM	7,970	→	29,800	→
4-2B	.690	4.02	→	→	7,970	→	21,592	→
4-2C	.695	4.02	→	→	7,690	→	53,900	→
4-4C	.709	4.02	→	→	7,690	→	74,500	→
4-3B	.699	4.02	→	→	7,510	→	91,500	→
4-1B	.693	4.01	→	→	7,250	→	82,000	→
4-5C	.716	4.02	→	→	7,000	→	274,100	→
4-1C	.694	4.02	→	→	6,500	→	10,105,500	→
5-1C	.740	3.99	→	→	8,300	→	989,400	→
5-2C	.748	4.03	→	→	7,780	→	5,592,100	→
5-3C	.752	4.03	→	→	7,680	→	6,087,700	→
5-4C	.747	4.04	→	→	8,300	→	1,119,200	→
5-5C	.733	4.02	→	→	8,200	→	3,442,800	→

* Partially Augmented

** Sample Began to Warm, Test Terminated

+ No Failure, Test Terminated

TABLE XXIIa. - COMPRESSION ELASTIC MODULUS MEASUREMENTS

Sample No.	Type	Elastic Modulus (million psi)
2-10C	Control (Unaugmented) ↓	2.10
2- 9C		2.00
2-10J		2.00
1-10J		2.30
1- 9C		2.20
2- 2B	Augmented (ORCOWEB) ↓	2.60
2- 1C		2.40
2- 2J		2.90
1- 2J		2.80
1- 1C		3.10
1- 1K	(FIBERITE) ↓	3.10
3- 1A		3.10

TABLE XXIII. - TENSION RAMP-TO-FAILURE RESULTS

AUGMENTED AND UNAUGMENTED SAMPLES

Specimen Number	Crosssection (inches ²)	Length (inches)	Pullout Load (pounds)	Test Temperature (°F)	Ramp Length (secs)	Failure Mode	Augmentation Type
1-6G	5.76	48.00	36,550	75	300	Wood/Shear	None
1-8A			36,100				
2-6A			30,850				
2-8A			31,550				
3-3A			32,600				
3-4G			33,250				
1-5G	4.54	48.00	41,500	75	300	Wood/Shear	ORCOWEB
1-3A			42,400				
2-3G			36,700				
2-5A			39,150				
3-2A			42,200				
3-1G			41,750				FIBERITE

TABLE XXIV. - TENSION FATIGUE RESULTS
AUGMENTED AND UNAUGMENTED SAMPLES (R = 0.1)

Specimen Number	Crosssection (inches ²)	Length (inches)	Maximum Tensile Load (pounds)	Test Temperature (°F)	Accumulated Cycles	Test Frequency (Hertz)	Failure Mode
1-8G	5.76	48.00	24,000	75	44,340	3.0	Epoxy/Shear
2-7A			19,000		288,610	3.5	Epoxy/Shear
1-7G			19,000		323,670 ⁺	3.5	Stud
1-7A			19,000		436,780 ⁺	3.5	Stud
2-8A			17,000		479,510 ⁺	4.0	Stud
2-7G			24,000		8,127	3.3	Lam./Shear
1-3G	5.76	48.00	24,000	75	115,450	3.0	Epoxy/Shear
2-4G			24,000		46,870	3.0	Lam./Shear
1-4G			28,000		40,100	3.5	Epoxy/Shear
2-4A			28,000		19,650	3.5	Epoxy/Shear
3-2G			24,000		149,030	3.5	Stud
1-4A			19,000		319,460 ⁺	4.0	Stud
2-3A			17,000		781,820 ⁺	4.0	Stud

⁺ No Failure, Test Terminated

TABLE XXV. - SUMMARY OF RAMP-TO-FAILURE COMPRESSION TESTS DATA ANALYSES
FOR GRAPHITE AUGMENTED, WOOD/EPOXY LAMINATE TESTS
(300 Sec Ramps, Data Unadjusted to Standard Wood Moisture Content)

Sample Configuration	Number of Samples	Mean Ultimate Stress	Coefficient of Variation*	Percent of Billet 1 & 2 Control Lam. Performance
Control - Billets 1 & 2 At Room Temp	10	9570 psi	0.068	---
Control - Billet 3 At Room Temp	2	9600	0.037	100
Control - Billet 4 At Room Temp	2	9080	0.011	95
Control - Billet 5 At Room Temp	3	10650	0.012	111
Control - Billets 1 & 2 At ~ 120°F	11	8290	0.066	87
Control - Billets 1 & 2 At ~ -40°F	7	12020	0.075	126
Fully Augmented - Billets 1 & 2 At Room Temp	10	13180	0.085	138
Fully Augmented - Billet 3 At Room Temp	2	15150	0.108	158
Fully Augmented - Billets 1 & 2 At ~ 120°F	9	10300	0.133	108
Fully Augmented - Billets 1 & 2 At ~ -40°F	5	16310 ⁺	0.057	170 ⁺
Partially Augmented - Billet 4	2	9270	0.001	97

* C.O.V. = Stand. Deviation/Mean Stress

+ Three Samples Exceeded Machine Capability

TABLE XXVI. - SUMMARY OF FATIGUE DATA ANALYSES
FOR GRAPHITE AUGMENTED, WOOD/EPOXY LAMINATE TESTS

(TESTS CONDUCTED AT ROOM TEMP, R = 0.1, DATA UNADJUSTED TO STANDARD WMC)

Sample Configuration	Number of Samples	No. Runouts Included in Regression	Equation of Linear Regression Line	Stress (or Load) Intercept	
				At 10 ⁴ Cycles	At 10 ⁶ Cycles
Compression Unaugmented	7	2	$S = -9471 + \log N \cdot 287.6$	-8320 psi	-7744 psi
Compression Aug. Transition Samples	13	1	$S = -8047 + \log N \cdot 65.3$	-7785	-7655
Compression Fully Augmented	9	1	$S = -11511 + \log N \cdot 0.73$	-11,508	-11,506
Tension Stud Unaugmented	6	2	$S = 38,362 - \log N \cdot 3449$	24,566 lbs (4265 psi)	17,669 lbs (3068 psi)
Tension Stud Fully Augmented	7	2	$S = 57,589 - \log N \cdot 6778$	30,476 lbs (6713 psi)	16,920 lbs (3727 psi)

TABLE XXVII. - SUMMARY OF RAMP-TO-FAILURE TENSION STUD TESTS DATA ANALYSES
FOR GRAPHITE AUGMENTED, WOOD/EPOXY LAMINATE TESTS
(300 SEC RAMPS, DATA UNADJUSTED TO STANDARD WMC)

Sample Configuration	Test Population	Mean Ultimate Stress	Percent of Billet 1 Control Laminate Performance
Control - Billet 1	2	36,325 lbs/6306 psi ¹	-----
Control - Billet 2	2	31,200 lbs/5417	86 (86) ²
Control - Billet 3	2	32,925 lbs/5716	91 (91)
Fully Aug - Billet 1	2	41,950 lbs/9240	115 (147)
Fully Aug - Billet 2	2	37,925 lbs/8354	104 (132)
Fully Aug - Billet 3	2	41,975 lbs/9246	116 (147)

¹ Lam. Crosssection for Controls = 5.76 sq.in., Augmented = 4.54 sq.in.

² lbs basis (psi basis)

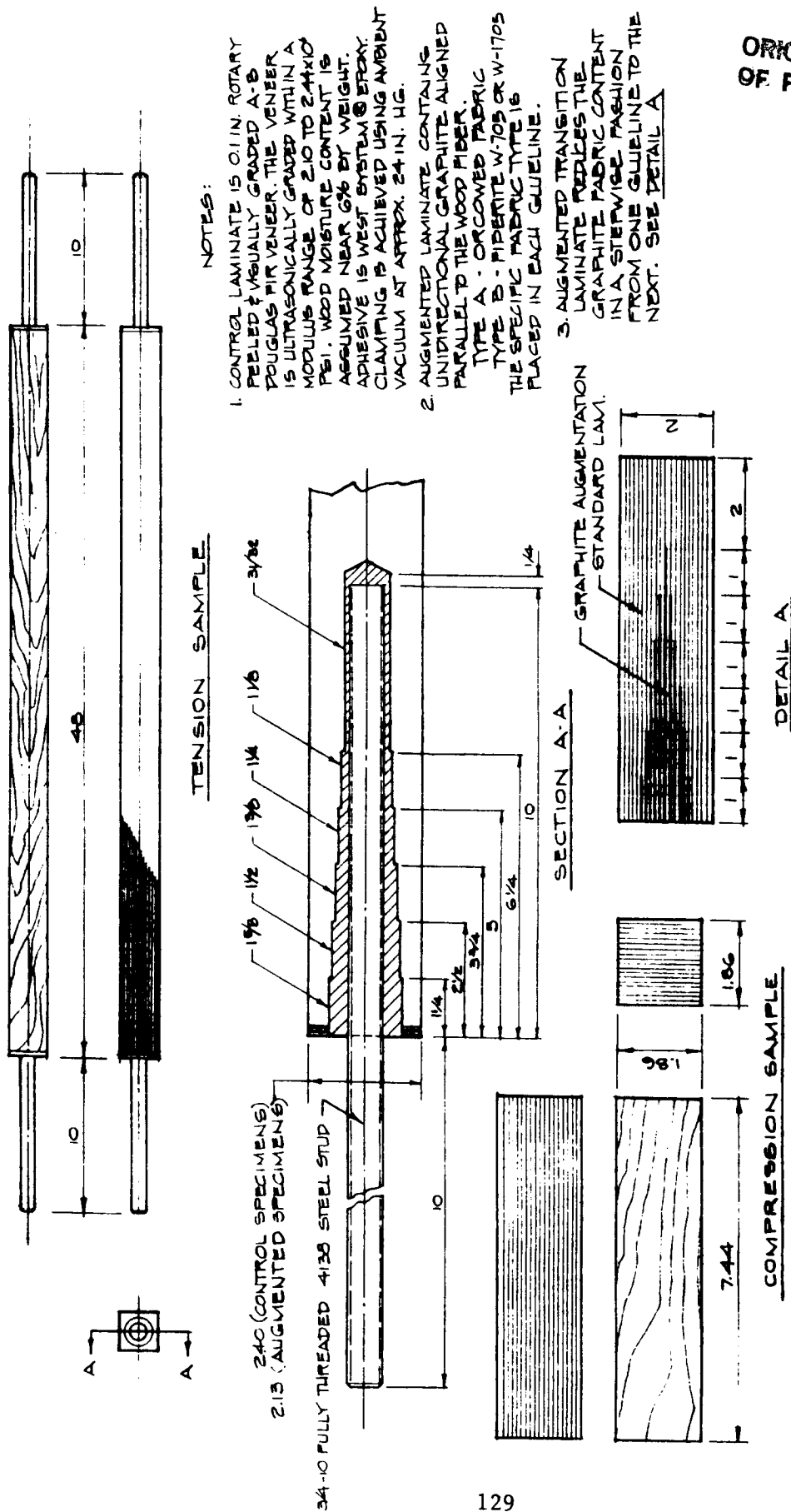


Figure 70. - Compression Sample and Tension Stud Sample Details

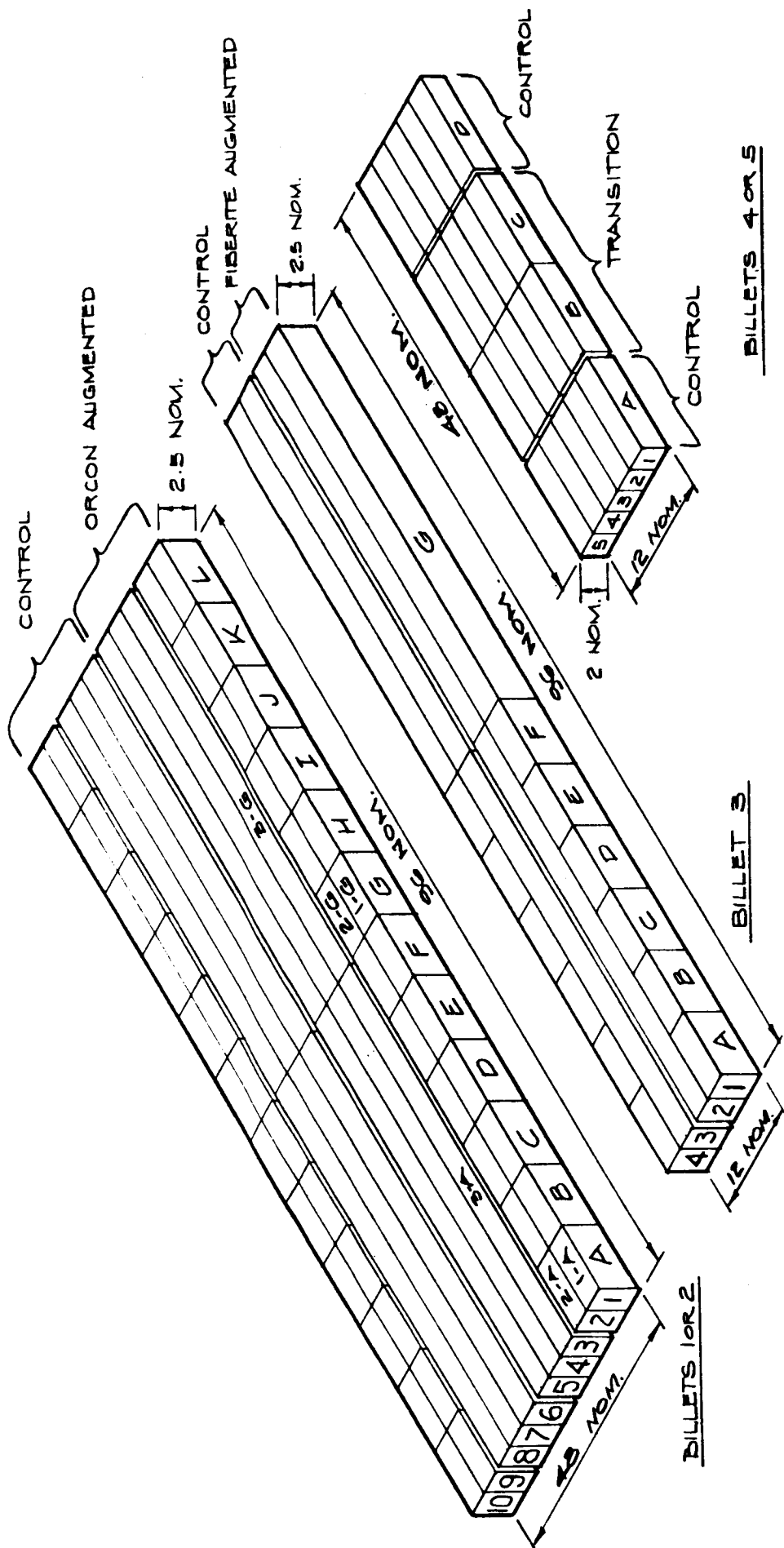
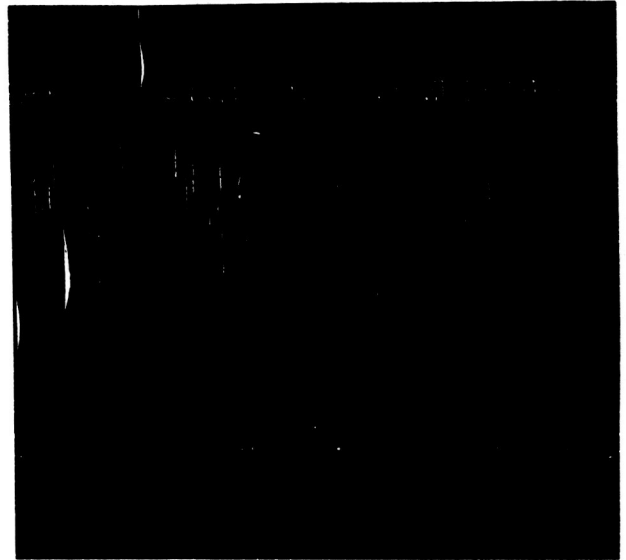


Figure 71. - Laminate Billet Partitioning Scheme



Side A



Side B

Figure 72. - ORCOWEB Graphite Cloth (4.75 oz/sq yd, 0.010 in dry thickness)

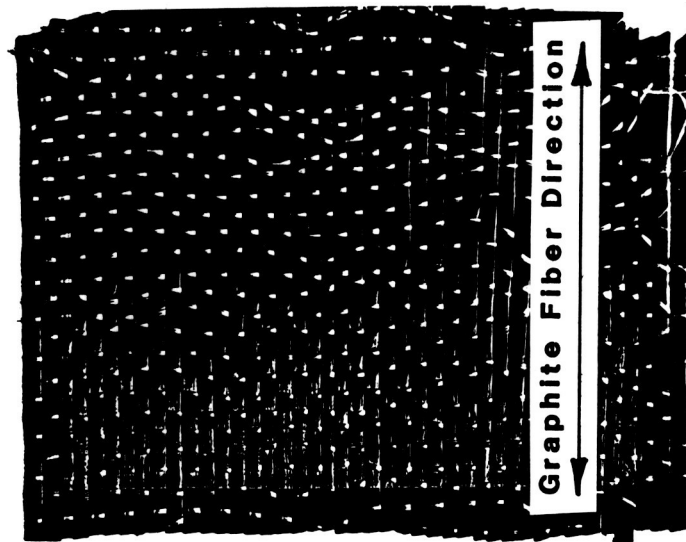


Figure 73. - FIBERITE Style W-1705 Graphite Cloth (5.86 oz/sq yd, 0.015 in dry thickness)

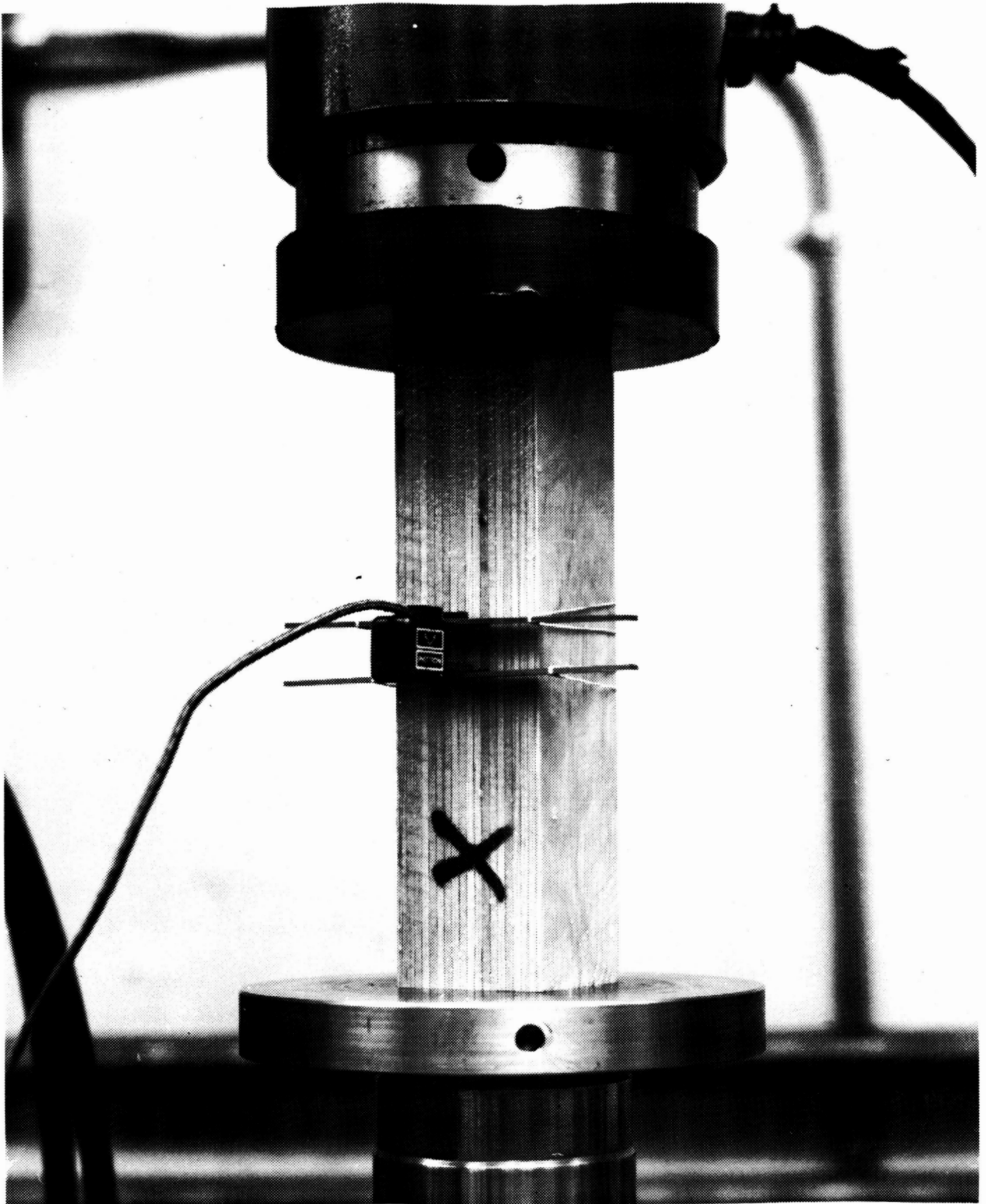


Figure 74. - Typical Compression Test Set-Up, Mounted Extensometer Shown

ORIGINAL PAGE IS
OF POOR QUALITY

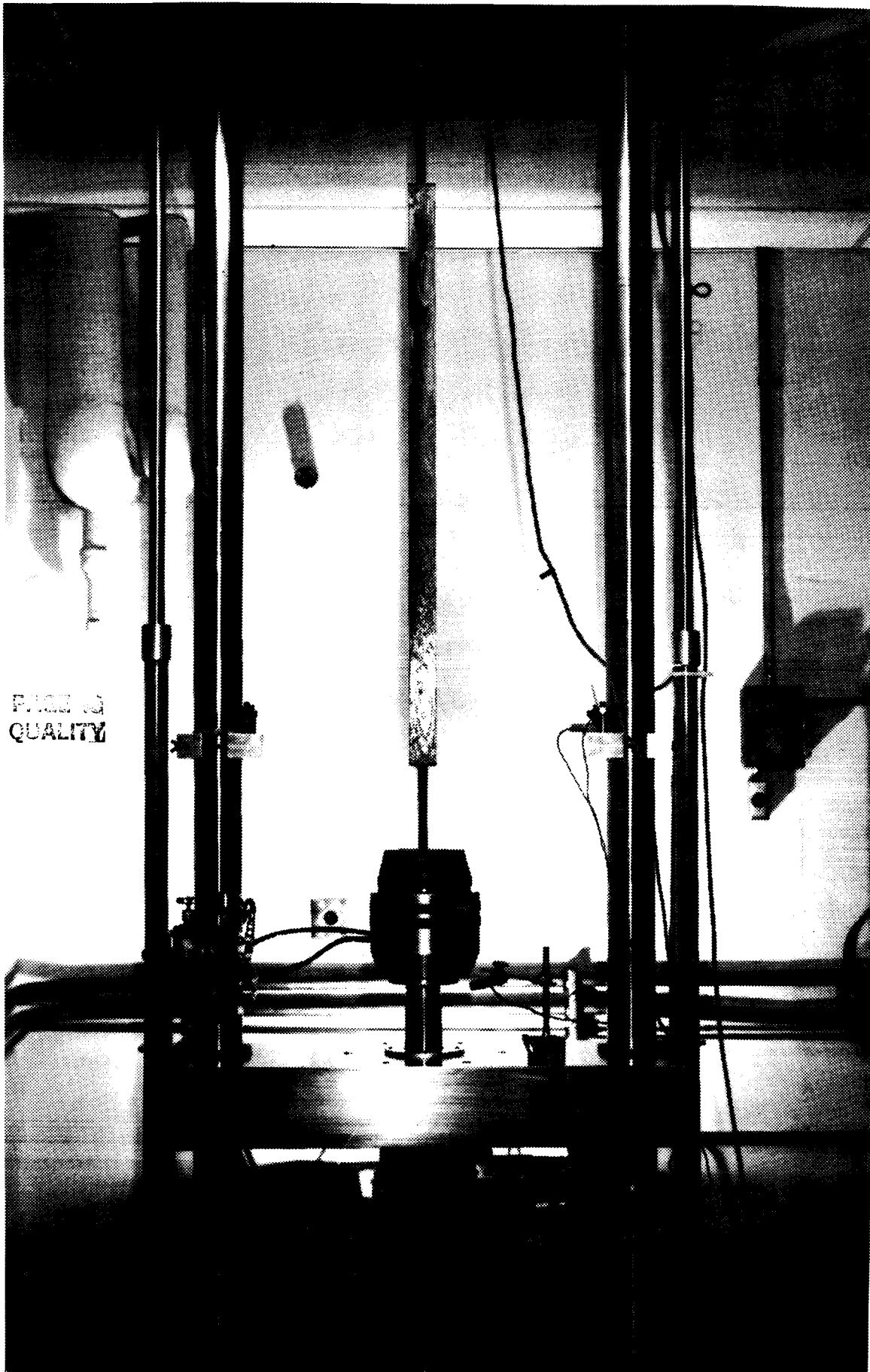


Figure 75. - Typical Tension Test Set-Up

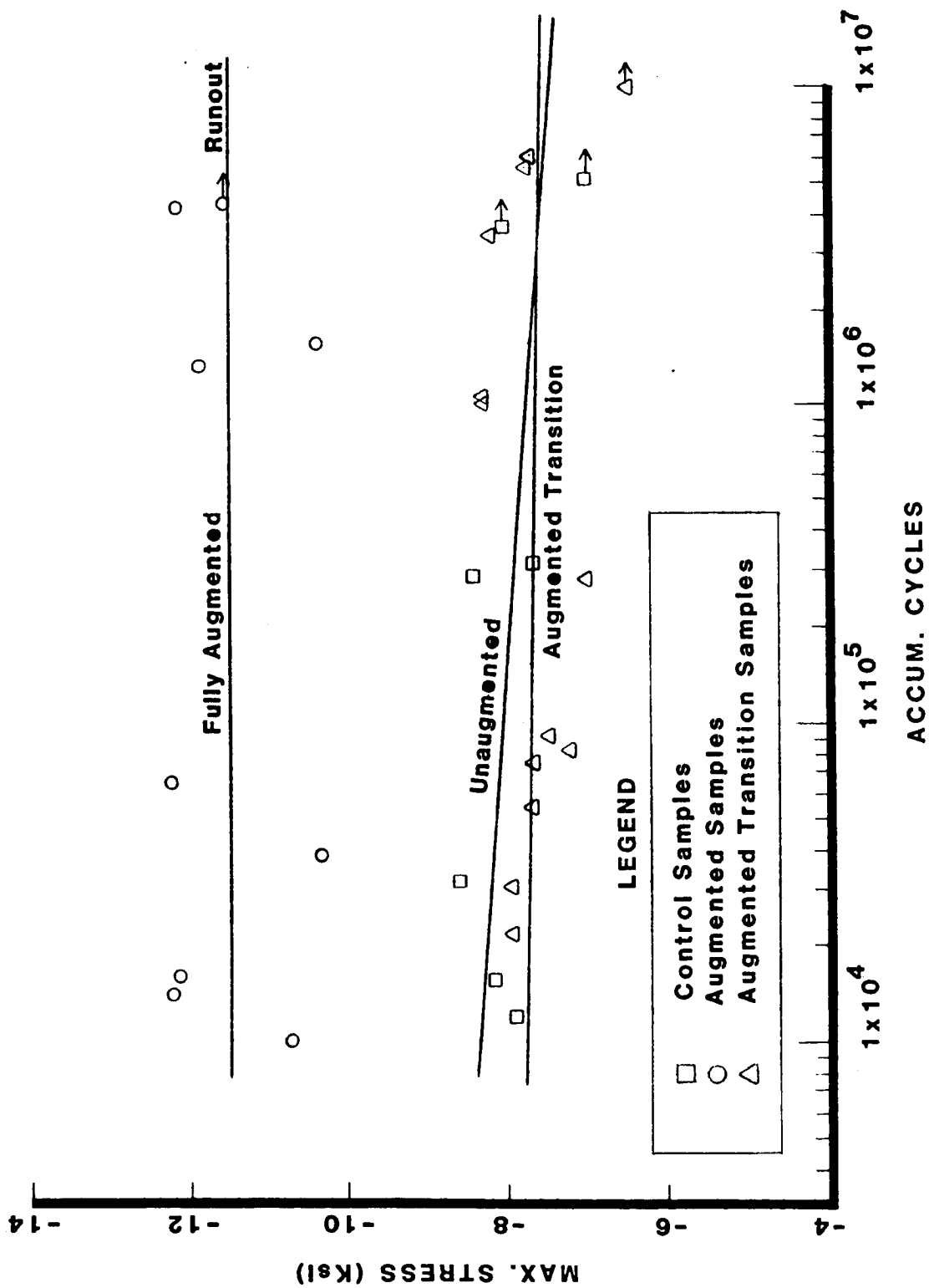


Figure 76. - Augmented Composite Qualification Tests, Compression Fatigue Results (R.1)

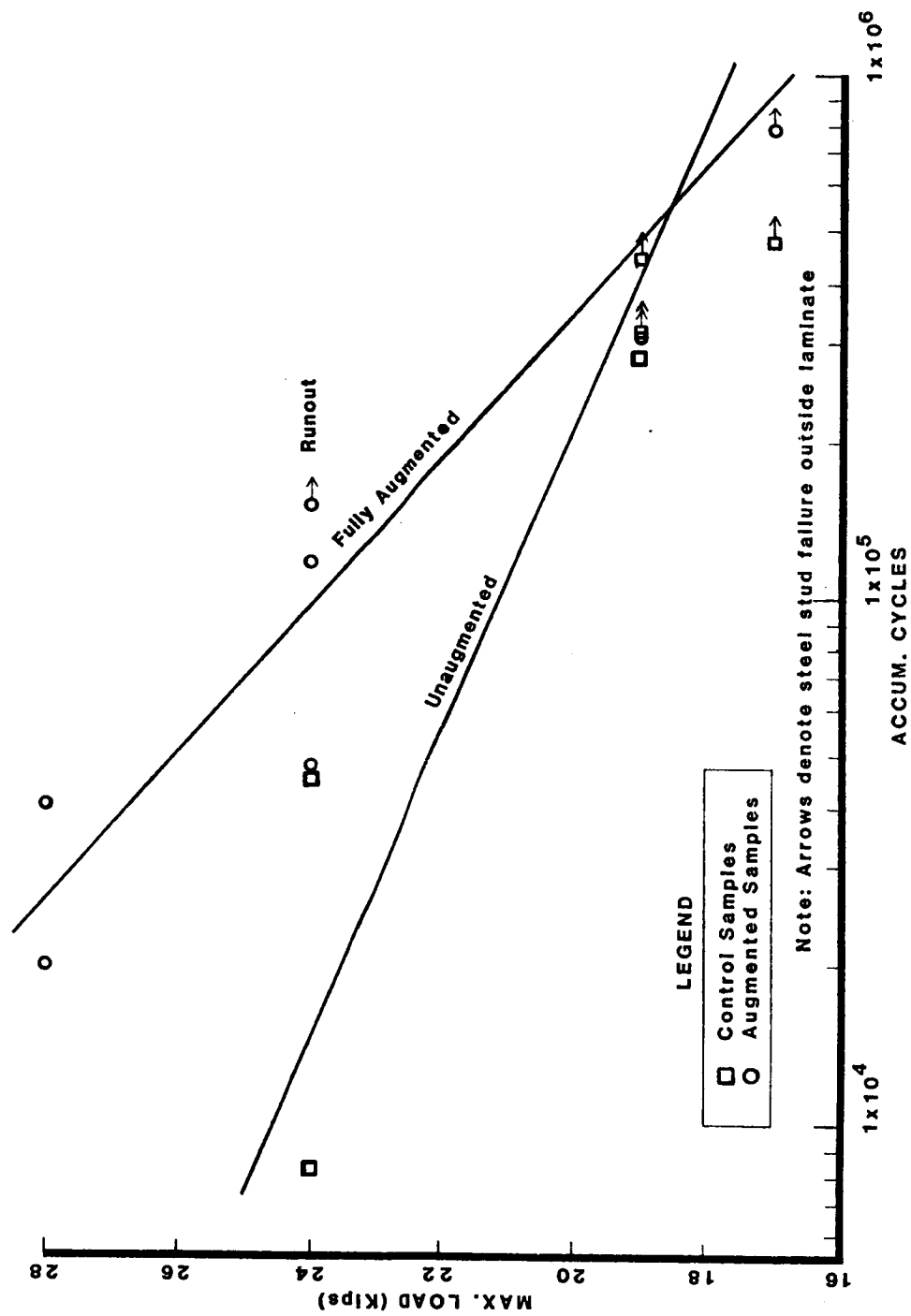


Figure 77. - Augmented Composite Qualification Tests, Tension Fatigue Results (R.1)

17.0 APPENDIX E - An Evaluation of Wood/Epoxy Laminate with Scarf Jointed Plies in Compression

Summary

An exploratory test program was designed and implemented by Gougeon Brothers, Inc. (GBI) to investigate the performance of wood/epoxy laminate featuring staggered scarf jointed plies in compression. Tests were conducted in ramp-to-failure and cyclic fatigue. Variables examined were scarf joint slope and non-optimum scarfs. The non-optimum scarfs featured joint overrides or gaps of two different magnitudes.

As expected, shallower slope scarf joints outperformed steeper sloped joints, particularly in fatigue. Other tests suggest that fairly substantial scarf overrides degrade compressive fatigue performance insignificantly relative to ideal joints. On the other hand, gaps or less substantial overrides seem to degrade performance noticeably relative to ideal joints.

Background

Contract DEN3-260 was awarded with one of its objectives being that of developing wood composite blade technology. A concurrent DOE/NASA program, the design of the MOD-5A rotor, was taxing the limits of the wood composite materials data base. Existing design allowables data were predominantly established from wood composite samples featuring plies with either no joints or staggered butt joints. Under fatigue conditions, especially tension fatigue, it was evident that damage originated frequently in the butt joints of individual plies.

Within the context of this contract's goals, as well as supporting possible needs of the MOD-5A rotor, some testing of laminate featuring scarf-jointed plies was of considerable interest. At the same time, some testing of scarf jointed plies had been conducted within the framework of the MOD-5A program. That testing concentrated on optimum 12:1 slope scarfs. It also evaluated, to a lesser degree, the effect of various quality joints and the effect of high moisture content on the performance of laminate with scarf jointed plies. A report of those tests is being generated under the MOD-5A program.

The thrust of this test program was to evaluate scarfs of three different slopes, nominally 4:1, 10:1, and 16:1. It was expected that this data could aid in determining whether the expected higher performance of shallower slope scarfs would justify the increased handling difficulty of veneer with more damage prone edges. In addition, future tolerancing of manufacturing processes would be aided by knowing which deviations from optimum assembly of plies would least adversely influence the performance of the laminated structure. Therefore testing of 10:1 slope scarfs with 0.25 and 0.50 inch gaps and overlaps was also undertaken.

Compression tests were proposed primarily due to lower specimen cost. Nevertheless, compression tests were expected to offer useful insights into the performance of laminate with scarf jointed plies. Compression testing tends to yield results which are less sensitive to ply joint configuration than are tension test results.

Test Program Design

The test program matrix is shown in Table XXVIII (Note that Tables and Figures for this appendix are included within this section). Numbers of samples are indicated for each defined sample configuration and test type. Control samples (containing no scarf joints) were also taken from each laminate billet to both characterize the laminate and to allow relative performance comparisons of scarf jointed laminate to be made.

All testing was to be conducted at room temperatures (65 to 75 degrees Fahrenheit). Tests prescribed included compression ramp-to-failure, and compression fatigue tests with a constant stress ratio (R) of 0.1 (R = minimum magnitude stress/maximum magnitude stress). Fatigue tests were to be targeted to 10,000, 100,000 and 1,000,000 cycles.

The basic sample design was a 2 inch thick by 2 inch wide by 12 inch tall laminate block. Grain was to be aligned parallel to the major dimension. The block would be composed of 19 to 20 Douglas fir veneer plies and WEST SYSTEM (R) Epoxy. The middle three plies would each have a single scarf joint (except control samples). The middle ply would have a scarf joint centered 6 inches from each end of the sample. Each adjacent ply would also contain a single scarf joint, staggered on centers 3 inches from the center scarf joint such that each scarf joint center would be nominally three inches from the next scarf joint center. This essentially symmetrical configuration, as shown in Figure 79, simulates a typical volume taken from structural laminate assembled with scarf joints.

Sample Fabrication

Two billets (designated NA and NB) of test laminate (nominally 96 inches by 24 inches by 2.1 inches) were fabricated from GBI specified Blade Grade 1 (BG1), 1/10th inch thick, rotary peeled Douglas fir veneers. BG1 is the highest structural classification for ultrasonically screened veneer used by GBI in wind turbine blade construction. The adhesive used was WEST SYSTEM (R) 105 Epoxy Resin and 206 Hardener. Billets were laminated under 24 inches (mercury) of vacuum.

Veneers for each billet were conditioned to average wood moisture contents of 7.4 and 7.1 percent for billets NA and NB respectively. Although the veneers were generally taken at random from available BG1 veneer inventory, individual veneers were weighed and assigned to the two billets on an equitable basis to minimize density variation.

To further minimize variation among test sample groups, each laminate billet was designed so that a large dispersion of variable groups would be fabricated from the same material. This scheme is illustrated in Figure 80.

The scarf joint detail is generalized in Figure 81 for non-optimum scarf joints.

Testing Methods

Compression ramp-to-failure and cyclic fatigue tests were all conducted at GBI's Materials Test Laboratory. An MTS (Model 810.14-2) two column, 110,000 pound load capacity, servo-hydraulic, closed-loop test system was utilized to perform all tests. Calibration of the system electronics for accuracy of both load and stroke measurements was conducted within 6 months of all tests.

Five minute ramp-to-failure tests were conducted per ASTM Standard D198. The selected ramp was 7900 pounds per minute. Tests were conducted at room temperatures ranging from 64 to 72 degrees Fahrenheit. A uniform failure criterion of 0.2 inch actuator deflection (from start of ramp) was established.

Compression fatigue tests were conducted at a constant stress ratio of 0.1. A 6 Hz sinusoidal load was applied to the fatigue test samples while under closed-loop load control. Progressive damage could be monitored via measurement of peak-to-peak actuator movement as a constant peak-to-peak load was applied to the sample. This feature was useful in establishing failure trends and aided in identifying runout tests (tests which were excessively outperforming a failure prediction) which required termination. A failure criterion identical to that for ramp-to-failure tests was used for fatigue samples. All fatigue tests were conducted at room temperatures ranging from 64 to 75 degrees Fahrenheit.

A typical test configuration is illustrated in Figure 82. A typical failed sample is shown in Figure 83.

On a selected basis, laminate moisture content (LMC), of failed ramp-to-failure and fatigue specimens, was determined using oven drying method (ASTM Method D143, Sections 124 and 125). LMC is lower than the expected wood moisture content due to the presence of epoxy adhesive in the bulk mass being evaluated. This value of wood fiber weight to total laminate weight typically is 82 percent. Therefore a general conversion of LMC to wood moisture content (WMC) can be made by multiplying WMC by a factor of 1.22. LMC is computed by the following method:

$$\text{LMC (\%)} = \frac{100 \times (\text{Post Test Weight} - \text{Oven Dry Weight})}{\text{Oven Dry Weight}}$$

Test Results and Conclusions

Based on available LMC data shown in Table XXIX, it can be seen that little variation existed from sample to sample. Nevertheless, test result stress levels have all been adjusted to a nominal WMC value of 12% in an attempt to reduce the effect of moisture content variation. This adjustment also allows data to be compared to other wood composite data which has been similarly corrected. This adjustment is documented at the end of this section.

Test results for ramp-to-failure tests are given in Table XXIX. Test results for fatigue tests are tabulated in Table XXX and are plotted in Maximum Stress versus Total Cycle (S-N) format in Figures 84 and 85. These results are summarized and discussed later in this section.

For the purpose of improving the quality of comparative conclusions, samples taken along similar longitudinal portions of the billets were targeted to similar cycles-to-failure. This selection of specific billet locations was such that near one edge of each billet, samples were typically targeted to the lowest number of cycles-to-failure while at the other end samples were typically targeted to the highest number of cycles-to-failure. Because on billet NA the laminate strip from which low cycle samples were taken was generally weaker than the laminate strip from which high cycle samples were taken, the slope of the S-N curves tend to be artificially low. Larger sample populations and more random sample selection would remedy this.

Ramp-to-failure results are summarized in Table XXXI. The results of control sample tests reveal a somewhat higher level of performance (4.6%) from billet NB when compared to billet NA controls. Ramp-to-failure samples featuring 10:1 scarfs with 0.50 inch overlaps were also tested from each billet and showed a somewhat more modest (2.1%) performance difference. Again, NB samples outperformed NA samples.

Ramp-to-failure results are characterized by relatively low scatter even with small populations. Nevertheless, ramp-to-failure results provide less dramatic conclusions than do fatigue results. Two trends are detectable:

1. Shallower slope scarf joints seem to offer slightly better static performance.
2. Overlap defects are better tolerated than are gap defects.

Compression fatigue results as shown in Table XXXII, although also clouded somewhat by scatter and small populations, suggest more significant trends. A comparison of non-scarf jointed (control) results to the results from different scarf jointed plies, is consistent with intuitive expectations of improved performance with shallower scarf slopes. Comparing linear regression values from the developed S-N curves at 10,000 and 1,000,000 cycles shows that 4:1 scarfed material performed at 86 percent of the

control material level. Similar comparisons show 10:1 scarfed material performing at 94 percent of control while the 16:1 material performed at 99 percent of control.

Performance comparisons of 10:1 scarfed material with overlaps and gaps also is consistent with expectations. Samples with 50% scarf overlaps performed at 96 percent of the level of unscarfed samples using the same comparison criteria described for the comparison of 4:1, 10:1, and 16:1 scarfed material. This value is essentially the same as the 94 percent value for optimum 10:1 scarfed material. On the other hand, 10:1 scarfed material with 50% gaps performed at 91 percent of the level of unscarfed samples. The net performance difference between 50% overlapped and gapped samples is 6 percent, in favor of the overlapped samples. Even with the relatively small sample populations, it is reasonable to view this result to be significant due to the consistent relationship of the linear regression curves of both data groups.

Sample populations of 10:1 scarfed material with 25% overlaps and gaps were extremely small, and therefore these results must be interpreted in very general terms. The samples with 25% gaps and overlaps tended to perform more in line with the 50% gap samples.

Three conclusions of reasonable significance can be drawn from the fatigue tests:

1. Compressive fatigue performance of material with 16:1 scarf jointed plies approaches the performance of material without joints. 10:1 (and steeper) scarf jointed plies show apparent degradations in compressive fatigue performance.
2. The compressive fatigue performance of material with 50% scarf joint overlaps is superior to material with 50% scarf joint gaps.
3. The compressive fatigue performance of 10:1 scarf-jointed laminate is not appreciably degraded when the joints are overlapped by 50% during manufacture.

ADJUSTMENT OF WOOD LAMINATE MECHANICAL PROPERTIES FOR MOISTURE CONTENT

From Reference 8, Pages 4-32 to 4-33:

$$P = P(12) \times [P(12)/P_g]^{-[(M-12)/(M_p-12)]}$$

Where:

M = moisture content (%) of wood

M_p = wood moisture content at which changes in property due to drying are first observed (for Douglas fir, M_p = 24%)

P = property at wood moisture content, M

P(12) = property at 12% wood moisture content

P_g = property for all wood moisture contents > M_p

$$P(12)/P_g = \text{constant, } K$$

$$K(t) = 1.21 \text{ (tension)}$$

$$K(c) = 1.92 \text{ (compression)}$$

$$K(s) = 1.26 \text{ (shear)}$$

If:

M(L) = measured moisture content of fir/epoxy laminate

M = wood moisture content = 1.22 x M(L)

P(t) = physical property as tested

Then:

$$P(12) = P(t) \times K^{[(1.22 \times M(L) - 12)/12]}$$

TABLE XXVIII. - LAMINATE WITH SCARF JOINTED PLIES - COMPRESSION TEST MATRIX

Test Type	Number of Specimens							
	Control (No Scarf)	Nominal Scarfs			Variation of 10:1 Scarf			
		4:1	10:1	16:1	50% Overlap	25% Overlap	25% Gap	50% Gap
Ramp-To-Failure	16	4	4	4	8	4	8*	4*
Fatigue, Target 10 ⁴ Cycles	3	2	2	2	2	0	0	2
Fatigue, 5 Target 10 ⁵ Cycles	2	2	2	2	2	1	1	2
Fatigue Target 10 ⁶ Cycles	2	2	2	2	2	1	1	2

* Original Test Matrix Design Called For 4 Specimens in the 25% Gap Group and 8 Specimens in the 50% Gap Group.
The Change Was Due to Test Billet Design Error.

TABLE XXIX. - COMPRESSION RAMP-TO-FAILURE RESULTS
(300 SEC. RAMP)

Sample No.	Scarf Configuration	Maximum Actual Stress (psi)	Laminate Moisture Content (percent)	Max Stress At 12% WMC (psi)	Mean Max Stress @ 12% WMC (psi)
NAA1 NAA4 NAA7 NAA10	None (Control)	9120 8940 8910 8930	6.4 6.2* 6.2* 5.9	7260 7020 7000 6880	7040
NAG1 NAG4 NAG7 NAG10		7720 8810 9140 9680	5.9 6.0* 6.0* 6.0	5940 6830 7090 7510	6840
NBA1 NBA4 NBA7 NBA10		9260 9270 9450 9290	6.1 6.1* 6.1 6.1	7230 7240 7370 7250	7270
NBF1 NBF4 NBF7 NBF10		9430 9350 9300 9000	6.1 6.1* 6.1* 6.1	7360 7300 7260 7020	7240
NAB1 NAB4 NAB7 NAB10	4:1, Nominal	8880 9000 9030 9200	6.1* 6.1* 6.1* 6.1*	6930 7030 7050 7180	7050

*Estimated Laminate Moisture Content

TABLE XXIX. (continued) - COMPRESSION RAMP-TO-FAILURE RESULTS
(300 SEC. RAMP)

Sample No.	Scarf Configuration	Maximum Actual Stress (psi)	Laminate Moisture Content (percent)	Max Stress At 12% WMC (psi)	Mean Max Stress @ 12% WMC (psi)
NAC1 NAC4 NAC7 NAC10	10:1, Nominal ↓	9320 9040 9140 9450	6.0* 6.0* 6.1 6.0*	7220 7010 7140 7330	7170
NAD1 NAD4 NAD7 NAD10	16:1 Nominal ↓	9240 9020 9200 9470	6.1* 6.1 6.1* 6.0	7210 7040 7180 7340	7190
NAF1 NAF4 NAF7 NAF10	10:1, 25% Overlap ↓	8540 9150 9270 9240	6.2* 6.3 6.2* 6.2*	6710 7240 7280 7260	7120
NAE1 NAE4 NAE7 NAE10	10:1, 50% Overlap ↓	8990 8980 9200 9150	6.0* 6.0* 5.9 6.0*	6970 6960 7090 7100	7030
NBD1 NBD4 NBD7 NBD10	↓	9430 9200 9220 9170	6.0 6.0* 6.0* 6.0*	7310 7140 7150 7110	7180

*Estimated Laminate Moisture Content

TABLE XXIX. (continued) - COMPRESSION RAMP-TO-FAILURE RESULTS
(300 SEC. RAMP)

Sample No.	Scarf Configuration	Maximum Actual Stress (psi)	Laminate Moisture Content (percent)	Max Stress At 12% WMC (psi)	Mean Max Stress @ 12% WMC (psi)
NBE1 NBE4 NBE7 NBE10	10:1, 50% Gap ↓	9210 8970 8980 9050	5.9* 5.9* 5.9 5.9*	7100 6910 6920 6970	6970
NBB1 NBB4 NBB7 NBB10	10:1, 25% Gap ↓	9300 9180 9310 9260	5.9* 5.9* 5.9* 5.9*	7160 7070 7170 7140	7130
NBC1 NBC4 NBC7 NBC10	↓	9240 8970 9340 9080	5.7* 5.4 5.7* 6.0	7030 6680 7100 7040	6960

*Estimated Laminate Moisture Content

TABLE XXX. - COMPRESSION FATIGUE RESULTS

(R = 0.1, FREQ = 4Hz)

Sample No.	Scarf Configuration	Maximum Actual Stress (psi)	Laminate Moisture Content (percent)	Max Stress At 12% WMC (psi)	Cycles At Failure
NBA2	None (Control) ↓	8300	6.1*	6480	7,650
NAA2		8300	6.4	6610	10,120
NAA9		7900	6.2	6210	14,180
NAC3		7100	6.1	5540	56,530
NBA9		7400	6.1*	5780	69,700
NBF3		7400	6.1*	5780	547,030 [†]
NAC9		6000	6.0*	4650	2,835,500 [†]
NAB2	4:1, Nominal ↓	8300	6.3	6560	1,530
NAB6		7400	6.2	5810	10,930
NAB3		6100	6.1*	4760	47,550
NAB5		5900	5.9	4540	128,270
NAB8		5600	6.1*	4370	1,569,500 [†]
NAB9		5400	6.1*	4220	2,907,540 [†]
NAC2	10:1, Nominal ↓	7900	6.1	6170	11,870
NAC6		7900	6.1	6170	13,810
NAC3		7100	6.0	5500	35,850
NAC8		6700	6.0*	5200	64,840
NAC5		6300	5.8	4820	525,900
NAC9		6500	6.0*	5040	1,019,500 [†]
NAD2	16:1, Nominal ↓	7900	6.3	6250	10,030
NAD6		7900	5.8	6040	16,980
NAD3		7200	6.1	5620	73,260
NAD8		7200	6.1*	5620	114,930
NAD5		6500	6.1*	5070	938,460
NAD9		6500	6.1*	5070	2,337,140 [†]

*Estimated Laminate Moisture Content

[†]No Failure, Test Terminated

TABLE XXX. (continued) - COMPRESSION FATIGUE RESULTS
(R = 0.1, FREQ = 4Hz)

Sample No.	Scarf Configuration	Maximum Actual Stress (psi)	Laminate Moisture Content (percent)	Max Stress At 12% WMC (psi)	Cycles At Failure
NAF3 NAF5	10:1, 25% Overlap ↓	6900 6300	6.0 6.2*	5350 4950	55,400 261,190
NAE2 NBD2 NBD3 NAE3 NBD5 NAE5	10:1, 50% Overlap ↓	7600 7700 7100 6900 7100 6400	6.1 6.0* 5.9 6.0* 6.0* 6.0*	5930 5970 5470 5350 5500 4960	18,630 19,510 61,370 65,860 499,420 529,890
NBE2 NBE6 NBE3 NBE5 NBE8 NBE9	10:1, 50% Gap ↓	7700 7400 6900 6400 6800 6300	6.0 5.8 5.9* 5.9* 5.9 5.6	5970 5660 5320 4930 5240 4760	5,430 21,520 45,630 115,790 156,640 976,100
NBB3 NBB5	10:1, 25% Gap ↓	6900 6200	5.9 5.9*	5320 4780	59,530 1,260,000+

*Estimated Laminate Moisture Content

+No Failure, Test Terminated

TABLE XXXI. - SUMMARY OF COMPRESSION RAMP-TO-FAILURE DATA ANALYSES
FOR LAMINATE CONTAINING SCARF JOINTED PLIES
(300 SEC. RAMPS, DATA NORMALIZED TO 12% WMC)

Scarf Joint Configuration	Number of Specimens	Mean Stress (psi)	Coefficient Of Variation*	Percent Of Control Lam Performance
None (Control/Billet NA)	8	6940	0.066	---
None (Control/Billet NB)	8	7260	0.015	---
None (Control/All)	14	7100	0.051	---
4:1, Nominal	4	7050	0.015	102
10:1, Nominal	4	7170	0.019	103
16:1, Nominal	4	7190	0.017	104
10:1, 25% Overlap	4	7120	0.039	103
10:1, 50% Overlap	8	7100	0.015	100
10:1, 50% Gap	4	6970	0.012	96
10:1, 25% Gap	8	7040	0.022	97

*C.O.V. = Stand. Dev./Mean Stress

TABLE XXXII. - SUMMARY OF COMPRESSION FATIGUE DATA ANALYSES
FOR LAMINATE CONTAINING SCARF JOINTED PLIES
(TESTS CONDUCTED AT R = 0.1, DATA NORMALIZED TO 12% WMC)

Scarf Joint Configuration	Number of Specimens	No. Runouts Included*	Equation Of Linear Regression Line	Stress Intercept At 10 ⁴ Cycles	Stress Intercept At 10 ⁶ Cycles
None (Control)	7	1	$S = -9995 \times N^{-.0484}$	-6400 psi	-5120 psi
4:1, Nominal	6	2	$S = -9570 \times N^{-.0574}$	-5640	-4330
10:1, Nominal	6	1	$S = -9654 \times N^{-.0507}$	-6050	-4790
16:1, Nominal	6	1	$S = -8900 \times N^{-.0396}$	-6180	-5150
10:1, 25% Overlap	2	0	$S = -9133 \times N^{-.0490}$	-5820	-4640
10:1, 50% Overlap	6	0	$S = -8393 \times N^{-.0369}$	-5980	-5040
10:1, 50% Gap	6	0	$S = -8734 \times N^{-.0450}$	-5770	-4690
10:1, 25% Gap	2	1	$S = -7860 \times N^{-.0355}$	-5670	-4810

*Runouts Lie Above Trend Lines and Do Appear To Uniformly Improve Data Sets

NOTE: CONTROL SAMPLES HAVE THE SAME OVERALL DIMENSIONS BUT CONTAIN NO SCARF JOINTS

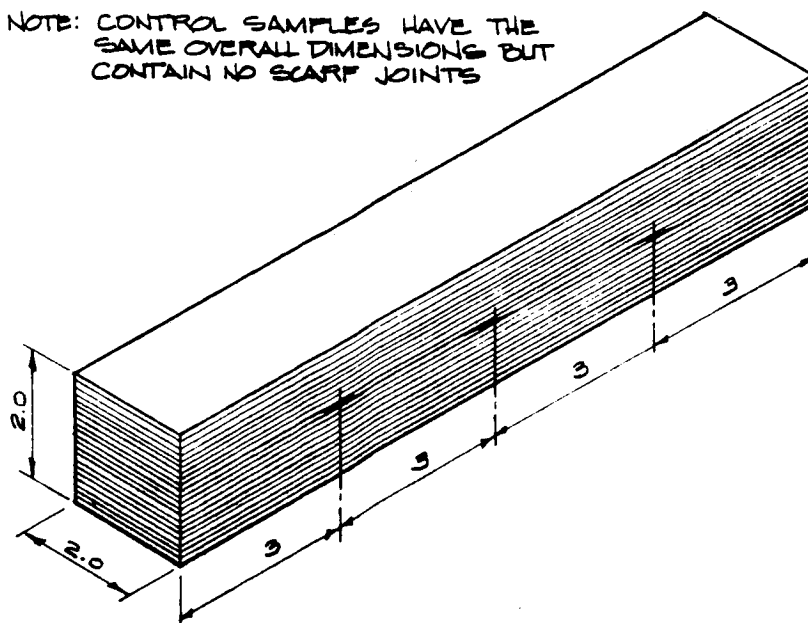


Figure 79.- Staggered Scarf Joint Test Sample Configuration

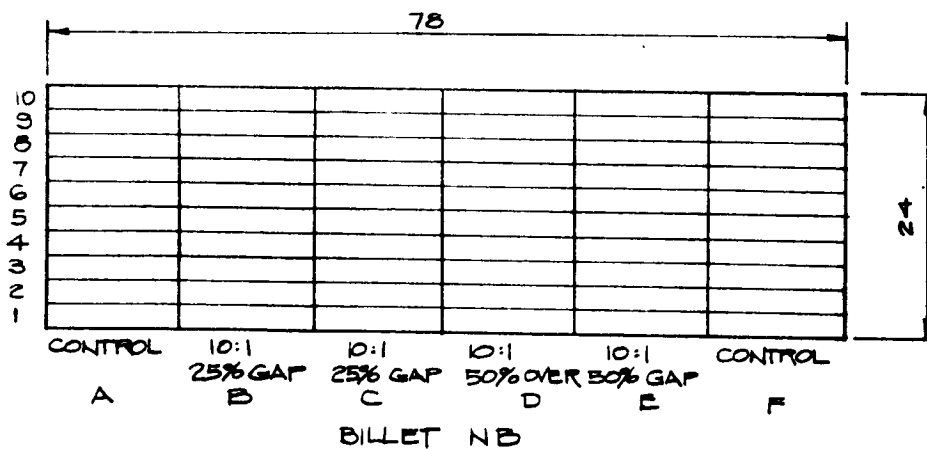
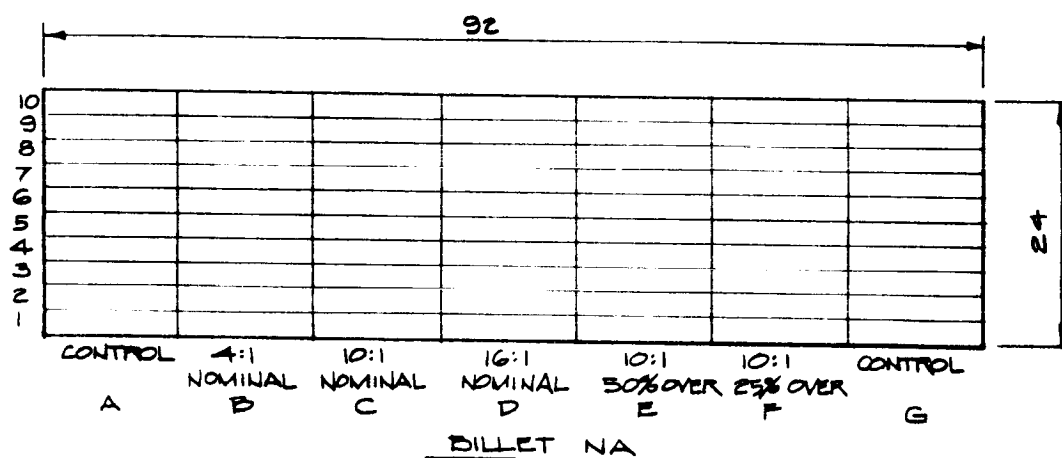
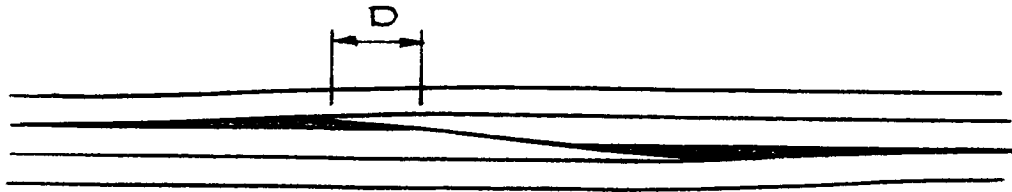


Figure 80.- Test Billet Allocation

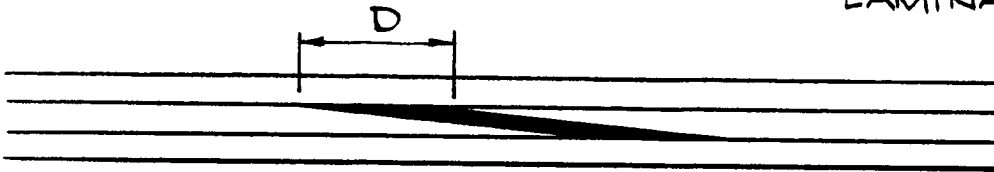
ORIGINAL PAGE IS
OF POOR QUALITY



OVERLAP JOINT

50% OVERLAP, $D = 0.50$
25% OVERLAP, $D = 0.25$

NOTE 1: OVERLAP JOINTS
TEND TO DISTORT
SOMEWHAT WITHIN THE
LAMINATE.



GAP JOINT

50% GAP, $D = 0.50$
25% GAP, $D = 0.25$

NOTE 2: SCARF SLOPE 10:1
FOR ALL NON-OPTIMUM
CONFIGURATIONS.

Figure 81. - Non-Optimum, Single Ply, Scarf Joint Details

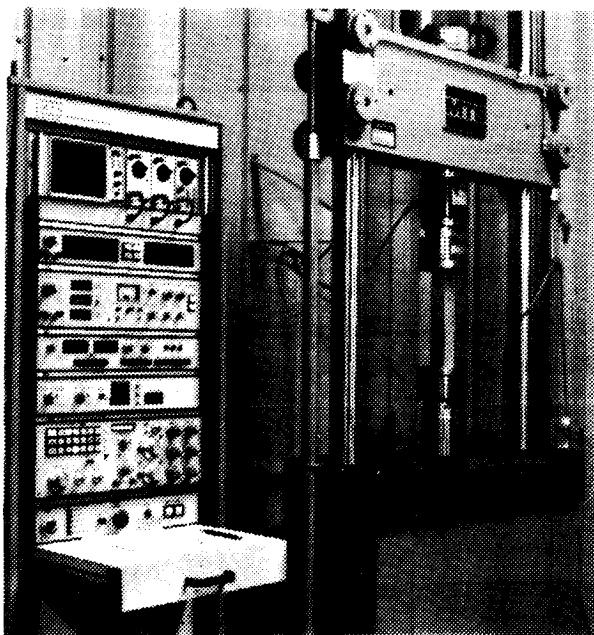


Figure 82. - General Test
Configuration

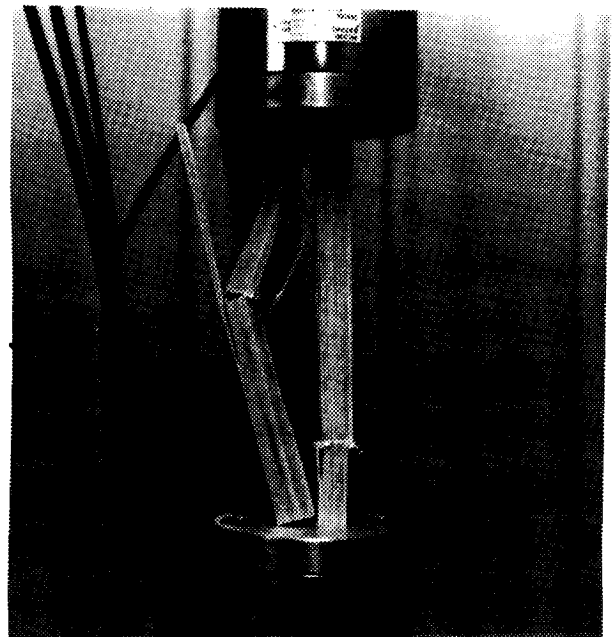


Figure 83. - Typical Failed
Fatigue Specimen

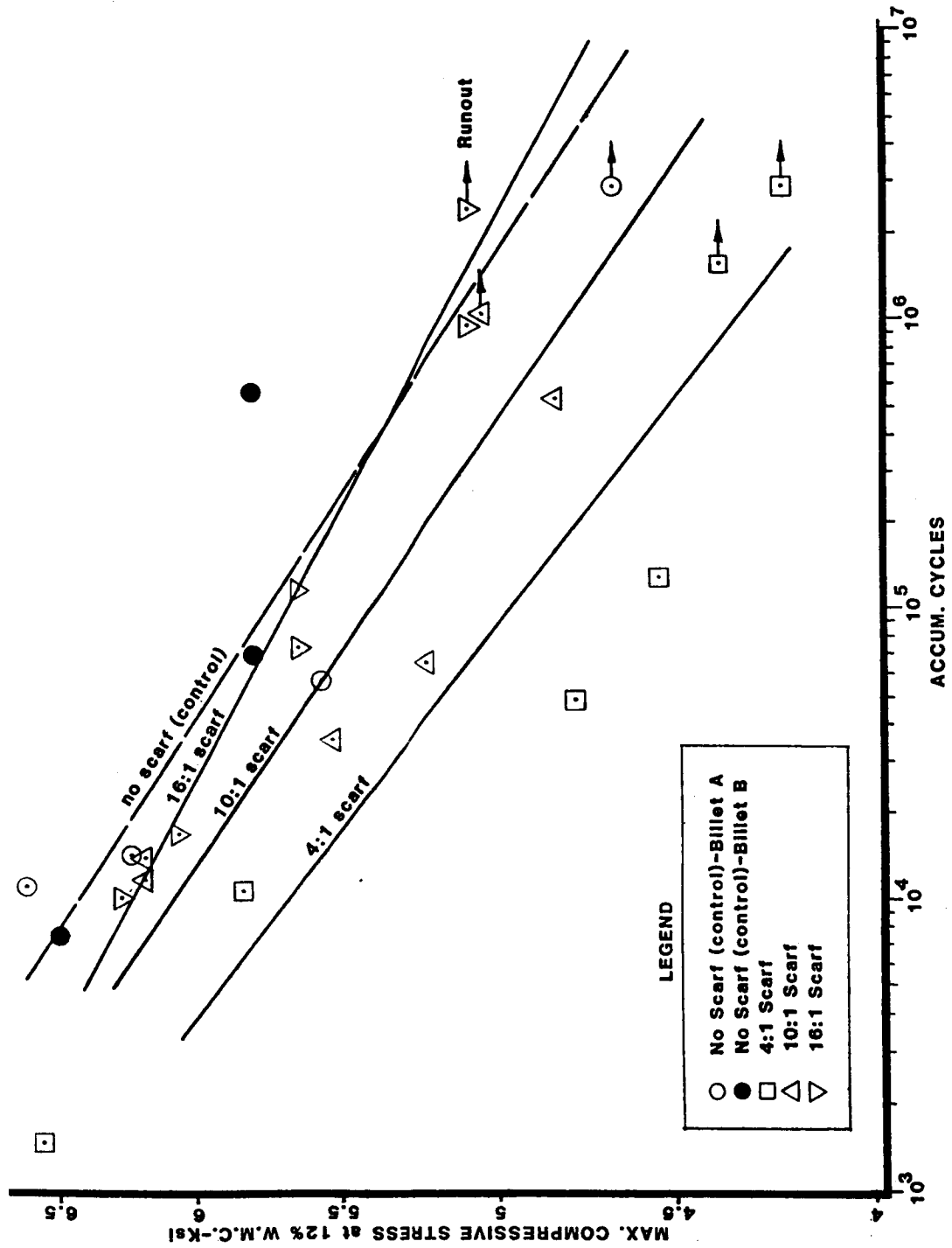


Figure 84. - Fatigue Performance Comparisons Of Laminates With Staggered Optimum Scarf Joints Of Different Slopes

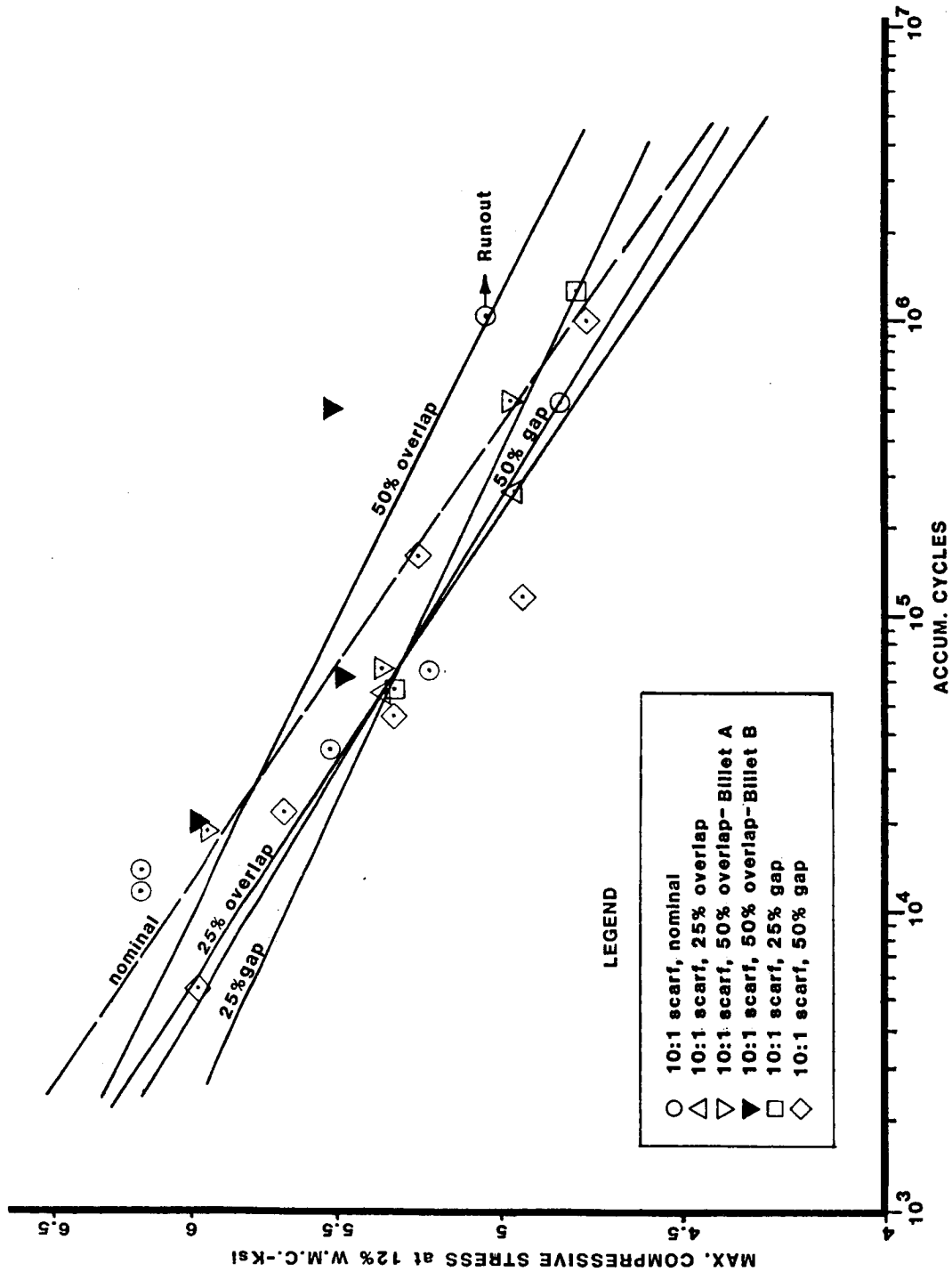


Figure 85. - Fatigue Performance Comparisons of Laminate With Staggered Non-Optimum 10:1 Slope Scarf Joints Of Various Types

18.0 APPENDIX F - Prototype Rotor Manufacturing Plan

TABLE OF CONTENTS

<u>Item No.</u>	<u>Description</u>	<u>Page No.</u>
18.1	Manufacturing Plan - Purpose	156
18.2	Manufacturing Plan - Objective	156
18.3	Hardware Description	156
18.4	Manufacturing Processes and Procedures	156
18.5	Quality Assurance Plan	156
18.6	Equipment, Tooling, Special Fixtures and Facilities	157
18.7	Materials Handling	157
18.8	Packaging and Shipping	157
18.9	Safety	157
18.10	Schedule	158

TABLES

XXXIII.	List of Engineering Drawings	159
XXXIV.	Blade Manufacturing Process/Quality Specification	160

FIGURES

86	Proposed Manufacturing Area	187
87	Proposed Fabrication Schedule	188

18.1 MANUFACTURING PLAN - PURPOSE

To provide accurate documentation of processes and procedures used in fabricating a prototype 90-foot diameter MOD-0 rotor as designed under Contract DEN3-260.

18.2 MANUFACTURING PLAN - OBJECTIVES

Objectives are as follows:

18.2.1 Demonstrate suitability of processes and procedures for fabricating and assembling the prototype 90-foot diameter MOD-0 rotor.

18.2.2 Maximize efficient use of resources for fabrication of prototype rotor

18.2.3 Develop baseline manufacturing plan which could serve as reference frame for production manufacturing plans

18.3 HARDWARE DESCRIPTION

18.3.1 Description of Rotor

The 90-foot diameter rotor is fabricated from six principal structural elements. These are namely one high pressure composite hub half shell, one low pressure composite hub half shell, two high pressure outer rotor (blade) half shells, and two low pressure outer rotor half shells. Each pair of half shells will be bonded to each other, after which fingers shall be cut into the root end of each outer rotor assembly and into both ends of the hub assembly. The two outer rotor assemblies will then be bonded to the hub by use of the finger joints to create an integral rotor structure. Engineering drawings describing the prototype rotor and associated hardware are listed in Table XXXIII.

18.4 MANUFACTURING PROCESSES AND PROCEDURES

18.4.1 Process Specifications

Table XXXIV is a series of process specifications defining each individual process and procedure required to complete the manufacturing operations. Included in the process specifications are specific requirements for inspections and tests for quality assurance.

18.5 QUALITY ASSURANCE PLAN

18.5.1 Quality Assurance - General

All veneers utilized within the rotor structure will be either Blade Grade 1 (BG1) or Blade Grade 2 (BG2) per Gougeon Brothers, Inc. Materials Specification GMS-001. All epoxy used (except where noted in Table XXXIV.) will be WEST SYSTEM Resin (105 BG) and Hardener (206 BG) in compliance with GMS-002 (pending final release).

18.5.2 Quality Assurance - Specific

The Manufacturing Process/Quality Specifications in Section 18.4 include specific requirements for quality assurance inspections and tests. Such activities are checked off by the individuals responsible for quality assurance as they are performed. Copies of these specifications accompany and govern all operations of the project.

18.6 EQUIPMENT, TOOLING, SPECIAL FIXTURES AND FACILITIES

Table XXXVIII is a list of equipment, tooling and special fixtures used in performing work on this project. The list includes descriptions, sources, specifications, quantities and availability of these items.

The south end of the Bay City manufacturing plant is scheduled for use on fabrication and assembly work under this project. Figure 86 shows the location of major equipment and fixtures.

18.7 MATERIALS HANDLING

Material, fabricated items and assemblies are to be moved and transported using the materials handling equipment listed in Table XXXVIII.

18.8 PACKAGING AND SHIPPING

Provisions for packaging and shipping prototype rotor components to the finger joint machining subcontractor and for final shipment to NASA's Plumbrook Test site are contained in the Design Drawings (see Table XXXVIII).

18.9 SAFETY

The foremost consideration in all activities is safety. All persons working on the project shall be provided with on-the-job training covering all aspects of safety, including:

1. Respiratory protection, involving handling of epoxy mixtures, sanding and grinding operations.
2. Eye protection at all times.
3. Proper operation of equipment, lift trucks, etc.
4. Wearing of gloves and aprons in handling epoxy coated materials.
5. Fire protection, including no smoking policy and use of and location of fire extinguishers.
6. Avoidance of injury due to improper lifting or other strenuous physical activities.
7. Installation of guards on equipment capable of cutting or pinching.
8. Good housekeeping, work area clean-up, and common sense while on the job.

18.10 SCHEDULE

Figure 87 is a schedule showing anticipated times to complete various milestones of the project.

TABLE XXXIII

ENGINEERING DRAWINGS, 90 FOOT, MOD-O PROTOTYPE ROTOR

<u>Drawing No.</u>	<u>Drawing Title</u>
<u>Prototype Rotor</u>	
CF-10-060	Final Design Rotor Planform & Tolerances
CF-10-061	Outer Rotor Open Planform
C -10-062	Outer Rotor Lofting
C -10-063	Inner Rotor Lofting
CD-10-064	Ice Detector Access Detail & Tip Vent/Tip Weight Detail
CF-10-066	Hub - Upwind Configuration
CF-10-067	Hub - Downwind Configuration
CD-10-068	Outer Rotor Sectional, Station 540, Tip
CF-10-069	Outer Rotor Sectional, Station 156 & 348
CF-10-070	Hub Internal Structure - High Pressure Shell View
CF-10-071	Hub Internal Structure - Low Pressure Shell View
CF-10-072	Hub Closed Planform & Finger Joint Details
CF-10-073	Hub Section
CF-10-074	External Blade Detail - High Pressure Side & Finger Joint Detail
CF-10-075	Hub Veneer Schedule
CF-10-078	Hub Center Cutout Detail - High Pressure Shell - Full Size
CF-10-079	Outer Rotor Instrumentation Details
CF-10-080	Outer Rotor Sectional, Station 252 & Instrumentation Enclosure Detail
CF-10-081	Outer Rotor Sectionals, Stations 372 & 468
CF-10-082	Outer Rotor Pressure Tap Sectional, Station 276
CF-10-083	Outer Rotor Pressure Tap Sectionals, Stations 396 & 492
CC-10-084	Hub-Crossgrain Fasteners - Concept "A" - Preliminary
CC-10-085	Hub-Crossgrain Fasteners - Concept "B" - Preliminary
C -10-086	Outer Rotor Veneer Schedule
CC-10-087	Final Shipping Configuration
CC-10-090	Preliminary Shipment Configuration
CD-10-096	Finger Joint Assembly Details
<u>Equipment, Tooling and Special Fixtures</u>	
CD-10-065	Twist Gauge Detail
CF-10-088	Aft Bunk for Final Shipment
CF-10-089	Forward Bunk for Final Shipment
CD-10-091	Bunks for Preliminary Shipment of Blades
CD-10-092	Bunks for Preliminary Shipment of Blades
CC-10-093	Handling Provisions
CD-10-094	Hub Mold Schematic
CF-10-095	Outer Rotor Mold - Schematic (L.P. Mold Shown)
CB-10-097	Sleeve Installation Schematic - Exploded View
CF-10-098	Hub Fastener Sleeve Installation Hardware Details
CF-10-099	Splice Joint Assembly - Tip Jack

TABLE XXXIV.

GOUCEON BROTHERS, INC., BLADE MANUFACTURING PROCESS/QUALITY SPECIFICATION NO: NASA-7 Pg. 1 of 27
 Process Description: 90 Foot MOD-O Prototype Rotor Fabrication Program: Contract DEN 3-260 Date: 3-8-83 Rev.

Completed & Accepted
 MFG SUP Q.A. ENGR. DATE

Oper. No.	Operation Description
1.0	<u>Materials Preparation</u>
1.1	<u>Douglas Fir Veneers</u>
1.1.1	Veneer Selection - Refer to design drawings and veneer schedules and determine quantity of Blade Grade 1 and 2 veneers (per specification GMS-001) required for complete rotor fabrication. Remove required number of veneers of each grade plus 20%, alternating from the top of a minimum of three stacks to randomize the veneers. Reject veneers having improper grade marking, excessive rough peel or excessive knots per GBI standards. Record accepted and rejected quantities in Manufacturing Log. Label and move rejected veneers to reject storage area.
1.1.2	Moisture Control Stabilization - Maintain veneer in a stable environment which supports an equilibrium wood moisture content of 7-9%. Prior to use in a laminating operation, wood moisture content of 7-9% must be measured in at least 4 of 5 10 inch x 10 inch coupons taken from 5 veneers being conditioned in the stack requiring verification. These sampled veneers should be located at the top, bottom and at approximately at 25%, 50%, and 75% locations with respect to the height of the stack. Following trimming of coupons, the five veneers are to be indelibly marked for later retrieval and returned to their respective locations. Mark coupons with stack number and location of sampled veneer (0% is TOP, 50% is MIDDLE and 100% is BOTTOM, etc.) Submit samples immediately to Materials Test Lab with a written request for m.c. tests.

TABLE XXXIV.

<u>GOUGEON BROTHERS, INC., BLADE MANUFACTURING PROCESS/QUALITY SPECIFICATION NO:</u>			<u>NASA-7</u>	<u>Pg. 2 of 27</u>
<u>Process Description: 90 Foot MOD-0 Prototype Rotor Fabrication</u>		<u>Program:</u>	<u>Contract DEN 3-260</u>	<u>Date: 3-8-83 Rev.</u>
<u>Oper. No.</u>	<u>Operation Description</u>	<u>Completed & Accepted</u>		
		<u>MFG SUP</u>	<u>Q.A. ENGR.</u>	<u>DATE</u>

Record results of above tests in Manufacturing Log. Veneers may be used for laminating operations for three consecutive days from any stack which has been qualified providing there are no known or recorded variations in the veneer conditioning environment which would jeopardize veneer m.c. stability.

Trimming and Lift Assembly - This operation may take place prior to qualification of m.c. (per 1.1.2). However, the requirements of 1.1.2 do still apply to any lift of veneers prior to laminating. M.C. stabilized lifts must remain in conditioning facility until one hour prior to commencement of laminate assembly.

Trim veneers to required width and length, using veneer trim fixture and saw. Also cut scarfs as required in skin designated veneers. After trimming, stack veneers on Lift Table in proper sequence for layup per the specific veneer schedule. Mark each veneer with numbers identifying position in lift. Label each lift with Grade, Lot Numbers, Total Lift Weight, Intended Use, Date, and

Name of Inspector.

Fiberglass Fabric and Graphite Tape

Verify Material Quantities - Refer to design drawings and determine quantities of E-glass fabric and graphite tape required for complete component and rotor fabrication.

Obtain from stock, rolls of proper grade E-glass and graphite tape and roll onto inspection table. Measure lengths and widths of available rolls. Number and label each roll with the quantity measured. Verify proper quantity is available for particular operation.

TABLE XXXIV.

GOUGEON BROTHERS, INC., BLADE MANUFACTURING PROCESS/QUALITY SPECIFICATION NO: <u>NASA-7</u>			Pg. <u>3</u> of <u>27</u>	
Process Description: <u>90 Foot MOD-O Prototype Rotor Fabrication</u>			Date: <u>3-8-83</u>	Rev. <u> </u>
			Completed & Accepted	
			MFG SUP	Q.A. ENGR. DATE

Operation Description	
Oper. No. <u>1.2.2</u>	Verify Material Quality - Review manufacturer's Materials Certification for each lot or roll to be used and place copy of the Material Certification in the Manufacturing Log. Inspect each roll of material intended for use for areas including cuts or misweaving and indelibly mark these areas as not to be used in manufacture.
1.2.3	Cutting and Marking - Cut fabric to sizes required using fabric shears. Mark each cut piece with position in layup. Roll cloth pieces onto paper tubes. Label cloth rolls with Cloth Type, Lot Number, Intended Use, Inspector's Name, and Date.
1.3	<u>Aluminum Lightning Protection Screen</u>
1.3.1	Verify Material Quantities - Refer to design drawings and determine quantities of aluminum screen required for continuous (and unspliced) outer rotor coverage.
	Obtain from stock, roll (or rolls) of proper grade aluminum screen and roll onto inspection table. Measure lengths and widths. Number and label each roll with the quantity measured. Verify proper quantity is available for particular application.
1.3.2	Verify Screen Quality - Inspect each roll of screen intended for use. Any cuts, punctures or significant mis-weaving may constitute cause for rejecting the material and must be reviewed.
1.3.3	Cutting and Marking - Cut screen to sizes required using metal shears. Mark each piece with intended location and roll up. Label each roll with Screen Type, Intended Use, Inspector's Name and Date.

TABLE XXXIV.

GOUGEON BROTHERS, INC., BLADE MANUFACTURING PROCESS/QUALITY SPECIFICATION NO: NASA-7. Pg. 4 of 27
 Process Description: 90 Foot MOD-0 Prototype Rotor Fabrication Program: Contract DEN 3-260 Date: 3-8-83 Rev.

Oper. No.	Operation Description	Completed & Accepted	
		MFG SUP	Q.A. ENGR. DATE
1.4	<u>Vacuum Bagging Materials</u>		
1.4.1	Peel Ply Preparation - Obtain from stock rolls of peel ply. Determine from Section 2.0 and design drawings quantity and sizes required. Cut peel ply to sizes required for each bagging operation, roll up and label with Intended Use, Inspector's Name and Date.		
1.4.2	Prepare Venting Material - Apply same measures as in 1.4.1 to Venting Material.		
1.4.3	Prepare Plastic Film - Apply same measures as in 1.4.1 to Plastic Film.		
1.4.4	Prepare Sealant and Vacuum Manifolds - Obtain and mark necessary quantities of Sealant to support each bagging operation and label each bundle with Intended Use, Inspector's Name and Date. Verify availability of unconstricted manifolds for use in each bagging operation. Manifolds may be reused when appropriate.		
1.5	<u>Miscellaneous Materials</u>		
	For each of the listed items verify appropriate quantities and quality to support requirements as defined in the design drawings. Prepare items into sizes or configurations ready for use and label with Quantity Information, Intended Use, Inspector's Name, and Date.		
1.5.1	Instrumentation and Ice Detector Conduit		
1.5.2	Plywood for shear web, bulkheads, instrumentation enclosures, tip caps and jig fabrication.		
1.5.3	Douglas fir for shear web stringers.		
1.5.4	Douglas fir/epoxy laminate for hydraulic damper attachment and for tip blocking.		
1.5.5	Aluminum lightning protection system ground straps.		
1.5.6	Hub crossgrain fastener sleeves.		

TABLE XXXIV.

GOUGEON BROTHERS, INC., BLADE MANUFACTURING PROCESS/QUALITY SPECIFICATION NO: NASA-7 Pg. 5 of 27
 Process Description: 90 Foot MOD-O Prototype Rotor Fabrication Program: Contract DEN 3-260 Date: 3-8-83 Rev.
 Completed & Accepted
 MFG SUP Q.A. ENGR. DATE

Oper. No.	Operation Description
1.5.7	Hydraulic damper attachment studs
1.5.8	NASA furnished Instrumentation Hardware: Pressure Taps, Tubing and Clamps. Angle of attack probe mounting hardware and ice detector plates and cabling.
1.5.9	Electrically conductive epoxy.
1.5.10	Nylon machine screws for cover plates.
1.5.11	Bulkhead inspection ports.
1.5.12	Special jigs and tooling as required.
1.5.13	Asbestos
1.5.14	Finishing paint.

TABLE XXXIV.

<u>GOUGEON BROTHERS, INC., BLADE MANUFACTURING PROCESS/QUALITY SPECIFICATION NO:</u>			<u>NASA-7</u>	<u>Pg. 6 of 27</u>
<u>Process Description: 90 Foot MOD-0 Prototype Rotor Fabrication</u>			<u>Program: Contract DEN 3-260</u>	<u>Date: 3-8-83</u> <u>Rev.</u>
<u>Oper. No.</u>	<u>Operation Description</u>	<u>Completed & Accepted</u>		
		<u>MFG SUP</u>	<u>Q.A. ENGR.</u>	<u>DATE</u>

2.0 Component Molding2.1 Outer Rotor Principal Structures (2 High and 2 Low Pressure Shells)

2.1.1 Mold Preparation - Wipe mold surface with clean, soft cloth, including alignment marks. Apply mold release agent to the mold surface. Apply vacuum bag sealant.

2.1.2 Gelcoat Application - Roll one coat of unpigmented epoxy gelcoat into mold and allow to cure. Use 205 hardener with 105 resin.

2.1.3 Vacuum System Check - Check pumps for normal operation and verify vacuum gage operation.

2.1.4 Glue Machine Checkout - Fill out Glue Machine Log. Check operation of pumps and rollers. Start up machine. Stabilize glue rate at sixty pounds per thousand square feet. Prior to coating any veneers from lift:

- Number in sequence approximately 20 to 30 12"x12" veneer coupons
- Dry weigh coupons and record on coupon
- Pass a coupon through machine rollers, weigh and record glue weight for coupon number on Glue Machine Log
- Repeat process with next coupon
- Glue application rate is considered stabilized when three successive samples show rates with $\pm 10\%$ (24.5-30.0 grams/ft²). Take two syringe samples of epoxy at the roller, mark and set aside.

2.1.5 Apply Exterior Glass Fabric - Check gelcoat for proper cure. Wash gelcoat with warm water. Wipe and allow to dry. Squeegee on two layers of fiberglass cloth over gelcoat using 105 resin and 206 hardener from glue machine.

2.1.6 Apply Lightning Screen - Lay a 4-inch wide strip of peel cloth chordwise over the fiberglass at Station 60. Roll aluminum lightning protection screen into the fiberglass. The screen should be 105/206 epoxy saturated.

TABLE XXXIV.

GOUGEON BROTHERS, INC., BLADE MANUFACTURING PROCESS/QUALITY SPECIFICATION NO: NASA-7 Pg. 7 of 27
 Process Description: 90 Foot MOD-0 Prototype Rotor Fabrication Program: Contract DEN 3-260 Date: 3-8-83 Rev.

Completed & Accepted
 MFG SUP Q.A. ENGR. DATE

Oper. No.	Operation Description
2.1.7	<p>Laminate Assembly - Pass veneers in proper order from lift through glue machine and place in mold per design drawings. Apply asbestos thickened 105/206 epoxy to longitudinal butt joints and any knot holes or other defects.</p> <p>Check for proper wetout and alignment of scarf joints, overlapped butt joints, missing veneers, lack of epoxy coating. Correct and record any irregularities on Manufacturer's Log.</p> <p>At the mid-point of the assembly operation take two more syringe samples of epoxy at the roller, mark and set aside.</p> <p>Apply Interior Glass Fabric - After top layer of veneers is in place, place two layers of dry fiberglass fabric on top of assembly. Lightly smooth fabric into position. Take two final syringe samples of epoxy at the roller, mark and set aside before shutting down the glue machine.</p> <p>Bagging and Cure - Place layer of peel ply over last layer of fiberglass cloth. Smooth into position.</p> <p>Place vacuum manifolds in spanwise direction on top of peel ply near center of assembly. Place venting material over manifolds and entire assembly.</p> <p>Seal entire assembly using plastic film and sealant at mold edges.</p> <p>Start up vacuum pumps and evacuate air from assembly. Place three vacuum gauges at three distributed locations. Allow vacuum to stabilize to 20 to 25 inches Mercury. Repair any leaks if necessary. Record initial stabilized vacuum levels on Glue Machine Log. Complete filling out remainder of Glue Machine Log.</p>
2.1.8	
2.1.9	

TABLE XXXIV.

GOUGEON BROTHERS, INC., BLADE MANUFACTURING PROCESS/QUALITY SPECIFICATION NO:		NASA-7	Pg. 8 of 27
Process Description: 90 Foot MOD-0 Prototype Rotor Fabrication		Program: Contract DEN 3-260	Date: 3-8-83 Rev.
Oper. No.	Operation Description	Completed & Accepted	
		MFG SUP	Q.A. ENGR. DATE

2.1.9	Bagging and Cure (continued)
	Check and record vacuum and room temperature each hour for first four hours of cure. Turn off vacuum system after minimum of eight hours.
2.1.10	Bagging Removal - Remove plastic film, other covering material and manifold. Complete wetout of interior layers of glass cloth by use of roller brush and 105/206 epoxy.
2.2	Inner Rotor (Hub) Principal Structure (1 High and 1 Low Pressure Shell)
2.2.1	Mold Preparation - See 2.1.1
2.2.2	Gelcoat Application - See 2.1.2
2.2.3	Vacuum System Check - See 2.1.3
2.2.4	Glue Machine Checkout - See 2.1.4
2.2.5	Apply Exterior Glass Fabric - See 2.1.5
2.2.6	Laminate Assembly - (High and Low Pressure Shells) - Pass first layer of veneers from lift through glue machine and place in mold per design drawings. Apply asbestos thickened 105/206 epoxy to longitudinal butt joints and any knot holes or other defects. Check for overlapped butt joints, missing veneers or fabric and lack of full epoxy coating. Correct and record on Manufacturer's Log. Next, place full layer coverage of fiberglass fabric over veneer layer, wetout and squeegee smooth. Align fabrics such that fibers are oriented at $\pm 45^\circ$ with respect to spanwise axis of blade. Continue alternating between veneer and fiberglass plies until completing approximately half of the laminate assembly or 90 minutes

TABLE XXXIV.

COUGEON BROTHERS, INC., BLADE MANUFACTURING PROCESS/QUALITY SPECIFICATION NO: NASA-7				Pg. 9 of 27	
Process Description: 90 Foot MOD-0 Prototype Rotor Fabrication		Program:	Contract DEN 3-260	Date:	3-8-83 Rev.
Oper. No.	Operation Description	Completed & Accepted			
		MFG SUP	Q.A. ENGR.	DATE	

2.2.6	Laminate Assembly (continued)
	have elapsed. At approximately the halfway point and at the end of the assembly phase, take two syringe samples of epoxy at the glue machine roller, mark and set aside.
	Apply vacuum bag as in 2.1.9. Following full eight-hour cure cycle, remove plastic film, other covering material and manifolds. Prepare surface for resumption of assembly by lightly sanding entire surface to remove any shine and also any localized high points or bubbles. Clean sanding dust by brushing and/or vacuuming away dust. Resume assembly of remaining shell laminate by going through Vacuum System Check and Glue Machine Check sequence as defined in 2.1.3 and 2.1.4. Take epoxy samples as defined previously in this section.
2.2.7	Apply Interior Glass Fabric - See 2.1.8
2.2.8	Bagging and Cure - See 2.1.9
2.2.9	Bagging Removal - See 2.1.10
2.2.10	Preparation of Low Pressure Shell for Buildup - Prepare surface for resumption of assembly by lightly sanding entire buildup bond area per design drawings to improve adhesion and remove any localized high points or bubbles. Clean sanding dust from surface by brushing and/or vacuuming away dust.
2.2.11	Assemble Buildup - Conduct Vacuum System Check and Glue Machine Check sequence as defined in 2.1.3 and 2.1.4
	Assemble buildup in identical manner to that described for High and Low Pressure Hub Shells in 2.2.6
2.2.12	Bagging and Cure - See 2.1.9
2.2.13	Bagging Removal - See 2.1.10

TABLE XXXIV.

GOUGEON BROTHERS, INC., BLADE MANUFACTURING PROCESS/QUALITY SPECIFICATION NO: NASA-7				Pg. 10 of 27	
Process Description: 90 Foot MOD-0 Prototype Rotor Fabrication				Program: Contract DEN 3-260	Date: 3-8-83 Rev. _____
Oper. No.	Operation Description	Completed & Accepted			
		MFG SUP	Q.A. ENGR.	DATE	

2.3 High Pressure Hub Shell Reinforcement

2.3.1 Manufacture and Prepare Mold for Reinforcement Fabrication. Per design drawings, manufacture a simple male mold to the interior dimensions and tolerances of the desired reinforcement. Coat with epoxy and wax when epoxy has hardened.

2.3.2 Check and Mix Glue Components - Obtain from gear pumps in separate containers, desired amount of WEST SYSTEM 105 resin and 206 hardener. Record in Manufacture Log Lot Numbers and Weights of the two components. Mix components thoroughly.

2.3.3 Layup Reinforcement - Wind epoxy wetted out tape onto mold in a continuous fashion squeezeing the material in place to smooth and remove excess air and epoxy. Before each epoxy batch runs out or begins to gel, take a syringe sample, label with date and job description. Return to 2.3.2 for additional epoxy to complete job. Tape ends should be cut square and overlapped by 3 inches whenever one tow runs out and a new tow is required. Apply total number of wraps to achieve dimension required, then set aside to cure.

2.3.4 Reinforcement Removal - Following complete cure of layup, (if reinforcement will not readily part from mold), cut away mold structure from inside of reinforcement. Leave a minimum of one eighth inch clearance between cuts and reinforcement. Remove mold in pieces as necessary.

2.4 Low Pressure Hub Shell Reinforcement

2.4.1 Manufacture and Prepare Mold for Reinforcement Fabrication - See 2.3.1

2.4.2 Check and Mix Glue Components - See 2.3.2

2.4.3 Lay Up Reinforcement - See 2.3.3

2.4.4 Reinforcement Removal - See 2.3.4

TABLE XXXIV.

GOUGEON BROTHERS, INC., BLADE MANUFACTURING PROCESS/QUALITY SPECIFICATION NO: <u>NASA-7</u>			Pg. <u>11</u> of <u>27</u>	
Process Description: <u>90 Foot MOD-0 Prototype Rotor Fabrication</u>			Date: <u>3-8-83</u>	Rev. <u> </u>
			Contract DEN <u>3-260</u>	
			Completed & Accepted	
			MFG SUP	Q.A. ENGR. DATE

Oper. No.	Operation Description
2.5	<u>Instrumentation and Ice Detector Access Plates</u>
2.5.1	Mold Preparation - Prepare low pressure mold surface as defined in 2.1.1.
2.5.2	Gelcoat Preparation - Per 2.1.1.2, apply gelcoat into mold areas where plates are defined in design drawings.
2.5.3	Check and Mix Glue Components - See 2.3.2.
2.5.4	Lay Up Parts - Check gelcoat for proper cure. Wash gelcoat with warm water. Wipe and allow to dry. Squeegee onto gelcoat areas necessary layers of 105/206 epoxy wetted-out fiberglass fabric to obtain desired plate thickness. Cloth should be oriented at 0 and 90 degrees to spanwise blade axis. Before each epoxy batch runs out or begins to gel, take a syringe sample, label with date and job description. Return to 2.5.3 for additional epoxy to complete job.
2.5.5	Plate Removal and Trimming - Following complete cure of layups, remove plates from mold surface. Using molded reference lines and templates, trim parts to dimensions required on design drawings.

TABLE XXXIV.

GOUGEON BROTHERS, INC., BLADE MANUFACTURING PROCESS/QUALITY SPECIFICATION NO:		NASA-7	Pg. 12 of 27
Process Description: 90 Foot MOD-0 Prototype Rotor Fabrication		Program: Contract DEN 3-260	Date: 3-8-83 Rev.
Oper. No.	Operation Description	Completed & Accepted	
3.0	Component Assembly	MFG SUP	Q.A. ENGR. DATE

Blade A (Instrumented Blade) Assembly

- 3.1.1 Half Shell Trimming - Remove molding battens from mold edges. Taking care to handle properly, place circular saw against the cut angle control surface with the lower saw motor housing surface resting against the cut height control guide. Start up saw and begin cutting into edge laminate. Maintain solid index against both angle control surfaces and cut height control guide at all times. Feed through laminate at rates appropriate to power and sharpness of saw and thickness of laminate. Replace saw blade immediately upon evidence of dulling.
- 3.1.2 Shell from Mold Removal - Remove low and high pressure shells from molds. Place upon saw horses, outer surface up, for pressure tap installation. Place supports against interior structure to prevent structure curvature from distorting under its own load.
- 3.1.3 Install Pressure Taps - Using locating templates mark desired pressure tap locations on blade at designated spanwise locations per design drawings. Drill holes to dimensions specified perpendicular to rotor surface at locations marked.
- Cut and form pressure tap tubing to approximate lengths indicated in design drawings. On a table belt sander, square off exterior end. By hand, using a small diameter twist drill remove any burrs on the inside of the exterior end. On a belt sander, lightly chamfer interior end to reduce wear on flexible tubing.

TABLE XXXIV.

GOUGEON BROTHERS, INC., BLADE MANUFACTURING PROCESS/QUALITY SPECIFICATION NO: NASA-7 Pg. 13 of 27

Process Description: 90 Foot MOD-0 Prototype Rotor Fabrication Program: Contract DEN 3-260 Date: 3-8-83 Rev.

Completed & Accepted
MFG SUP Q.A. ENGR. DATE

Oper. No.	Operation Description
3.1.3	<p>Install Pressure Taps (continued)</p> <p>Using small diameter grinder, remove gelcoat and fiberglass layers, and lightly expose the lightning screen to bare aluminum over a diameter as defined in the design drawings. Bond pressure tap in place using electrically conductive epoxy as specified. Measure weights of component parts of epoxy and record in Manufacturer's Log. Check exterior surface for flushness of pressure tap orifices due to epoxy shrinkage and fill with clear WEST SYSTEM 105/205 epoxy as required. Measure weights of component parts of epoxy and record in Manufacturer's Log. Fair when epoxy has hardened by lightly block sanding the area.</p>
3.1.4	<p>Return Shells to Molds - Following pressure tap installation return shells to molds. Bend interior of pressure taps to approximate shape indicated in design drawings. In trailing edge, remove just sufficient laminate to allow aft most pressure taps to avoid interfering with trailing edge joint. See design drawings for clarification.</p>
3.1.5	<p>Install Angle of Attack Probe Base Supports - Mark desired base location as specified on design drawings on high pressure shell leading edge. Install blocking and ribs for probe base and support anchors at locations required and to shape specified in design drawings. Machine away blocking material sufficient to place base support into low pressure shell leading edge blocking such that base supports can be centered along their respective section chord lines. Machine away corresponding spanwise blocking material on the high pressure shell leading edge. Total material removed should allow slight freedom for aligning base supports. Place low pressure shell upon five saw horses. Support at each end and under each installation station and</p>

TABLE XXXIV.

COUGEON BROTHERS, INC., BLADE MANUFACTURING PROCESS/QUALITY SPECIFICATION NO: <u>NASA-7</u>		Pg. 14 of 27	
Process Description: <u>90 Foot MOD-O Prototype Rotor Fabrication</u>		Date: <u>3-8-83</u> Rev. <u> </u>	
Program: <u>Contract DEN 3-260</u>			
Operation Description		Completed & Accepted	
Oper. No.		MFG SUP	Q.A. ENGR. DATE

- 3.1.5 Install Angle of Attack Base Supports (continued)
 check leading edge for straightness. Place base supports in their respective locations. Insert waxed rigid tubing into bearing bases and extend tubing toward respective section trailing edge. Using plywood support jigs, align tubing such that each bearing base is aligned parallel with its section chordline. Place high pressure shell over low pressure shell to verify proper fit up. Manufacture and bond to base support, required number of hard epoxy spacers to ensure proper centering of base in hole. Remove high pressure shell and return to mold.
 Coat machined blocking on low pressure shell with clear WEST SYSTEM 105/206 epoxy. Measure weights of component parts of epoxy and record in Manufacturer's Log. Before epoxy hardens, apply asbestos thickened 105/206 epoxy to base supports and low pressure blocking and place base supports with alignment tubes into position. Again, measure weights of component parts of epoxy and record in Manufacturer's Log. Check alignment of base supports, and wipe away excess thickened epoxy. Return low pressure shell to mold when epoxy has hardened.
- 3.1.6 Fabricate Shear Webs - Manufacture shear webs and shear web stringers from materials and per dimensions and tolerances contained within the design drawings for both Blades A and B.
- 3.1.7 Install Shear Web -
 a) Locate shear web stringers in both low and high pressure shells by use of snapped chalk line and per locations and tolerances contained in design drawings.

TABLE XXXIV.

GOUGEON BROTHERS, INC., BLADE MANUFACTURING PROCESS/QUALITY SPECIFICATION NO: NASA-7 Pg. 15 of 27
 Process Description: 90 Foot MOD-0 Prototype Rotor Fabrication Program: Contract DEN 3-260 Date: 3-8-83 Rev.

Completed & Accepted
MFG SUP Q.A. ENGR. DATE

Oper. No.	Operation Description
3.1.7	<p>Install Shear Web (continued)</p> <p>b) Dry check fit of shear web into both high and low pressure shell stringers. Fit should not be too snug; correct if necessary.</p> <p>c) Dry fit stringers at required chordwise location and mark any local areas which have slight interference with installed pressure taps. Remove minimum stringer material necessary to allow slight clearance for pressure taps.</p> <p>d) Bond stringers to respective shells by precoating both sides of the intended joint with clear 105/206 epoxy and then asbestos thickened 105/206 epoxy, stapling shear web stringers in place. Measure weights of component parts of epoxy and record in Manufacturer's Log.</p> <p>(e) Following cure of stringer to shell joint, apply clear 105/206 epoxy to interface areas of shear web to the low pressure shell stringer. Before clear epoxy has hardened, apply asbestos thickened epoxy to same area and place shear web into stringer. Brace shear web into proper design position during cure.</p>
3.1.8	<p>Install Ice Detector and Instrumentation Enclosure Blocking - Per design drawings, install blocking trimmed to required dimensions at specified locations on the low pressure shell by coating both sides of the intended joint with clear 105/206 epoxy and then applying thickened 105/206 epoxy before applying staples and weights to the blocking to locate the clamp.</p>
3.1.9	<p>Assemble Instrumentation Enclosures - Using materials specified in the design drawings fabricate three instrumentation enclosures at the locations specified.</p>

TABLE XXXIV.

GOUGEON BROTHERS, INC., BLADE MANUFACTURING PROCESS/QUALITY SPECIFICATION NO:		NASA-7	Pg. 16 of 27	
Process Description: 90 Foot MOD-0 Prototype Rotor Fabrication		Program: Contract DEN 3-260	Date: 3-8-83 Rev.	
Operation Description		Completed & Accepted		
Oper. No.		MFG SUP	Q.A. ENGR.	DATE

- | | |
|--------|--|
| 3.1.9 | <p>Assemble Instrumentation Enclosures (continued)</p> <p>All surfaces and joints are to be treated with clear and/or asbestos thickened WEST SYSTEM 105/206 epoxy as called out on the drawings. Measure weights of component parts of epoxy and record in Manufacturer's Log. Apply thickened epoxy fillets where required and apply a single layer of fiberglass cloth with 105/206 epoxy to the exterior of the enclosure for joint reinforcement as specified. Again, measure weights of component parts of epoxy and record in Manufacturer's Log.</p> |
| 3.1.10 | <p>Conduit Installation - Lead required size plastic conduit to locations specified on the design drawings. Leave sufficient amount at root end of the blade to span the splice joint and run to rotor centerline. Tie conduit down using fiberglass strips with clear WEST SYSTEM 105/206 epoxy per design drawings. Measure weights of component parts of epoxy and record in Manufacturer's Log. Coil up extra length at root end and tape to inner surface of low pressure shell.</p> |
| 3.1.11 | <p>Pressure Tap Hookup - On both high and low pressure shells, attach and clamp tubing to pressure tap outlet. Cut low pressure shell tubing to length necessary to lead in an orderly fashion along shell interior to respective enclosure. Allow sufficient additional length to allow freedom to lead to the interior of the instrument enclosure. On the high pressure shell, an additional two feet of length must be given to each tube to allow for practical lead to enclosure as blade halves are bonded. When all hookups</p> |

TABLE XXXIV.

GOUCEON BROTHERS, INC., BLADE MANUFACTURING PROCESS/QUALITY SPECIFICATION NO: NASA-7 Pg. 17 of 27
 Process Description: 90 Foot MOD-O Prototype Rotor Fabrication Program: Contract DEN 3-260 Date: 3-8-83 Rev.

Completed & Accepted
 MFG SUP Q.A. ENGR. DATE

Oper. No.	Operation Description
3.1.11	Pressure Tap Hookup (continued) are made, bundle the tubes and anchor them in place per the design drawings.
3.1.12	Install Tip Blocking and Drill Vent Hole - Trim Douglas fir/epoxy laminate blocking to fit tip region per design drawings. Verify that blocking allows blade halves to join at the tip by dry fitting both blades. Machine tip vent hole and bond pre-manufactured glass-epoxy insert per design drawings using clear WEST SYSTEM 105/206 epoxy. Measure weights of component parts of epoxy used and record in Manufacturer's Log.
3.1.13	Install Ribs and Damper Attachment Blocking - Install WEST SYSTEM epoxy coated plywood ribs as specified into blades A and B and into high pressure hub shell. Bond in place using asbestos thickened 105/206 epoxy and filletting where appropriate. Plastic inspection port may be pre-installed in ribs. Measure weights of component parts of each epoxy batch used and record in Manufacturer's Log. Per design drawings, dry fit interior attachment blocking in both ends of hub structure and into each root end of the outer blades. When dry fits are acceptable, apply clear WEST SYSTEM 105/206 epoxy to bonding surfaces. Before clear epoxy hardens, apply asbestos thickened 105/206 epoxy to joint surfaces of each blocking piece and with the aid of internal braces, position each internal blocking piece and establish moderate pressure to enhance the joint. Measure weights of component parts of each epoxy batch used and record in Manufacturer's Log. Also, before each batch gels or is expended, take a syringe sample, mark with date and operation and set aside. Allow eight hour minimum cure prior to disturbing bonded structure.

TABLE XXXIV.

GOUGEON BROTHERS, INC., BLADE MANUFACTURING PROCESS/QUALITY SPECIFICATION NO: NASA-7 Pg. 18 of 27
 Process Description: 90 Foot MOD-O Prototype Rotor Fabrication Program: Contract DEN 3-260 Date: 3-8-83 Rev.

Oper. No.	Operation Description	Completed & Accepted	
		MFG SUP	Q.A. ENGR. DATE

3.1.14

Bond Half Shells -

- a) Keeping high pressure shell in mold, suspend low pressure mold over it with approximately nine to twelve inches of clearance. Lifting points can only be at extreme ends of low pressure shell due to shear web interference. Be certain lifting slings are secure.
- b) Dry Fit - Ease root end of low pressure shell onto high pressure shell while feeding shear web into stringer located on high pressure shell. Then ease tip end of low pressure shell down while checking interior with light to verify proper shear web placement within stringer.
- c) At time of dry fit up, using templates for cover plates and scribed lines on gelcoat indicating design plate locations, scribe line defining desired plate perimeter. Cut away enough of the shell where the cover plates are to be installed so that a hand may fully access the interior.
- d) Following successful dry fit up of the shells, lift low pressure shell off again so that just enough access exists to reach the unbonded shear web stringer on the high pressure shell. Lead all pressure tap tubes into their respective enclosures through the minimum dimension holes necessary in the enclosure side wall. Tubes should pass snugly through holes, but should not be pinched.
- e) Apply clear WEST SYSTEM 105/206 epoxy to all bonding areas - namely the leading and trailing edge joint faces, the lower edge of the shear web, the interior of the high pressure shell shear web stringer, and tip blocking to interior rotor shell interfaces. Before the epoxy hardens, mix and apply

TABLE XXXIV.

GOUCEON BROTHERS, INC., BLADE MANUFACTURING PROCESS/QUALITY SPECIFICATION NO: NASA-7		Pg. 19 of 27
Process Description: 90 Foot MOD-O Prototype Rotor Fabrication		Date: 3-8-83 Rev. _____
Program: Contract DEN 3-260		
Operation Description		Completed & Accepted
MFG SUP		Q.A. ENGR. DATE

Oper. No.	Operation Description
3.1.14	<p>Bond Half Shells (continued)</p> <p>asbestos thickened epoxy to these same joint areas. Measure weights of component parts of each epoxy batch used and record in Manufacturer's Log. Also, before each batch gels or is expended, take a syringe sample, mark with date and operation and set aside.</p> <p>f) While gently pulling out slack of all pressure tap tubes, ease root end of low pressure shell onto high pressure shell while feeding shear web into stringer located on high pressure shell. Also check alignment of tip blocking before proceeding. With interior of blade lighted, ease the tip end of the low pressure shell down while verifying proper shear web placement within stringers. Apply moderate pressure and let blade cure a minimum of twelve hours prior to removing from mold.</p>
3.2	Blade B Assembly
3.2.1	Half Shell Trimming - See 3.1.1
3.2.2	Install Shear Web - See 3.1.7 (disregard Para. c)
3.2.3	Install Ice Detector Blocking - See 3.1.8
3.2.4	Conduit Installation - See 3.1.10
3.2.5	Install Tip Blocking and Drill Vent Hole - See 3.1.12
3.2.6	Bond Half Shells - See 3.1.14 (disregard all references to pressure tap tubes and instrumentation enclosures.
3.3	Hub Assembly
3.3.1	Interior Glass Wetout - Using roller brush and clear WEST SYSTEM 105/206 epoxy, complete wetout of interior glass fabric. Measure weights of component parts of each batch of epoxy and record in Manufacturer's Log.
3.3.2	Half Shell Trimming - See 3.1.1

TABLE XXXIV.

GUGEON BROTHERS, INC., BLADE MANUFACTURING PROCESS/QUALITY SPECIFICATION NO: NASA-7 Pg. 20 of 27
 Process Description: 90 Foot MOD-0 Prototype Rotor Fabrication Program: Contract DEN 3-260 Date: 3-8-83 Rev.

Oper. No.	Operation Description	Completed & Accepted	
		MFG SUP	Q.A. ENGR. DATE
3.3.3	Fastener Sleeve Installation Setup - Place low pressure shell onto saw horses and secure in place. Hang aluminum drill guide plate defined in the design drawings from the machined edges of the low pressure shell. Shim, brace and clamp where necessary to achieve optimum alignment of plate with respect to cut plane, rotor centerline and spanwise centerline.		
3.3.4	Drill Fastener Holes - Drill out holes for inserts using slip type guide bushings, which are located by use of the guide plate, and a hand-held drill with motor. After each hole is drilled check for plate movement against drawn match lines.		
3.3.5	Install Fastener Sleeves - After holes are all drilled, keep guide plate in position for use as a sleeve installation alignment plate. Using waxed sleeve insert guides, as shown in the design drawings, secure inspected and approved sleeves onto locating pins.		

With a fabric swab and clear WEST SYSTEM 105/206 epoxy, wet out interiors of machined holes. Before clear epoxy hardens, apply asbestos thickened 105/206 epoxy to hole interiors, and to threaded exteriors of sleeves. Measure weights of component parts of each epoxy batch used and record in Manufacturer's Log. Also, before each batch gels or is expended, take a syringe sample, mark with date and operation and set aside.

As each sleeve insert is placed into the alignment plate, seal region where insert exits hub exterior to prevent excessive epoxy bleed through. When all sleeves are in place, recheck the alignment plate to assure position is correct.

TABLE XXXIV.

COUGEON BROTHERS, INC., BLADE MANUFACTURING PROCESS/QUALITY SPECIFICATION NO: NASA-7			Pg. 21 of 27	
Process Description: 90 Foot MOD-O Prototype Rotor Fabrication		Program: Contract DEN 3-260	Date: 3-8-83	Rev. _____
Operation Description			Completed & Accepted	
Oper. No.			MFG SUP	Q.A. ENGR. DATE

Oper.
No.

Operation Description

- 3.3.5 Install Fastener Sleeves - (continued)
Then attach clamping plate to alignment plate per design drawings to force each plate insert to a common plane.
Following a minimum of 12 hours cure time, remove all sleeve installation hardware.
- 3.3.6 Bond Half Shells - Keeping low pressure shell in mold, dry fit high pressure shell to it. Check correspondence of spanwise centerlines and rotor centerlines scribed on both high and low pressure shell exterior gelcoat.
Following satisfactory dry fit, lift high pressure shell off with sufficient clearance to apply epoxy to both sides of joint. Apply clear WEST SYSTEM 105/206 epoxy, wet out all joint surfaces. Before clear epoxy hardens, apply asbestos thickened 105/206 epoxy to low pressure shell joint surface. Measure weights of component parts of each epoxy batch used and record in Manufacturer's Log. Also, before each batch gels or is expended, take a syringe sample, mark with date and operation and set aside.
Lower high pressure shell onto low pressure shell and apply moderate pressure. Clean up excess epoxy which oozes from joint. Recheck relationship of scribed lines. Let hub cure a minimum of twelve hours prior to removing from mold.
- 3.3.7 Install Hub Hole Reinforcement - Lightly abrade outside surface of hole reinforcements. Using templates for hub holes and scribed lines on gelcoat indicating rotor and spanwise centerlines, scribe lines defining hub holes. Machine away laminate until holes are to design specification. Check for fit against pre-manufactured hole reinforcements and provide subtle clearances, if necessary.

TABLE XXXIV.

GOUGEON BROTHERS, INC., BLADE MANUFACTURING PROCESS/QUALITY SPECIFICATION NO: NASA-7 Pg. 22 of 27Process Description: 90 Foot MOD-O Prototype Rotor Fabrication Program: Contract DEN 3-260 Date: 3-8-83 Rev.

Oper. No.	Operation Description	Completed & Accepted			
		MFG	SUP	Q.A. ENGR.	DATE
3.3.7	<p>Install Hub Hole Reinforcement - (continued)</p> <p>Lightly sand or wipe mating surfaces of insert and hole. Then apply clear 105/206 epoxy to mating surfaces. Before clear epoxy hardens, apply asbestos thickened 105/206 epoxy to edges of holes and install reinforcements. Check reinforcement alignment and correct if necessary.</p> <p>Measure weights of component parts of each epoxy batch used and record in Manufacturer's Log. Also, before each batch gels or is expended take a syringe sample, mark with date and operation and set aside. Allow eight hour minimum cure prior to disturbing hub structure.</p>				

TABLE XXXIV.

GOUGEON BROTHERS, INC., BLADE MANUFACTURING PROCESS/QUALITY SPECIFICATION NO: <u>NASA-7</u>			Pg. <u>23</u> of <u>27</u>	
Process Description: <u>90 Foot MOD-0 Prototype Rotor Fabrication</u>			Date: <u>3-8-83</u> Rev. <u> </u>	
			Contract DEN <u>3-260</u>	
			Completed & Accepted	
			MFG SUP <u>Q.A. ENGR.</u>	DATE <u> </u>

Oper. No.	Operation Description
4.0	<u>Component Machining</u>
4.1	<u>Blade A Machining</u>
4.1.1	<p>Install Cover Plates - Machine cover plate holes to final dimension and configuration shown on design drawings. Check respective cover plates for fit. When suitable fit is obtained, machine and cast fastener holes as specified. After completing fastener hole manufacture, remove cover plates and apply a thin silicone rubber bead around perimeter of access hole lip. Let bead harden. Reinstall cover plate to half of maximum fastener torque specified. Note where plate is non-flush with rotor surface and correct by lightly filing or adding epoxy coatings to inner surface perimeter of cover plate as required.</p> <p>4.1.2 Finish Tips - Using router, face off each blade tip as specified in design drawings. Then install plywood tip cap as required. Bond plywood in place by first applying clear WEST SYSTEM 105/206 epoxy to all mating surfaces and then applying asbestos thickened 105/206 epoxy before clamping plywood in place. Measure weights of component parts of each epoxy batch used and record in Manufacturer's Log. Wipe away excess epoxy and let cure for eight hours minimum before removing clamps.</p> <p>4.1.3 Prior to machining of finger joints, balance Blades A and B using non-metallic ballast cast in epoxy. Dummy weights simulating the weight of the instruments should be added to Blade A. Balancing weight should be added through the ice detector hole and kept as well inboard as is practical to avoid developing blade frequency problem.</p>

TABLE XXXIV.

GOUGEON BROTHERS, INC., BLADE MANUFACTURING PROCESS/QUALITY SPECIFICATION NO: NASA-7 Pg. 24 of 27
 Process Description: 90 Foot MOD-O Prototype Rotor Fabrication Program: Contract DEN 3-260 Date: 3-8-83 Rev. _____

Oper. No.	Operation Description	Completed & Accepted	
		MFG SUP	Q.A. ENGR. DATE
4.1.4	Face Off Root - Using router, face off inner blade, face within .25 to .50 inches of final specified dimension. Apply two coats of clear WEST SYSTEM epoxy to moisture seal laminate.		
4.1.5	Machine Fingers -		
	a) Pending NASA approval, a machining qualification structure (box beam) is recommended. Align structure with Horizontal Boring Mill per design drawings, high pressure side up. Face off structure at location specified. Make angled cuts using large circular cutter at locations and to depth specified.		
	b) Check dimensions of qualification piece and fit, if satisfied repeat process on actual rotor structure. Cover joint during any stop in the machining process of over 15 minutes with a layer of plastic film. Cover with several layers of plastic film for shipment. Include weighed cut out wedges within packing to monitor laminate moisture content changes.		
4.2	<u>Blade B Machining</u>		
4.2.1	Install Cover Plates - See 4.1.1		
4.2.2	Finish Tips - See 4.1.2		
4.2.3	Face Off Root - See 4.1.4		
4.2.4	Machine Fingers - See 4.1.5b		
4.3	<u>Hub Machining</u>		
4.3.1	Face Off Ends - See 4.1.4 (treat each hub end as an inner blade face)		
4.3.2	Machine Fingers - See 4.1.5b		

TABLE XXXIV.

GOUGEON BROTHERS, INC., BLADE MANUFACTURING PROCESS/QUALITY SPECIFICATION NO: NASA-7 Pg. 25 of 27
 Process Description: 90 Foot MOD-O Prototype Rotor Fabrication Program: Contract DEN 3-260 Date: 3-8-83 Rev.

Completed & Accepted
 MFG SUP Q.A. ENGR. DATE

Oper. No.	Operation Description
5.0	<u>Rotor Assembly</u>
5.1	<u>Splice Joint Bonding - Blade A to Hub</u>
5.1.1	Dry Fit - Roughly align both structures, install clamping system and pull joint together to check fit. With fingers engaged, verify adjustability for alignment. Withdraw fingers.
5.1.2	Adhesive Application - Coat all mating surfaces with clear WEST SYSTEM 105/206 epoxy liberally to both sides of the joint. Before clear epoxy gels, apply asbestos thickened epoxy to all bonding surfaces. Measure weights of component parts of each epoxy batch used and record in Manufacturer's Log. Also, before each batch gels or is expended, take a syringe sample, mark with date and operation and set aside.
5.1.3	Bond Joint - Pull joint together by tightening the clamping system. Inspect exterior and interior for liberal and complete oozing of epoxy. Check and adjust blade to hub alignment while also setting joint engagement within specified tolerances. Wipe away excess epoxy. Let structure cure undisturbed for 12 hours minimum.
5.1.4	Finish Joint - Following cure, fair hub to blade discontinuity and fill any voids with microballoon thickened 105/206 epoxy. Any significant voids should be filled with asbestos thickened 105/206 epoxy. Measure weights of component parts of each epoxy batch used and record in Manufacturer's Log. When completed, apply fiberglass wrapping over joint area per design drawings. Measure weights of component parts of each epoxy batch used and record in Manufacturer's Log.

TABLE XXXIV.

COUGEON BROTHERS, INC., BLADE MANUFACTURING PROCESS/QUALITY SPECIFICATION NO:		NASA-7	Pg. 26 of 27
Process Description: 90 Foot MOD-0 Prototype Rotor Fabrication		Program: Contract DEN 3-260	Date: 3-8-83 Rev.
Oper. No.	Operation Description	Completed & Accepted	
		MFG SUP	Q.A. ENGR. DATE

5.2 Splice Joint Bonding - Blade B to Hub

5.2.1 Dry Fit - See 5.1.1

5.2.2 Adhesive Application - See 5.1.2

5.2.3 Bond Joint - See 5.1.3

5.2.4 Finish Joint - See 5.1.4

5.3 Rotor Completion

5.3.1 Install Lightning Strap - Remove gelcoat and underlying peel ply at location specified on design drawings for lightning protection system, ground strap installation. Using grinder lightly expose the lightning screen to bare aluminum over the entire installation area. Bond and fasten ground strap in place using electrically conductive epoxy as specified. Measure weights of component parts of epoxy and record in Manufacturer's Log. Clean up excess epoxy.

5.3.2 Guy Wire Anchors - Install attachments for support wires of angle of attack probes on Blade A per design drawings. Bond fasteners in place using clear WEST SYSTEM 105/206 epoxy. Measure weights of component parts of epoxy and record in Manufacturer's Log.

5.3.3 Final Rotor Balance - Suspending rotor at centerline, statically balance using non-metallic ballast cast in epoxy in location described in 4.1.3.

5.3.4 Final Finishing - Sand entire rotor surface until smooth and fair. Check contour against defined lofting lines using templates. Record in Manufacturer's Log any noted deviations from lofted contour.

TABLE XXXIV.

GOUGEON BROTHERS, INC., BLADE MANUFACTURING PROCESS/QUALITY SPECIFICATION NO:		NASA-7	Pg. 27 of 27
Process Description: 90 Foot MOD-O Prototype Rotor Fabrication		Program: Contract DEN 3-260	Date: 3-8-83 Rev. _____
Oper. No.	Operation Description	Completed & Accepted	
		MFG SUP	Q.A. ENGR. DATE

5.3.4 Final Finishing (continued)

Paint rotor with paint and color scheme as defined in design drawings. Spraying is preferred, but roller application may be substituted. When final coat is dry, verify that pressure tap orifices are unclogged - clean out if necessary with compressed air and thin wire.

5.3.5

Shipment - Using manufactured bunks as identified in design drawings, prepare rotor for delivery to NASA specified facility. Measure final weights and confirm centerline center of gravity prior to loading onto shipment trailer.

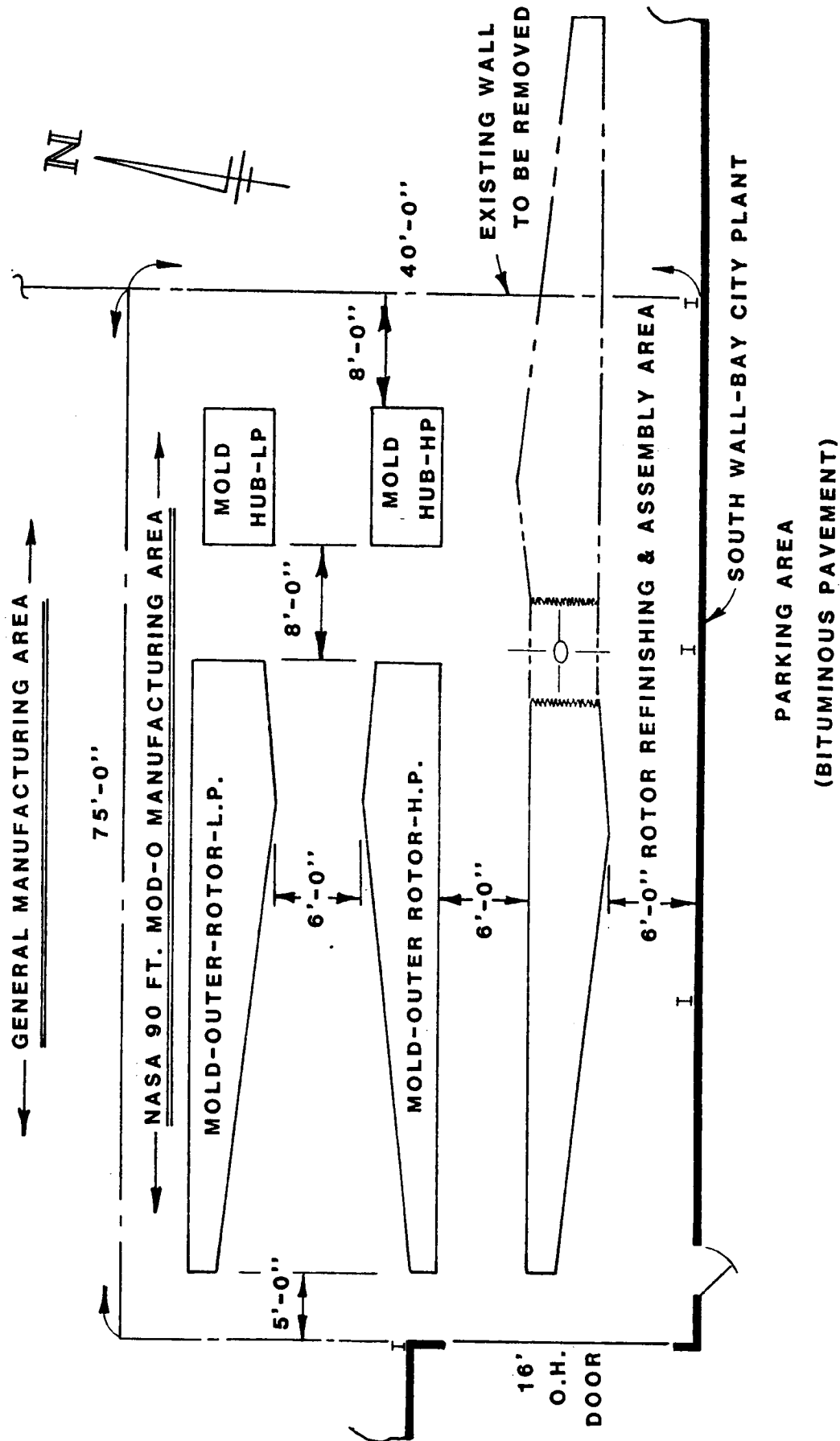


Figure 86. - Proposed Manufacturing Area

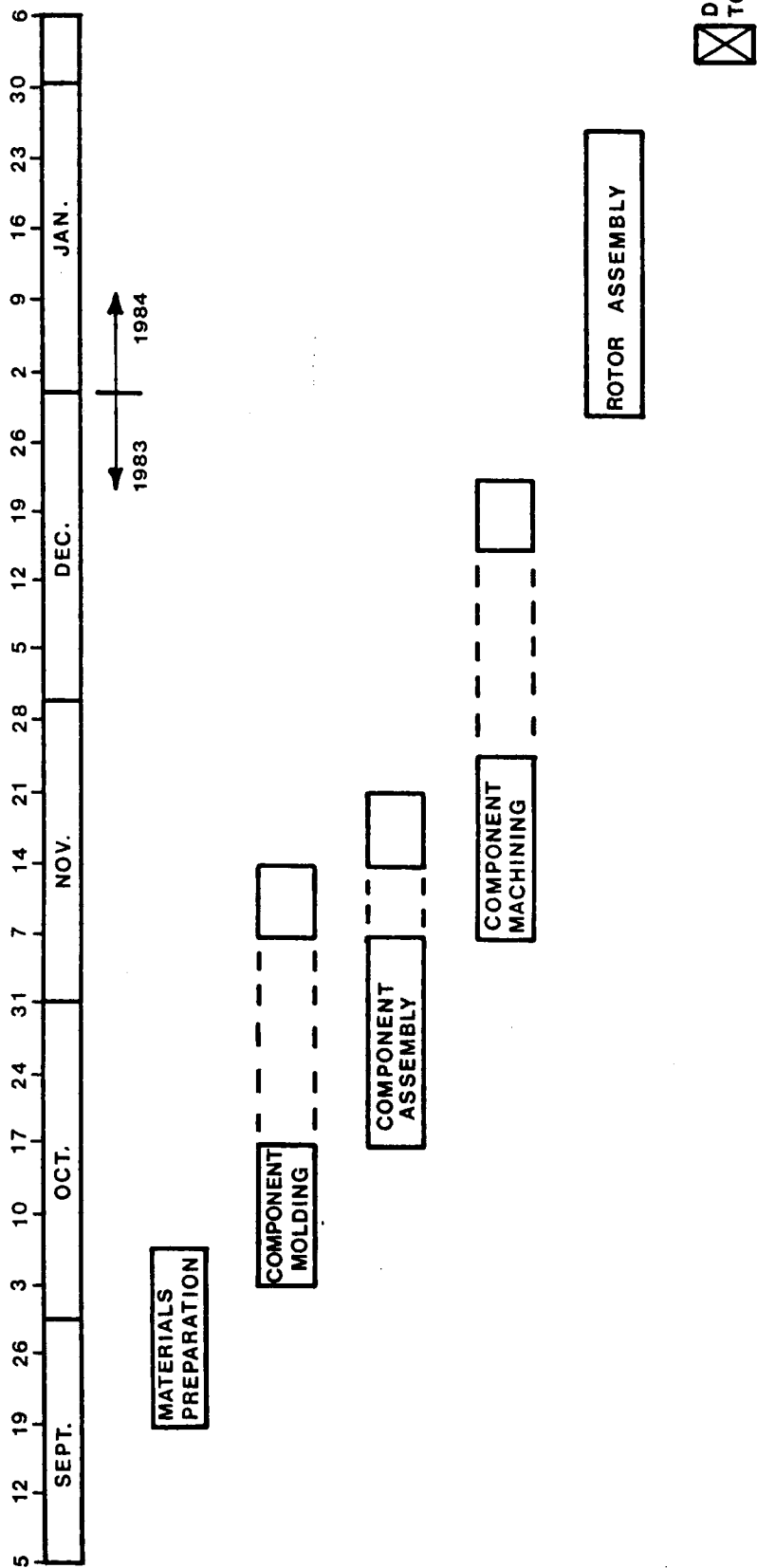


Figure 87. - Proposed Fabrication Schedule

19.0 REFERENCES

1. Gougeon, M.; and Zuteck, M.: The Use of Wood for Wind Turbine Blade Construction. Large Wind Turbine Design Characteristics and R&D Requirements, S. Lieblein, Ed., NASA CP-2106, CONF-7904111, 1979, pp. 293-308.
2. Zuteck, M.D.: The Development and Manufacture of Wood Composite Wind Turbine Rotors. DOE/NASA Horiz. Axis Wind Turbine Workshop, July 27, 1981.
3. Faddoul, J.R.: Examination, Evaluation, and Repair of Laminated Wood Blades After Service on the Mod-0A Wind Turbine. DOE/NASA/20320-53, NASA TM-83483, Oct. 1983.
4. Glasgow, J.C.; and Corrigan, R.D.: Results of Free Yaw Tests of the Mod-0 100-Kilowatt Wind Turbine. DOE/NASA/20320-46, NASA TM-83432, June 1983.
5. Hohenemser, K.H.; and Swift, A.H.P.: The Investigation of Passive Blade Cyclic Pitch Variation Using an Automatic Yaw Control System. Solar Energy Research Institute; SERI/TR-11052-2, Aug. 1982.
6. Bankaitis, H.: Evaluation of Lightning Accommodation Systems for Wind-Driven Turbine Rotors. DOE/NASA/20320-37, NASA TM-82784, Mar. 1982.
7. Lark, R.F.; Gougeon, M.; Thomas, G.; and Zuteck, M.: Fabrication of Low-Cost Mod-0A Wood Composite Wind Turbine Blades. DOE/NASA/20320-45, NASA TM-83323, Feb. 1983.
8. Anon.: Wood Handbook; Wood as an Engineering Material. Forest Products Laboratory, Forest Service, U.S. Dept. of Agriculture, Agriculture Handbook No. 72, Aug. 1974.
9. Forrest, R.C.: Effects of Circular Holes on Strength of Douglas Fir/Epoxy Laminates. General Electric Co./AEPD MOD-5A Project. June 1983.
10. Thomas, G.; rev. Forrest, R.: Fatigue Strength Testing of Douglas Fir/Epoxy Laminates for MOD-5A Wind Turbine Blade Project - Phase B1. General Electric Co./AEPD MOD-5A Project. Dec 1982.
11. Lieblein, S.; Gougeon, M.; Thomas, G.; and Zuteck, M.: Design and Evaluation of Low-Cost Laminated Wood Composite Blades for Intermediate Size Wind Turbines: Blade Design, Fabrication Concept, and Cost Analysis. DOE/NASA/0101-1, NASA CR-165463, Nov. 1982.
12. Faddoul, J.R.: Test Evaluation of a Laminated Wood Wind Turbine Blade Concept. DOE/NASA/20320-30, NASA TM-81719, May 1981.

1. Report No. NASA CR-174713		2. Government Accession No.		3. Recipient's Catalog No.	
4. Title and Subtitle DESIGN OF AN ADVANCED WOOD COMPOSITE ROTOR AND DEVELOPMENT OF WOOD COMPOSITE BLADE TECHNOLOGY				5. Report Date DECEMBER 1984	
				6. Performing Organization Code	
7. Author(s) T. Stroebel, C. Dechow, and M. Zuteck				8. Performing Organization Report No. GBI ER-11	
				10. Work Unit No.	
9. Performing Organization Name and Address Gougeon Brothers, Inc. 706 Martin Street P.O. Box X908 Bay City, Michigan 48707				11. Contract or Grant No. DEN 3-260	
				13. Type of Report and Period Covered Contractor Report	
12. Sponsoring Agency Name and Address U.S. Department of Energy Wind Energy Technology Division Washington, DC 20545				14. Sponsoring Agency Code Report No. DOE/NASA/0260-1	
15. Supplementary Notes Final Report. Prepared Under Interagency Agreement DE-AI01-79ET20320. Project Manager, R. F. Lark, Wind Energy Project Office, NASA Lewis Research Center, Cleveland, OH 44135.					
16. Abstract In support of a program to advance wood composite wind turbine blade technology, a design was completed for a prototype, 90-foot diameter, two-bladed, one-piece rotor, with all wood/epoxy composite structure. The rotor was sized for compatibility with a generator having a maximum power rating of 400 kilowatts. Innovative features of the rotor include: a teetering hub to minimize the effects of gust loads, untwisted blades to promote rotor power control through stall, joining of blades to the hub structure via an adhesive bonded structural joint, and a blade structural design which was simplified relative to earlier efforts. The prototype rotor was designed to allow flexibility for configuring the rotor upwind or downwind of the tower, for evaluating various types of teeter dampers and/or elastomeric stops, and with variable delta-three angle settings of the teeter shaft axis. The prototype rotor was also designed with provisions for installing pressure tap and angle of attack instrumentation in one blade. A production version rotor costing analysis was conducted. Included in the program were efforts directed at developing advanced load take-off stud designs for subsequent evaluation testing by NASA, development of aerodynamic tip brake concepts, exploratory testing of a wood/epoxy/graphite concept, and compression testing of wood/epoxy laminate, with scarf-jointed plies.					
17. Key Words (Suggested by Author(s)) Wind turbine; rotor blades; teetered rotor; one-piece rotor; laminated wood; wood composite; wood/epoxy composite; wood/epoxy/graphite composite				18. Distribution Statement [REDACTED] [REDACTED]	
19. Security Classif. (of this report) Unclassified		20. Security Classif. (of this page) Unclassified		21. No. of pages 196	
22. Price*					